Empirical Studies of Over-the-counter Currency Option Contracts

A dissertation submitted in fulfilment of the requirements

for the degree of

Doctor of Philosophy

Alfred Huah-Syn Wong

B.Com(*Qld*), MFM(*Qld*), FRM®

Discipline of Finance

School of Economics, Finance and Marketing
Business Portfolio
RMIT University
Melbourne, Australia
December 2009

DEDICATION

With profound respect to my late father, Kee-Lieng,

and to my dearest mother, Chiew-Hiong,

in honour of their

selfless love,

trust,

support

and guidance throughout my life.

DECLARATION

I certify that except where due acknowledgement has been made, the work is that of the author alone; the work has not been submitted previously, in whole or in part, to qualify for any other academic award; the content of the thesis is the result of work which has been carried out since the official commencement date of the approved research program; and, any editorial work, paid or unpaid, carried out by a third party is acknowledged.

Alfred Huah-Syn Wong

ACKNOWLEDGEMENTS

This dissertation would not be completed without the generous assistance from several individuals over the candidature period of my doctorate degree. My gratitude to these individuals is boundless. I express my upmost appreciation to my Ph.D supervisors at RMIT University, Associate Professor Amalia Di Iorio and Professor Richard Heaney. Associate Professor Amalia Di Iorio is highly regarded for her work in the area of international finance. I am grateful for her time, support and guidance on my research. Professor Richard Heaney is a well-known and highly respected academic in the field of finance both in Australia and overseas. His passion for research is inspiring and I thank Richard for his constant patience, genuine interest, trust and expert guidance on my work.

I am also thankful to several other individuals who had provided generous research guidance at various stages of my dissertation. I thank Associate Professor Greg Walker who had provided supervision support at the early stage of my study; Professor Mark Morrison and Dr. Roderick Duncan at Charles Sturt University, for encouragement and useful suggestions; Professor Alex Frino at Sydney University, for useful discussion on data-related issues and Associate Professor Heather Mitchell at RMIT University, for critical comments on my work. I am also indebted to Perio Musio of UBS Investment Bank, Switzerland; John Ewan of British Bankers' Association (BBA), London; Eric Chan of UBS Investment Bank, Singapore and Alex Wong of Mizuho Investment Bank, Singapore for their invaluable market insights on over-the-

counter currency option and generous data support. Funding support from the Faculty of Business, Charles Sturt University for the completion of this dissertation is also gratefully acknowledged.

This Ph.D endeavour would not come to fruition without the affection, support, encouragement and understanding from my lovely wife, Annie, who had endured many family commitments throughout the progress and completion of this onerous task. To my dear children, Joshua, Esther and Sarah, I thank them for the joy they bring into my life. I am also grateful to my dear brother, Winston Wong, for help with proofreading the early version of this dissertation.

Last but most importantly, I thank my Lord and Saviour, Jesus Christ, for His daily blessings. His grace and mercy filled every aspects of my life.

LIST OF FIGURES

Figure 2-1: Over-the-counter Foreign Exchange Derivatives by Instruments 12
Figure 2-2: OTC Currency Derivatives by Instrument and Maturity 13
Figure 2-3: OTC Currency Derivatives by Currency Type 14
Figure 2-4: Growth of OTC and Exchange-traded Currency Options 15
Figure 2-5: AUD/USD At-the-money Forward Straddle 18
Figure 2-6: AUD/USD Strangle 20
Figure 2-7: 25-delta Risk Reversal 22
Figure 2-8: AUD/USD One-Month Implied Volatility on 1 October 2003 24
Figure 2-9: EUR/USD Implied Volatility Term Structure 25
Figure 2-10: AUD/USD One-month Implied Volatility on 1 October 2003 27
Figure 4-1: Variance Ratio versus Maturity (q=10) 93
Figure 4-2: Variance Ratio versus Maturity (q=20) 93
Figure 4-3: Total RMSE versus Maturity 106
Figure 5-1: Time Series Plots of Spot Exchange Rate, At-the-money Forward 123
Figure 5-2: The Simple Moving Average Trading Rule 125
Figure 5-3: EUR/USD Buy and Sell Signals (Trigger Value =1) 128
Figure 5-4: EUR/USD Buy and Sell Signals (Trigger Value =2) 128
Figure 6-1: One-month Quoted Implied Volatility versus Delta on 21/08/2003 165
Figure 6-2: Implied Volatility versus Moneyness (X/F) for AUD/USD 171
Figure 6-3: Time Series Plots of Curvature and Slope Coefficients 178
Figure 6-4: Impulse Reponses for Smile Slopes due to Volatility Shock 199
Figure 6-5: GBP/USD Impulse Reponses for Trivariate VAR 201
Figure 6-6: EUR/USD Impulse Reponses for Trivariate VAR 202
Figure 6-7: AUD/USD Impulse Reponses for Trivariate VAR 203
Figure 6-8: USD/JPY Impulse Reponses for Trivariate VAR 204
Figure 6-9: Estimated Jumps for AUD/USD 208
Figure 6-10: Estimated Jumps for USD/JPY 208
Figure 7-1: Movement of Implied Volatility and Smile Curvature over Time 234
Figure 7-2: Volatility Smiles for GBP/USD 235
Figure 7-3: Volatility Smile Dynamics for GBP/USD 237

LIST OF TABLES

Table 2-1: A Comparison of Over-the-counter Currency Options and Exchange-traded Currency Options 28
Table 4-1: Descriptive Statistics for the First-Differenced Implied Volatility Series 73
Table 4-2: Augmented Dickey-Fuller (1981) and Phillips-Perron (1988) Unit Root Tests 75
Table 4-3: Autocorrelation Coefficients and the Ljung-Box Q-statistic 76
Table 4-4: Variance Ratio Estimation and Hypothesis Testing of Unity Variance Ratios Using Zs(q) 83
Table 4-5: Variance Ratio Estimation and Hypothesis Testing of Unity Variance Ratios Using Z(q) 85
Table 4-6: Hypothesis Testing of Unity Variance Ratios Using Ranks and Signs 88
Table 4-7: Sidack-adjusted $\widetilde{P}_{ji}^{S}$ *-values for Ranks and Signs* 91
Table 4-8: Out-of-Sample One-day Ahead Forecast Performance for the Random Walk and Competing Models 102

Table 4-9: RMSE Ratios Relative to the Random Walk Model *104*
Table 4-10: Diebold-Mariano (1995) Test of Equal Forecast Accuracy *107*
Table 5-1: Descriptive Statistics for At the Money Forward Straddle Quotes *120*
Table 5-2: Descriptive Statistics for Risk Reversal Quotes *121*
Table 5-3: Calculation of Total Option Premium *134*
Table 5-4: Naïve Models for At-the-money Forward Straddles *140*
Table 5-5: Naïve Models for Risk Reversals *141*
Table 5-6: Results for At-the-money Forward Straddle Trades *143*
Table 5-7: Results for Risk Reversal Trades *148*
Table 5-8: Aggregate Result for At-the-money Forward Straddles *152*
Table 5-9: Aggregate Result for Risk Reversals *153*
Table 6-1: Summary Statistics for the Implied Volatility Datasets *167*
Table 6-2: Estimated Smile Coefficients Using Quadratic Approximation *175*
Table 6-3: Statistics for the Shape Proxies and Conditional Volatility *180*
Table 6-4: Estimated GARCH (1,1) Parameters *182*
Table 6-5: Granger Causality Tests on Dynamics of Volatility Smile (CF & PF) *187*
Table 6-6: Granger Causality Tests on Dynamics of Volatility Smile (SKW and CE) *190*
Table 6-7: Granger Causality Test on Individual Slope for Put Options *193*
Table 6-8: Granger Causality Test on Individual Slope for Call Options *194*
Table 6-9: Residuals Autocorrelation Tests for VAR (3) Model *197*
Table 6-10: Test Results for the Trivariate VAR Model *197*
Table 6-11: Jump Frequencies and Window Sizes *207*
Table 6-12: Probit Regressions for the Aggregate Sample *211*
Table 6-13: Aggregate Results for Probit Regressions *213*
Table 7-1: Descriptive Statistics for Implied Volatility and Estimated Series *227*
Table 7-2: Phillips-Perron(1988) Unit Root Tests *229*
Table 7-3: Correlations Between Parameter Estimates and Implied Volatility *231*
Table 7-4: Estimated Shape Proxies and Volatility Smile *236*
Table 7-5: Univariate Regression Tests Using Shape Proxies of Volatility Smile *239*
Table 7-6: Univariate Regression Tests Using At-the-money Implied Volatility *241*
Table 7-7: Regression Tests Using At-the-money Implied Volatility and CF *243*
Table 7-8: Regression Tests Using At-the-money Implied Volatility and PF *244*
Table 7-9: Regression Tests Using At-the-money Implied Volatility and AS *245*
Table 7-10: Regression Tests Using At-the-money Implied Volatility and CE *246*
Table 7-11: Regression Tests with At-the-money Implied Volatility and GARCH (1,1) Estimates *248*
Table 7-12: Regression Tests Using At-the-money Implied Volatility with CF and GARCH (1,1) Estimates *250*
Table 7-13: Regression Tests Using At-the-money Implied Volatility with PF and GARCH (1,1) Estimates *251*
Table 7-14: Regression Tests Using At-the-money Implied Volatility with AS and GARCH (1,1) Estimates *252*
Table 7-15: Regression Tests Using At-the-money Implied Volatility with CE and GARCH (1,1) Estimates *253*

ABSTRACT

It is a well-established fact that the foreign exchange market is the largest financial market in the world[1]. However, it is relatively less well-known that currency options and other foreign exchange-related derivatives have become more popular and prominent in size since the mid-1980's. Today, currency options are used by numerous players in the financial market, including portfolio managers, hedgers, speculators and even central bankers. Despite their popularity amongst market participants, research in currency options has received little attention in comparison with options on stocks and other underlying assets. This is not surprising as most of the currency option contracts are written by commercial and investment banks in the privately negotiated over-the-counter option markets rather than the exchange-traded markets.

This thesis provides empirical investigations into the behaviour of implied volatility quotes for currency options on the British pound/U.S. dollar (GBP/USD), the euro/U.S. dollar (EUR/USD), the Australian dollar/U.S. dollar (AUD/USD) and the U.S. dollar/Japanese yen (USD/JPY). The analyses are performed using dealer-quoted implied volatility and spot exchange rate datasets collected from the over-the-counter currency option market.

[1] According to the Triennial Central Bank Survey conducted by the Bank for International Settlements, global foreign exchange market recorded a daily turnover of USD3.21 trillion in April 2007 (See Table B.1 of the survey released in December 2007).

Two main aspects of the implied volatility quotes are examined in this dissertation. First, the time series behaviour of implied volatility of various maturities is analysed. Second, analysis concerning the dynamics of implied volatility smiles for these four currency-pairs is undertaken.

The first empirical chapter examines the random walk hypothesis using implied volatility quotes of various maturities. Conventional and nonparametric variance ratio tests are performed on the volatility levels and first-differences. The results provide evidence of random walk violations in the volatility series across all currency pairs examined. Specifically, strong rejections are found in the short-dated volatility of one week and one month. Further, out-of-sample robustness tests suggest that forecasting implied volatility changes using a random walk model produce significantly higher forecasting errors compared with two alternative models based on the artificial neural networks (ANNs) and autoregressive integrated moving average (ARIMA) frameworks. These findings suggest that short-dated implied volatility are better characterised as a mean-reverting process while the random walk process captures long-dated implied volatility more accurately.

The analysis in the second chapter extends the key findings by examining the profitability of volatility trading using a simple technical trading strategy. This study concludes that the trading rules generated positive returns in the majority of the currency pairs even after allowing for volatility and exchange rate spreads. The buy straddle signals generate positive average holding-period returns for three of the four currency pairs examined. Further, the average holding-period return of the buy trade is statistically different from the average holding-period return of the sell trade. This is

especially evident for the USD/JPY straddles. Conversely, risk reversal trades produced less compelling outcomes with lower winning trades and holding-period returns. Thus the overall results suggest that moving average trading rules are useful in volatility trading. In addition the profits from the option strategies are often large enough to offset the transaction costs.

The third analysis chapter examines a well-known empirical anomaly in the currency option market. Specifically, the relation between the dynamics of the volatility smile and the anticipated volatility for the GBP/USD, EUR/USD, AUD/USD and USD/JPY currency pairs is investigated. The analysis uses a unique trader-quoted implied volatility dataset to construct the volatility smile over the sample period. To fully capture the time series dynamics of the volatility smile, different measures of volatility smile dynamics are employed, namely, (i) the slope coefficient of the call and put volatility curves, (ii) a measure of curvature, and (iii) the degree of skewness in the daily volatility smile. The Granger-causality tests show that the lagged coefficients for the recursive GARCH estimates are statistically different from zero over the optimal lag choice. This evidence of a unidirectional relationship is particularly strong when the tests are performed using put volatility curves. The results also reveal significant feedback between the curvature of the volatility smile and the quoted volatility. Further, tests are performed using a trivariate vector autoregressive model and impulse response functions to trace the impact of a volatility shock. A robustness test using probit regression suggests evidence of predictability of jumps using the smile curvature and out-of-money options. Consistent with recent literature, this study suggests that the behaviour of the volatility smile is driven by trading activities induced by the anticipated risk in the foreign exchange market.

The final analysis chapter extends earlier empirical work on volatility forecasting using information subsumed in the volatility smile dynamics. Specifically, it combines volatility smile dynamics with corresponding at-the-money implied volatility and GARCH(1,1) volatility estimates to forecast realised exchange rate volatility. The relative information content of the forecasting models is analysed using encompassing regression tests. The coefficients for smile curvature are both significant and negatively related to the level of implied volatility. The validity of the unbiasedness and efficiency hypothesis for the implied volatility forecasts is found to be related to the shape of the volatility smile. In particular, when the smile effect is more pronounced, the forecast performance of the implied volatility series deteriorates.

TABLE OF CONTENTS

DEDICATION I
DECLARATION II
ACKNOWLEDGEMENTS III
LIST OF FIGURES V
LIST OF TABLES V

CHAPTER 1 – INTRODUCTION **1**

1.1 OBJECTIVE OF THE DISSERTATION 1
1.2 MOTIVATION OF THE DISSERTATION 2
1.3 THE IMPORTANCE OF AN EMPIRICAL EXAMINATION OF OPTION-IMPLIED VOLATILITY 3
1.4 SCOPE AND STRUCTURE OF THIS DISSERTATION 4

CHAPTER 2 - AN OVERVIEW OF THE OVER-THE-COUNTER CURRENCY OPTION MARKET **9**

2.1 INTRODUCTION 9
2.2 SIZE AND STRUCTURE OF THE OVER-THE-COUNTER FOREIGN EXCHANGE DERIVATIVE MARKET 11
2.3 GROWTH OF OVER-THE-COUNTER AND EXCHANGE TRADED CURRENCY OPTIONS 14
2.4. VOLATILITY TRADING IN THE OVER-THE-COUNTER CURRENCY OPTION MARKET 16
2.4.1 At-the-money Forward Straddles *18*
2.4.2 Strangle Trades *19*
2.4.2 Risk Reversal Trades *21*
2.5 DATA FROM THE OVER-THE-COUNTER CURRENCY OPTION MARKET 22
2.5.1 The BBA-Reuters Implied Volatility Data *23*
2.5.2 The UBS Implied Volatility Data *26*
2.6 A COMPARISON OF CONTRACT FEATURES 27
2.7 CONCLUSION 29

CHAPTER 3 - LITERATURE REVIEW **30**

3.1 INTRODUCTION 30
3.2 IMPLIED VOLATILITY ESTIMATION 35
3.2.1 Implied Volatility Estimation Error *38*
3.3 THE QUALITY OF OVER-THE-COUNTER CURRENCY OPTION-IMPLIED VOLATILITY 40
3.4 TIME SERIES BEHAVIOUR OF IMPLIED VOLATILITY 42
3.4.1 Random Walks and Implied Volatility *43*
3.4.2 Term Structure of Implied Volatility *50*
3.5 MONEYNESS EFFECT OF IMPLIED VOLATILITY 52
3.5.1 Lognormal Distribution and Volatility Smile *53*
3.5.2 Option Trading and Volatility Smile *55*
3.5.3 Other Explanations for the Volatility Smile Anomaly *58*
3.6 CONCLUSION 60

CHAPTER 4 - FOREIGN EXCHANGE IMPLIED VOLATILITY AND THE RANDOM WALK HYPOTHESIS **61**

4.1 INTRODUCTION 61
4.1.1 Implied Volatility Estimation *65*
4.1.2 Random Walk and Foreign Exchange Volatility *66*
4.2 RANDOM WALKS AND VARIANCE RATIO TESTS 66
4.3 DATA AND METHODOLOGY 68
4.3.1 Quoting Convention for Implied Volatility Data *70*

4.3.2 Descriptive Statistics ... *72*
4.3.3 The Conventional Variance Ratio Test ... *78*
4.3.4 The Nonparametric Variance Ratio Test ... *80*
4.4 EMPIRICAL RESULTS FOR THE CONVENTIONAL VARIANCE RATIO TEST ... 82
4.5 EMPIRICAL RESULTS FOR THE NONPARAMETRIC VARIANCE RATIO TEST ... 87
4.6 MEAN REVERSION ... 91
4.7 MODEL COMPARISON TESTS ... 94
4.7.1 The Random Walk Model ... *96*
4.7.2 The ARIMA(p,1,q) Model ... *97*
4.7.3 Artificial Neural Networks Model ... *98*
4.8 THE FORECAST PERFORMANCE TEST ... 99
4.8.1 Forecast Results ... *101*
4.8.2 Diebold- Mariano (1995) Forecast Accuracy Test ... *106*
4.9 CONCLUSION ... 109

CHAPTER 5 – VOLATILITY TRADING USING SIMPLE TRADING RULES ... 111

5.1 INTRODUCTION ... 111
5.2 APPLICATION OF TECHNICAL TRADING RULES ... 112
5.3 VOLATILITY TRADING IN THE OVER-THE-COUNTER CURRENCY OPTION MARKET ... 115
5.3.1 Straddle Trades ... *115*
5.3.2 Risk Reversal Trades ... *116*
5.4 DATA ... 117
5.4.1 Descriptive Statistics ... *119*
5.5 METHODOLOGY ... 124
5.5.1 Options Premia Estimations ... *129*
5.5.2 Estimation of Holding-period Return ... *133*
5.5.3 Examples of Holding-period Return Calculations ... *136*
5.5.4 The Naïve Strategy and the Simple Moving Average Strategy ... *138*
5.6 EMPIRICAL RESULTS ... 142
5.6.1 Buy and Sell At-the-money Forward Straddle ... *144*
5.6.2 Risk Reversal Trades ... *148*
5.6.3 Straddle Aggregate Result by Trigger Values ... *151*
5.6.4 Risk Reversal Aggregate Result by Trigger Values ... *153*
5.7 CONCLUSION ... 154

CHAPTER 6 – THE DYNAMICS OF VOLATILITY SMILE AND FOREIGN EXCHANGE RISK ... 156

6.1 INTRODUCTION ... 156
6.2 VOLATILITY SMILE ANOMALY ... 157
6.2.1 Currency Option Trading and Volatility Smiles ... *160*
6.2.2 Data ... *161*
6.2.3 Implied Volatility vs Deltas ... *164*
6.2.4 Descriptive Statistics ... *166*
6.3 THE VOLATILITY SMILE ... 170
6.3.1 Smile Asymmetry ... *172*
6.3.2 Slope Coefficients for Call and Put Volatility Curves ... *172*
6.3.3 Measure of Skewness for Volatility Smile ... *173*
6.4 QUADRATIC APPROXIMATION OF VOLATILITY SMILE ... 174
6.4.1 Measure of Curvature for Volatility Smile ... *175*
6.5 DYNAMICS OF CURVATURE AND SLOPES COEFFICIENTS OVER TIME ... 176
6.5.1 Summary Statistics for Smile Dynamics ... *180*
6.6 ESTIMATION OF ONE-MONTH CONDITIONAL VOLATILITY ... 181
6.6.1 Recursive GARCH(1,1) of Kroner et al (1995) ... *182*

6.7 VOLATILITY SMILES DYNAMICS AND FUTURE EXCHANGE RATE VOLATILITY 183
6.8 EMPIRICAL RESULTS 186
6.8.1 Bilateral Granger-causality Test along Volatility Smile *188*
6.8.2 Granger-causality Test at Individual Delta Levels *191*
6.8.3 Trivariate vector autoregressive model *195*
6.8.4 Residuals Autocorrelation and Results for VAR(3) model *196*
6.8.5 Impulse Response Analysis *198*
6.9 JUMPS AND THE SMILE DYNAMICS 205
6.9.1 Probit Model Analysis *209*
6.9.2 Results for Probit Model Analysis *210*
6.10 CONCLUSION 214

CHAPTER 7 – FOREIGN EXCHANGE VOLATILITY PREDICTION: INTEGRATING VOLATILITY SMILE WITH IMPLIED VOLATILITY **215**

7.1 INTRODUCTION 215
7.2 SHAPES OF VOLATILITY SMILES AND VOLATILITY OF THE UNDERLYING ASSETS 216
7.3 PREVIOUS STUDIES ON VOLATILITY FORECASTING 217
7.4 DATA 218
7.5 METHODOLOGY 219
7.5.1 The Relationship between Implied Volatility and the Shape of Volatility Smile *220*
7.5.2 Estimation of Realised Volatility *221*
7.5.3 Estimation of Conditional Volatility *222*
7.5.4 The Relationship between Realised Volatility and the Shape of Volatility Smile *223*
7.5.5 Forecasting Realised Volatility using Smile-adjusted Implied Volatility *224*
7.5.6 Forecasting Realised Volatility Using, Smile Characteristics, Implied Volatility and Rolling-GARCH (1,1) Model *225*
7.6 DESCRIPTIVE STATISTICS 226
7.7 STATIONARITY TESTS 228
7.8 AT-THE-MONEY IMPLIED VOLATILITY AND THE SHAPE OF VOLATILITY SMILE 229
7.9 UNIVARIATE REGRESSION TEST RESULTS 238
7.9.1 Regressing RV on SM *238*
7.9.2 Regressing RV on IV *240*
7.10 MULTIPLE REGRESSION TEST RESULTS 241
7.10.1 Regressing RV on IV and SM *242*
7.10.2 Regressing RV on IV, SM and GV *247*
7.11 CONCLUSION 254

CHAPTER 8 – CONCLUSIONS AND FUTURE RESEARCH **256**

8.1 INTRODUCTION 256
8.2 CONTRIBUTIONS OF THE DISSERTATION 257
8.3 FURTHER EXTENSIONS TO THE DISSERTATION 259
8.4 CONCLUSION 261

APPENDIX A – CONDITIONAL AND IMPLIED VOLATILITY **262**

APPENDIX B – ADDITIONAL PROBIT MODEL ANALYSIS **263**

BIBLIOGRAPHY **265**

"Traders now use the formula [the Black and Scholes (1973) option pricing formula] *and its variants extensively. They use it so much that market prices are usually close to formula values even in situations where there should be a large difference."*

- Fisher Black (1989a), *The Journal of Portfolio Management*, 15(2), pp.7 and pp.8. (bracket added by the author of this dissertation)

"The language and conventions that traders in the over-the-counter currency option markets use are borrowed from the Black-Scholes model, even though traders are fully aware that the model is at best an approximation."

- Allan Malz, 1997, *The Journal of Derivatives*, 5(2), pp.19.

CHAPTER 1 – INTRODUCTION

1.1 Objective of the Dissertation

This dissertation provides four empirical analyses that are centred upon one subject matter – the implied volatility characteristics of currency options. The analyses are performed using trader-quoted implied volatility according to standard market convention. In essence, the volatility of an asset over the remaining life of an option contract is unobservable and thus it is often assumed to follow a random walk process. Whether the volatility parameter can be adequately described as a random walk process for all option maturities remains an empirical question. A better understanding of implied volatility characteristics is critical to the pricing of currency option contracts and offers insights into the implied volatility "smile" anomaly reported in the currency option market.

Each analysis in this dissertation offers empirical examination of dealer-quoted implied volatility data for options on four major currency pairs: the British pound against the U.S dollar (GBP/USD), the euro against the U.S. dollar (ERU/USD), the Australian dollar against the U.S. dollar (AUD/USD) and the U.S. dollar against the Japanese yen (USD/JPY). The empirical analyses are original studies and they employ a unique and rich option dataset from the over-the-counter market, consisting of options with various maturities and moneyness.

The key objective of this dissertation is to extend existing empirical literature on the characteristics of currency option-implied volatility. This is achieved through the consideration of how implied volatility data at various maturities may vary over time, investigating the use of simple trading rules for volatility trading, examining the dynamics of the volatility smile, and finally testing the usefulness of information embedded in the volatility smile for the prediction of realised volatility.

1.2 Motivation of the Dissertation

There are three main reasons for undertaking empirical analyses on currency option contracts using data from the over-the-counter market. The first reason relates to the size of the over-the-counter currency option. Most currency option contracts are traded in the over-the-counter market. A recent survey by the Bank for International Settlements indicates that the notional amount of the over-the-counter currency option contracts grew from USD 9,597 billion in December 2006 to USD 12,748 billion in December 2007 globally [2]. In sharp contrast, exchange traded currency options amounted to USD 78.6 billion in December 2006 and rose to USD 132.7 billion in December 2007. This survey suggests that the over-the-counter currency option is about 96 times larger than the exchange traded equivalent. The sheer size of the over-the-counter market indicates that it plays a central role in the provision of currency option contracts to various market players. It is also potentially a more reliable source for information extraction due to its liquidity.

[2] See Table 20A, BIS Quarterly Review, March 2009.

Second, a clear understanding of implied volatility behaviour facilitates price discovery for currency options and thus enhances dissemination of market information to different participants in the over-the-counter option markets, including central banks, hedger, speculators and arbitragers. This is crucial as market transparency is lacking due to the highly customised nature of option contracts traded in this market. Further, recent over-the-counter derivative losses sustained by banks imply that more careful scrutiny of price behaviour in these markets would provide useful information to risk management professionals and policy makers for supervisory purposes.

Third, empirical research into the price dynamics of over-the-counter currency options is still relatively sparse. The current literature that employs information from over-the-counter currency option markets focuses mainly on the forecasting ability of implied volatility data in two aspects: the information content of implied volatility and the estimation of risk-neutral density functions for exchange rates. In contrast, this research is mainly concerned with the dynamics of implied volatility and how the implied volatility smile relates to anticipated volatility in the exchange rate market.

1.3 The Importance of an Empirical Examination of Option-implied Volatility

An empirical study of currency option-implied volatility is important for a number of reasons:

a) It allows a better understanding of implied volatility characteristics for different option maturities. In practice, implied volatility varies across maturities and this contradicts the constant volatility assumption of the Garman-Kohlhagen (1983) currency option pricing model. However, little is known about whether or not a

common time series process can be used to describe implied volatility across all maturities.

b) Empirical evaluation of implied volatility behaviour has both theoretical and practical implications for risk forecasting, hedging decisions and the construction of volatility trading strategies. Since implied volatility provides an *ex-ante* view of an asset's volatility over the remaining life of the option, it can potentially forecast future volatility more accurately than volatility forecasts based on historical data.

c) It offers a better understanding of volatility smile dynamics in terms of how the smile is related to the anticipated risk in the currency market. This assessment can help to explain option pricing biases that are reported in empirical studies.

d) The analysis fills a gap in the volatility forecasting literature by investigating how the forecasting performance of at-the-money implied volatility is related to the shape of the volatility smile. Such analysis reveals relationships that exist between different proxies of volatility smile dynamics and how these proxies may improve the accuracy of the implied volatility forecasts.

1.4 Scope and Structure of this Dissertation

This dissertation is structured in the following manner. Chapter 2 provides an overview of the over-the-counter currency option market. All of the analyses presented in this dissertation are concerned with currency options that are traded in the over-the-counter market. The chapter documents the unique features of over-the-counter currency options, including the contract details, volatility trading strategies, market structure and implied volatility data available from this market. It also compares

contract features between the over-the-counter option and the exchange-traded equivalent.

Chapter 3 provides a broad review of the main published research papers concerning theoretical and empirical characteristics of implied volatility, with emphasis on currency options. It presents two main areas of literature concerning implied volatility – first, the time series behaviour of implied volatility, and second, the moneyness characteristics of implied volatility. The literature that constitutes the basis of the empirical chapters (that is Chapter 4 through to Chapter 7) is briefly revisited in each relevant chapter.

The empirical analyses are presented in Chapter 4 through to Chapter 7. Chapter 4 is concerned with the behaviour of quoted implied volatility at various maturities. Specifically, the chapter extends the literature dealing with implied volatility in several aspects. First, by testing the random walk hypothesis across implied volatility of different maturities, the implied volatility characteristics across the term structure can be better understood. The results using in-sample tests provide evidence of random walk violations in the volatility series across all currency pairs. Notably, rejections of a random walk are particularly strong for the short-dated options maturing in one week and one month. Contrary to Garman-Kohlhagen (1983) and Hull-White (1987), the empirical evidence reported in this chapter suggests that option-implied volatility are not constant over time and they do not always vary strictly according to a random walk process. Second, the results from this study suggest that option pricing and volatility models that assume a random walk component across the entire volatility term structure are not consistent with empirical findings. Third, out-of-sample tests involving

forecasting implied volatility changes from a random walk model produce significantly higher forecasting errors compared with two alternative models using artificial neural networks (ANNs) and autoregressive integrated moving average (ARIMA) frameworks. These findings confirm the in-sample test results and suggest that short-dated implied volatility are better characterised as a mean-reverting process while the random walk process may better capture time series variation in long-dated implied volatility. The results are broadly consistent with the recent innovations in option pricing methodology of Sabanis (2003) who assumes volatility follows a mean-reverting process, at least for maturities of one week and one month.

Chapter 5 extends the key findings of Chapter 4 by examining the profitability of volatility trading using simple technical trading strategies. This is largely motivated by the evidence of random walk violations in the volatility process documented in Chapter 4. The trading rules assume that when the prevailing volatility price departs considerably from its moving average price, a buy or sell trade will emerge. Two main contributions stem from Chapter 5. First, this chapter documents profitability of option combination trades including straddles and risk reversals which have received little attention in the literature. Second, consistent with Brock, Lakonishok and LeBaron (1992) the results presented in this chapter indicate that volatility trading using moving average trading rules can result in profitable trades even after adjusting for transaction costs. In particular, the buy straddle trades generate positive holding-period returns for three of the four currency pairs tested. The evidence is particularly strong for the USD/JPY straddles. Conversely, risk reversal trades produced less compelling outcomes with lower winning trades and holding-period returns. Even so, positive holding-period returns still exist for these trades.

The dynamics of the volatility smile anomaly are examined in Chapter 6. Little empirical research exists with respect to how the volatility smile evolves over time. This chapter examines the relationship between different proxies for volatility smile dynamics and the anticipated volatility for the GBP/USD, EUR/USD, AUD/USD and USD/JPY currency pairs. The volatility smile is constructed daily using a unique trader-quoted implied volatility dataset. This chapter provides two important findings with regard to the dynamics of the volatility smile. First, the results indicate that the dynamics of the volatility smile are related to variation in risk of the underlying currency. Second, the analysis also reveals significant feedback between the curvature of the volatility smile and the anticipated volatility of the underlying currencies. Consistent with recent literature (for example, Ederington and Guan (2002) and Bollen and Whaley (2004)), the results show that the behaviour of the volatility smile is related to trading activities induced by anticipated changes in foreign exchange risk.

The analysis presented in Chapter 7 extends the empirical work on volatility forecasting of Christensen and Prabhala (1998) and Covrig and Low (2003) using information subsumed in the volatility smile dynamics. This is the first empirical research to investigate how the shape of the volatility smile may affect the forecasting ability of implied volatility forecasts. The rationale for incorporating the volatility smile dynamics is based on the results from Chapter 6 which indicate that the smile dynamics are related to the future volatility of the underlying currency. Two important contributions to the existing literature on volatility forecasting are offered in this chapter. First, the curvature and slope coefficients of the volatility smile are strongly correlated with at-the-money implied volatility. In particular, these coefficients are both significant and negatively related to the level of implied volatility. This finding is

consistent with the results of Pena, Rubio, and Serna (1999). Furthermore the chapter also finds significant relationship between the shape of the volatility smile and the realised volatility. Second, the validity of the unbiasedness and efficiency hypothesis is found to be related to the shape of the volatility smile. When the smile effect is more pronounced, the predictive ability of the implied volatility deteriorates. Chapter 8 concludes with the key findings of this dissertation and future research directions are also offered.

CHAPTER 2 - AN OVERVIEW OF THE OVER-THE-COUNTER CURRENCY OPTION MARKET

2.1 Introduction

This chapter provides an overview of the over-the-counter foreign exchange derivative market with emphasis on aspects of the currency option market that are relevant to this dissertation. First it traces the growth of the market. This is followed by a discussion of the standard market conventions for currency option trading and a review of the two data sources used in this dissertation. The chapter concludes by presenting some unique features of over-the-counter currency option contract, when compared with the exchange-traded counterparts.

Derivative contracts are traded in privately negotiated over-the-counter market or on organised exchanges. The origin of the over-the-counter call option on olive presses can be traced back to the dawn of civilisation at around 350 B.C. according to the Greek philosopher Aristotle[3]. Today, derivative instruments play a very crucial role in financial markets all around the world. They are used by various market participants, including portfolio managers, hedgers and even central bankers for protection against adverse movements in the underlying assets. Speculators are also involved in this market, often taking the other side of the contract in the hope of making gains. This, in turn, provides liquidity to the derivatives markets.

[3] A brief discussion of this event is provided in Whaley (2003).

During his Nobel Prize lecture on 9th December 1997, Myron Scholes argued that the over-the-counter derivative industry will continue to grow and evolve in sophistication. He also highlighted that academic research into this market will become increasingly important over time due to the dynamic nature of the industry[4]. Indeed the size of the over-the-counter derivative market has grown tremendously - the total notional amount of this market grew by approximately seven times since 1998 to USD 591.96 trillion[5] in December 2008. In comparison, the world gross domestic product stood at USD 60.12 trillion[6] over the same period. The size of the over-the-counter derivative market is also several times larger than the global outstanding value of stocks and bonds which is estimated to be around USD 115.6 trillion[7].

Currency option contracts were first introduced in the organised exchange market through the Philadelphia Stock Exchange (PHLX). Option contracts on the British pound were first introduced in December 1982, followed by the Canadian dollar, German mark, Japanese yen and Swiss franc in early 1983[8] (Smithson, 1998). In response to the introduction of currency option trading on the PHLX, commercial banks offered their clients customised currency options in the over-the-counter market.

The over-the-counter currency option market has become very prominent in size since the mid-1980. In 1984, the British Bankers' Association established a working group to draw up the terms and conditions of the British London Interbank Currency Option Market (Hicks, 2000). This documentation received universal

[4]The lecture was subsequently published. See Scholes, Myron, S.(1998) *The American Economic Review*, 88(3).
[5]See Table 19 on pp.103 of the Statistical Annex, BIS Quarter Review, June 2009.
[6] World Bank Development Indicators database, World Bank, 1 July 2009
[7] International Financial Services, London (IFSL), extracted from the June and July 2009 Equity Markets and Bond Markets Reports. Bonds and stocks had notional values of USD 83 trillion and USD 32.6 trillion respectively in 2008.
[8] Options on the Australian dollar became available in 1987.

acceptance in the following years[9]. By 1987, trading in this market became very efficient through 'volatility trading' and delta-hedging[10]. Its rapid growth is largely attributable to the highly customised nature of the contracts where the strike price and the transaction size can be negotiated between a customer and the bank.

2.2 Size and Structure of The Over-the-counter Foreign Exchange Derivative Market

Due to the decentralised nature of the over-the-counter market, collection of market information is an extremely onerous task. Since 1998, however the Bank for International Settlements (BIS) has been actively involved in the collection of global financial markets statistics through regular surveys[11]. Amongst other statistics, the survey provides detailed information on over-the-counter, as well as exchange traded, derivatives relating to the size and structure of these markets.

Figure 2-1 displays the aggregate notional amount of the over-the-counter foreign exchange derivatives classified according to instrument types. The notional amount as estimated by the Bank for International Settlements in December 2008 was USD 49.8 trillion. This represents the total outstanding contractual payment in the derivatives markets on the reporting date and gives an indication of the equivalent positions in the underlying spot exchange rates markets.

[9] The London Interbank Currency Option Market (LICOM) Terms and Conditions was subsequently renamed the International Currency Options Market (ICOM) Terms and Conditions due to its world-wide appeal.
[10] *Ibid, p.3*
[11] This survey was introduced by the central banks of the G10 countries in 1998 to track the size and structure of the global financial markets.

Figure 2-1: Over-the-counter Foreign Exchange Derivatives by Instruments

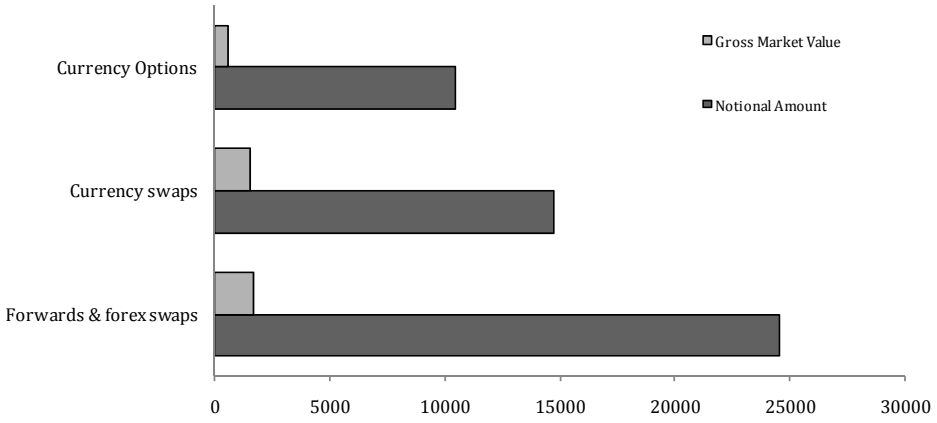

Source: Table 19 of BIS Quarterly Review, June 2009. The notional amount and market value are reported in billions of U.S. dollars.

The total gross market value for the same foreign exchange derivatives is much less. The global foreign exchange derivatives market is estimated to have a total gross market value of USD 3.9 trillion which is approximately 8 percent of the total notional amount of the over-the-counter foreign exchange derivatives. This represents the liquidation value of these contracts and is a measure of market risk exposure in these derivatives instruments[12].

Forward and foreign exchange swap contracts are the most common form of foreign exchange derivatives. This is followed by currency swaps and currency options. For currency option contracts, the global notional amount was USD 10.5 trillion in December 2008. This represents about 21 percent of the total notional amount for foreign exchange derivatives and reflects a very large and liquid market.

[12] The gross market value approach provides more useful information from a risk management perspective.

Figure 2-2: OTC Currency Derivatives by Instrument and Maturity

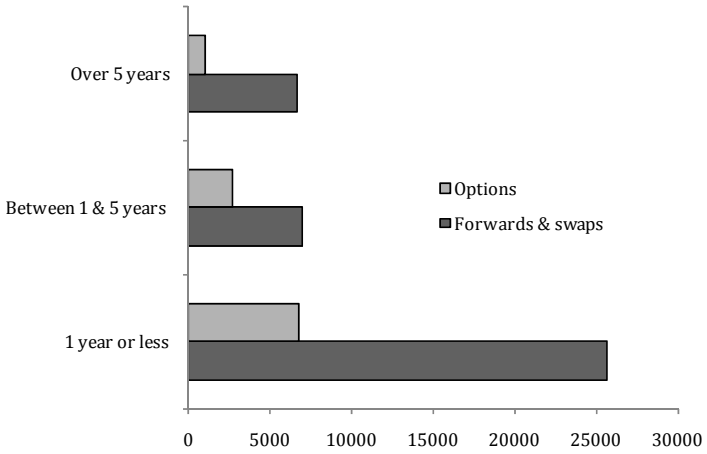

Source: Table 20C of BIS Quarterly Review June 2009. The notional amount is reported in billions of U.S. dollars.

Figure 2-2 shows the foreign exchange derivatives by maturity buckets. The use of short-dated contracts with maturities of one year or less is most common across all derivative types. This suggests that short-dated contracts are more liquid than the long-dated contracts. In comparison, short-dated currency options are much smaller in notional amount than forwards and swaps. However, relative to the short-dated maturities, currency options with maturities of one to five years occupy a larger proportion of the maturity bucket, which is about 40% of forwards and swaps. Overall, the one to twelve month options have the greatest market liquidity while it is also possible to negotiate a contract with maturity of five years and above.

The global positions of over-the-counter foreign exchange derivatives by currency type are provided in Figure 2-3. The data includes both currency sides of every foreign exchange transaction. Not surprisingly, the U.S dollar has the highest notional amount, followed by the euro, Japanese yen and pound sterling. These currencies contribute about 80 percent of the global notional amount. This pattern is consistent with the popularity of the underlying currencies in which most of the global foreign

exchange transactions are denominated. The notional amount for the Australian dollar is slightly below the Canadian dollar which had a notional amount of USD 127.5 billion in December 2008.

Figure 2-3: OTC Currency Derivatives by Currency Type

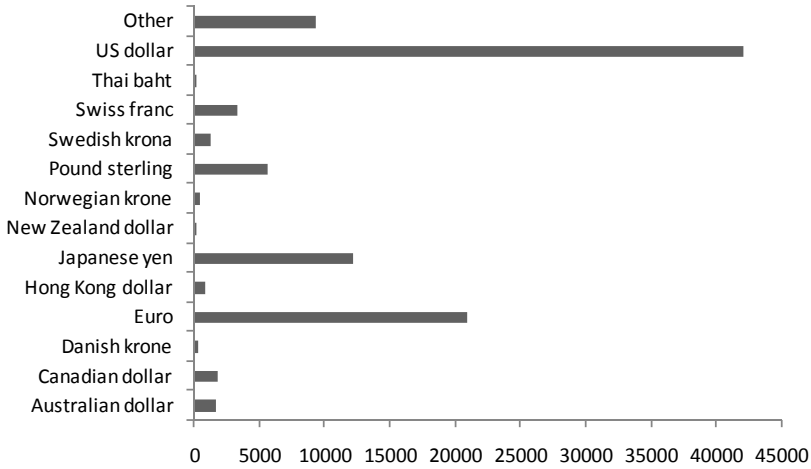

Source: Table 20B of BIS Quarterly Review June 2009. The notional amount is reported in billions of U.S. dollars.

2.3 Growth of Over-the-counter and Exchange Traded Currency Options

Figure 2-4 traces the size of the over-the-counter and exchange traded currency option contracts in notional amounts. A similar upward growth pattern can be noted in both markets although, on average, the size of the over-the-counter currency option market is about one hundred times larger than the exchange traded currency option market. This suggests that a large majority of currency option trading activities take place in the over-the-counter currency option market rather than on organised exchanges. In terms of the global derivative market share, the over-the-counter derivative market has also grown steadily from 85.2% in December 1998 to 91.10% in

December 2008[13]. Taken together, the limited growth in the exchange-traded currency option markets reflects intense competition between the two market types. The growth pattern for the exchange-traded currency option market is in line with the over-the-counter currency option. Such patterns are consistent with the results of Cincibuch (2004) who finds that intensive arbitrage activity occurs between currency options traded on organised exchanges and those traded in the over-the-counter market.

Figure 2-4: Growth of OTC and Exchange-traded Currency Options

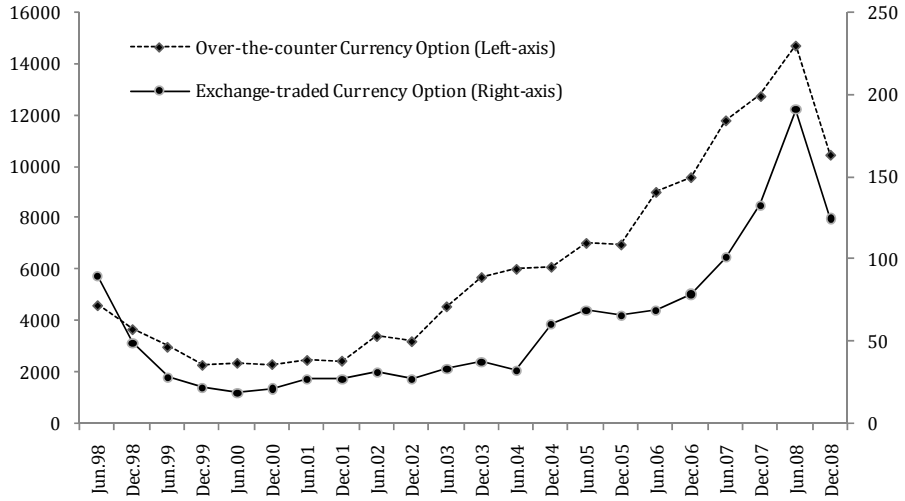

Source: Table 19 and Table 23A of BIS Quarterly Review, June 2009.
The notional amount is reported in billions of U.S. dollars.

[13] These figures are estimated from Tables 19 and 23A of the BIS Quarterly Review, 2009. See page 103 and 108 of the survey.

2.4. Volatility Trading in the Over-the-counter Currency Option Market

Currency option traders quote option prices in terms of implied volatility instead of dollar premium[14]. This is also known as "quoted implied volatility" which is sometimes referred to by traders[15]in the interbank currency option market. For instance, on a given trading day, a trader may provide a volatility quote for the one-month EUR/USD at-the-money forward call option by stating "one-month at-the-money forward dollar call are 11 at 11.5", meaning the trader is prepared to buy the call at the implied volatility of 11 percent per annum and sells it at a higher implied volatility of 11.5 percent per annum. Quoting implied volatility facilitate the comparison of relative option values across different contract specifications.

Once a deal is struck between the bank and the customer, the quoted implied volatility is then entered into the Garman-Kohlhagen (1983) currency option pricing model with the other contract details (eg agreed strike price) so that the dollar premium can be calculated. The application of this standard market convention is in contrast with the implied volatility literature since the option's implied volatility is known before the option dollar premium is calculated. Specifically, in the implied volatility literature, the model price of an option contract is set equal to the observed market price so that the implied volatility parameter can be determined using the Garman-Kohlhagen (1983) model[16]. In practice, the use of the term "quoted" implied volatility does not alter the original concept of implied volatility - it represents the market assessment of the

[14] This gives rise to the term "volatility trading" in the over-the-counter currency option market.

[15] These are mostly market makers who provide their customers with bid and ask quotes at which they are willing to buy or sell options.

[16] Mayhew (1995) provides a detailed discussion on implied volatility estimations.

underlying spot exchange rate volatility over the remaining maturity[17] of the option contract.

Another distinct feature of the implied volatility quoting convention used by traders in the over-the-counter currency option market relates to the moneyness of an option contract. Instead of providing the strike price and spot exchange rate that correspond to each maturity, traders provide implied volatility quotes for a given option delta. The delta of an option is defined as the rate of change of the option value with respect to the change in the spot exchange rate. The delta for a call equals $N(d_1)$ in the Garman-Kohlhagen (1983) currency option pricing model[18] while the delta of a put is defined as $N(d_1)$ minus one (Hull, 2006). Therefore for a given strike price and maturity, if a call option has a delta of 0.7, the delta for a put will be -0.3[19].

Traders in the over-the-counter currency option market express delta in percentage terms instead of decimal form. The negative signs for put option deltas are also omitted in practice. For example a "35 delta put" for a one-month EUR/USD may have an implied volatility of 10 percent per annum. This means the put option has a delta value of -0.35 for the dollar premium calculation using the Garman-Kohlhagen (1983) pricing model. The measure of moneyness in the form of delta is related to the

[17] This is sometimes referred to as "tenor".
[18] This model is described in Section 5.5.1 of Chapter 5. For European put options, $-1 \leq \delta \leq 0.0$.
[19] This relationship can be shown mathematically using the put-call parity. Under the put-call parity, $C = P + S - \frac{X}{(1+r)^T}$, where X= strike price, r = risk-free interest rate and T is time to maturity. By treating the present value of the strike price as a constant, differentiating the put-call parity with respect to S gives $\frac{\partial C}{\partial S} = \frac{\partial P}{\partial S} + 1$.

risk management of traders' open positions against price risks, which need to be delta-hedged when an option is purchased or sold in the over-the-counter market[20].

2.4.1 At-the-money Forward Straddles

Although customisation is available in the over-the-counter currency option market, there is also a wide variety of currency options traded in combinations[21]. The most common trade is known as a "straddle" which involves a combination of an "at-the-money forward" call and an "at-the-money forward" put with the same maturity. These European calls and puts share the same strike price which is equal to the prevailing forward exchange rate. In terms of moneyness, the at-the-money forward has a delta value of 0.50. As the call and put move away from the common strike price with a delta value of 0.5 (or X / F ≈ 1.0), they become more in or out-of -the-money.

Figure 2-5: AUD/USD At-the-money Forward Straddle

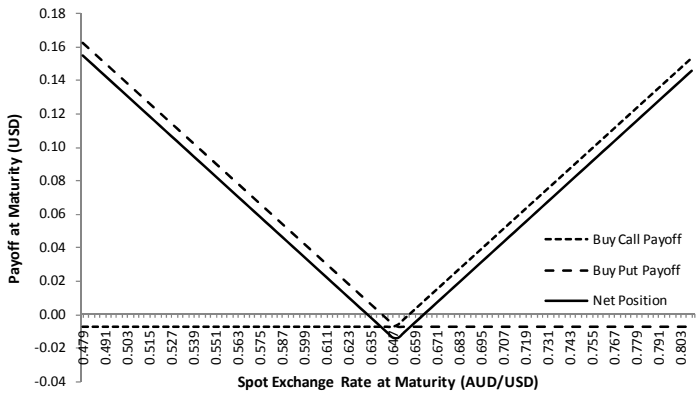

Payoff diagram of AUD/USD at-the-money straddle at maturity: Spot exchange rate = AUD/USD 0.6463 (5 September 2003), 1-month AUD BBA-LIBOR = 4.8025% p.a., 1-Month USD BBA-LIBOR = 1.12% p.a., at-the-money implied volatility = 10.34% p.a.

[20] Traders provide the bid and ask quotes upon demand but do not know which position would be taken by their customers until the contracts have been finalised.

[21] The popularity of combination trades in the over-the-counter may be attributable to the highly liquid market where even out-of-the money options are actively traded. For instance, trading of 25-delta calls and 25-delta puts is very common.

The payoff diagram of the AUD/USD straddle at maturity has a v-shaped pattern as illustrated in Figure 2-5. The long call and put positions have the same strike price of AUD/USD 0.64855 (which corresponds with the delta value of 0.5[22]). On 5 September 2003, the spot exchange rate was AUD/USD 0.6463 and the respective BBA-LIBOR interest rates for the Australian and the U.S dollar were 4.80 percent per annum and 1.12 percent per year. The observed implied volatility for the 50-delta option on the same day was recorded as 10.34 percent per annum. Using these parameters, the estimated premium for the put and call was approximately USD 0.0076 per Australian dollar[23]. Thus the estimated break-even points for the call and put are approximately at the exchange rates of AUD/USD 0.6562 and AUD/USD 0.6409[24] respectively. Outside these break-even points, the straddle will generate profitable outcomes. The difference between these break-even prices is USD 0.0152. This difference also reflects the total premium incurred for the long call and long put positions.

2.4.2 Strangle Trades

The payoff diagram for the "strangle" is displayed in Figure 2-6. Similar to the straddle, this combination is comprised of two long positions – one long position in a European call and one long position in a European put option. However, the call and put do not share a common strike price. In this case, the 25-delta call and the 25-delta put[25]

[22] This is also referred to as "50-delta" according to market convention.

[23] The premium is estimated using the Garman-Kohlhagen (1983) currency option pricing model. The total premium due depends on the notional amount of the contract. If the call option allows the holder to purchase 100 million Australian dollars one month from the inception of the contract, then the total premium due is 2x0.0076x 100,000,000 = USD 1.511 million. All things being equal, an implied volatility of 14% p.a. would increase the total premium to USD 2.056 million.

[24] For call options, at break-even point, $S_{BE} - X - P = 0$. Therefore, S_{BE} = AUD/USD 0.64855 + AUD/USD 0.0076 ≈ AUD/USD 0.6562. For puts the break-even point is estimated as X-P = AUD/USD 0.64855 - AUD/USD 0.0076≈ AUD/USD 0.6409.

[25] This is also equivalent to a 75-delta call which is in-the-money. See the discussion in the previous section. Estimation of the strike price is explained in Chapter 5 of this dissertation.

are used to construct the strangle trade. The payoff diagram resembles a u-shaped pattern in contrast with the straddle trade. These options have strike prices of AUD/USD 0.6623 and AUD/USD 0.6333 with moneyness values, S/X of 0.9765 and 1.0168 respectively.

Figure 2-6: AUD/USD Strangle

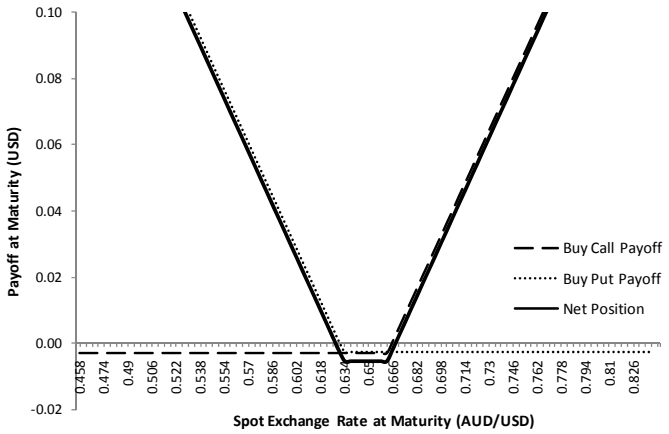

Payoff diagram of AUD/USD 25-delta strangle at maturity: Spot exchange rate = AUD/USD 0.6463 (5 September 2003), 1-month AUD BBA-LIBOR = 4.8025% p.a., 1-Month USD BBA-LIBOR = 1.12% p.a., 25-delta call implied volatility = 10.783% p.a., 25-delta put implied volatility =10.393% p.a.

The total premium incurred is USD 0.0054 per Australian dollar which is relatively cheaper than the straddle trade. This is not surprising as a larger movement is needed in the underlying spot exchange rate before the options start to move in-the-money. The gap between the break-even points is USD 0.0344 which is about two times larger than the straddle trade. The holder of the strangle will lose both premiums if the underlying spot exchange rate closes within the break-even strike prices at the expiration of the option contracts. In practice, traders are often involved in the buying or selling out-of-money options and the strangle combination is quoted as a spread between the at-the-money forward implied volatility and the 25-delta put or call implied volatility. Thus if the difference between these quoted implied volatility departs from zero, the degree of curvature for the volatility smile can be measured (Malz, 1997).

2.4.2 Risk Reversal Trades

The risk reversal combination is constructed by a simultaneous purchase and sale of out-of-money options of equal moneyness. This is considered to be an aggressive directional trade (DeRosa, 2000). For instance, a risk reversal trade can be created by taking a long position in a 25-delta call and a short position in a 25-delta put. Alternatively, the combination can also be constructed by taking a short position in the call and a long position in the put option.

The payoff from a risk reversal combination (long call and short put) is shown in Figure 2-7 for the one-month AUD/USD trade. In this case, the trader receives a premium from the put and the put moves in-the-money when the spot exchange rate is above the break-even price of AUD/USD 0.6309[26] while the long call position will move in-the-money above the break-even price of AUD/USD 0.6653 at maturity. Between the two break-even points, the net cost of the combination is close to zero[27].

[26] This is estimated as $-(X-S_{BE}-P) = 0$, S_{BE} = AUD/USD 0.6309.
[27] The estimated premium incurred for the call option is 0.0030 per Australian dollar and 0.0024 per Australian dollar is received from short put position. The net position over this range is therefore -0.0030 + 0.0024 = loss of USD 0.0006.

Figure 2-7: 25-delta Risk Reversal

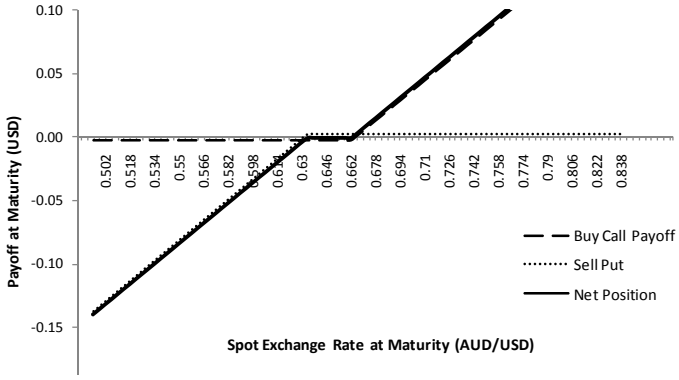

Payoff diagram of AUD/USD 25-delta risk reversal at maturity: Spot exchange rate = AUD/USD 0.6463 (5 September 2003), 1-month AUD BBA-LIBOR = 4.8025% p.a., 1-Month USD BBA-LIBOR = 1.12% p.a., 25-delta call implied volatility = 10.783% p.a., 25-delta put implied volatility =10.393% p.a.

Market traders provide risk reversal quotes in terms of net volatility spread between the implied volatility for the put and call options of the same moneyness. For instance a one-month 25-delta call may have an implied volatility of 10 percent per annum while a put with of the same delta value and maturity may be priced at 11.2 percent per annum. Thus the one-month risk reversal on the AUD/USD is quoted as 1.2 percent per year. Since the put option is bid over the call option, the Australian dollar is expected to depreciate against the U.S. dollar over the maturity of the option contracts.

2.5 Data from the Over-the-counter Currency Option Market

This section provides a brief examination of implied volatility data obtained from two sources[28]: the British-Bankers' Association-Reuters (BBA-Reuters) in London and UBS Investment Bank in Switzerland[29]. The BBA-Reuters data is used in Chapters Four and Five while Chapter Six and Seven use data from UBS. The implied volatility

[28] Statistical examinations of the implied volatility data are provided in Chapters 4, 5, 6 and 7.

[29] The author thanks John Ewan of BBA and Perio Musio of UBS.

quotes for four selected major currencies, namely, the GBP/USD, the EUR/USD, the AUD/USD and the USD/JPY currency pairs of various maturities and moneyness are obtained from these sources.

2.5.1 The BBA-Reuters Implied Volatility Data

The British-Bankers' Association-Reuters implied volatility data comprises of the average daily implied volatility[30] of twelve contributors in the London interbank market[31]. These contributors are major market makers in the London over-the-counter currency option market. The data consists of at-the-money forward implied volatility of European options for six different maturities: one-week, one-month, three-month, six-month, one-year and two-year. Strangles and risk reversals are available in three different maturities of one-month, three-month and one-year[32]. These series are available for thirteen different currency pairs.

The implied volatility data are supplied daily by the contributors between 3:30 pm and 3:50 pm London time. The average of each series is calculated and this forms the benchmark for the currency option implied volatility in the over-the-counter market. The establishment of the BBA-Reuters dataset promotes market transparency and allows independent valuation of currency option contracts consistent with the

[30] The average bid and ask implied volatility are supplied by the contributors.
[31] While banks customise option deals for their customers, an active interbank market also exists where traders are linked with several currency option brokers.
[32] Amongst others, the contributing banks include BNP Paribus, Barclays Capital, UBS AG, HSBC and Citibank. These are major market makers in the over-the-counter currency option market.

requirements of the International Accounting Standards (IAS) 39 on fair value of financial instruments[33].

The option-implied volatility data is also useful for the estimation of foreign exchange rates probability distribution and the volatility smile. McCauley and Melick (1996) and Malz (1997) showed how the at-the-money forward implied volatility, the strangle and the risk reversal data can be used jointly to recover market traders' probability distribution. These volatility data can also be used to estimate the volatility smile for currency options. An estimated volatility smile, using a second order Taylor's approximation method, is displayed in Figure 2-8[34]. More importantly, for the purpose of this dissertation, the at-the-money forward implied volatility of different maturities can be used to examine the behaviour of implied volatility across the term structure.

Figure 2-8: AUD/USD One-Month Implied Volatility on 1 October 2003

$$\hat{\sigma}_{\delta}(\delta) = ATM_t - 2RR_t(\delta - 0.5) + 16STR_t(\delta - 0.5)^2$$

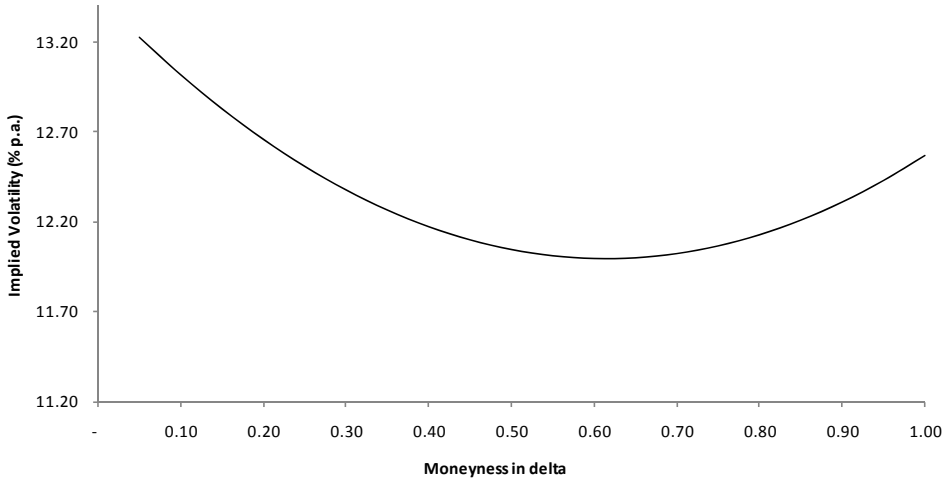

Data Source: BBA-Reuters, London. Used with permission. "ATM" represents at-the-money forward implied volatility, "RR" is the risk reversal quote, "STR" is the strangle quote and "δ" denotes the delta value.

[33] The IAS 39 Fair Value and Hedging provision became operational in the European Union countries in 2005. The equivalent accounting standard in the United States is FAS 133.
[34] A detailed discussion is provided in Malz (1997).

Figure 2-9 displays the time series of the at-the-money implied volatility series for the one-month, three-month, six-month and two-year maturities[35] for the EUR/USD currency pair. Evidently, the volatility for the EUR/USD currency pair are not constant over time and exhibit differences across maturities.

The variation in the implied volatility levels is greater for the short-dated series than for the long-dated series. For instance, one-month implied volatility varied between 6.87 percent per annum and 12.75 percent per annum while the two-year series fluctuates from 8.76 percent per annum to a peak of 12.48 percent per annum. The pattern of the implied volatility contradicts the theoretical assumptions of the Garman-Kohlhagen (1983) currency option pricing model but is consistent with the studies on term structure of implied volatility by Xu and Taylor (1994) and Campa and Chang (1995) that use currency option data.

Figure 2-9: EUR/USD Implied Volatility Term Structure

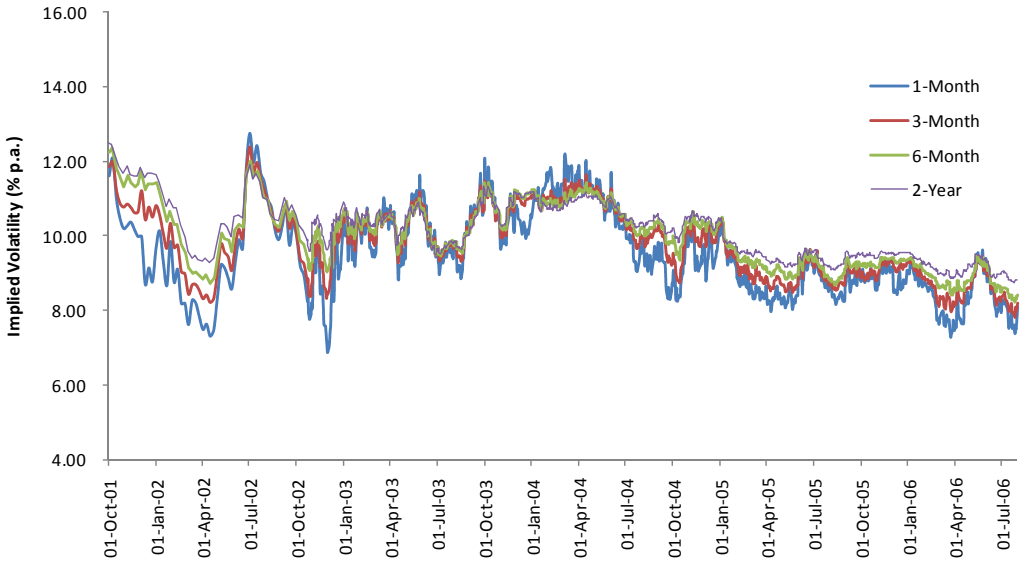

Data Source: BBA-Reuters, London. Used with permission.

[35] For brevity, the one-week and one-year implied volatility are not shown in Figure 2-9.

2.5.2 The UBS Implied Volatility Data

The daily data from UBS Investment Bank consists of one-month implied volatility quotes[36] for different values of delta. These are daily implied volatility quotes for European call and put options collected at 6:00 p.m. New York trading time. This is a more refined dataset and is useful for investigating the behaviour of the volatility smile in the over-the-counter currency option market. For any given day of the sample period, a cross-section of nineteen data points can be observed for each currency pair. These are implied volatility that correspond with delta values of 5-delta, 10-delta, 15-delta, 20-delta, 25-delta, 30-delta, 35-delta, 40-delta, 45-delta for put options; and 5-delta, 10-delta, 15-delta, 20-delta, 25-delta, 30-delta, 35-delta, 40-delta, 45-delta for call options. The 50-delta implied volatility are also available.

Figure 2-10 provides the volatility smile constructed using implied volatility for call and put options that correspond with different values of delta. In contrast with the volatility smile constructed using the BBA-Reuters dataset in Figure 2-8, the volatility smile constructed using the UBS implied volatility data avoids the use of interpolation and thus provides a richer cross-sectional representation of volatility smile on any given day of the sample period. The u-shaped pattern is very pronounced and is consistent with the analysis of implied volatility smiles found in Taylor and Xu (1994). The quadratic approximation for the volatility smile seems to fit the currency option market data quite well. Again, the existence of a u-shaped pattern across

[36] These are averages of bid and ask quotes.

moneyness lends support for the violation of the constant volatility assumption implicit in the Garman-Kohlhagen (1983) currency option pricing model.

Figure 2-10: AUD/USD One-month Implied Volatility on 1 October 2003

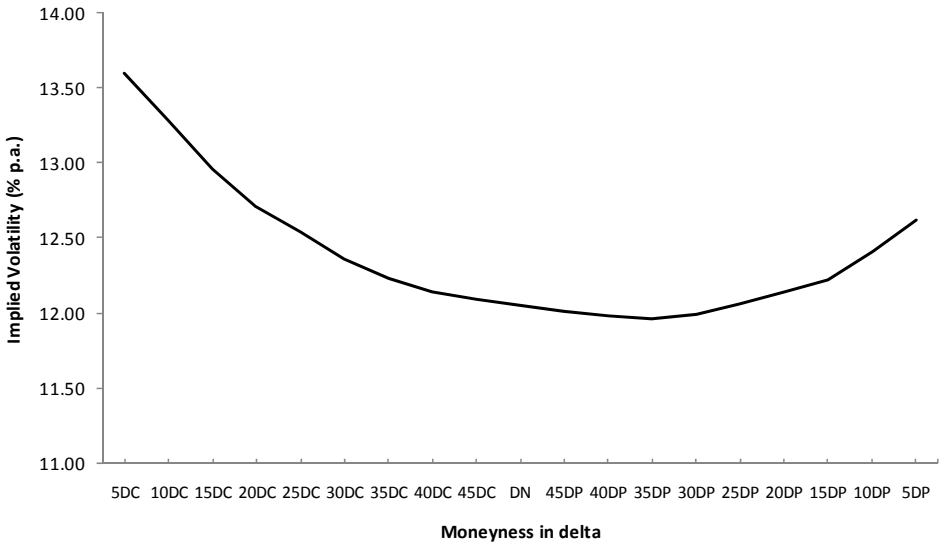

Data Source: UBS Investment Bank, Switzerland. Used with permission.

2.6 A Comparison of Contract Features

There are several differences between options traded in the over-the-counter markets and the exchange-traded equivalents. The main differences between the over-the-counter and exchange-traded currency options are summarised in Table 2-1. In essence, the over-the-counter markets are attractive because they offer tailor-made option contracts to their customer. The highly flexible nature of these contracts allows banks to offer option contracts in numerous currencies with any strike price or maturity to their customers. Furthermore odd lots are available from this market in contrast with the highly standardised contracts offered on the exchange traded currency option

market. This means that market participants are able to hedge a specific amount of foreign exchange risk over any horizon or any strike price. On the other hand, the privately negotiated deal between the bank and the customer in the over-the-counter market suggests that there is a lack of price transparency – it is difficult for the customer to know for certain if the premium charged by the bank equals a fair market value. In contrast, the option premium for contracts traded in centralised exchanges is publicly available.

Table 2-1: A Comparison of Over-the-counter Currency Options and Exchange-traded Currency Options

Attribute	Over-the-counter Option	Exchange-traded Options
Access to Contract	Through a bank	Traded on PHLX, CME and FINEX through a broker
Strike Price	Negotiated between a bank and the customer	Limited strike prices
Underlying Spot	Any currency pair that has a spot and forward market	Limited to currency pairs listed on exchanges
Regulation	Not regulated by a single regulatory body but governed by codes of conduct[37]	Regulated by the exchanges and clearinghouses
Transaction Size	Negotiable	Standardised
Option Type	European	American
Credit Risk	Customer at risk of bank defaulting	No default risk, clearinghouse becomes counterparty
Trading Method	Use of telephone, 24-hour market	Open outcry, restricted trading hours
Brokerage	None on bank	Mandatory

Source: Adapted from Sutton (1990) and Hicks (2000).

[37] The International Swaps and Derivative Association provides standard legal documents for most of the over-the-counter contracts. Further, indirect supervision is also in place through bank capital adequacy requirements for off-balance sheet activities under "Pillar 1" of the Basel II Accord.

2.7 Conclusion

This chapter provides a brief overview of the over-the-counter currency option market. The over-the-counter currency option market has grown significantly in size and is substantially larger than its exchange-based competitors. Such explosive growth provides an important justification for conducting empirical research into this market. Further, implied volatility data obtained from this market is available for empirical analysis of currency options traded on the over-the-counter market. Such empirical investigation creates a better understanding of implied volatility and option valuation as well as the various trading activities that take place in these markets.

CHAPTER 3 - LITERATURE REVIEW

3.1 Introduction

Empirical studies on volatility of asset price returns are crucial to many aspects of the financial markets. It is not surprising that this is a subject of interest amongst the investment and academic communities as evidenced by the extensive body of literature devoted to the study of volatility modelling and forecasting. From a practical standpoint, if market volatility is expected to increase, portfolio managers may purchase more insurance or rebalance their portfolio positions in order to reduce their exposure to particular classes of asset. Furthermore, since investors have different risk preferences, predictable volatility suggests that a more appropriate and effective asset allocation strategy can be designed to achieve investor risk-return trade-off requirements.

In the practice of risk management, the volatility parameter serves as an important proxy for financial asset risk which is frequently estimated for a single security or a portfolio of assets over a given period of time. The measurement of such risk first requires the estimation of asset price volatility. The estimated volatility is then used as an input parameter for probability models, such as the benchmark Value-at-Risk[38] (VaR) measure or other simulation-based procedures that provide risk estimates for an expected maximum loss at a given confidence level over a target time horizon[39].

[38] An extensive review of this methodology is provided by Jorion (2000).

[39] Under the Basel Accord, the VaR estimate is calculated with 99 percent confidence interval over a 10-business day period. Under "Pillar 1" of the Basel II Accord banks are required to set up an internal model to forecast their financial risk exposure.

These procedures have become industry-standard for internal and external risk reporting and are now reported by financial institutions all around the world.

An accurate representation of market volatility is also important for the pricing of derivative instruments whose trading volumes have grown sharply since the 1980s. Black and Scholes (1973) developed the well-known option pricing formula that depends on five input parameters, namely, the spot price of the underlying asset, the strike price, the risk free rate of interest, the time to maturity, and the volatility of asset price returns. All of these parameters are directly observable, with the exception of the volatility, which must be estimated. Thus, the usefulness of the Black-Scholes model and its variants rests upon the forecast quality of the volatility parameter. Indeed, it is shown in Hull (2006) that the price of an option is a monotonically increasing function of volatility. This is true for both call and put options.

In an early paper by Black and Scholes (1972), it was shown that a better estimate of the volatility parameter can lead to more accurate pricing of option contracts using their formula[40]. Consistent with this view, Rendleman and O'Brien (1990) analysed the effect of volatility mis-estimation on a synthetic portfolio insurance[41] program and show that understatement of the volatility parameter is associated with an under-insured portfolio while overestimation of the underlying asset's volatility results in the portfolio manager purchasing more insurance than is needed.

[40] See pp.408-409 of Black and Scholes (1972).

[41] This involves keeping the portfolio's delta position to be very close to the delta position of the desired put option. See Smithson (1998).

The literature on volatility modelling and estimation can be broadly classified into two strands: an historical-based approach and an option-based approach. Under the former, volatility is estimated from historical price returns while the latter infers volatility from traded option prices. The development of the historical-based approach is largely attributed to the early work of Engle (1982)[42] with estimation of the conditional asset return volatility using an autoregressive conditional heteroskedasticity (ARCH) model. A multitude of variants and extensions to the ARCH model have been developed since the groundbreaking work of Robert Engle, including *inter alia* the work of Bollerslev (1986) on the generalised autoregressive conditional heteroskedasticity (GARCH) model, the integrated GARCH(IGARCH) model of Engle and Bollerslev (1986), the exponential GARCH (EGARCH) model of Nelson (1991), the threshold ARCH(TARCH) model of Zakoian (1994) and the quadratic ARCH (QARCH) model of Sentana (1995) and the fractional integrated exponential GARCH(FIEGARCH) of Bollerslev and Mikkelsen (1996). These models have generally assumed that the volatility parameter is time-varying. In other words, the variances of the error terms are not equal - the error terms may be larger in some periods and smaller in others. The methodology rests upon the notion that asset price returns observed in the recent past might provide information about the conditional variance for the current period. Parameter estimation for these models usually involves the implementation of least squares or maximum likelihood (Engle, 1982), where with sufficiently, large return time series[43], estimated parameters[44] converge to their true values.

[42] The ARCH model was initially used to model inflation rates. Bollerslev (2001) noted that improvement in computing power and the availability of high quality data have allowed wide applications of these models in the field of finance.

[43] For instance, Jorion (1995) uses approximately 1500 observations of daily spot exchange rate data to estimate the GARCH parameters.

[44] For instance, the implementation of the popular GARCH (1,1) model requires estimates of the average variance rate (ω), the coefficient of the lagged conditional variance (α) and the correlation coefficient of the lagged conditional variance (β).

The option-based approach to volatility estimation was first formalised by Henry Latane and Richard Rendleman when they published an empirical study on volatility estimation titled 'Standard Deviations of Stock Price Ratios Implied in Option Prices' in 1976[45]. The paper shows that volatility implied in call option prices are significantly correlated with the actual volatility of the underlying stocks over the corresponding periods. The volatility parameter imputed from an option price using their estimation procedure is known as the 'implied volatility' or the 'implied standard deviation' of the option[46]. In essence, the implied volatility of an option contract represents a trader's view of the market sentiment over the remaining life of the option contract. Thus its forward-looking nature can be viewed as an *ex-ante* approach to volatility estimation.

The procedure for volatility estimation using option price is distinctly different from the historical approach. Specifically, the estimation of volatility does not require a long history of asset price returns or complex econometric procedures. This is a relatively straight-forward approach that uses observed option prices and the corresponding input parameters from an option contract, including the prevailing risk-free interest rate, the option time to expiration, the price of the underlying asset and the stipulated strike price. Given the observed option price and the input parameters, one can recover the corresponding value of the volatility parameter using the Black-Scholes (1973) formula and some iterative search algorithm.

Recent empirical studies suggest that implied volatility of traded option contracts are superior to the historical-based estimates for the prediction of future

[45] See Latane and Rendleman (1976).
[46] The term *implied volatility* is used interchangeably with *implied standard deviation*.

volatility. For example, studies by Jorion (1995) and Covrig and Low (2003) both show that option-implied volatility subsume all information contained in time series models in the currency market. Similar results are also reported in the stock market by Jiang and Tian (2005) using model-free implied volatility estimates. Thus, implied volatility can be used to monitor market behaviour over a given time period. Indeed, central banks such as the Bank of England, provide regular updates of market sentiment using an option-implied probability density functions, estimated from implied volatility,[47] that correspond with various strike prices and different time intervals.

This chapter aims to survey the main literature pertaining to option-implied volatility with particular emphasis on currency options. It highlights two key areas of the literature – the time series and the moneyness characteristics of implied volatility. Since the volatility parameter that is required to price an option contract cannot be directly observed, a number of estimation procedures have been suggested in the literature. The theoretical basis and development of these procedures are briefly presented in Section 3.2. Measurement errors due to non-synchronous trading and market frictions have led to a number of authors employing quoted implied volatility data from the over-the-counter currency option market. These issues are discussed in Section 3.3. Studies on modelling the time series behaviour of implied volatility are discussed in Section 3.4 while the moneyness characteristic of implied volatility known as the 'volatility smile effect' is discussed in Section 3.5. Several explanations for the existence of such anomalies are also presented. The conclusion of this chapter is offered in Section 3.6.

[47] See Clews, Panigirtzoglou and Proudman (2000) for the methodology adopted by the Bank of England for the estimation of the probability density function.

3.2 Implied Volatility Estimation

In their study on the option pricing framework, Black and Scholes (1973) assumed that the volatility of the underlying stock remained constant over the maturity of the option contract. The volatility parameter was estimated using historical stock price returns calculated as the annualised standard deviation of the continuous compounded returns[48]. It was shown that the model systematically overvalued stocks with high variance while low variance stocks are largely undervalued. They also demonstrated that when the same test was repeated using actual variance of price returns over the maturity of the option contracts, the model provide estimates of option prices more accurately.

As an alternative to historical volatility estimation, the market price of an option contract can be set to equal the theoretical option price to determine the volatility of the underlying asset. This relationship is expressed in Equation 3-1, where $C_{T,i}^{Mkt}$ is the observed call option market price with strike price X_i at time t with maturity T. The corresponding spot price, model price, risk-free rate of interest and volatility are denoted as S_t, C_{Mod}, r and $\sigma_{T,i}$ respectively:

$$C_{T,i}^{Mkt} = C_{Mod}(S_t, X_i, T, r, \sigma_{T,i}) \tag{3-1}$$

[48] Stock price returns are estimated by taking the natural logarithm of price relative, $(p_t / p_t\text{-}1)$ where p represents stock price at time t. The empirical results of the Black-Scholes (1973) option pricing framework were published separately in Black and Scholes (1972).

Using this method, a unique implied volatility $\sigma_{T,i}$ that corresponds with each cross-section[49] option market price i can be found. As no closed-form solution is available, the volatility parameter $\sigma_{T,i}$ is often estimated using numerical procedures such the Newton-Raphson algorithm.[50] Manaster and Koehler (1982) provide the necessary conditions to arrive at a positive implied volatility using this procedure.

Under the strict assumption of the Black-Scholes (1973) model, options written on the same underling asset with various strike prices and maturities should have identical implied volatility. Often this assumption is violated in empirical studies[51]. Consequently, a number of researchers have developed various weighting schemes to estimate implied volatility. Latane and Rendleman (1976)[52] estimate the implied standard deviations for various options written on a particular stock and the weighted average of the implied standard deviations is then used as an estimator of the future volatility over the maturity of the option. Their results show that while the weighted implied standard deviation for a particular stock is not constant and produce biased results, the estimated volatility correlates strongly with the actual volatility over the sample period. This technique has been criticised for the use of improper weights since the individual weights do not sum to one. In a similar vein, Chiras and Manaster

[49] This refers to options on the same underlying asset with different levels of moneyness.

[50] This is essentially a simple iteration technique for solving one-dimensional nonlinear equations.

[51] The empirical evidence for this anomaly is known as the "volatility smile" which is discussed in Section 3.5 of this chapter.

[52] $WISD_{it} = \left[\sum_{j=1}^{N} ISD_{ijt}^2 d_{ijt}^2\right]^{0.5} \left[\sum_{j=1}^{N} d_{ijt}\right]^{-1}$, where WISD is the weighted average implied standard deviation for company i in period t, and d_{ijt} is the partial derivation of the price of option j of company i in period t with respect to its implied standard deviation using the Black-Scholes (1973) model. The weights are also known as the "vega" of the option.

(1978)[53] propose that the implied standard deviation should be weighted by the price of an option with respect to its implied standard deviation. They argue that investors are concerned with the size of their investments and thus price elasticity of options with respect to their implied standard deviations should be considered in the weighting scheme. Beckers (1981) [54] propose a relatively straight-forward implied standard deviation estimation technique that allocates more weight to at-the-money options. The implied standard is then estimated by minimising the difference between the market and model option prices. Instead of weighting schemes, Whaley (1982) employs a nonlinear cross-sectional regression model to estimate the implied volatility that minimises the difference between the observed and the model price. This technique is found to be superior to its predecessors.

A special case of implied volatility estimation using a closed-form solution is provided by Brenner and Subrahmanyam (1988)[55]. Consistent with Beckers (1981), this technique makes use of at-the-money European options to provide an accurate estimate of implied volatility. More recently, Corrado and Miller (1996) extend the Brenner-Subrahmanyam formula to estimate implied volatility over a wide range of moneyness. The study shows that the improved formula generates accurate estimates of implied

---

[53] $WISD = \sum_{j=1}^{N} ISD_j \frac{\partial W_j}{\partial \upsilon_j} \frac{\upsilon_j}{W_j} \left[\sum_{j=1}^{N} \frac{\partial W_j}{\partial \upsilon_j} \frac{\upsilon_j}{W_j} \right]^{-1}$, where N is the number of options recorded on a particular stock for the observation date ISD_j is the implied standard deviation of option j for the stock, $\frac{\partial W_j \upsilon_j}{\partial \upsilon_j W_j}$ is the price elasticity of option j with respect to its implied standard deviation (υ).

[54] $f(ISD) = \sum_{i=1}^{I} w_i [C_i - BS_i(ISD)]^2 \left[\sum_{i=1}^{I} w_i \right]^{-1}$, where C_i is the market price of an option, BS_i is the Black-Scholes option price as a function of implied standard deviation, i is the total number of options on a given stock with the same maturity, and w_i denotes the weight for the i th option.

[55] $ISD_T \approx \sqrt{\frac{2\Pi}{T}} \frac{e^{rT}}{F} MV_T$,where ISD_T is the estimated implied standard deviation with T-period(s) to maturity (as a fraction of a year) , r is the risk free rate of interest, F is the forward rate and MV_T is the market price of the option contract with maturity T period(s) from now. Under the put-call parity condition, this approximation can be directly applied to both at-the-money call and put options.

volatility and the approximations are less sensitive to various levels of moneyness compared with the original Brenner-Subrahmanyam formula.

3.2.1 Implied Volatility Estimation Error

Irrespective of the techniques discussed in the preceding section, implied volatility estimates based on the methodology defined by Equation 3-1 implicitly assume that data from listed options on exchanges can be precisely observed and are accurately matched with their corresponding parameters. This concept holds in the frictionless world of Black and Scholes (1973). In reality, these techniques suffer from estimation error caused by measurement biases and various forms of market frictions. Specifically, Stoll and Whaley (1993) note that weighting with an option's vega effectively places more weight on near-the-money options which are more sensitive to volatility. On the other hand, illiquid out-of-the-money options receive more emphasis when the elasticity of the option price is used in implied volatility estimations. Furthermore, the pooling and averaging of implied volatility is inconsistent with the smile anomaly and term structures of implied volatility reported by Bollen and Rasiel (2003) and Xu and Taylor (1994) in currency option markets. Hull and White (1987) also note that estimates of implied volatility from options listed on exchanges are contaminated by option pricing errors.

Hentschel (2003) posits that the application of weighted average schemes assumes that implied volatility measurement error is attributed to the sensitivity of implied volatility to option price error and ignores other possible sources of error. He argues that, since prices in the cash and option markets are observed imprecisely, small errors in the input parameters can amplify implied volatility measurement error. While

options' strike prices and maturities can be observed with certainty, the values for the option market price, the underlying spot price, risk-free rate of interest and volatility are all subject to market structure constraints such as minimum tick sizes and bid-ask spreads. The study shows that the ideal Black-Scholes (1973) option price is a monotonic function of moneyness. The option bid-ask spread is however, characterised as a step function of moneyness. Using variance decomposition analysis, Hentschel (2003) finds that for the majority of options, measurement errors from option and spot prices account for most of the total error variance.

Another source of friction that gives rise to implied volatility measurement error is attributable to non-synchronous trades between the option market and the cash market. In other words, the option and the underlying asset price quotations are often available at different times of the day. Bookstaber (1981) developed a probability model that can be used to evaluate the extent of option mispricing due to non-synchronous trading. The results indicate that the problem of non-synchronous trades is more severe when the volatility of the underlying asset is higher. Conversely, the probability of non-synchronous trades decreases when option trading volumes are higher.

The lack of liquidity in the option market is another important source of bias. A study of Israel stock market by Brenner, Eldor and Hauser (2001) reveals that lack of liquidity has important pricing implications for currency options. In particular, they show that the average illiquidity discount value, defined as the ratio of option price for non-traded options divided by the price for options traded on the exchange, has an average value of 0.21 in the total sample. This finding suggests that illiquid currency options auctioned by the Bank of Israel are priced, on average, 21 percent lower than

those traded on the Tel-Aviv Stock Exchange. These results are robust across three different subperiods.

3.3 The Quality of Over-the-counter Currency Option-implied Volatility

Most empirical studies on implied volatility employ data from exchange-listed option contracts. As articulated in the preceding section, the use of option data from this market can produce measurement errors arising from various forms of market frictions. In order to obtain better estimates of implied volatility, a number of researchers have proposed the use of implied volatility data obtained from the over-the-counter currency option market. These studies include Dunis and Keller (1995), Campa and Chang (1995), Malz (1997), Campa, Chang and Reider (1998), Bollen and Rasiel (2003), Covrig and Low (2003), and more recently Carr and Wu (2007).

In comparison with exchange-traded option contracts, the use of option data from the over-the-counter currency option market has several advantages. First, over-the-counter currency option markets are generally more liquid than organised exchanges. This is largely attributable to the highly customised nature of these contracts, which is advantageous to market participants. For instance, specific strike price and notional value of an option contract can be negotiated between a writing bank and its customer. Other benefits to the users of over-the-counter options are discussed in Chapter 2[56].

[56] See Table 2-1 of this thesis for a comparison of key differences between currency options traded in the over-the-counter market and an organised exchange.

Second, option prices are quoted in terms of implied volatility by traders in the over-the-counter currency option market, in sharp contrast with option quotes available in dollar premium through organised exchanges. In other words, these options are quoted in the form of implied volatility and thus the application of the back-solving procedure using the methodology presented in Equation 3-1 is not required. This mitigates implied volatility measurement errors arising from the matching of option parameters and non-synchronous trades for the researcher.

Third, currency option contracts traded in the over-the-counter currency market are available as European style options and pay no dividend. This is in contrast with stock options traded on stock exchanges which are mostly American style. The early exercise feature embedded in these contracts is another potential source of bias for implied volatility estimates since additional assumptions are needed with respect to the timing of dividends and the behaviour of stock prices on ex-dividend date[57]. Consistent with this view, Whaley (1982) suggests that the option valuation model would become more complex, with high additional computational costs when multiple dividends are paid before the expiration of an option contract.

Fourth, options traded on exchanges mature on fixed dates and therefore the prices observed successively relate to options with lower time-to-maturity. In contrast, volatility quotes from the over-the-counter currency option markets are available with fixed maturities. For instance, the BBA-Reuters at-the-money implied volatility[58] are available in maturities of one-week, one-month, three-month, six-month, one-year and two-year. On any given period *t*, the one-week option will expire exactly in one week

[57] It is usually assumed that stock prices will fall by the amount of the dividend on the ex-dividend date (Hull, 2006).
[58] Further details of the BBA-Reuter data are provided in Chapter 2 of this thesis.

from period *t*. Thus, time series of implied volatility for fixed maturity can be constructed. The use of implied volatility data with constant maturity also avoids the complexities arising from varying time-to-expiration[59].

3.4 Time Series Behaviour of Implied Volatility

In the previous sections it has been established that research into improving the accuracy of volatility estimates has received some attention in the literature. Considerable research effort has been dedicated to the accuracy of volatility estimates using historical data. On the other hand, researchers have employed a more forward-looking approach to the use of option prices in recovering volatility estimates. These studies are motivated by the observation that asset price volatility tends to vary over time and such variation is not entirely predictable. Consistent with this widely held view, the study by Geske and Roll (1984) advocates that empirical biases reported for the Black-Scholes (1973) model are related to the volatility parameter. They conjecture that the "variance bias" is attributable to the nonstationary behaviour of volatility over time and hence an option pricing model with changing volatility would alleviate such a bias. Black (1989b) concurs with this view and suggests that since asset price volatility is not constant in reality, the dynamics of asset price volatility should be incorporated into the option pricing formula in order to improve its pricing performance.

Garman-Kohlhagen (1983) modified the Black-Scholes (1973) formula to include interest rates for both the domestic and the foreign currency. This is achieved by replacing the price of the underlying asset with the spot foreign exchange rate which is

[59] Since the option price decreases as maturity approaches, the corresponding implied volatility is also expected to fall over time.

then discounted by the foreign interest rate. As with the assumption used in the frictionless world of Black and Scholes (1973), the Garman-Kohlhagen (1983) currency option pricing model takes on the assumption that the volatility of the underlying exchange rate remains constant throughout the remaining life of the option. Such a strong assumption is often violated in empirical studies evidenced by the time-varying behaviour of volatility and pricing biases resulting from model misspecification. The following section reviews key empirical studies that employ random volatility in the pricing of currency options. Studies on term structures of implied volatility for currency option are also discussed.

3.4.1 Random Walks and Implied Volatility

Since the implied volatility of the underlying asset represents uncertainty over the remaining life of the option contract, it cannot be directly observed. The elusive nature of volatility suggests that the variation of asset price returns can be generalised as a random walk process. Accordingly, a more realistic approach is to relax the constant volatility assumption in order to account for the time series dynamics of the volatility parameters. Specifically, currency option-pricing models that assume a random walk in the volatility process have been examined by several authors including Chesney and Scott (1989), Heston (1993), Xu and Taylor (1994), Melino and Turnbull (1995), and Gessner and Poncet (1997). These studies are largely motivated by the stochastic volatility option pricing framework of Hull and White (1987) which is based on empirical observations that indicate random characteristics of asset price volatility (Fouque, Pananicolaou and Sircar, 2000).

Hull and White (1987) introduced the stochastic volatility option pricing to price European call options on stocks. In this model the volatility of the underlying asset is time-variant and is governed by a random process:

$$ds = ØSdt + \sigma S\, dw \tag{3-2}$$

$$dV = \mu V dt + \xi V\, dz \tag{3-3}$$

where dz and dw are the Weiner process and ξ is the volatility of the volatility. The variable V is the underlying asset's variance rate which is assumed to revert to a mean value at a known rate. They point out that although there are an infinite number of paths that give the same mean variance when the variance term is stochastic, all paths produce the same terminal distribution of the asset price. Accordingly, under this model, it is shown that when volatility is random and uncorrelated to the underlying price, an option's price is the Black-Scholes (1973) integrated price that corresponds with the distribution of the mean variance over the remaining maturity of the option[60]. They argue that although the variance is treated as a random process, the asset price distribution at the expiration of the option remains lognormal.

Hull and White (1987) also show that when volatility is stochastic, the Black-Scholes (1973) model tends to overprice at-the-money options and underprice deep-in-the-money and deep-out-of-the-money options. This observation is consistent with the smile pattern observed in the currency option market (Campa, Chang and Reider 1998). Hull and White (1987) report such a pattern is sensitive to the size of the ξ coefficient that measures the volatility of the volatility parameter. Further, the mispricing becomes more severe when the coefficient becomes larger. In addition, they note that an estimate

[60] The Monte Carlo simulation procedure can be used to examine pricing biases when asset price and volatility are correlated.

of the volatility change coefficient is by no means a straightforward procedure. It can be approximated from changes in implied volatility using option prices traded on organised exchanges, such as the Philadelphia Stock Exchange (PHLX). However such estimates are contaminated by pricing errors in line with Hentschel (2003).

Similar to Hull and While (1987), Scott (1987) also considers an option pricing model that allows the variance rate to vary randomly over the maturity of the option contract. Consistent with the findings of Hull and White (1987), the random variance[61] model has the lowest sum of squared errors compared with the two other Black-Scholes (1973) models specified with daily revised variance rate and constant variance rate respectively. The pricing error reported for the constant variance Black-Scholes (1973) model is nearly two times larger than the error reported for the random variance model. However, the pricing error for random variance is only about 8.8 percent lower[62] than the Black-Scholes (1973) model that uses daily variance estimates. This suggests that the random variance model performed only marginally better than the daily revised variance Black-Scholes (1973) model. The study also identifies some evidence of random changes in stock returns with a mean-reverting tendency.

Chesney and Scott (1989) investigated the performance of the random variance model for European calls and puts on the Swiss franc. They advocate that the violation of the lognormal assumption in foreign exchange rates is attributed to the random behaviour of the variance rate. Building upon the stochastic volatility framework of Hull and White (1987) and Scott (1987), they suggest that the volatility process of the

[61] Although the term "Random Variance" is used in Scott (1987) and Chesney and Scott (1989), the models are based on the same premise of Hull and White (1987) that allows the underlying asset price volatility to vary randomly over time.
[62] See Table 3 on pp.435 of Scott (1987).

underlying exchange rate can be set up in a manner that allows the log of the volatility parameter to follow a mean-reverting process. The parameter estimation involves running the following model:

$$\ln\sigma_t = \alpha + \rho\ln\sigma_{t-1} + \varepsilon_t \qquad (3\text{-}4)$$

The regression model provides estimates of α, ρ and σ_ε using daily exchange rates data from November 1979 to December 1983. These estimates are then used to simulate values of volatility for the random variance option pricing model. Similar to Scott (1987), they calculate the mean squared error and mean absolute deviation from both the random variance model and the Garman-Kohlhagen (1983) model. The estimated option prices are compared with call and put option values traded in Geneva for the year 1984. The random variance model uses two different volatility specifications for the underlying exchange rates: first, using the mean-reverting procedure described in Equation (3-4) and second, by setting $\alpha = 0$ and $\rho = 1$ that permits the volatility process to evolve as a random walk process.

Chesney and Scott (1989) show that the Garman-Kohlhagen (1983) model performed poorly when the volatility parameter is either constant or when it is estimated using the historical method, with high mean squared errors of 24.725 and 21.384 respectively. On the other hand, the random variance model, with a mean-reverting volatility parameter, dominates the random walk volatility model, with mean squared errors of 0.125. This is more than ten times lower than the random variance model with a random walk volatility specification. Notably, the Garman-Kohlhagen model with daily revised implied volatility has the lowest mean squared error amongst the five

models[63], which is about one and a half times lower than the random variance model with mean-reverting volatility process. In contrast with previous studies, this result raises doubts about the random behaviour of volatility since an option pricing model that uses daily revised variance estimates can outperform models that employ mean-reverting and random walk specifications.

Furthermore, for the Garman-Kohlhagen (1983) model, Chesney and Scott (1989) observe that strike price bias alone explains model pricing error. In contrast, two additional biases (time-to-maturity and volatility biases) are found to be significant explanatory variables for pricing bias under the random variance model. Finally, these results also suggest that the random variance model has a tendency to overvalue long-dated options and undervalue short-dated options.

In contrast with a number of previous studies that employ Monte Carlo simulation procedures, Heston (1993) developed a stochastic volatility model with a closed-form solution for European currency options when the underlying spot price is correlated with volatility. The model assumes that the mean-reverting volatility process can be modelled using four different components, namely, mean reversion, long-run variance, current variance and volatility of volatility. Heston (1993) observes that when the correlation between spot returns is positively correlated with volatility, a fat-tail effect is reported to the right of the spot returns distribution. This increases the price of out-of-the-money options and decreases the price of in-the-money options relative to the Garman-Kohlhagen (1983) model. However, when the parameter is set to zero, the spot returns exhibit a normal distribution. Further, in this study, the volatility of the volatility

[63] These are: 1) random variance model with mean-reverting volatility process, 2) random variance model with random walk volatility process, 3) Garman-Kohlhagen model with daily revised variance, 4) Garman-Kohlhagen model with historical variance, and 5) Garman-Kohlhagen model with a constant variance estimate.

parameter is shown to be related to the shape of the spot price returns when the volatility is uncorrelated with the spot price, increasing the parameter increases the kurtosis of spot returns. On the contrary, when the volatility and the spot price are correlated, a skewed distribution exists. Thus, the study suggests that within the stochastic volatility framework, the correlation between volatility and spot price is an important precursor for leptokurtic and skewed asset price returns, which affects the pricing of in-the-money options relative to out-of-the-money options. This result is generally consistent with pricing biases reported in the currency option market[64].

Melino and Turnbull (1995) analyse the pricing and hedging performance of the constant volatility and stochastic volatility model by constructing a portfolio to replicate the payoffs of European options on the USD/CAD exchange rate. They argue that since option writers are able to fully and perfectly hedge their exposures, the cost of hedging via replication will be the price of the option. This procedure can be used to price options even when an active secondary market for long-term options is not available.

The replication of option positions in Melino and Turnbull (1995) are performed for four different maturities of ninety-day, one-year, two and a half-year and five-year from January 1975 to December 1986. This results in approximately one hundred portfolios for each maturity over the entire sample period. These options are held until maturity and the mean square hedging errors are recorded[65]. The constant volatility Garman-Kohlhagen (1983) currency option pricing model is applied using

[64] See for instance, Bollen and Rasiel (2003).

[65] The errors are calculated based on the difference between predicted option prices and the value of the replicating portfolio.

implicit volatility estimated from a sixty-day European option to value options of different maturities. In other words, a flat term structure is assumed under this approach and the results indicate that the implicit volatility characteristics of short-dated options are consistent with the volatility behaviour of long-dated options. This contradicts the term structure of volatility model reported in Xu and Taylor (1994) and Campa and Chang (1995).

Compared with the constant volatility model, Melino and Turnbull (1995) find lower mean square errors when the stochastic volatility model is used to construct the weights used for option replications. This result is consistent with the earlier findings of Hull and White (1987) and Chesney and Scott (1989). It further shows that the total hedging error is consistently lower with positive values across all maturities with the stochastic volatility model is used. Thus, contrary to the constant volatility model, improvement in hedging is noted when the time varying nature of the volatility term structure is taken into consideration. However, using simulated option prices, the magnitude of the total hedging error tends to increase with time-to-maturity. Taken together, the implication is that treating volatility as a random process may be more appropriate for short-dated option than for long-dated options.

The joint hypothesis that the volatility spread[66] and the long term implied volatility follow a random walk process is suggested by Xu and Taylor (1994). The reported likelihood-ratio indicates that this hypothesis is doubtful. Instead, the study suggests that it is more probable to model long-dated volatility alone as a random walk

[66] This is estimated as the difference between the estimated short-term and long-term volatility.

process. Indeed Xu and Taylor (1994) find support for the latter at the five per cent significance level using the British pound and the German marks option datasets.

Gessner and Poncet (1997) examine the ability of both the Hull and White (1987) and Heston (1993) stochastic volatility model to generate volatility smiles and volatility term structures using currency option data from the over-the-counter market[67]. The option data are available in various maturities, one-week, one-month, two-month, three-month, six-month, nine-month and twelve-month. Notably, the derived smile convexity using the Hull-White (1987) model is distinctly different from the observed short-dated and long-dated elements of the smile. Thus, contrary to the initial findings of Hull and White (1987), modelling volatility as a random process does not appear to be strictly consistent with empirical observations. The authors argue that the use of random walk model in volatility modelling contradicts practitioners' belief that volatility is better modelled as a mean-reverting process. This lends support for the use of Heston's model in favour of the Hull and White (1987) model.

3.4.2 Term Structure of Implied Volatility

The constant volatility Garman-Kohlhagen (1983) model suggests that implied volatility should be independent of the options' maturities. This assumption is often violated in empirical studies evidenced by different levels of volatility for different maturities. Xu and Taylor (1994), for instance estimate the short-dated volatility and long-dated volatility using currency option data for the British pound, Japanese yen, Swiss franc, and German mark obtained from the Philadelphia Stock Exchange. The

[67] Distinct from previous studies, the study employs a relatively limited sample covering one month, ranging from 2 February to 29 February, 1996.

study finds the difference between a 15-day and a long-term implied volatility usually differ by several percent (several 100 basis points). Further the slope of the term structure varies widely in a fairly random manner over time. Such variations are more prevalent for short-dated volatility.

In a similar vein, Campa and Chang (1995) examine the consistency between current term structure of volatility and the behaviour of future volatility quotes using option data from the over-the-counter market. Under the expectation hypothesis, it is expected that movement in long-term volatility should be consistent with future short-term volatility. For most of the cases, regressing short-dated volatility against current long-dated volatility give a slope coefficient close to one. This indicates that future increases in the short-dated volatility behave in line with the expectations hypothesis. Further, the paper is unable to reject the expectations hypothesis in the majority of cases. Thus, for all currencies and maturity pairs, current spreads between long-dated and short-dated volatility seems to predict the right direction for future short-rate and long-rate changes. Similar to Xu and Taylor (1994), the study also finds short-dated volatility quotes have significantly higher variability compared with long-dated options. More recently, Byoun, Kwok and Park (2003) investigate the implied volatility term structure using an alternative approach that incorporates implied volatility from various strike prices. Although they find some evidence of predictability of future short-dated volatility under the expectation hypothesis, the increase in long-term volatility incorrectly predicts the direction in the subsequent change in long-term volatility.

3.5 Moneyness Effect of Implied Volatility

It is well-established that the cross-sectional pattern of implied volatility recovered from the Garman-Kohlhagen (1983) model contradicts the constant volatility assumption. Several researchers have concluded that implied volatility of out-of-the-money and in-the-money options are consistently higher than at-the-money options. For instance, Taylor and Xu (1994) show that implied volatility of currency options can be approximated as a quadratic function of the strike price. Another study by Campa, Chang and Reider (1998) reveals asymmetrical U-shaped patterns when the three-month implied volatility of the DEM/USD and JPY/USD exchange rates are graphed against the strike prices relative to the forward rates. Using similar data from the over-the-counter market, however, Bollen and Rasiel (2003) report a more symmetrical U-shape pattern when daily average implied volatility data is presented against moneyness measured in terms of delta. Further Malz (1997) proposed an accurate second-order Taylor approximation to obtain the volatility smile from option combinations constructed with puts and calls.

The volatility smile anomaly has attracted much attention in the literature. Several authors have attempted to explain and understand the existence of such a pattern from two perspectives - some believe that the anomaly is attributable to error of the option pricing model while others argue that the existence of the volatility smile is related to market demand for out-of-money options. The following section reviews the theoretical framework and empirical findings relating to the volatility smile with an emphasis on currency options.

3.5.1 Lognormal Distribution and Volatility Smile

The literature offers two explanations for the existence of the volatility smile. First, it is widely held that the volatility smile pattern is attributable to the erroneous assumption used in the Garman-Kohlhagen (1983) option pricing model where the probability distribution of the exchange rate over the maturity of the option contract is assumed to be lognormal distributed. In reality, exchange rate distributions are found to exhibit significant skewness and kurtosis. For instance, Campa, Chang and Reider (1998) show that the foreign exchange probability density function derived from an asymmetric volatility smile deviates significantly from the lognormal distribution. Along with skewness the estimated distributions reveal extreme kurtosis. A similar finding is also provided by Malz (1997) who suggests that skewed distributions inferred from the volatility smile are useful for measuring future market sentiment.

It is therefore no surprise that several studies have examined the ability of "smile-consistent" models to generate the volatility smile behaviour observed in the currency option market. Although Bates (1996a) finds improved explanatory power when fitting a stochastic jump-diffusion model to German mark options over 1984 to 1991 though the model fit was not strong. For the call options, the model tends to over-estimate actual prices for options of three to six months maturity; such a pattern is reported across all levels of moneyness. On the other hand, in-the-money calls are under-estimated by the model. The average errors for put options are generally lower but they remain under-valued for maturities of three to six months. He noted that the poor fit of the model is related to parameter instability since skewness, implicit in the exchange rates distribution, appears to vary over time.

Gessner and Poncet (1997) posit that leptokurtosis and skewness in the foreign exchange rate returns give rise to the smile anomaly in the currency option market. Accordingly, the Hull and White (1987) model is used to fit the smile pattern observed in the over-the-counter market and the derived volatility smile is markedly different from the empirical smile. In particular, for one-month volatility, the Hull-White estimated smile is more pronounced than the actual smile, while the three-month and one-year smiles appear too flat relative to the observed smile.

In a related literature, Das and Sundaram (1999) applied a similar approach to Bates (1996a) by introducing jumps into the return process and allowing the volatility parameter to follow a stochastic process. The model was found to exhibit term structure patterns inconsistent with the smile anomaly observed in actual data. Specifically, the term structure from the model is too flat relative to actual data. The difference between short and long-dated volatility is also found to be negligible, which contradicts the two to three percentage point spreads reported in the literature. The estimated smiles for long-dated options also flatten too rapidly. For instance, the generated three-month smile is almost a constant function of moneyness even though high levels of skewness and kurtosis are assumed in the model.

Sarwar and Krehbiel (2000) evaluate the pricing performance of the Heston (1993) and Garman-Kohlhagen (1983) model for European call options written on the British pound. The study reports root mean square errors (RMSE) of 0.36 for the Garman-Kohlhagen model with daily revised volatility estimates, while the RMSE for the Heston model is 0.37 in the aggregate option sample. The Heston model performed slightly less favourably for in-the-money and out-of-the money options, with RMSE of

1.03 and 0.24 respectively, versus the corresponding RMSE values of 0.96 and 0.21 reported from the Garman-Kohlhagen model. Both models fit the observed option data equally well for near and at-the-money options.

Taken together, these studies offer no conclusive support for the argument that the smile anomaly is explained or reproduced by including jump processes and stochastic volatility components into the Garman-Kohlhagen (1983) option-pricing model. At best, these extensions produce marginal improvement in the Garman-Kohlhagen model and only offer a partial explanation for the smile anomaly. Contrary to the more complex stochastic volatility model, when daily revised estimates of implied volatility are used in the Garman-Kohlhagen (1983) model, lower pricing errors relative to the more complex stochastic volatility models can be attained (Chesney and Scott, 1989). Thus it is apparent that skewness and leptokurtic effects alone may not be sufficient to explain the empirical smile puzzle.

3.5.2 Option Trading and Volatility Smile

More recently, a number of authors have explored an alternative explanation for the existence of the volatility smile based on the demand for out-of-money call and put options. According to this view, market participants actively use calls and puts as an effective tool for hedging their exposure against adverse movements in the underlying assets returns. In related work, Ederington and Guan (2002) suggest that the existence of the smile pattern is driven by hedging pressure. They report that the average daily trading volume for out-of-the-money put options are consistently higher than for at-the-money and in-the-money put options for index options. The average trading volumes for

far out-of-the-money puts is approximately ten times larger than the volumes reported for in-the-money puts. The study finds that when a significant movement in the cash market is expected, out-of-the money options are purchased by market players in order to protect their positions from potential downside risks. Such hedging activities would generate upward pressure on option premia as option trading volume increases. This eventually bids up the prices for out-of-money calls and out-of-the money puts. In line with this view, the Granger-causality test results of Sarwar (2003) indicate that lagged option trading volumes from the currency option market have significant forecasting power with respect to the implied volatility of the British pound, although the result is much stronger for the in-the-money options than the out-of-money options.

In another related literature, Bollen and Whaley (2004) present the "net buying pressure"[68] hypothesis which posits that supply and demand imbalances driven by trading activities in the index option market, will eventually push up implied volatility for out-of-the-money index options. The authors suggest that option writers will not leave their positions unhedged – as their positions grow and become imbalanced, they are exposed to increasing risk[69] and they are therefore forced to sell their options at a higher price. This causes implied volatility to exceed the actual volatility thus causing the slope of volatility smile to change. The study shows that the net buying pressure coefficients for both call and put options are significant explanatory variables for the change in implied volatility of at-the-money options. Furthermore, in most instances, positive coefficients are reported for both call and put options, although stronger support is noted for put options.

[68] This is estimated as the difference between the number of buyer-driven contracts less the number of seller-driven contracts.

[69] Option writers are exposed to unlimited downside risk.

A recent study by Doran, Peterson and Tarrant (2007) finds evidence of predictability of extreme movements in the stock market using information embedded in volatility smiles. The authors construct measures of volatility skew by taking the difference between the implied volatility of deep-out-of-the-money option and the implied volatility that corresponds with various level of moneyness. Using probit model analysis, the coefficient estimates are found to be positively related to the incidence of large negative jumps at the 5% level of significance. They note that large skew coefficients are related to large negative jumps. The relationship is stronger when out-of-money puts are used in the probit models. This supports the findings of Bollen and Whaley (2004) and is consistent with the hedging pressure argument presented by Ederington and Guan (2002). It further implies that skewness in option prices reflected in the volatility smile is capable of generating information about future movements of the underlying market, specifically when a large decline in the underlying asset price is expected.

In their study of pricing performance of currency option pricing model, Bollen and Rasiel (2003) find pronounced smiles when the one to three months implied volatility are graphed against moneyness measured in deltas. They suggest that the presence of symmetrical smiles reflects foreign exchange market sentiment over the option expiration periods. Thus a symmetrical smile indicates that on average, there is demand from hedgers against depreciation as well as appreciation of the underlying exchange rates. They perform a regression of implied volatility on moneyness and find the slope coefficients vary widely. Notably, put options have negative slopes while positive coefficients are reported for the calls. These observations are consistent with the "net buying pressure" hypothesis of Bollen and Whaley (2004) and imply that the

dynamics of the volatility smile may be related to future volatility over the remaining life of the option contract. Also, consistent with the hedging hypothesis of Ederington and Guan (2002), the 'skewness premium'[70] reported in Bates (1996b) fluctuated drastically over the Exchange Rate Mechanism (ERM)[71] crisis period and became more negative preceding the withdrawal of the British pound from the ERM, when the Bank of England failed to support the pound sterling above its lower limit of DM2.778[72]. Campa and Chang (1995) also note that implied volatility quotes rose sharply one month prior to the ERM crisis in September 1992.

3.5.3 Other Explanations for the Volatility Smile Anomaly

It is widely acknowledged that the volatility smile effect became more pronounced after the October 1987 stock market crash. In line with this, Liu, Pan and Wang (2005) introduce the notion of 'rate-event premium' and develop a model that can be used to explain implied volatility skew. According to this model, out-of-money put options are sensitive to this premium. When a rare event such as a market crash occurs, investors react by assigning such premium to rare-event-sensitive instruments particularly out-of-money put options. It is shown that a large portion of volatility skew can be explained by the rare-event premium hypothesis. The model is consistent with the belief that out-of-money options are often used as a cheap form of insurance against large movements in the underlying asset. It also explains the information content of volatility skew proposed by Doran *et al* (2007) by showing that option prices are

[70] This is defined as (C/P -1), where c and p are call and put option premia. These options are equally out-of-money.
[71] The Exchange Rate Mechanism was operational from 12 March, 1979 to 2 August, 1993.
[72] See Figure 1 and Figure 4 of Bates (1996b); Malz (1996) provides extensive discussion and analysis on the ERM crisis using over-the-counter currency option prices.

sensitive to large negative movements in the underlying asset. This is particularly the case for put options.

Pena, Rubio and Serna (1999) argue that the volatility smile observed empirically is usually twice the size of the predicted smile using a "smile-consistent model". Motivated by this observation, the study investigates several possible determinants of the volatility smile using various explanatory variables including bid and ask spreads, share volumes, option volumes, a day-of-the-week dummy variables, and the standard deviation of the underlying asset. Using the Granger-causality model, the study shows that the magnitude of volatility smile curvature is significantly and positively related with option bid-ask spreads. The volatility of the underlying asset is also found to be significant but negatively associated with the volatility smile curvature. Thus during periods of high volatility, the curvature of smile tends to be lower. This indicates that transaction costs proxied by bid and ask spreads has an important impact on the pricing of out-of-money options relative to at-the-money options. This finding also supports the dynamic nature of the volatility smile in response to the impending risk of the underlying market.

3.6 Conclusion

This chapter provides an overview of empirical studies in the area of implied volatility with an emphasis on currency options. Despite the overwhelming efforts devoted to the estimation and characterisation of implied volatility, the performance of option pricing models that assume a random volatility process remain mixed and inconclusive. In addition, there is evidence to suggest that strike price bias in the Garman-Kohlhagen (1983) option pricing model may not be solely attributed to erroneous assumptions used in the model.

Chapter 4 provides further investigation into the random behaviour of implied volatility across the term structure using time series of quoted implied volatility collected from the over-the-counter currency option market. The test results are further explored using simple trading rules in Chapter 5. Chapter 6 examines the moneyness behaviour of quoted implied volatility in the currency option market. The dynamics of the volatility smile is investigated using proxies of slopes and curvatures. The information content of these proxies is considered in Chapter 7.

CHAPTER 4 - FOREIGN EXCHANGE IMPLIED VOLATILITY AND THE RANDOM WALK HYPOTHESIS

4.1 Introduction

The study of foreign exchange volatility has attracted considerable interest in the literature due to its vital role in the financial markets, including for instance, pricing in the currency option market, risk forecasting, portfolio diversification, multinational investment activities and the implementation of foreign exchange policies by the central banks. Indeed, since the early 1980s, the study of volatility modelling in the foreign exchange market has become an important part of the finance literature.

Although the volatility of asset returns is considered elusive, some stylized facts are well documented: mean-reversion, pronounced persistence and an "asymmetric pattern" induced by market innovations. Such attributes are discussed in Poon and Granger (2005) and Engle and Patton (2001). While the existing literature is dominated by volatility forecasting using time series techniques[73], studies into the dynamics of option-implied volatility have received little attention. This examination is necessary as it has important implications for the implementation of relatively recent option-pricing frameworks and time series models that treat foreign exchange volatility as an unobservable component. These approaches often assume a random walk process in the estimation of the underlying foreign exchange volatility. Studies on currency option pricing that assume volatility follows a random walk process include for example,

[73] A comprehensive literature survey by Poon and Granger (2003) reports a total of 93 studies on asset volatility prediction have been studied in various market contexts.

Chesney and Scott (1989), Heston (1993), Melino and Turnbull (1995), Bates (1996), Duffie, Pan and Singleton (2000). These are largely motivated by the work of Hull and White (1987). Time series modelling techniques used by Harvey, Ruiz and Shephard (1994) and Chowdhury and Sarno (2004) also assume a random walk component in the modelling of foreign exchange volatility. Further, Nelson (1991) suggests that the logarithm of the conditional variance takes on the characteristic of a random walk process.

Modelling foreign exchange volatility as a random walk process is largely motivated by the skewness and kurtosis effects observed in empirical data. However, such models ignore the 'term structure' effect reported in the currency option market, asset returns and volatility changes are generally assumed to be independent. Gessner and Poncet (1997) argue that modelling of asset price volatility as a random walk process contradicts empirical findings and market convention. Traders often argue that the market data exhibits a mean reverting pattern rather than a random walk process. In line with this view, Sabanis (2003) extended the work of Hull and White (1987) by allowing the volatility of the underlying asset to follow a mean reverting process. More recently, Bali and Demirtas (2008) present evidence of mean reversion in asset price volatility using data from the index futures market.

A number of authors have shown that foreign exchange volatility is not well described by a random process. A study by Scott (1987) shows that only marginal improvement is made to the option pricing model when volatility of the underlying asset is assumed to vary randomly over time. Chesney and Scott (1989) compared the performance of the random variance option-pricing model with the Garman-Kohlhagen

(1983) model; the random variance model takes on the assumption that the log of volatility follows a random walk process over time while a constant volatility parameter is used in the Garman-Kohlhagen (1983) model. The results indicate a mean squared error of 1.431 for the former while the latter has a value of 0.056 against the observed price[74]. This suggests that option pricing models that assume a random walk in the volatility process do not provide a better fit to market prices than a constant variance model. Instead, Chesney and Scott (1989) suggest that allowing the volatility of the U.S. dollar/Swiss franc exchange rate to follow a mean-reverting process generates a lower pricing error for the calls and puts compared with the constant volatility model. Xu and Taylor (1994) examine the term structure of implied volatility using currency option data from the Philadelphia Stock Exchange. Their joint test for a random walk process over the implied volatility spread (between the short and long-term volatility) and long-term volatility is rejected. However, the same hypothesis for the long-term implied volatility series is not rejected at the five percent significance level.

This chapter examines the dynamics of the implied volatility series by performing various in-sample and out-of-sample tests on quoted implied volatility of four major currencies. It focuses on the over-the-counter European currency options of different maturities. Since implied volatility are actively traded in this market, daily quoted implied volatility can be observed and this provides a reliable data source for empirical examination. Tests are performed for the implied volatility series with maturities of one-week, one-month, three-month, six-month, one-year and two-year.

[74] See Table 3 on pp.276 of Chesney and Scott (1989).

While former studies test for random walk property in asset prices, empirical tests based on implied volatility data have yet to be undertaken. This study provides an extension to the existing literature on the random walk hypothesis using option-implied volatility estimates. It further adds to a growing interest in the option-implied volatility literature driven by a greater appreciation of the information content of option prices.

In this analysis, both conventional and nonparametric variance ratio methodologies are employed. These include the distribution-free variance ratio test of Wright (2000) in order to avoid the potential sensitivity of the test results induced by non-normality, heteroscedasticity and excess kurtosis frequently observed in volatility data. To confirm the robustness of the variance ratio test results, the Sidack-adjusted *p*-values are also calculated for all maturities and currency pairs. This controls for possible biases due to sample size distortions. For completeness, the standard unit root tests are also reported in this study. Finally, out-of-sample tests are performed using various forecasting models to check robustness of the variance ratio test results.

The following section provides a brief review of implied volatility estimation. Section 4.2 introduces the implied volatility data and the variance ratio literature. In Section 4.3, the variance ratio method and the nature of the datasets are described. The empirical findings for the variance ratio tests are presented in Section 4.4 and Section 4.5. Section 4.6 examines the mean reverting nature of the volatility series while robustness tests using out-of-sample forecasting tests are discussed in Sections 4.7 and 4.8. The conclusion of this study is provided in Section 4.9.

4.1.1 Implied Volatility Estimation

Early research into option-implied volatility by Latane and Rendleman (1976), Schmalensee and Trippi (1978), and Beckers (1981) suggests that implied volatility is a better estimate of realised volatility than historical data based estimates. In essence, the estimation of implied volatility involves solving the level of volatility that equates the observed option price with the theoretical price according to the Black-Scholes (1973) model. The application of this procedure suffers from various measurement error problems due to market frictions (Hentschel, 2003). This raises doubt about the precision of implied volatility estimated in the traditional way. Dunis and Keller (1995) propose the use of quoted implied volatility traded in the over-the-counter currency option market to mitigate such measurement errors. Another study by Covig and Low (2003) also uses at-the-money implied volatility from the over-the-counter currency option market to eliminate data biases induced by maturity effects, the nonsynchronisation problem and moneyness effects commonly found in empirical studies.

Another possible concern for the estimation of implied volatility relates to the liquidity of the option market. Indeed, empirical work by Brenner, Eldor and Hauser (2001) suggests that market liquidity is important for the pricing of option contracts. Their study shows that illiquid currency options are priced 21% less than liquid options. A recent industry survey conducted by the Bank for International Settlements suggests that most currency options are traded in the over-the-counter market[75]. The over-the-counter currency option market is quite liquid thus allowing a more accurate estimate of

[75] See BIS Quarterly Review, March 2009, Table 19 and Table 23A.

implied volatility and this further alleviates measurement error problems that arise from various market frictions.

4.1.2 Random Walk and Foreign Exchange Volatility

Where volatility follows a random walk model the time series process is non-stationary as its variance fluctuates randomly over time. Such a process is said to contain a unit root. Traditionally, the presence of a random walk process can be identified using a unit root test on the time series data. Taylor (1994), Bollerslev, Engle and Nelson (1994), report evidence against a unit root process in foreign exchange volatility sampled from the 1980s to the 1990s. Wright (1999) uses the log-squared volatility series for currencies and rejects the null of a nonstationary stochastic process. In a more recent paper, Chowdhury and Sarno (2004) report that the volatility process in the foreign exchange market is better characterised as a persistent stationary process rather than as a unit root process.

4.2 Random Walks and Variance Ratio Tests

The random walk hypothesis has been the central focus of the finance literature over the last three decades. Arguably, improved time series modelling techniques, the availability of superior quality, and larger sample sizes over a longer time horizon in the 1980s have allowed researchers to re-examine the price dynamics of security returns more effectively.

Lo and MacKinlay (1988) examine the time series behaviour of asset prices using data spanning from 1962 to 1985. Their study proposes that if a price series

follows a random walk process, then the variance of the asset returns should be proportional to the return interval. However, if the estimated variance ratio is statistically different from the value of one, then the random walk hypothesis is rejected. Specifically, this method assumes that the variance of an asset's volatility increments increase linearly with the holding-period. Therefore the variance of $Y_t - Y_{t-2}$ is twice the variance of $Y_t - Y_{t-1}$. This property is used to test the random walk hypothesis by calculating a ratio based on the variance of qth differences divided by the product of q and the variance of the first difference. The ratio should yield a value of one if no violation of the random walk exists. Deviation from the expected ratio of one is statistically tested using a Z-test statistic. Their study provides strong support for rejection of the random walk hypothesis for the entire sample period using NYSE Indexes. In their following paper[76], the authors re-examine the robustness of the variance ratio test using Monte Carlo simulation and concluded that under the null hypothesis of a random walk with heteroscedasticity, their Z-test statistic provides a better test than the traditional Dickey-Fuller (1979) unit root test or the Box-Pierce (1970) test for autocorrelation.

Numerous researchers have since adopted the variance ratio test with the Lo and MacKinlay's (1988) Z-test statistic to investigate the random walk hypothesis. For instance, studies by Alam, Hasan and Kadapakkam (1999), Darrat and Zhong (2000), Lima and Tabak (2004), Chang (2004), Abraham, Seyyed, and Alsakran (2002), Smith and Ryoo (2003), Lai, Balachander, and Mat Nor (2002) have tested the random walk hypothesis in different markets using the variance ratio method. A more recent study on share prices by Belaire-Franch and Opong (2005) examines the behaviour of FTSE

[76] See Lo and MacKinlay (1989).

indices and it also uses the variance ratio approach. In contrast with previous studies, a more robust nonparametric version of variance ratio test based on signs and ranks of Wright (2000) was also used in this study.

Using spot exchange rate data, Liu and He (1991) examine weekly exchange rate series for five currency pairs and find evidence of deviation from the random walk process using the variance ratio test. The Z-test statistic of Lo and MacKinlay (1988), which is robust to heteroscedasticity, rejected the variance ratio test in three of the five currency pairs. Another study by Pan, Chan and Fok (1997) investigates the behaviour of currency futures prices from 1977 to 1987 and it also employs the variance ratio methodology. The study uses prices of individual currency futures for the British pound, the German mark, the Japanese yen and the Swiss franc. With the exception of the yen currency futures, they find little evidence of random walk violation in the currency futures market.

4.3 Data and Methodology

The data used in this study comprises of daily implied volatility quotes for four currency options traded in the over-the-counter currency option market, namely the British pound against the U.S. dollar, euro against the U.S. dollar, Australian dollar against the U.S. dollar and the U.S. dollar against the yen. At-the-money options on forward contracts where the strike prices of the option contracts are set to equal the forward exchange rate. As most of the option contracts are dealt at the forward exchange rate, such contracts have high liquidity and therefore provide a reliable source of data for this study. Indeed a number of researchers have relied on this attribute to

estimate the risk-neutral probability density function of future exchange rates, including studies by McCauley and Melick (1996), Malz (1997) and Campa, Chang and Reider (1998), and more recently Carr and Wu (2007).

Quoted volatility are obtained from the British Bankers' Association (BBA) database. BBA provides the average volatility quotes estimated daily from a total of 12 major market makers in the over-the-counter currency option market. Daily closing implied volatility quotes are provided by the market makers between 3:30 pm and 3:50 pm London time. BBA excludes the two highest and lowest rates for each trading day and the average of the remaining rates is stored in the BBA-Reuters database.

Option contracts with maturities of one-week, one-month, three-month, six-month, one-year and two-year are obtained from this database. The range of maturities allows examination of the random walk hypothesis across the term structure of the volatility series. Since the database became available from August 2001, daily sampling provides a reasonably large number of observations with an average sample size for each maturity of approximately 1,140 observations from 29 August, 2001, to 28 April, 2006. This generates a total of 27,450[77] usable data points over the sample period.

[77] This study uses four currency pairs with 6 respective maturities, therefore 6 x (1133+1145+1151+1146) = 27,450 usable observations.

4.3.1 Quoting Convention for Implied Volatility Data

The quoted implied volatility series used in this study are provided in the standard form and following the interbank quoting conventions. The British pound, euro and the Australian dollar are available in the "American" form while the Japanese yen are quoted in the "European" form (also known as the "bankers' quotes"). The former provides the value of the base currency (that is the British pound, euro and the Australian dollar) in American dollars while the latter gives the value of the American dollar in terms of the countercurrency (in this case, the Japanese yen). The level of the quoted implied volatility is unaffected by the quoting convention used.[78]

In the over-the-counter currency option market, quoted implied volatility are entered into the Garman-Kohlhagen model (1987) to calculate the dollar premium. Therefore the market price of an option contract is not known before the corresponding implied volatility is available.

A working example is used to demonstrate implied volatility estimation using the different quoting conventions discussed in the preceding paragraph, option market prices (in the "American" and "European" forms) are provided by DeRosa (2000, pp.63). An approximation of implied volatility for at-the-money options can be simplified using Equation (4-1). This is based on the study of Brenner and Subrahmanyam (1988) who demonstrate that the price of an at-the-money call option can be approximated as the product of the forward rate and the volatility of the underlying asset. This is then adjusted for time-value by the square-root of $T/2\Pi$.

[78] This is illustrated in the example following Equation 4-1.

Specifically, this approximation can be used to estimate the implied volatility of a call option traded at-the-money where the strike price equals the forward rate. This is specified as:

$$IV_T \approx \sqrt{\frac{2\prod}{T}} \frac{e^{rT}}{F} MV_T \qquad (4\text{-}1)$$

where IV_T is the estimated implied volatility with T-period(s) to maturity (as a fraction of a year) , r is the interest rate differential between the currency pair, F is the forward exchange rate and MV_T is the market price of the option contract with maturity, T period(s) from now. Under put-call parity, this approximation can also be directly applied to put options. Using the dollar premium and interest rate data provided in DeRosa (2000, pp.63), the implied volatility for the European and American quotes are estimated below:

Call option on USD/JPY (quoted in "European" form)

Spot exchange rate	=	JPY115
Strike price (forward outright)	=	JPY114.58
Interest rate (USD)	=	5.00% p.a.
Interest rate (JPY)	=	0.50% p.a.
Maturity	=	30 days
Dollar premium ("pips")	=	JPY2.6545

The estimated implied volatility using equation (4-1) gives:

$$IV_T \approx \sqrt{\frac{2\prod}{(30/365)}} \frac{e^{(\ 0.045x30/365)}}{114.58} 2.6545$$

$$IV_T \approx 20.18\% \text{ p.a.}$$

Call option on JPY/USD (quoted in "American" form)

Spot exchange rate	=	USD1/115
Strike price (forward outright)	=	USD1/114.58
Interest rate (USD)	=	5.00% p.a.
Interest rate (JPY)	=	0.50% p.a.
Maturity	=	30 days
Dollar premium ("pips")	=	USD0.0002015

The estimated implied volatility using equation (4-1) gives:

$$IV_T \approx \sqrt{\frac{2\Pi}{(30/365)}} \frac{e^{(0.045x30/365)}}{1/114.58} 0.0002020$$

$$IV_T \approx 20.16\% \text{ p.a.}$$

This example shows that the level of implied volatility is independent of the quotation form used.

4.3.2 Descriptive Statistics

Table 4-1 reports the descriptive statistics for the first differences of implied volatility calculated from the four currency options over five years from 29 August, 2001 through to 28 April, 2006. The change in volatility is calculated by taking the differences in logs between the closing implied volatility of two successive trading days. The mean change in volatility series for the implied volatility is negative for all maturities and currencies. The standard deviation of the implied volatility changes series consistently decreases as maturity increases. The variation in the mean change in volatility series confirms the existence of "term structure" effects of implied volatility reported in Campa and Chang (1995), Xu and Taylor (1994) and Byoun, Kwok and Park (2003). This result violates the constant volatility assumption underlying the Garman-Kohlhagen (1983) model.

An analysis of higher moments reveals high positive kurtosis in the implied volatility series. Except for the one-week GBP/USD and the two-year AUD/USD volatility return series, the skewness coefficients are all above zero.

Table 4-1: Descriptive Statistics for the First-Differenced Implied Volatility Series

	Mean	Std Dev	Kurt	Skew	Autocorrelations				
					ρ_1	ρ_2	ρ_3	ρ_4	ρ_5
Panel A: GBP/USD (n = 1133)									
1-Week	-0.0002	0.525	48.237	-0.148	-0.143 ***	-0.047	-0.083 ***	-0.038	-0.063 **
1-Month	-0.0011	0.222	12.226	0.361	-0.036	-0.091 ***	-0.081 ***	0.031	0.088 ***
3-Month	-0.0014	0.188	10.372	0.451	-0.034	-0.068 **	-0.097 ***	0.040	0.088 ***
6-Month	-0.0011	0.096	34.350	1.222	0.013	0.022	-0.042	0.025	0.039
1-Year	-0.0012	0.077	28.626	1.113	0.055 *	-0.011	0.002	0.033	0.048
2-Year	-0.0012	0.068	22.567	0.585	0.101 ***	0.006	0.020	0.045	-0.008
Panel B: EUR/USD (n = 1145)									
1-Week	-0.0016	0.562	6.626	0.383	-0.033	-0.048	-0.098 ***	-0.096 ***	-0.061 **
1-Month	-0.0024	0.275	7.331	0.900	-0.001	-0.094 ***	-0.131 ***	0.023	0.083 ***
3-Month	-0.0026	0.178	12.412	1.157	0.011	-0.015	-0.094 ***	-0.042	0.081 ***
6-Month	-0.0028	0.137	21.211	1.161	0.013	-0.034	-0.069 **	-0.027	0.088 ***
1-Year	-0.0028	0.124	38.127	1.507	-0.032	-0.065 **	-0.052 *	-0.013	0.074 **
2-Year	-0.0026	0.118	52.479	1.607	-0.022	-0.067 **	-0.054 *	-0.037	0.084 ***
Panel C: AUD/USD (n = 1151)									
1-Week	-0.0034	0.548	8.980	1.077	0.008	-0.116 ***	-0.118 ***	-0.060 **	-0.012
1-Month	-0.0038	0.286	12.125	1.255	-0.008	-0.113 ***	-0.098 ***	0.000	0.125 ***
3-Month	-0.0033	0.190	22.090	1.237	-0.080 ***	-0.094 ***	-0.019	-0.040	0.066 **
6-Month	-0.0031	0.158	89.376	0.547	-0.105 ***	-0.154 ***	0.033	-0.052 *	0.032
1-Year	-0.0037	0.199	39.999	2.543	-0.047	-0.004	-0.059 **	-0.037	0.064 **
2-Year	-0.0027	0.156	175.121	-0.068	-0.191 ***	-0.200 ***	0.026	-0.014	0.025
Panel D: USD/JPY (n = 1146)									
1-Week	-0.0014	0.729	13.068	0.208	-0.100 ***	-0.009	-0.107 ***	-0.095 ***	-0.034
1-Month	-0.0015	0.361	9.972	0.819	-0.031	-0.051 *	-0.096 ***	-0.075 **	0.021
3-Month	-0.0015	0.210	10.474	0.876	-0.043	0.004	-0.035	-0.092 ***	-0.004
6-Month	-0.0016	0.149	12.649	0.557	-0.036	-0.001	-0.013	-0.054 *	-0.002
1-Year	-0.0018	0.121	19.633	0.118	-0.023	-0.013	0.015	-0.022	-0.017
2-Year	-0.0019	0.114	23.389	0.104	-0.015	-0.006	0.020	-0.018	-0.015

Notes: This table presents the mean, standard deviation, kurtosis, skewness and autocorrelation coefficients for the first differenced implied volatility series of the four currencies. The standard errors for the autocorrelation coefficients are calculated as $1/\sqrt{T}$ and T is the number of observations. The summary measures the statistics from 29 August, 2001 to 28 April, 2006 with an average sample size of 1140 for each volatility series.
**** Significant at the 1% level*
*** Significant at the 5% level*
** Significant at the 10% level*

The autocorrelations for the implied volatility returns are estimated from one to five lags and are reported in columns five to nine. These coefficients vary across maturities and currencies and remain significant after five lags. The signs of these coefficients become more consistent at lag five, where the one-week volatility returns have negative coefficients while the remaining maturities are all above zero (with the exception of the USD/JPY currency pair). The level of skewness increases with maturities in most instances. These findings are consistent with the "fat tail" effect, indicating that the distributions of the volatility series significantly depart from the normality assumption.

Table 4-2 provides the standard unit root tests on the daily implied volatility levels and the first differenced series using the Augmented Dickey-Fuller (1981) and Phillips-Perron (1988) unit root tests. In columns one and three, the null hypothesis of a unit root in the volatility process can be rejected in most instances when the tests are applied on the volatility levels. Specifically, stronger rejections are noted for the short-dated series. For the six-month, one-year and two-year GBP/USD series, the null hypothesis of a unit root cannot be rejected. The results are fairly consistent across the two methods. When the tests are repeated using the first differenced series, the null hypothesis of a unit root in the series is strongly rejected across all currency pairs and maturities. This result holds under both methods. Thus, the Augmented Dickey-Fuller (1981) and Phillips-Perron (1988) unit root tests provide evidence of stationary volatility in levels while the first differences of the volatility series are strictly stationary.

Table 4-2: Augmented Dickey-Fuller (1981) and Phillips-Perron (1988) Unit Root Tests

	Augmented Dickey-Fuller		Phillips-Perron	
	IV_t	ΔIV_t	IV_t	ΔIV_t
Panel A: GBP/USD (n=1133)				
1-Week	-2.727 *	-11.592 ***	-5.456 ***	-39.806 ***
1-Month	-2.910 **	-10.596 ***	-2.969 **	-35.133 ***
3-Month	-2.875 **	-10.313 ***	-2.832 *	-35.011 ***
6-Month	-2.123	-19.823 ***	-2.154	-33.223 ***
1-Year	-1.964	-23.400 ***	-1.977	-31.832 ***
2-Year	-1.893	-22.611 ***	-1.891	-30.438 ***
Panel B: EUR/USD (n=1145)				
1-Week	-3.340 **	-13.032 ***	-6.305 ***	-35.268 ***
1-Month	-3.707 ***	-11.781 ***	-3.762 ***	-34.102 ***
3-Month	-3.844 ***	-11.591 ***	-3.174 **	-33.506 ***
6-Month	-3.408 **	-11.224 ***	-2.820 *	-33.401 ***
1-Year	-3.316 **	-8.931 ***	-2.784 *	-35.083 ***
2-Year	-3.207 **	-8.953 ***	-2.874 **	-34.714 ***
Panel C: AUD/USD (n=1151)				
1-Week	-3.250 **	-16.174 ***	-4.305 ***	-33.957 ***
1-Month	-3.487 ***	-11.431 ***	-2.856 *	-34.430 ***
3-Month	-3.011 **	-11.919 ***	-2.458	-37.149 ***
6-Month	-2.695 *	-9.456 ***	-2.259	-38.513 ***
1-Year	-3.529 ***	-8.094 ***	-2.926 **	-35.617 ***
2-Year	-2.564	-8.334 ***	-2.286	-44.299 ***
Panel D: USD/JPY (n=1146)				
1-Week	-5.214 ***	-11.224 ***	-7.975 ***	-37.915 ***
1-Month	-4.310 ***	-15.654 ***	-5.408 ***	-35.143 ***
3-Month	-3.718 ***	-16.356 ***	-4.340 ***	-35.338 ***
6-Month	-3.606 ***	-15.590 ***	-3.531 ***	-35.066 ***
1-Year	-3.063 **	-8.812 ***	-3.172 **	-34.601 ***
2-Year	-3.001 **	-8.574 ***	-3.063 **	-34.352 ***

Note: This table reports the Augmented Dickey-Fuller (ADF) test statistic for the presence of a unit root. IV_t is the natural logarithm of the implied volatility; ΔIV_t is the first differences of IV_t. The appropriate number of lags in the ADF test is determined using the Akaike Information Criterion. The unit root tests are also performed with a constant and a deterministic trend individually. In order to conserve space, these results are not reported here since the overall pattern remains unchanged.
**** Significant at the 1% level*
***Significant at the 5% level*
**Significant at the 10% level*

The autocorrelation coefficient that corresponds with each volatility series for different lags is reported in Table 4-3. The joint tests for zero autocorrelation using the Ljung-Box Q statistics coefficients are performed on the first 200 lags[79] using the natural logarithm of the implied volatility levels. The test statistics are reported on the

[79] This is broadly consistent with Poon and Granger (2005) who find strong persistence in volatility process.

last row of each panel in Table 4-3. The relevant critical value of 249.455 at the 1% level of significance is from a χ^2 distribution with 200 degrees of freedom.

Table 4-3: Autocorrelation Coefficients and the Ljung-Box Q-statistic

Lag	1-Week	1-Month	3-Month	6-Month	1-Year	2-Year
Panel A: GBP/USD						
1	0.8884	0.9808	0.9816	0.9909	0.9926	0.9934
5	0.7527	0.9194	0.9199	0.9506	0.9580	0.9596
10	0.6926	0.8467	0.8464	0.8948	0.9092	0.9115
20	0.5891	0.7056	0.6947	0.7852	0.8131	0.8102
30	0.4308	0.5621	0.5430	0.6735	0.7119	0.6997
100	0.0075	0.0910	0.0348	0.2115	0.2482	0.2260
200	0.1688	0.0991	0.0163	-0.1001	-0.1642	-0.1588
Q(200-0)	20034.01*	30100.70*	27024.25*	41111.73*	45864.94*	43824.53*
Panel B: EUR/USD						
1	0.9268	0.9727	0.9835	0.9882	0.9887	0.9885
5	0.7131	0.8879	0.9241	0.9454	0.9543	0.9536
10	0.6282	0.7966	0.8551	0.8930	0.9119	0.9107
20	0.5791	0.6633	0.7343	0.7966	0.8253	0.8248
30	0.4065	0.5487	0.6322	0.7099	0.7465	0.7483
100	-0.0112	0.0526	0.2031	0.3196	0.3799	0.3956
200	0.1887	0.2175	0.2346	0.2600	0.2725	0.3097
Q(200-0)	19919.84*	31502.21*	45097.38*	60581.02*	68626.02*	72177.53*
Panel C: AUD/USD						
1	0.9665	0.9863	0.9885	0.9865	0.9886	0.9782
5	0.8646	0.9435	0.9589	0.9613	0.9485	0.9542
10	0.7998	0.8906	0.9235	0.9336	0.8982	0.9297
20	0.738	0.8022	0.8618	0.8803	0.7944	0.8791
30	0.6283	0.7175	0.7977	0.8232	0.6932	0.8267
100	0.1463	0.2186	0.3388	0.4136	0.1414	0.4439
200	0.1296	0.0957	0.035	0.018	0.1183	0.0269
Q(200-0)	36450.06*	47226.30*	61601.17*	71367.27*	42148.52*	75080.07*
Panel D: USD/JPY						
1	0.8958	0.9506	0.9711	0.9828	0.9879	0.9896
5	0.6188	0.8012	0.8715	0.9206	0.9423	0.9486
10	0.5242	0.6869	0.7838	0.8591	0.8944	0.9037
20	0.4149	0.4821	0.6040	0.7274	0.7889	0.8056
30	0.2297	0.3220	0.4675	0.6289	0.7146	0.7353
100	0.0362	0.0771	0.2003	0.3301	0.4171	0.4574
200	-0.0495	-0.0828	-0.0064	0.1315	0.2334	0.2946
Q(200-0)	11663.17*	18732.55*	33193.57*	54343.61*	70890.21*	78869.43*

Note: This table presents the autocorrelation coefficients of different lags. The Ljung-Box Q statistics on the last row of each panel test for the joint hypothesis of zero autocorrelation up to 200 lags. The asterisk (*) shows that the test statistic is significantly difference from zero at the 1% level of significance. The sample period spans from 29 August, 2001 to 28 April, 2006. The statistics are calculated using the log of daily implied volatility quotes.

The first-order autocorrelation coefficients estimated using implied volatility levels show very high autocorrelation. For the GBP/USD series reported in Panel A of Table 4-3, the autocorrelation coefficients fall within the range of 0.1688 (200^{th} lag) to

0.888 (first lag) for the one-week implied volatility series. For the two-year volatility series, the autocorrelation coefficient of the first lag is 0.993 which is larger than the corresponding one-week autocorrelation coefficient. These coefficients indicate "half-lives" from 6 calendar days to 98.7[80] calendar days. The significant persistence in the long-dated volatility series suggests that the change in the prevailing volatility series has a significant effect on the volatility series approximately five months into the future[81].

Relative to the short-dated volatility series, the long-dated volatility series take about sixteen times longer to move halfway back towards their unconditional mean. The Ljung-Box test statistic for the joint null hypothesis of zero autocorrelation is strongly rejected across all implied volatility series at the 1% level of significance. This result holds across all currency-pairs. The autocorrelation coefficients reported in Table 4-3 show strong persistence in the implied volatility series and they remain significant across a range of lag choices. For instance, in Panel C, the one-week and two-year AUD/USD series have autocorrelation coefficients of 0.6283 and 0.8267 respectively after 30 lags.

In contrast with the long-dated volatility series, the autocorrelation coefficients for the short-dated series declined more rapidly at the same lags length. For instance, the one-week GBP/USD series in Panel A has a coefficient of 0.0075 at 100 lags. In comparison, the autocorrelation coefficients for the one-year and two-year series remain at 0.2482 and 0.2260 respectively.

[80] $0.888^{h} = 0.5$, h=5.83; $0.993^{h} = 0.5$, h =98.7

[81] This is estimated as: h / trading day per year x 12 months. For the two-year series, 98.7/250 x 12=4.73, assuming there are 250 trading days in a year.

Overall, the size of the autocorrelation coefficients reported in Table 4-3 are broadly consistent with the persistent nature of financial market volatility noted in Poon and Granger (2003), where the autocorrelation coefficients for realised volatility were found to be significantly greater than zero even after 1000 lags. These results indicate that volatility levels can be characterised as a stationary series with very slowly decaying autocorrelation coefficients.

4.3.3 The Conventional Variance Ratio Test

The preceding analyses suggest that the null hypothesis of a unit root in the volatility data can be rejected across all currencies and maturities. Since both a unit root and uncorrelated increments are required for the random walk process to hold (Liu and He, 1991), variance ratio tests are employed in the following section to investigate the violation of the uncorrelated increments requirement.

The variance ratio test of Lo and MacKinlay (1988) relies on an important property of the random walk process; that is, if the random walk hypothesis holds, the variance of the first difference of a series should be proportionally related to the variance of the q differences. For example, the variance of monthly change in volatility should be thirty times as large as the variance of daily change in volatility under the null hypothesis if the daily volatility series follows a random walk process. Thus the variance ratio estimated at lag q, can be expressed as:

$$VR(q) = \frac{1}{q}\frac{Var(R^q)}{Var(R^1)} \quad (4\text{-}2)$$

The notation R is the natural logarithm of the first difference of the implied volatility (V) series measured as $logV_t$ - $logV_{t-1}$ and R^q and R^1 represent q-period and 1-period change in volatility respectively. The variance ratio (VR) has a value of one if the random walk null hypothesis holds. That is, if the estimated variance ratio is equal to one over q intervals, the implied volatility series can be characterised as a random walk process. The standard normal test statistics under homoscedasticity, $Zs(q)$ is given by:

$$Zs(q) = \frac{\sqrt{(N-1)}[VR(q)-1][2(2q-1)(q-1)]/3}{\sqrt{q}} \tag{4-3}$$

The heteroscedastic-consistent standard normal test statistics $Z(q)$ is given by:

$$Z(q) = \frac{\sqrt{(N-1)}[VR(q)-1]}{\sqrt{V(q)}} \tag{4-4}$$

where N is the number of observations of $R_{t,}$ and $V(q)$ is the consistent estimate of the variance ratio at interval q. The standard normal test statistics $Zs(q)$ has independent and identically distributed standard normal error terms while the heteroscedastic-robust test statistic, $Z(q)$, has a less restrictive assumption that allows heteroscedastic and non-normal error terms.

In testing the random walk hypothesis using the implied volatility series, both Zs and Z statistics are calculated for different levels of q. Daily closing implied volatility are used as the base observation interval. The Zs and Z statistics are calculated for each q by comparing the variance of the base interval with the variance for two-day, five-day, ten-day, twenty-day and thirty-day periods. The VR for each level of q is calculated for the volatility series with maturities of one-week, one-month, three-month, six-month, one-year and two-year. Since both $Zs(q)$ and $Z(q)$ statistics are asymptotic normal, the usual critical values are used for hypothesis testing. For completeness, the

variance ratio test is also performed using volatility levels for the selected currency pairs.

4.3.4 The Nonparametric Variance Ratio Test

Wright (2000) developed a nonparametric version of the variance ratio test that uses ranks and signs in place of the underlying change in volatility. In contrast with the conventional asymptotic normal variance ratio tests of Lo and MacKinlay (1988), this method avoids making the limiting assumptions about the underlying distribution. This is an important consideration as the implied volatility first differences reported in Table 4-1 exhibit significant leptokurtic distributions.

Wright (2000) tests six different time series models, including two long memory models using Monte Carlo simulation. The test statistics are found to be more robust to size distortion in the presence of conditional heteroscedasticity than the conventional variance ratio test. Given that the distribution-free method is more precise than the conventional asymptotic tests, more reliable results can be expected when the implied volatility first difference series are characterised by skewness, kurtosis and persistence. The rank-based variance ratio test statistics are defined as:

$$RK_1 = \frac{\left(\frac{1}{Tk} \sum_{t=k+1}^{T} (R_{1t} + R_{1t-1} + ...R_{1t-k})^2 - 1 \right)}{\sqrt{\left(\frac{2(2k-1)(k-1)}{3kT} \right)}} \qquad (4\text{-}5)$$

$$RK_2 = \frac{\left(\frac{1}{Tk}\sum_{t=k+1}^{T}(R_{2t} + R_{2t-1} + ...R_{2t-k})^2 - 1\right)}{\sqrt{\left(\frac{2(2k-1)(k-1)}{3kT}\right)}} \quad (4\text{-}6)$$

where

$$RK_{1t} = \left(R(y_t) - \frac{T+1}{2}\right) / \sqrt{\frac{(T-1)(T+1)}{12}}$$

$$RK_{2t} = \Phi^{-1}\left(R(y_t)/(T+1)\right)$$

Φ is the standard normal cumulative distribution function and $R(y_t)$ is ranked amongst T observations of differences in logs in the volatility series from $y_1, y_2, ...y_T$ with simple linear transformation used to produce a ranking with sample mean of zero and variance of one. The sign-based variance ratio tests are specified as:

$$S_1 = \frac{\left(\frac{1}{Tk}\sum_{t=k+1}^{T}(S_t + S_{t-1} + ...S_{t-k})^2 - 1\right)}{\sqrt{\left(\frac{2(2k-1)(k-1)}{3kT}\right)}} \quad (4\text{-}7)$$

where $S_t + ... + S_{t-k}$ are the signs of the differences in logs in the volatility series, which are assumed to be independent and identically distributed (*iid*) with mean of zero and variance of one. The test statistics for RK_1, RK_2 and S_1 for a given T and interval k can be compared with the critical values found in Wright (2000)[82]. The test statistics are estimated for each of the volatility series.

[82] Refer to Table 1 on pp.3 of Wright (2000).

4.4 Empirical Results for the Conventional Variance Ratio Test

The results for the conventional variance ratio tests are presented in Table 4-4. The tests are performed on differences in logs of the volatility series as well as the volatility levels. The first column shows the respective maturities of the volatility series for each of the currency-pairs. The test results for the GBP/USD currency pair are presented in columns two to five. The second and the fourth columns report the estimated variance-ratio, *VR*, for each holding-period *q*. The corresponding standard normal Zs-test statistics under the assumption of homoscedasticity are displayed in columns three and five. For the rest of the currency pairs, the results are tabulated in the same manner.

Table 4-4 reveals that the variance ratio test under homoscedasticity rejects the unit variance hypothesis overwhelmingly when the test is applied on the volatility levels. In fact, the null hypothesis of unity variance ratio can be rejected at the 1% level of significance in all cases. The Zs-test statistic ranges from 18.3 for the two-year AUD/USD volatility series to 148.5 for the one-year GBP/USD volatility series. The high homoscedastic Zs-test statistic corresponds with large deviation in variance ratio from unity where in most cases, the estimated variance ratios are well in excess of five. Drawing from the autocorrelation analysis reported in Table 4-3, the Ljung-Box Q statistics and the variance ratio statistics are consistent with one another up to this point. This suggests that the rejection of the variance ratio test may be attributed to the presence of autocorrelation in the implied volatility series.

Table 4-4: Variance Ratio Estimation and Hypothesis Testing of Unity Variance Ratios Using *Zs*(q)

		GBP/USD				EUR/USD				AUD/USD				USD/JPY			
		Diff. in logs		Levels		Diff. in logs		Levels		Diff. in logs		Levels		Diff. in logs		Levels	
	q	*VR*	*Zs*	*VR*	*Zs*	*VR*	*Zs*	*VR*	*Zs*	*VR*	*Zs*	*VR*	*Zs*	*VR*	*Zs*	*VR*	*Zs*
1-Week	5	0.440	-8.609 ***	4.419	52.528 ***	0.786	-3.300 ***	4.163	48.880 ***	0.813	-2.895 ***	4.110	48.159 ***	0.735	-4.097 ***	4.266	50.466 ***
	10	0.271	-7.271 ***	8.330	73.078 ***	0.509	-4.920 ***	7.594	66.115 ***	0.604	-3.982 ***	6.388	54.137 ***	0.459	-5.419 ***	7.504	65.206 ***
	20	0.180	-5.557 ***	15.576	98.719 ***	0.285	-4.871 ***	13.538	85.401 ***	0.391	-4.159 ***	6.587	38.137 ***	0.284	-4.876 ***	12.866	80.823 ***
	30	0.165	-4.557 ***	22.264	116.075 ***	0.269	-4.010 ***	18.905	98.296 ***	0.372	-3.456 ***	5.085	22.474 ***	0.253	-4.104 ***	17.514	90.659 ***
1-Month	5	0.831	-2.603 ***	4.888	59.730 ***	0.824	-2.724 ***	4.287	50.794 ***	0.828	-2.666 ***	4.213	49.750 ***	0.810	-2.936 ***	4.643	56.292 ***
	10	0.789	-2.106 **	9.591	85.643 ***	0.748	-2.527 **	8.228	72.469 ***	0.807	-1.944 *	6.606	56.327 ***	0.639	-3.619 ***	8.715	77.350 ***
	20	0.753	-1.675 *	18.474	118.343 ***	0.604	-2.697 ***	15.208	96.777 ***	0.727	-1.864 *	6.453	37.224 ***	0.532	-3.190 ***	15.626	99.625 ***
	30	0.748	-1.374	26.683	140.195 ***	0.537	-2.540 **	21.208	110.943 ***	0.697	-1.668 *	4.850	21.181 ***	0.471	-2.906 ***	21.325	111.585 ***
3-Month	5	0.856	-2.211 **	4.887	59.723 ***	0.929	-1.093	4.091	47.767 ***	0.717	-4.379 ***	4.216	49.803 ***	0.894	-1.631	4.780	58.411 ***
	10	0.817	-1.820 *	9.579	85.520 ***	0.888	-1.127	7.886	69.040 ***	0.669	-3.330 ***	6.610	56.370 ***	0.752	-2.482 **	9.152	81.736 ***
	20	0.805	-1.320	18.371	117.651 ***	0.800	-1.363	14.691	93.258 ***	0.601	-2.726 ***	6.269	35.964 ***	0.694	-2.087 **	16.858	108.019 ***
	30	0.800	-1.091	26.371	138.495 ***	0.737	-1.443	20.594	107.572 ***	0.590	-2.254 **	4.538	19.467 ***	0.629	-2.036 **	23.539	123.738 ***
6-Month	5	1.091	1.397	4.952	60.720 ***	0.928	-1.113	3.924	45.180 ***	0.576	-6.564 ***	4.222	49.891 ***	0.928	-1.116	4.862	59.672 ***
	10	1.168	1.670 *	9.794	87.669 ***	0.912	-0.886	7.574	65.911 ***	0.495	-5.076 ***	6.618	56.453 ***	0.821	-1.795 *	9.445	84.674 ***
	20	1.189	1.281	19.085	122.486 ***	0.858	-0.967	14.200	89.911 ***	0.440	-3.821 ***	6.190	35.429 ***	0.800	-1.362	17.829	114.628 ***
	30	1.226	1.231	27.904	146.865 ***	0.818	-1.001	19.971	104.152 ***	0.436	-3.103 ***	4.406	18.738 ***	0.735	-1.452	25.419	134.060 ***
1-Year	5	1.150	2.310 **	4.961	60.859 ***	0.815	-2.855 ***	3.772	42.829 ***	0.906	-1.463	4.238	50.143 ***	0.962	-0.592	4.895	60.182 ***
	10	1.251	2.500 **	9.829	88.019 ***	0.789	-2.117 **	7.274	62.909 ***	0.901	-0.991	6.673	57.002 ***	0.877	-1.233	9.568	85.901 ***
	20	1.286	1.938 *	19.222	123.416 ***	0.778	-1.513	13.670	86.303 ***	0.898	-0.697	6.297	36.161 ***	0.883	-0.797	18.265	117.599 ***
	30	1.348	1.898 *	28.204	148.500 ***	0.756	-1.339	19.243	100.153 ***	0.900	-0.548	4.588	19.743 ***	0.804	-1.074	26.299	138.894 ***
2-Year	5	1.262	4.027 ***	4.962	60.875 ***	0.808	-2.963 ***	3.655	41.017 ***	0.422	-8.954 ***	4.232	50.050 ***	0.989	-0.165	4.903	60.305 ***
	10	1.393	3.915 ***	9.827	87.994 ***	0.781	-2.195 **	7.032	60.478 ***	0.325	-6.787 ***	6.642	56.688 ***	0.922	-0.786	9.595	86.176 ***
	20	1.504	3.416 ***	19.181	123.136 ***	0.764	-1.604	13.183	82.985 ***	0.276	-4.942 ***	6.142	35.098 ***	0.937	-0.430	18.353	118.198 ***
	30	1.624	3.405 ***	28.052	147.673 ***	0.736	-1.449	18.513	96.148 ***	0.266	-4.041 ***	4.321	18.272 ***	0.858	-0.778	26.462	139.786 ***

Note: This table reports the variance ratios and the corresponding test statistics. The sample period spans from 29 August, 2001 to 28 April, 2006 using volatility levels and differences in logs of the quoted implied volatility series. VR denotes the estimated variance ratio at each holding-period q and Zs is the test statistics under the homoscedasticity assumption. The tests are conducted with small sample size adjustment.

****significant at the 1% level*

***significant at the 5% level*

**significant at the 10% level*

In sharp contrast, rejections of the null hypothesis are most evident for short-dated series when the test is repeated using first differences of the implied volatility series. For these series, the Zs-test statistics are above 1.96 suggesting the random walk hypothesis can be comfortably rejected at the 5% level of significance (two-tailed test). Notably, the one- week and one-month series are consistently rejected across all four currency-pairs. For the USD/JPY currency-pair, rejections of the null hypothesis at 1% level of significance can be found for the one-week and one-month series at various holding-periods (q). However for the AUD/USD and the GBP/USD currency pairs, rejections of the null hypothesis are more widespread and can be found across all maturities. Consistent with this pattern, the variance ratios estimated using first differences are also closer to unity compared with those estimated with volatility levels. This can be seen across all currency-pairs.

Since the *Zs*-test statistics are calculated based on the assumption of homoscedasticity, rejection of the null hypothesis of a random walk process could be largely the result of heteroscedasticity or autocorrelation in the data series. To confirm this conjecture, the heteroscedastic-consistent Z-test statistic of Lo and MacKinlay (1988) is used to test for the rejection of the null hypothesis. The results are displayed in Table 4-5.

Notably, the results in Table 4-5 are considerably different from those reported in Table 4-4 when heteroscedastic adjustment is applied to the Z-test statistics. Specifically, the heteroscedastic-consistent z statistics are substantially lower than the unadjusted equivalent in Table 4-4 when the variance ratio test is applied on the volatility levels. This pattern is observed across all series in the sample.

Table 4-5: Variance Ratio Estimation and Hypothesis Testing of Unity Variance Ratios Using *Z*(q)

		GBP/USD				EUR/USD				AUD/USD				USD/JPY			
		Diff. in logs		Levels		Diff. in logs		Levels		Diff. in logs		Levels		Diff. in logs		Levels	
	q	*VR*	*Z*	*VR*	*Z*	*VR*	*Z*	*VR*	*Z*	*VR*	*Z*	*VR*	*Z*	*VR*	*Z*	*VR*	*Z*
1-Week	5	0.440	-1.588	4.419	30.390 ***	0.786	-3.019 ***	4.163	33.880 ***	0.813	-2.519 **	4.110	6.784 ***	0.735	-3.376 ***	4.266	34.086 ***
	10	0.271	-2.245 **	8.330	43.122 ***	0.509	-4.453 ***	7.594	47.938 ***	0.604	-3.540 ***	6.388	8.150 ***	0.459	-4.488 ***	7.504	46.867 ***
	20	0.180	-2.446 **	15.576	59.498 ***	0.285	-4.496 ***	13.538	63.504 ***	0.391	-3.847 ***	6.587	6.286 ***	0.284	-4.111 ***	12.866	62.116 ***
	30	0.165	-2.311 **	22.264	70.923 ***	0.269	-3.750 ***	18.905	74.249 ***	0.372	-3.253 ***	5.085	4.056 ***	0.253	-3.525 ***	17.514	72.751 ***
1-Month	5	0.831	-1.864 *	4.888	29.552 ***	0.824	-2.328 **	4.287	32.883 ***	0.828	-2.238 **	4.213	6.931 ***	0.810	-2.037 **	4.643	38.461 ***
	10	0.789	-1.852 *	9.591	42.697 ***	0.748	-2.170 **	8.228	49.159 ***	0.807	-1.704 *	6.606	8.225 ***	0.639	-2.638 ***	8.715	54.828 ***
	20	0.753	-1.657 *	18.474	59.867 ***	0.604	-2.380 **	15.208	67.572 ***	0.727	-1.722 *	6.453	5.939 ***	0.532	-2.475 **	15.626	73.796 ***
	30	0.748	-1.465	26.683	71.954 ***	0.537	-2.285 **	21.208	78.122 ***	0.697	-1.575	4.850	3.720 ***	0.471	-2.346 **	21.325	85.711 ***
3-Month	5	0.856	-1.800 *	4.887	30.853 ***	0.929	-0.778	4.091	29.878 ***	0.717	-1.697 *	4.216	6.824 ***	0.894	-1.072	4.780	39.237 ***
	10	0.817	-1.738 *	9.579	44.519 ***	0.888	-0.824	7.886	45.488 ***	0.669	-1.548	6.610	8.074 ***	0.752	-1.761 *	9.152	56.278 ***
	20	0.805	-1.426	18.371	62.105 ***	0.800	-1.056	14.691	62.604 ***	0.601	-1.414	6.269	5.629 ***	0.694	-1.598	16.858	77.395 ***
	30	0.800	-1.225	26.371	74.132 ***	0.737	-1.156	20.594	72.471 ***	0.590	-1.215	4.538	3.358 ***	0.629	-1.619	23.539	92.037 ***
6-Month	5	1.091	0.144	4.952	33.339 ***	0.928	-0.522	3.924	26.312 ***	0.576	-1.289	4.222	6.784 ***	0.928	-0.638	4.862	36.491 ***
	10	1.168	0.304	9.794	48.444 ***	0.912	-0.459	7.574	40.589 ***	0.495	-1.248	6.618	8.016 ***	0.821	-1.162	9.445	52.702 ***
	20	1.189	0.291	19.085	68.639 ***	0.858	-0.546	14.200	56.413 ***	0.440	-1.087	6.190	5.498 ***	0.800	-0.969	17.829	73.789 ***
	30	1.226	0.386	27.904	83.524 ***	0.818	-0.592	19.971	65.741 ***	0.436	-0.927	4.406	3.207 ***	0.735	-1.079	25.419	89.170 ***
1-Year	5	1.150	0.507	4.961	36.169 ***	0.815	-0.984	3.772	24.003 ***	0.906	-0.860	4.238	6.856 ***	0.962	-0.283	4.895	33.777 ***
	10	1.251	0.740	9.829	52.647 ***	0.789	-0.849	7.274	37.601 ***	0.901	-0.617	6.673	8.127 ***	0.877	-0.697	9.568	48.918 ***
	20	1.286	0.711	19.222	74.877 ***	0.778	-0.676	13.670	52.816 ***	0.898	-0.460	6.297	5.635 ***	0.883	-0.504	18.265	68.945 ***
	30	1.348	0.846	28.204	91.471 ***	0.756	-0.625	19.243	61.750 ***	0.900	-0.371	4.588	3.395 ***	0.804	-0.709	26.299	83.760 ***
2-Year	5	1.262	1.153	4.962	37.057 ***	0.808	-0.872	3.655	23.035 ***	0.422	-1.379	4.232	6.761 ***	0.989	-0.074	4.903	33.001 ***
	10	1.393	1.379	9.827	53.886 ***	0.781	-0.766	7.032	36.167 ***	0.325	-1.325	6.642	7.983 ***	0.922	-0.425	9.595	47.785 ***
	20	1.504	1.499	19.181	76.422 ***	0.764	-0.629	13.183	50.602 ***	0.276	-1.125	6.142	5.403 ***	0.937	-0.261	18.353	67.335 ***
	30	1.624	1.742 *	28.052	93.027 ***	0.736	-0.593	18.513	58.909 ***	0.266	-0.968	4.321	3.104 ***	0.858	-0.493	26.462	81.790 ***

Note: This table reports variance ratios with the corresponding test statistics. The sample period spans from 29 August, 2001 to 28 April, 2006 using volatility levels and differences in logs of the quoted implied volatility series. VR denotes the estimated variance ratio at each holding-period q and Z is the Lo and MacKinlay (1988) test statistics robust to heteroscedasticity. The tests are conducted with small sample size adjustment.

****significant at the 1% level*

***significant at the 5% level*

**significant at the 10% level*

A similar pattern also exists when the test is applied on the differences in logs of the volatility series, although the reduction in the estimated test statistics is less pronounced when compared to the volatility levels. For instance, the homoscedastic Zs reported in Table 4-4 is 139.786 (q=30) for the two-year USD/JPY volatility series but it has a considerably lower test statistic of 81.790 (q=30 in Table 4-5) when the heteroscedastic robust Z statistic is tested on the volatility levels.

A relatively small reduction in the test statistics is noted when the test is repeated using differences in logs of the implied volatility series. This can be seen in the z-test statistic for the two-year USD/JPY volatility series which reduced from -0.778 to -0.473 when the homoscedastic adjustment is applied to the standard z-test statistic. This suggests that heteroscedasticity is more severe in the implied volatility levels than the first difference in the logs of implied volatility. The reductions in the test statistics do not alter the test results for the volatility levels and the null hypothesis remains strongly rejected at the 1% level of significance in all cases.

Together, the results presented in Tables 4-4 and 4.5 suggest that most of the rejections of the null hypothesis under homoscedasticity are not robust to heteroscedasticity when the variance ratio test is performed on the difference in log volatility series. In particular, the long-dated series of six-month, one-year and two-year are no longer rejected under the heteroscedastic-consistent Z statistic. Therefore it is clear that the variance ratios of these series are significantly different from one due to the presence of heteroscedasticity in the volatility process. More importantly, this is consistent with the findings of Diebold and Nerlove (1989) who find strong ARCH effects in the volatility patterns of spot exchange rates.

In contrast, short-dated implied volatility series of one-week and one-month remain significant in Table 4-5 with the heteroscedastic adjusted z-test statistic. The only exception is the two-year GBP/USD series which is marginally rejected with a Z-test statistic of 1.742 over an interval of 30 days.

The rejection of the null hypothesis is particularly strong for the Japanese yen. For example, the heteroscedastic-consistent z-statistics associated with time interval, q of 5, 10, 20 and 30, are -3.376, -4.488, -4.111, -3.525 for the one-week USD/JPY series. Clearly, the null hypothesis is strongly rejected at the 1% level of significance.

For the three-month series, rejections of the unity variance ratio assumption are also reported for time intervals of 10 and 20 days. For the EUR/USD and AUD/USD currency pairs, rejections of the null are also reported for the one-week and one-month series. These short-dated series results are robust to heteroscedasticity and thus the rejections of the variance ratio test appear to be related to autocorrelation rather than heteroscedasticity.

4.5 Empirical Results for the Nonparametric Variance Ratio Test

Although the preceding test results reported in Table 4-5 are robust to heteroscedasticity, the conventional variance ratio assumes the sampling distribution of the variance ratio test statistic is normally distributed. As the quoted volatility series are far from normally distributed, violation of the underlying assumption in the variance ratio test statistics can produce erroneous test results.

Table 4-6: Hypothesis Testing of Unity Variance Ratios Using Ranks and Signs

		GBP/USD			EUR/USD			AUD/USD			USD/JPY		
	K	***RK₁***	***RK₂***	***S₁***	***RK₁***	***RK₂***	***S₁***	***RK₁***	***RK₂***	***S₁***	***RK₁***	***RK₂***	***S₁***
1-Week	5	-2.702 ***	-3.031 ***	-2.360 **	-3.140 ***	-3.302 ***	-2.844 ***	-2.354 **	-2.746 ***	-0.939	-4.229 ***	-4.447 ***	-3.030 ***
	10	-3.963 ***	-4.554 ***	-3.177 ***	-4.319 ***	-4.803 ***	-3.322 ***	-3.481 ***	-4.016 ***	-1.572	-5.220 ***	-5.638 ***	-3.524 ***
	20	-3.735 ***	-4.216 ***	-2.914 ***	-3.925 ***	-4.595 ***	-2.840 ***	-3.347 ***	-4.101 ***	-1.498	-4.645 ***	-5.020 ***	-3.390 ***
	30	-3.102 ***	-3.475 ***	-2.548 **	-3.167 ***	-3.751 ***	-2.231 **	-2.544 **	-3.305 ***	-1.107	-3.872 ***	-4.189 ***	-3.099 ***
1-Month	5	-2.494 **	-2.773 ***	-1.425	-3.103 ***	-2.926 ***	-2.594 ***	-3.042 ***	-2.917 ***	-3.655 ***	-3.439 ***	-3.271 ***	-2.714 ***
	10	-1.678 *	-2.240 **	-0.579	-2.925 ***	-2.899 ***	-2.386 **	-2.405 **	-2.278 **	-2.763 ***	-3.944 ***	-4.038 ***	-2.870 ***
	20	-1.396	-1.941 *	0.147	-2.610 ***	-2.799 ***	-2.129 **	-2.001 **	-2.088 **	-1.993 **	-3.362 ***	-3.544 ***	-2.720 ***
	30	-1.046	-1.582	0.516	-2.394 **	-2.578 ***	-1.935 *	-1.807 *	-1.871 *	-1.574	-3.021 ***	-3.172 ***	-2.701 ***
3-Month	5	-1.797 *	-2.034 **	0.003	-0.991	-1.103	-0.436	-1.117	-1.466	0.228	-0.867	-1.045	-0.679
	10	-1.316	-1.731 *	0.761	-0.845	-1.044	-0.654	-0.885	-1.218	-0.042	-2.185 **	-2.394 **	-1.868 *
	20	-1.075	-1.406	1.081	-0.725	-1.244	-0.341	-1.017	-1.394	-0.043	-2.190 **	-2.276 **	-1.977 **
	30	-0.698	-1.102	1.381	-0.775	-1.374	-0.344	-0.839	-1.237	0.392	-1.922 *	-2.089 **	-1.679 *
6-Month	5	3.586 ***	3.328 ***	1.079	1.877 *	1.186	1.248	1.926 *	1.475	1.826 *	0.790	0.497	1.270
	10	3.359 ***	3.076 ***	1.045	1.319	0.905	0.535	1.723 *	1.372	1.630	-0.809	-1.014	0.124
	20	2.692 ***	2.263 **	0.439	0.426	0.143	-0.388	0.999	0.790	0.996	-0.904	-1.020	-0.175
	30	2.903 ***	2.335 **	0.600	0.183	-0.143	-0.446	0.895	0.697	0.927	-0.749	-1.004	-0.340
1-Year	5	3.662 ***	3.961 ***	1.576	1.475	0.951	1.053	-0.065	-0.670	0.005	2.542 **	2.310 **	2.710 ***
	10	3.321 ***	3.646 ***	1.716 *	1.251	1.022	0.570	0.701	0.038	0.587	0.867	0.647	1.429
	20	2.706 ***	2.772 ***	1.441	0.824	0.783	-0.052	0.967	0.474	0.565	0.487	0.374	0.515
	30	2.837 ***	2.768 ***	1.289	0.635	0.543	-0.217	0.762	0.400	0.327	0.165	-0.011	0.018
2-Year	5	4.115 ***	4.912 ***	2.671 ***	2.611 ***	2.192 **	1.797 *	1.292	1.206	-0.713	3.010 ***	2.995 ***	1.815 *
	10	3.667 ***	4.434 ***	2.446 **	2.227 **	2.010 **	1.393	2.151 **	2.268 **	-0.197	1.455	1.369	0.343
	20	2.957 ***	3.617 ***	1.989 **	1.552	1.416	1.058	1.609	2.024 **	-0.779	0.889	0.946	-0.483
	30	3.028 ***	3.646 ***	1.900 *	1.155	0.961	0.717	1.478	1.949 *	-0.939	0.343	0.369	-0.833

Note: The table reports nonparametric variance ratio test of Wright (2000) with a null hypothesis of one. The sample period spans from 29 August, 2001 to 28 April, 2006 using differences in logs of implied volatility quotes. The rank tests statistics are denoted as RK_1 and RK_2 while S_1 denotes the results for the sign tests.
****significant at the 1% level*
***significant at the 5% level*
**significant at the 10% level*

In order to confirm the robustness of the test results, additional variance ratio tests are conducted using the nonparametric ranks and signs tests of Wright (2000), which are free from distribution assumptions. The methodology is presented in Equations (4-5), (4-6) and (4-7). Table 4-6 provides the ranks and signs test statistics R_1, R_2 and S_1 with time intervals of 5-day, 10-day, 20-day and 30-day. This is consistent with the conventional variance ratio tests previously reported in Tables 4-4 and 4-5.

As indicated in Table 4-6, the nonparametric ranks and signs statistics show that there is sufficient evidence to reject the null hypothesis of unity variance ratio across all currency pairs. Notably, the three-month contracts have the lowest rejection rate among the various maturities. For maturities of one month or less, there is strong rejection of the random walk hypothesis across all currency pairs at various values of k. The rejections are stronger with the rank-based tests RK_1 and RK_2. These test statistics are mostly significant at the 5% level and constitute convincing evidence against the random walk hypothesis across all currency pairs. The test statistics are larger for short-dated volatility. These results are fairly consistent with the heteroscedasticity adjusted conventional variance ratio tests reported in Table 4-5 for the EUR/USD and USD/JPY currency pairs.

In contrast with the rank-based test results, the sign-based tests provide some evidence of rejection of the null of unity variance ratio for the one-year and two-year volatility series. However, as demonstrated by Wright (2000), the sign-based test statistics are normally less robust than the rank-based tests but they can still be more powerful than the conventional variance ratio tests. Following a recent paper by Belaire-

Franch and Opong (2005), Sidack-adjusted *p*-values[83] are used to control for possible test-size distortions in the ranks and signs tests. The adjusted *p*-value is estimated as:

$$\widetilde{p}_{ji}^{S} = 1 - (1 - P_{ji})^{\alpha} \tag{4-8}$$

where

$\alpha =$ Number of *k* values

$P_{ji} =$ *p*-value computed for nonparametric variance ratio test *j* for a given value *k*,

$i = 1,2,\ldots\ \alpha$

To perform this adjustment, the *p*-value of each variance ratio test that corresponds to the ranks and signs tests are estimated for each currency pair. Since the tests are performed over four different intervals, the number of *k* values used to estimate the corrected *p*-values is set to four. Thus, for each currency pair, the *p*-values are estimated for every maturity using intervals of 5, 10, 20 and 30 days, resulting in a total of 72 adjusted *p*-values for the entire sample.

The final test results for the adjusted *p*-values are reported in Table 4-7. As can be seen, the rejections of the random walk hypothesis persist even after controlling for data bias due to size distortions. Notably, strong rejection of the unity variance ratio assumption is found for the one-week series. However, in contrast with the results in Table 4-6, rejections of the null hypothesis are only reported for the one-month EUR/USD and USD/JPY series. Overall, the results are fairly consistent with those reported previously (see Table 4-5) in the conventional variance ratio test with heteroscedestic-robust test statistics. With the exception of the GBP/USD currency pair,

[83] This is consistent with Psaradakis (2000).

no rejection of unity variance ratio is reported for series with maturity of three month and above. It is interesting to note that for the GBP/USD currency pair, the six-month, one-year and two-year volatility series still reject the ranks tests using RK_1 and RK_2 although only marginal rejection was reported for the two-year volatility in Table 4-5.

Table 4-7: Sidack-adjusted $\widetilde{P}_{ji}^{S}$ -values for Ranks and Signs

	1-Week		1-Month		3-Month	6-Month		1-Year		2-Year	
Panel A: GBP/USD											
RK1	0.011	**	0.431		0.662	0.014	**	0.015	**	0.007	***
RK2	0.004	***	0.183		0.441	0.051	*	0.014	**	0.001	***
S1	0.041	**	0.897		0.794	0.750		0.368		0.120	
Panel B: EUR/USD											
RK1	0.004	***	0.029	**	0.867	0.688		0.694		0.306	
RK2	0.002	***	0.022	**	0.659	0.868		0.837		0.385	
S1	0.040	**	0.107		0.984	0.884		0.880		0.561	
Panel C: AUD/USD											
RK1	0.030	**	0.124		0.796	0.531		0.909		0.380	
RK2	0.007	***	0.116		0.557	0.701		0.978		0.271	
S1	0.590		0.146		0.998	0.552		0.981		0.910	
Panel D: USD/JPY											
RK1	0.000	***	0.003	***	0.305	0.880		0.717		0.579	
RK2	0.000	***	0.003	***	0.256	0.826		0.750		0.581	
S1	0.005	***	0.022	**	0.401	0.909		0.627		0.768	

Notes: This table presents the final test results using the Sidack-corrected p-values. The adjusted p-values are calculated from individual p-value that corresponds to the variance ratio test with four values of k (5,10,20,30).
****significant at the 1% level*
***significant at the 5% level*
**significant at the 10% level*

4.6 Mean Reversion

The variance ratio statistics is strictly unity when a stationary series is uncorrelated over time. Campbell, Lo and MacKinlay (1997) show that the ratio of the variance of a q-period variable and q times the variance of a one-period variable can be reduced to $(1+\rho_1)$, where ρ_1 is the first-order autocorrelation coefficient of the variable.

Under this rationale, the calculated variance ratio is simply one plus the zero autocorrelation (that is $\rho_1 = 0$) for an uncorrelated return series, and hence this gives rise to the notion of variance ratio is unity. However, if positive first-order autocorrelation is present in the return series, then the sum of one plus the first-order autocorrelation will be larger than one. Conversely, the presence of negative first-order autocorrelations will reduce $(1+\rho_1)$ to below a value of one.

If a series reverts toward its long-term mean over time[84] then the variance for *q*-period return will be less than *q* times the one period variance resulting in variance ratio being less than unity. In other words, negative first-order autocorrelation will reduce $(1+\rho_1)$ to less than unity. This property of variance ratios provides a simple and useful diagnostic tool for examining characteristics of asset price returns. Indeed, studies by Poterba and Summers (1988), Lo and MacKinlay (1989) and Kim, Nelson and Startz (1991) use this property to examine the presence of mean reversion in stock prices.

Figure 4-1 and 4-2 present the estimated variance ratios for each currency by maturity with a time interval of q=10 and q=20 respectively. This is based on the variance ratio statistics calculated using differences in logs of implied volatility reported in Table 4-5. The mean variance ratio is also calculated for each of the respective maturities. For the variance ratio estimated over a 10-day interval, the average variance ratio increases steadily from a value of 0.5 for the one-week series to 1.0 for the one-year series. Notably, the one-year series has the highest mean variance ratio which is close to one.

[84]This may due to the presence of transitory factors in the price series caused by speculative trades or changes in required rate of returns. See Poterba and Summers (1988).

Figure 4-1: Variance Ratio versus Maturity (*q=10*)

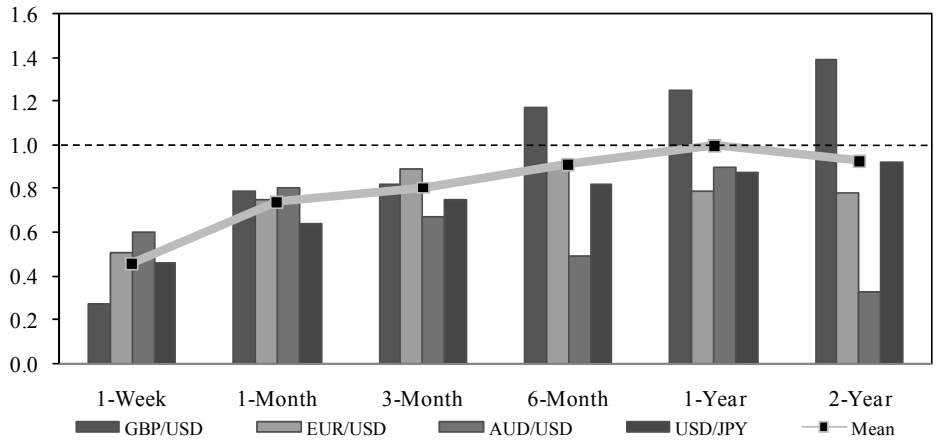

Figure 4-2: Variance Ratio versus Maturity (*q=20*)

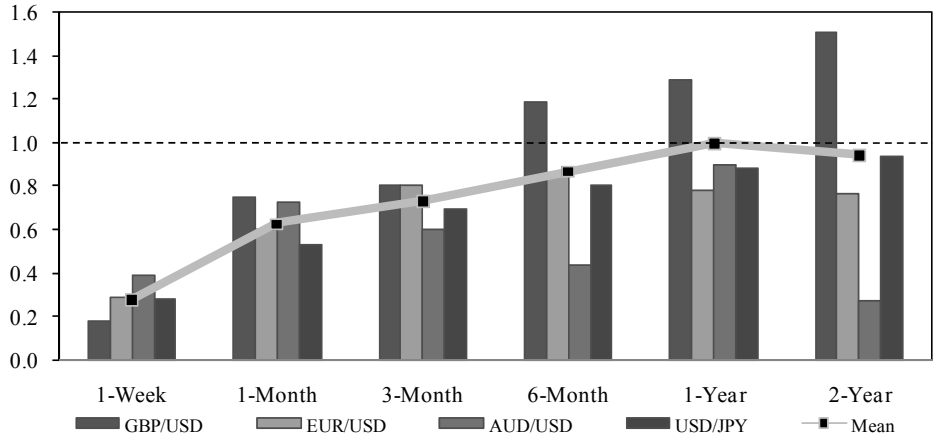

This is followed by the two-year series which has an average of approximately 0.9. For the short-dated series of one-month and three-month, the estimated variance ratios fall between 0.7 and 0.8. The lowest mean variance ratio is reported for the one-week series. On the whole, the mean variance ratio appears to increase steadily with maturity through to 12 months.

In terms of currency type, the GBP/USD currency pair exceeded the variance ratio of one for maturities of six-month, one-year and two-year with estimated variance

ratios between 1.2 and 1.4. This is indicative of positive autocorrelation in the volatility process and coincides with the test results presented in Table 4-7 which show rejection for the same series even after controlling for test size distortions. Thus, the rejection of the variance ratio test for these maturities is attributable to high positive autocorrelation in the GBP/USD volatility series.

On the other hand, the estimated variance ratios for the AUD/USD series are consistently below unity across all maturities. These exhibit the lowest variance ratios for the three-month, six-month and two-year series. In contrast with the GBP/USD series, this suggests the presence of negative autocorrelation in the volatility series and therefore there is a greater tendency for the volatility series to revert toward their mean. The pattern in Figure 4-2 constructed at a higher interval of twenty days, exhibits a similar trend.

4.7 Model Comparison Tests

It should be noted that while the results from the preceding analyses are unambiguous for the short maturities of one week and one month, evidence for the longer maturities is somewhat mixed. Furthermore, both the parametric and nonparametric variance ratio tests provide in-sample analysis for the null hypothesis of random walks. Such tests may not be very meaningful or have little practical value for market practitioners and forecasters. Therefore, to substantiate the validity of the test results, further evidence seems warranted. In view of this, implied volatility forecasts based on the random walk model is constructed. The forecasting ability of this model is

compared with two alternative competing models and the test results would render further insights into the behaviour of the implied volatility series and the forecasting ability of the alternative models.

In this section, further analysis is performed by examining the forecasting ability of two competing models against the random walk process. If the implied volatility series is best characterised as a random-walk process, then forecasting using a random-walk model should generate superior results compared to other competing models.

Three different time series forecasting models are constructed including a driftless random walk model, an autoregressive integrated moving average (ARIMA) model and an artificial neural networks (ANNs) model. These models are used to generate one-day ahead out-of-sample forecasts of implied volatility changes for each of the six maturities examined in the previous section. The out-of-sample prediction is adopted as a means of avoiding data mining issues associated with in-sample inference.

The implied volatility data is divided into two subsamples. The first subsample consists of 900 observations of daily log implied volatility changes from 29 August 2001 to 29 April 2005 and is used for modelling. For out-of-sample forecasting evaluations, the second subsample is used. This consists of 250 daily observations from 30 August 2005 to 28 April 2006. The modelling and forecasting tests are performed using first-differences in the implied volatility series. This specification is motivated by the lack of stationarity in the volatility levels according to the unit root results reported in Table 4-2, particularly for the longer maturities. For the competing models, the well-

established univariate autoregressive integrated moving average (ARIMA) model is used as the linear forecasting model, while the more flexible artificial neural networks (ANNs) model is chosen to capture possible nonlinear structure in the volatility series.

4.7.1 The Random Walk Model

Empirical evidence suggests that foreign exchange volatility is persistent with a root close to unity; for example, the studies by Engle and Bollerslev (1986) and Engle and Gonzalez-Rivera (1991). It appears reasonable to expect that the random walk is used as the first forecasting model. The persistent nature of implied volatility also suggests that an $I(1)$ process provides a better characterisation of the volatility series for the purpose of forecasting. Thus, the first specification considered is a driftless random walk model:

$$\Delta IV_t^M = \mu_t \tag{4-9}$$

where,

ΔIV_t^M = The first-difference of the implied volatility series for a given maturity M for period t,

μ_t = a white noise process.

4.7.2 The ARIMA(*p,1,q*) Model

This is a general univariate linear model to account for higher-order autoregressive processes combined with a moving-average processes to capture time series variation in the data. It allows the series, ΔIV_t, to depend linearly on its own past values plus a combination of current and previous values of a white noise error term:

$$\Delta IV_t^M = \sum_{i=1}^{p} \phi_i \Delta IV_{t-i}^M + \varepsilon_t + \sum_{j=1}^{q} \theta_j \varepsilon_{t-j} \qquad (4\text{-}10)$$

where,

ε_{t-j} = a white noise process,

p = order of autoregressive component,

q = order of moving-average component,

The parameters p and q are non-negative integers and the autoregressive and moving average-parameters are defined as $0 < |\phi| < 1$, $0 < |\theta| < 1$, $\phi + \theta \neq 0$ so that the series ΔIV_t is stationary.

The Schwarz's Bayesian information criterion (SBIC) is relied upon to determine the appropriate values for p and q (Brooks, 2002). The model is estimated for all six maturities that correspond to each of the four currency pairs. In most instances, the information criterion selects either an ARIMA(2,1,1) or an ARIMA(2,1,2) process for the short-dated series of one-week and one-month. For the three-month, six-month, one-year and two-year series, the SBIC criterion results in selection of an ARIMA(1,1,0) process.

4.7.3 Artificial Neural Networks Model

The artificial neural networks (ANNs) model is a nonparametric technique that is not new in the finance literature. For instance, Trippi and DeSieno (1992) and Altman, Marco and Varetto (1994) have previously examined the usefulness of this method in the trading of equity index futures and the prediction of corporate distress respectively. In a recent study, Ferland and Lalancette (2006) also adopt the ANNs model to estimate volatility in the EuroDollar futures market. Due to the flexibility of this approach, it can be used to approximate any nonlinear behaviour in the data series (Campbell, Lo and MacKinlay, 1997). The estimation procedure uses a feedforward neural network[85] model with two hidden layers.

$$\Delta IV_t^M = \alpha_0 + \sum_{l=1}^{k} \alpha_l g\left(\sum_{i=1}^{s} \psi_{il} \Delta IV_{t-i}^M + \psi_{0l} \right) + \varepsilon_t \qquad (4\text{-}11)$$

where

ΔIV_t^M	=	system output or the estimated change in the *IV* series for maturity *M* estimated at period *t*,
s	=	number of inputs or lagged first difference of the implied volatility series,
α_0	=	intercept coefficient of the model,
α_l	=	network weighting estimated from l =1,…to k,
ψ_{il}	=	the weights from the input i layer to the hidden unit,
ψ_{0l}	=	bias weights of the hidden unit l,
ε_t	=	error term of the model.

[85] Further exposition on ANNs is provided in Campbell, Lo, and MacKinlay (1997).

The inputs are connected to multiple nodes; weighting is applied at each node and $g(.)$ determines the connections between the nodes and is used as the activation function to enhance the nonlinearity of the model.

4.8 The Forecast Performance Test

The out-of-sample forecasting accuracy of the models is carried out using three different evaluation measures. The first measure is the root-mean-squared error (RMSE) while the mean-error (ME) and mean-absolute-error (MAE) are also reported in the test results. Out-of-sample forecasts of the series ΔIV_t^M are calculated using each of the models defined in the previous section and these one-day ahead forecasts are estimated using data from the second subsample (30 August 2005 to 28 April 2006). For a given maturity *M* at period *t*, the RMSE is defined as:

$$RMSE = \sqrt{\frac{1}{N}\sum_{t=1}^{N}(\Delta\hat{IV}_t^M - \Delta IV_t^M)^2} \tag{4-12}$$

where $\Delta\hat{IV}_t^M$ represents the forecast values for options with maturity *M* at period *t*, ΔIV_t^M is the actual value for maturity *M* at period *t* and *N* is the forecast horizon which is one day.

The second forecast performance test provides a relative measure of forecasting error for the rival models. A ratio, $RMSE_{CM}/RMSE_{RW}$, is calculated for the various models relative to a random walk process where $RMSE_{CM}$ denotes the root-mean-squared error for the competing models, while $RMSE_{RW}$ is the root-mean-squared error for the benchmark random walk model. A ratio of 1.0 suggests that the competing

model is as good as the random walk benchmark model. A ratio less than 1.0 indicates that the benchmark model is out-predicted by the competing model. No gain is achieved from using the competing models if the ratio is greater than 1.0. Inferences are based on the null hypothesis of zero difference in the forecast accuracy measured using RMSE, that is the competing models relative to the driftless random walk model.

In the third appraisal, the Diebold-Mariano statistics (Diebold and Mariano, 1995) are employed to examine the statistical significance of the forecast errors between the random walk and the competing model. The null hypothesis of zero difference in forecast error between the random walk and the competing model is assumed in this approach. Specifically, the loss differential is measured as the difference between the squared forecast error of the competing models and that of the benchmark random walk model. The test statistic is useful for comparing forecast accuracy as it allows the forecast errors to be "non-Gaussian, non-zero mean, serially correlated, and contemporaneously correlated" (pp.253, Diebold and Mariano, 1995). The Diebold-Mariano statistic is specified as:

$$DM = \frac{\bar{d}}{\sqrt{\hat{V}(\bar{d})}} \tag{4-13}$$

where the loss function differential, $d_t \equiv g(e_{RW,t|t-h}) - g(e_{CM,t|t-h})$ with h-step ahead forecast error, and

$\sqrt{\hat{V}(\bar{d})}$ = the estimated standard error for the sample mean loss differential, $\bar{d}$,

e_{RW} = the forecast error for the random walk model estimated as $\left(\Delta IV_t - \Delta\hat{IV}_{RW,t|t-h}\right)^2$

e_{CM} = the forecast error for the competing model estimated as $\left(\Delta IV_t - \Delta\hat{IV}_{CM,t|t-h}\right)^2$

4.8.1 Forecast Results

Table 4-8 provides the out-of-sample RMSE statistics associated with the driftless random walk, ARIMA and the ANNs model for one-day ahead forecasts. The RMSE statistics unambiguously favour the competing models over the random walk. Notably, in all cases the RMSE for the competing models is consistently lower than those reported for the benchmark model. For example, the one-week GBP/USD has a RMSE of 5.78 using the random walk model, while the ARIMA and ANNs have RMSEs of 4.93 and 4.88 respectively.

For the two-year series of the same currency, the RMSE reported for the random walk model is 0.54 while the ARIMA and ANNs models both have lower RMSE (0.45). This pattern is reported across all maturities and currency pairs. This suggests that the competing models have higher forecasting accuracy than the random walk model. Thus the random walk specification does not receive support against the two alternative models when using the RMSE criterion. This further validates the preceding random walk violations when using conventional and nonparametric variance ratio tests.

The predictive accuracy of the ARIMA and ANNs models is not distinctly different from each other although the ARIMA model has marginally lower RMSEs, particularly for the shorter maturities of one-week and one-month. For these maturities, the mean RMSE difference (mean RMSE for ARIMA less mean RMSE for ANNs) is -0.14 and -0.005 respectively, while differences for the three-month to two-year series fall between -0.003 and -0.013. In comparison, the mean RMSE gap between the random walk and the competing models is much larger, for instance forecasting using

Table 4-8: Out-of-Sample One-day Ahead Forecast Performance for the Random Walk and Competing Models

	Random-walk Model				ARIMA Model				Artificial Neural Network Model			
	GBP/USD	EUR/USD	AUD/USD	USD/JPY	GBP/USD	EUR/USD	AUD/USD	USD/JPY	GBP/USD	EUR/USD	AUD/USD	USD/JPY
1-week												
ME	0.030	0.036	-0.007	0.032	-0.071	-0.002	0.025	0.091	-0.022	-0.028	-0.015	0.121
MAE	4.343	4.599	3.985	4.907	3.806	3.368	3.190	3.711	3.651	3.471	3.275	3.884
RMSE	5.778	6.129	5.133	6.597	4.931	4.632	4.243	4.925	4.875	4.864	4.298	5.225
1-month												
ME	0.009	-0.001	0.008	0.010	-0.037	0.006	-0.004	0.057	-0.015	-0.025	0.023	0.032
MAE	2.067	2.222	2.287	2.330	1.558	1.626	1.653	1.746	1.553	1.613	1.704	1.747
RMSE	2.659	2.912	2.903	3.124	2.068	2.240	2.189	2.358	2.080	2.210	2.262	2.345
3-month												
ME	0.009	0.001	0.001	0.013	-0.033	0.004	-0.035	0.029	-0.025	0.052	0.001	-0.010
MAE	2.070	1.180	1.119	1.162	1.593	0.902	0.960	0.902	1.573	0.896	0.959	0.918
RMSE	2.664	1.537	1.475	1.543	2.108	1.243	1.277	1.205	2.090	1.237	1.291	1.224
6-month												
ME	0.001	0.000	-0.001	0.010	-0.029	-0.002	-0.053	0.020	-0.013	0.042	0.133	-0.003
MAE	0.567	0.671	0.781	0.703	0.446	0.519	0.684	0.550	0.442	0.514	0.677	0.552
RMSE	0.792	0.914	1.039	0.972	0.647	0.752	0.919	0.778	0.643	0.751	0.931	0.783
1-vear												
ME	-0.001	0.001	0.001	0.005	-0.030	-0.003	-0.051	0.010	-0.025	0.042	0.015	0.021
MAE	0.442	0.493	0.612	0.466	0.357	0.380	0.515	0.372	0.358	0.382	0.512	0.373
RMSE	0.612	0.682	0.816	0.641	0.503	0.553	0.698	0.518	0.505	0.556	0.698	0.517
2-vear												
ME	0.001	0.005	0.005	0.005	-0.028	0.002	-0.061	0.006	-0.022	0.046	-0.056	0.018
MAE	0.392	0.437	0.585	0.439	0.314	0.348	0.483	0.351	0.316	0.353	0.491	0.352
RMSE	0.537	0.597	0.769	0.610	0.445	0.498	0.654	0.501	0.446	0.505	0.677	0.502

Note: This table reports the mean error (ME), the mean average error (MAE), and the root mean square error (RMSE). These statistics are defined below. All figures are multiplied by 100. The modelling is performed from the first subsample which comprises of 900 daily observations from 29 August, 2001 to 29 April, 2005. The second subsample consists of 250 daily observations and is used to calculate the out-of-sample forecasting errors that correspond with the models above.

$$ME = \frac{1}{N}\sum_{i=1}^{N}(\Delta\hat{IV}_t^M - \Delta IV_t^M),\ MAE = \frac{1}{N}\sum_{i=1}^{N}\left|(\Delta\hat{IV}_t^M - \Delta IV_t^M)\right| \text{ and } RMSE = \sqrt{\frac{1}{N}\sum_{t=1}^{N}(\Delta\hat{IV}_t^M - \Delta IV_t^M)^2}$$

the random walk model results in a mean RMSE of 5.91 for the one-week volatility series while the ANN model gives a corresponding value of 4.82. The differences in RMSEs decrease steadily as maturity increases.

A consistent result across all three models is that the lowest RMSE is reported for the one-week AUD/USD volatility series while the GBP/USD recorded the lowest RMSEs for the one-month, six-month, one-year and two-year series. This tends to suggest that although improvement in predictive accuracy can be achieved using the ARIMA and ANN models, these models performed equally well for the AUD/USD and GBP/USD series.

However, the performance for the three-month volatility series appears mixed across all currency pairs. Specifically, in that while the lowest RMSE is reported for the AUD/USD currency pair under the random walk model, both the ARIMA and ANN models have the lowest RMSEs for the USD/JPY volatility series. By maturity, the forecasting performance for the two-year series has the lowest mean RMSEs while the one-month series has the highest RMSEs. Overall, a regular pattern of RMSEs across maturities can be noted – that is, the root-mean-squared errors decrease proportionately with maturity.

Results from the RMSE ratios in Table 4-9 paint a very similar picture. For each currency pair, the ratio for each maturity is estimated. In all instances, the RMSE ratios, which is measured as the ratio of RMSE from the competing model divided by the RMSE from the random walk model, is less than 1.0. This is suggestive of lower

forecasting error when using the competing models. Such a pattern is observed consistently across maturities and currencies.

Table 4-9: RMSE Ratios Relative to the Random Walk Model

Maturity	GBP/USD	EUR/USD	AUD/USD	USD/JPY	Mean
ARIMA Model					
1-Week	0.8535	0.7557	0.8268	0.7466	0.7956
1-Month	0.7776	0.7692	0.7538	0.7548	0.7638
3-Month	0.7911	0.8083	0.8658	0.7811	0.8115
6-Month	0.8169	0.8225	0.8852	0.8001	0.8312
1-Year	0.8219	0.8112	0.8551	0.8074	0.8239
2-Year	0.8278	0.8331	0.8505	0.8210	0.8328
ANN Model					
1-Week	0.8438	0.7936	0.8373	0.7920	0.8166
1-Month	0.7823	0.7589	0.779	0.7506	0.7677
3-Month	0.7845	0.8045	0.8758	0.7934	0.8145
6-Month	0.8118	0.8211	0.8962	0.8057	0.8337
1-Year	0.8246	0.8152	0.8552	0.8057	0.8251
2-Year	0.8299	0.8457	0.8802	0.8219	0.8444

Note: The RMSE ratios are measured as $RMSE_{CM}/RMSE_{RW}$, where $RMSE_{CM}$ and $RMSE_{RW}$ denote the root-mean-squared error for the competing and random walk model. The RMSEs are calculated using the out-of-sample forecasting results from the second subsample.

For short-dated maturities of one-week and one-month, the mean RMSE ratios for the ARIMA model are 0.796 and 0.764. These values are lower than the results for the one-year and the two-year series of 0.824 and 0.833 respectively. A similar observation can be made when the ratios are calculated using the ANNs model. Thus, forecasting using the ARIMA model can achieve an improvement of 17% to 24%[86] compared with the random walk model. On the whole, as maturity increases, the mean RMSE ratios move closer to 1.0, indicating that the choice of forecasting model becomes less important for the long-dated volatility series. The same result is reported when using the ANNs model.

[86] Using mean RMSE ratio for the one-month series, this is estimated as 1-0.7638 = 23.62%

Figure 4-3 plots the total RMSE of the models versus maturity. The total RMSE is calculated as the sum of the individual RMSE from each of the four currencies. Consistent with the preceding results, the RMSEs decreases proportionately against maturity. It is clear that the random walk model has the highest total RMSE amongst all the three models. This result holds across each of the six maturities. However, the total RMSE lines for all three models tend to converge as maturity increases. For the ANNs and ARIMA models the RMSE lines overlap each other in most instances thus suggesting the similar performance for both the ANN model and the ARIMA model. For majority of the currency pairs, the RMSEs for the ANN model are only marginally higher than RMSEs for the ARIMA model.

To this point, an important parallel can be drawn between Figure 4-1 and Figure 4-3. By examining the solid line that represents the total RMSE for the random walk model, it can be seen that the RMSEs for the short-dated maturities are higher than that of the long-dated maturities; at the same time, short-dated maturities also have lower variance ratio than the long-dated series. Conversely, the long-dated maturities have higher mean variance ratios. Indeed, the mean variance ratios for the long-dated maturities of six-month to two-year are close to 1.0. For example the mean variance ratio (with q=10) for the one-week volatility is 0.46 and this increases to 0.93 for the two-year series, while the corresponding RMSEs for the same series drops from 0.23 to 0.03 under the random walk model. Thus, it appears that the data-generating process for short-dated volatility is better characterised as a mean-reverting process, while long-dated maturities are better modelled using a unit root specification. Although the random walk model records lower RMSE for the long-dated series, it is still dominated by the ARIMA and ANNs models.

Figure 4-3: Total RMSE versus Maturity

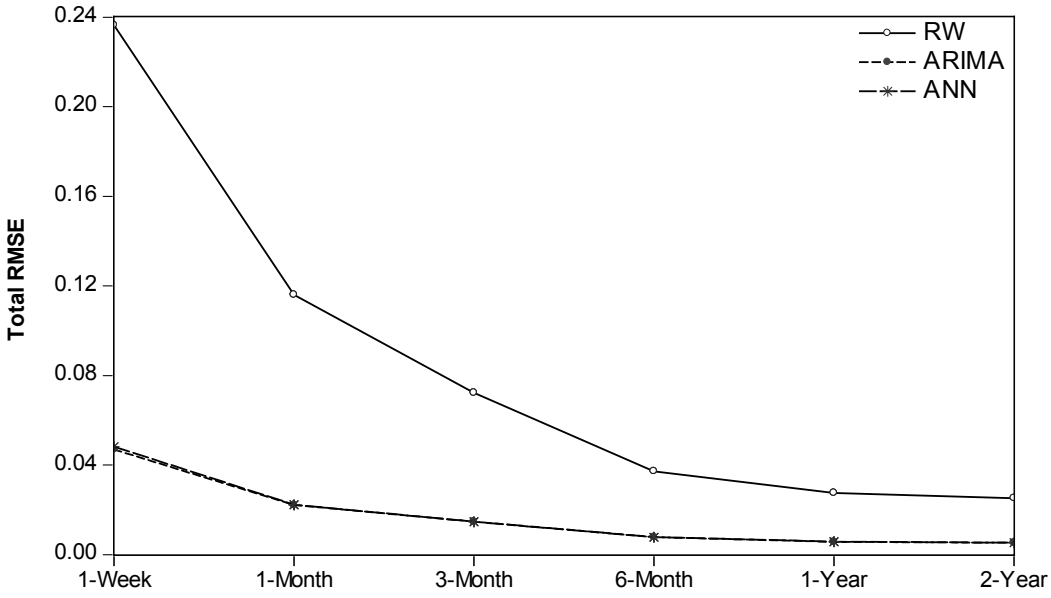

Note: This figure shows the total root-mean-squared errors (RMSEs) from the random walk (RW), autoregressive integrated moving average (ARIMA) and the artificial neural networks (ANNs) models. The total RMSE is calculated as the sum of the individual RMSE for each of the four currencies examined.

4.8.2 Diebold- Mariano (1995) Forecast Accuracy Test

In Table 4-10, the results for the out-of-sample one-day ahead forecast performance using the Diebold-Mariano (DM) statistics are displayed. The DM statistic tests for the null hypothesis of no difference in forecast errors between the random walk and competing models. Since the competing models perform almost as well as each other, the DM statistic is only used to assess the forecasting performance of the random walk model against one of the competing models. However, given previous results indicate that the mean RMSE for ANNs is marginally higher than the mean RMSE for the ARIMA model, the random walk model is evaluated against the ANNs model[87].

[87] This is a conservative approach as the ARIMA model performed marginally better than the ANNs model across all six maturities. Subsequent comparisons between the random walk and ARIMA model using the Diebold-Mariano (1995) statistic do not alter the findings reported in Table 4-10.

The Diebold-Mariano (1995) statistic is performed according to the specification provided in Equation (4-13). If the regression coefficient is positive and significant, then the random walk model's performance is worse than that of the ANNs model. The rejection of the null hypothesis is based on standard *t*-test statistics, and a linear regression of the loss function on a constant is performed to obtain the DM statistics. The standard errors of the test statistics are corrected for heteroscedasticity and autocorrelation using the Newey-West (1987) procedure.

Table 4-10: Diebold-Mariano (1995) Test of Equal Forecast Accuracy

Currency	1-Week	1-Month	3-Month	6-Month	1-Year	2-Year
GBP/USD	0.723 (2.838) ***	0.269 (5.514) ***	0.266 (5.554) ***	0.021 (3.550) ***	0.012 (4.122) ***	0.009 (3.619) ***
EUR/USD	1.471 (5.325) ***	0.368 (5.741) ***	0.081 (4.388) ***	0.026 (3.175) ***	0.014 (2.883) ***	0.006 (1.466)
AUD/USD	0.742 (3.585) ***	0.325 (4.993) ***	0.048 (2.333) **	0.019 (1.621)	0.016 (2.407) **	0.017 (3.175) ***
USD/JPY	1.697 (3.917) ***	0.423 (5.521) ***	0.092 (4.635) ***	0.036 (4.248) ***	0.016 (4.626) ***	0.014 (4.131) ***

Note: This table presents the Diebold-Mariano (1995) statistics for the null hypothesis of zero loss function differential (multiplied by 1000). The t-statistics are reported in the parentheses. The standard errors of the test statistics are corrected for heteroscedasticity and autocorrelation using the Newey-West (1987) procedure.
****significant at the 1% level*
***significant at the 5% level*
**significant at the 10% level*

The results in Table 4-10 provide resounding rejection of the null hypothesis across all maturities and currencies. Specifically, each of the reported Diebold-Mariano (1995) statistics is above zero and in virtually all instances show strong rejection of the null with coefficients significant at the 1% level. Across all currencies, the coefficients for the short-dated maturities are consistently larger than those of the long-dated maturities. For example, the DM statistic for the one-week GBP/USD is 0.723 while the

two-year DM statistic has a value of 0.009. The same observation can be made for all other currency pairs.

Although the size of the coefficients becomes smaller as maturity increases, they remain statistically significant except for the two-year EUR/USD and the six-month AUD/USD volatility series. These observations are consistent with the preceding findings reported in Table 4-9 and Figure 4-3. This empirical evidence can be interpreted as supporting of the superior forecasting performance of the ANNs model against the random walk model. This reaffirms the view that the implied volatility process is not well characterised as a random walk process.

These results are broadly consistent with the work of Sabanis (2003) that suggests the use of mean reverting volatility for pricing European options. Furthermore the notion of mean-reverting volatility in asset prices was recently investigated by Bali and Demirtas (2008) with support for this model. Thus, the result is consistent with recent literature and offers convincing evidence in favour of the ARIMA and ANNs models for implied volatility forecasting.

4.9 Conclusion

Previous studies have tested the random walk hypothesis for securities traded on stock exchanges. This chapter examines the random walk hypothesis using traded implied volatility data collected from the over-the-counter currency option market using various in-sample and out-of-sample tests, in addition to standard unit root tests. The test statistics are applied to the implied volatility levels and the differences in logs for the volatility series for four major currencies. Both parametric and nonparametric variance ratio tests are applied in analysis of the data. The null hypothesis of a random walk process in the implied volatility series is consistently rejected across all currency pairs examined. Specifically, for the one-week and one-month series, violations of the random walk persist even after controlling for data bias and test size distortions. These results are confirmed in out-of-sample forecasting tests.

The main empirical finding from the variance ratio tests appear to suggest that there is potential for variation with respect to the appropriateness of the random walk process for modelling quoted volatility process across various maturities and currencies. Thus time series in foreign exchange implied volatility is not well characterised by a random walk process. This implies that option pricing and volatility models that assume a random walk in volatility across all maturities is not consistent with empirical findings reported in this chapter. It further suggests that while it may be useful to model foreign exchange volatility as a random walk process, the volatility patterns that exist within the term structure need to be recognised. In particular, short-dated volatility series of one-week and one-month are better characterised as a mean reverting process. This proposition is supported by the out-of-sample test results.

The out-of-sample forecasting accuracy tests demonstrate the usefulness of alternative volatility modelling methods, namely the ARIMA and ANNs. In particular, autoregressive integrated moving average (ARIMA) process and artificial neural networks (ANNs) models produce superior volatility forecasts compared with the random walk model. This underscores the merit of such modelling techniques in capturing the nonlinear behaviour of volatility.

CHAPTER 5 – VOLATILITY TRADING USING SIMPLE TRADING RULES[88]

5.1 Introduction

The behaviour of option-implied volatility series is examined in Chapter 4 and the test results show that there are violations of the random walk hypothesis in the implied volatility process. This chapter considers a further extension to these test results using simple moving-average trading rules on at-the-money forward straddles and risk-reversals option combination trades.

Trading strategies that are based on technical rules rely on the existence of time series patterns over a particular time frame and assume that asset prices do not follow a random walk process. Users of technical rules believe that a buy or sell signal appears when a lower or upper price bound is breached.

The following section presents literature concerning technical trading. Section 5.3 introduces volatility trading in the currency option market. In Section 5.4, description of the datasets is provided while the methodology and test results are available in Section 5.5 and Section 5.6 respectively. Section 5.7 concludes the findings of this chapter.

[88] The early version of this chapter forms the basis of a paper presented to the 14th Global Finance Conference at Melbourne, Australia in April 2007. It was co-authored with Eric Chan of UBS Investment Bank and 70% of the paper is completed by the author of this dissertation. The work presented in this dissertation reflects the opinions of the author alone and does not necessarily reflect the views of UBS Investment Bank.

5.2 Application of Technical Trading Rules

Technical analysis has been practiced in the financial markets for more than two centuries. According to Brock, Lakonishok and LeBaron (1992), the oldest charting technique is attributed to Charles Dow in the late 1800s. Nison (1991) provides a detailed commentary on the ancient Japanese candlestick charting technique which can be traced back to the 17th century. It is widely held that technical trading provides useful buy and sell signals amongst market practitioners in futures, currencies, equities and bonds.

Contrary to the popularity of technical analysis, the classical random walk theory asserts that technical trading has no value in any investment decision making. Apparent predictability of future returns using such trading methods is considered to be spurious and can be eliminated out-of-sample. Further, such information cannot be exploited after allowing for transaction costs. As such, according to Campbell, Lo and MacKinlay (1997), this technique has been regarded as a "black sheep" and has never enjoyed the same degree of acceptance as fundamental analysis. The general attitude of academics to the use of such tools for investment decision making is one of doubt, as described by James (1968):

> "trends" are spurious or imaginary manifestations; and that tools of technical analysis, and tool such as charts and Dow Theory, are without investment value."

However, there is growing evidence that supports profitability of technical trading in various market contexts including studies by Blume, Easley and O'Hara (1994), Brock, Lakonishok and LeBaron (1992), Neely, Weller and Dittmar (1997), Chan, Hameed and Tong (2000). The Brock, Lakonishok and LeBaron (1992) study offers the most comprehensive empirical study on technical trading using 90 years of daily data from the Dow Jones Index. Using popular moving average technical trading rules, they find that such trading rules are useful in predicting stock price changes. Their results also hold when the bootstrap methodology is used to correct for problems with standard statistical tests. Consistent with this study, Chang and Osler (1999) investigate the profitability of technical trading rules in the foreign exchange market using six major currency pairs and they conclude that simple technical trading rules have the ability to generate a statistically significant profit. Another study by Pilbeam (1995) compares the forecasting techniques produced by fundamentalists and chartist using four major currency pairs: the British pound, Japanese yen, German mark and the French franc. The study finds no clear evidence of the superiority of fundamentalists over chartists despite the fact that fundamentalists have the advantage of possessing information on economic fundamentals.

A more recent work by Hsu and Kuan (2005) examines an extensive range of trading rules and strategies using daily closing prices for four main equity indices: the S&P500, NASDAQ, Russell 2000 and the DJIA. Compared with the buy-and-hold strategy, their results show that the best trading rule produced superior performance over the entire sample period for the Russell 2000 index and seven of the eleven in-sample periods for the NASDAQ Composite. Further, a questionnaire survey conducted by Taylor and Allen (1992) finds overwhelming evidence for the use of technical

analysis in the London foreign exchange market[89]. More than 90 per cent of the respondents used charting in their trading room. The survey also shows that 13.6 per cent of the respondents viewed technical analysis and fundamental analysis as complementary tools in their trading activities while 7.3 per cent consider them to be mutually exclusive.

In a strict sense, the efficient market hypothesis suggests that no predictable pattern should exist in asset returns. However research by DeBondt and Thaler (1985), Stein (1989), Jegadeesh and Titman (1993) and Barberis, Shleifer and Vishny (1998) casts doubt on the efficient market hypothesis. As a result, most researchers today are more willing to accept the notion that the market may not be fully efficient and market psychology should not be ignored.

Substantial liquidity in the over-the-counter currency option market allows different combinations of option positions to be initiated by traders. Combinations such as "butterfly", "condor", "straddle", "strangle" and "risk reversal" are frequently traded in the over-the-counter currency option market. However, limited attention has been given to empirical analysis of such option trades. Indeed, Chaput and Ederington (2005) note that although option combinations are heavily traded, they receive relatively little attention in empirical research. While their study is based on options on EuroDollar Futures contracts traded on the Chicago Mercantile Exchange (CME), this chapter considers two types of option combinations available in the over-the-counter currency option market, namely at-the-money forward straddles and risk-reversals.

[89] The study was conducted on behalf of the Bank of England. A total of 213 completed questionnaires were analysed.

5.3 Volatility Trading in the Over-the-counter Currency Option Market

Unlike other markets, traders in the over-the-counter interbank markets express their option quotes and execute their trades in terms of implied volatility. The volatility parameter which represents traders' subjective view of the future movement of the underlying currency is used to determine the option premium. By standard market convention, traders enter this parameter into the Garman-Kohlhagen (1983) to obtain the option premium. Specifically, traders use the prevailing volatility prices coupled with option contract details to back-solve for the option dollar premium. This produces a convenient method for traders to compare prices of different options over time.

The foreign exchange and currency option market have a unique 24-hour global market which trades daily except on New Year holiday and weekends. Financial institutions, especially investment banks, are active in providing customised currency option contracts to their clients. Unlike exchange-traded currency options[90] with fixed exercise prices, over-the-counter currency options are traded on fixed moneyness measured in terms of option delta with constant maturity.

5.3.1 Straddle Trades

An at-the-money forward straddle is a combination of a European call and a European put with identical strike prices, which are approximately equal to the forward exchange rate. The at-the-money forward straddle has the greatest liquidity in the over-the-counter market as most deals are done in these combinations. When a large increase

[90] These are traded on the Philadelphia Stock Exchange (PHLX) and the Chicago Board of Trade (CBOT).

in volatility is anticipated in the option market, the trader can purchase a combination of a call and a put. An upward or downward movement in the spot market will result in one of the options being deeply "in-the-money" while the other will expired unexercised. When the "in-the-money" option is sold in the market, the profit generated will be more than enough to pay for the option premia. Alternatively, when a drop in volatility is expected in the option market, the trader will sell the straddle to receive two option premia from the call and put[91]. This is a relatively risky strategy as an incorrect view of the market could result in a severe loss.

5.3.2 Risk Reversal Trades

Risk reversal is a widely used indicator amongst practitioners, policy makers and central banks to infer information about expected future foreign exchange rate movement[92]. A standard risk reversal instrument is the "25-delta" contract which is a combination of a long position in a 25-delta European call option and a short position of 25-delta European put option for the same currency pair. A combination of short call and long put position can also be created to reflect an opposite view of the market.[93] This is a standard market convention used in the over-the-counter currency option market where option prices are quoted in terms of implied volatility for a given level of delta.

The volatility of risk reversal is quoted as the difference in the implied volatility of the long option position and the short option position. For instance, if a 25-delta call has an implied volatility quote of 10% and a 25-delta put has a volatility of

[91] Under such market condition, the trader anticipates the call and put will not move in-the-money.
[92] For instance, see pp.72-73 of Cooper and Talbot (1999).
[93] Both call and put have delta values of 0.25 and -0.25 respectively.

9%, then the risk reversal[94] is quoted as 1% per annum. Therefore when a risk reversal is positive, the call is bid over the put.

Traders use the sign and the magnitude of risk reversals to gauge the degree of skewness in expected exchange rate movements. A positive risk reversal implies that the out-of-money call is more expensive than the out-of-money put. For instance, in the USD/JPY market, when the 25 delta risk reversal is trading at 0.3, the 25 delta call is trading at a volatility of 0.3 percentage points above the 25 delta put. This is an indication of skewness toward appreciation of the USD against the yen.

In essence, the simultaneous purchase of a call and sale of a put results in a synthetic foreign exchange forward position. A range between the two strike prices exists due to the different strike price for the call and put options. A combination of a long call and short put will result in a net gain when the spot exchange rate moves above the strike price for the call. On the other hand, a profitable position exists for the long put and short call position when the spot exchange rate moves below the strike price for the put.

5.4 Data

This study employs datasets available from the over-the-counter currency option market on four major currency pairs: the British pound against the U.S. dollar,

[94] This is also known as a "collar".

euro against the U.S. dollar, Australian dollar against the U.S. dollar and Japanese yen against the U.S. dollar quotes. The use of over-the-counter currency option data circumvents non-synchronisation problem and the expiration-day effect commonly addressed in the option pricing literature. The average of bid and ask implied volatility quotes is used to avoid bid and ask bounce effects.

The daily volatility quotes of European options are obtained from the British Bankers' Association (BBA) database which is contributed to by 12 major market makers in the London over-the-counter currency option market. The contributors provide the closing rates between 3:30 and 3:50 pm daily. BBA excludes two highest and lowest rates for the day and the average of the remaining rates is stored in the BBA database.

The corresponding spot exchange rates are recorded at the same time as the implied volatility quotes. Maturities for at-the-money-forward implied volatility are available for one-week, one-month, three-month, six-month, one-year and two-year. For the 25-delta risk-reversals and 25-delta strangles, daily data for the one-month, three-month and one-year contracts are available.

To allow for comparability in the test results with risk reversal trades, the one-week and the two-year at-the-money forward volatility are omitted in this study. Daily interest rate data for the respective currency pairs are also available from the BBA for the shortest maturity of overnight to 12 months. The BBA-LIBOR rates are released daily at approximately 11:00 am London time.

5.4.1 Descriptive Statistics

Table 5-1 reports the descriptive statistics for the natural logarithm of the at-the-money forward straddle quotes for the British pound, euro, Australian dollar and Japanese yen. The univariate statistics are calculated using the log series of the volatility levels to allow for comparison with an earlier study by Covrig and Low (2003)[95]. The sample mean, standard deviation, skewness, excess kurtosis and their respective *p*-values are reported for the period 1 October, 2001 to 31 July, 2006.

The mean of the log series increases with maturity for three out of four currency pairs. This supports the existence of "term structure" effects reported in Campa, Chang and Reider (1998), Xu and Taylor (1994) and Gessner and Poncet (1997). For the Japanese yen, the sample means decrease as the maturity increases.

Variations in the sample mean reported for each currency pair are consistent with the violation of the constant volatility assumption implicit in the Garman-Kohlhagen (1983) model. Table 5-1 also shows that as the horizon increases, the standard deviation of the respective maturities decreases. This pattern holds across all currency pairs. For instance, in the GBP/USD currency pair, the standard deviation for the one-month series is 0.136 while the one-year contract has a standard deviation of 0.075. This pattern is consistent with the work of Covrig and Low (2003). Overall, the values for excess kurtosis and skewness indicate that the distributions are not normal across all maturities.

[95] Their study is based on three currency pairs, namely USD/JPY, AUD/USD and GBP/USD and the sample period range from 5 June, 1996 to 25 April, 2000. Implied volatility for the 1-month, 2-month, 3-month and 6-month series are used.

Table 5-1: Descriptive Statistics for At the Money Forward Straddle Quotes

	N	Mean	*p*-value	Std Dev	Skw	*p*-value	Ex-Kurt	*p*-value	Min	Max
GBP/USD										
1-Month	1204	2.093	0.000	0.136	-0.294	0.000	1.375	0.000	1.647	2.453
3-Month	1204	2.111	0.000	0.112	0.327	0.000	1.285	0.000	1.775	2.453
6-Month	1204	2.142	0.000	0.084	0.044	0.531	0.472	0.001	1.905	2.371
1-Year	1204	2.156	0.000	0.075	0.128	0.071	-0.040	0.779	1.952	2.352
EUR/USD										
1-Month	1207	2.247	0.000	0.119	0.083	0.240	-0.616	0.000	1.927	2.560
3-Month	1207	2.276	0.000	0.098	-0.001	0.989	-0.947	0.000	2.054	2.535
6-Month	1207	2.299	0.000	0.088	0.019	0.785	-0.937	0.000	2.105	2.515
1-Year	1207	2.314	0.000	0.080	0.140	0.048	-0.818	0.000	2.152	2.525
AUD/USD										
1-Month	1204	2.314	0.000	0.154	0.327	0.000	-0.428	0.003	1.966	2.716
3-Month	1204	2.332	0.000	0.119	0.339	0.000	-0.574	0.000	2.074	2.629
6-Month	1204	2.344	0.000	0.100	0.330	0.000	-0.626	0.000	2.122	2.611
1-Year	1204	2.350	0.000	0.090	0.332	0.000	-0.633	0.000	2.153	2.592
USD/JPY										
1-Month	1207	2.222	0.000	0.113	0.407	0.000	-0.422	0.003	1.996	2.638
3-Month	1207	2.217	0.000	0.087	0.234	0.001	-0.611	0.000	2.044	2.479
6-Month	1207	2.216	0.000	0.079	0.366	0.000	-0.167	0.239	2.064	2.495
1-Year	1207	2.215	0.000	0.077	0.638	0.000	0.442	0.002	2.088	2.504

Note: This table presents the mean, standard deviation, skewness, excess kurtosis of the natural logarithm for the at-the-money forward implied volatility quotes from 1 October, 2001 to 31 July, 2006.

Table 5-2 presents the univariate statistics for the risk reversal series in the same format as the straddles series in Table 5-1. As the 25-delta risk reversals series can be above or below zero, the statistical tests are performed on the volatility levels without applying natural logarithm transformations. The sample mean is significantly different from zero and this pattern is consistently reported across all currency pairs. Standard option pricing theory suggests that equally out-of-money call and put options[96] should have identical implied volatility (Malz, 1997) but this is not the case.

[96] In this case, moneyness in terms of delta.

Table 5-2: Descriptive Statistics for Risk Reversal Quotes

	N	Mean	*p*-value	Std Dev	Skw	*p*-value	Kurt	*p*-value	Min	Max
GBP/USD										
1-Month	1201	0.091	0.000	0.302	0.279	0.000	-0.370	0.009	-0.660	1.030
3-Month	1201	0.123	0.000	0.251	0.125	0.078	-0.661	0.000	-0.510	0.770
1-Year	1201	0.153	0.000	0.218	-0.063	0.376	-0.964	0.000	-0.290	0.630
EUR/USD										
1-Month	1206	0.295	0.000	0.396	0.294	0.000	-0.179	0.206	-0.650	1.450
3-Month	1206	0.373	0.000	0.367	0.032	0.651	-0.429	0.002	-0.560	1.320
1-Year	1206	0.429	0.000	0.331	-0.053	0.457	-0.824	0.000	-0.280	1.120
AUD/USD										
1-Month	1204	-0.302	0.000	0.376	0.441	0.000	-0.381	0.007	-1.450	0.710
3-Month	1204	-0.333	0.000	0.328	0.560	0.000	-0.451	0.001	-1.170	0.580
1-Year	1204	-0.365	0.000	0.285	0.512	0.000	-0.885	0.000	-0.880	0.340
USD/JPY										
1-Month	1205	-0.686	0.000	0.592	-0.801	0.000	3.890	0.000	-3.470	1.270
3-Month	1205	-0.883	0.000	0.653	-0.207	0.003	1.362	0.000	-3.320	1.100
1-Year	1205	-1.128	0.000	0.841	-0.124	0.079	-0.034	0.809	-3.220	0.870

Note: This table presents the mean, standard deviation, skewness, excess kurtosis, risk reversal of the implied volatility quotes for different maturities from 1 October, 2001 to 31 July, 2006.

In column two, positive means are reported for the GBP/USD and the EUR/USD series while the AUD/USD and the USD/JPY series record negative means. The *p*-values for the null hypothesis of zero mean in column three suggest that equality of the implied volatility spread between the 25-delta call and 25-put is overwhelmingly rejected across currencies and maturities. Thus, on average, the market anticipates an appreciation of the GBP/USD and EUR/USD exchange rates while the AUD/USD is expected to depreciate over the sample period.

Figure 5-1 provides the time series plots for the spot exchange rates, one-month at-the-money implied volatility and the one-month 25-delta risk reversals in their respective panels. Upward trends in the spot exchange rates are shown for the

GBP/USD and EUR/USD series while the USD/JPY[97] has a downward trend over the sample period. These patterns are consistent with the statistics reported in Table 5-2. The one-month at-the-money implied volatility varied considerably over time with common spikes around early 2002 and late 2003 for the GBP/USD, EUR/USD and AUD/USD currency pairs. For the 25-delta risk reversal, considerable variation in the daily movement is also noted. The risk reversal pattern for the USD/JPY currency pair is below zero in most instances over the sample period.

[97] The volatility spread between the call and put appears to be more severe for USD/JPY. As the value of the U.S. dollar is quoted in yen term, this reflects the strengthening of the yen against the U.S. dollar over the sample period.

Figure 5-1: Time Series Plots of Spot Exchange Rate, At-the-money Forward Implied Volatility and Risk Reversal from 1 October, 2001 to 31 July, 2006.

Panel A: Daily Movement of GBP/USD, 1-Month at-the-money forward and 1-Month Risk Reversal

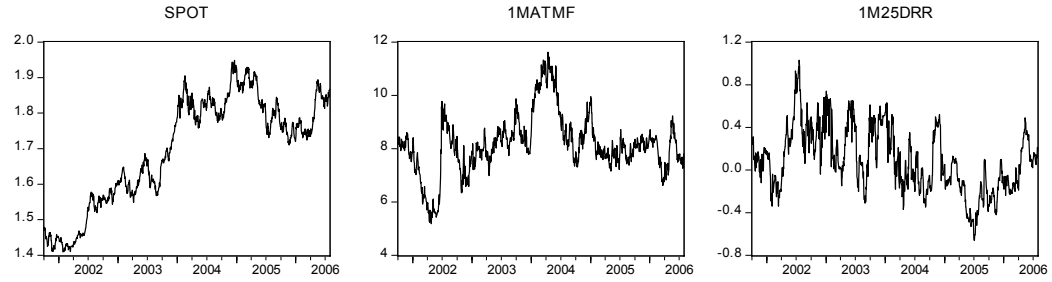

Panel B: Daily Movement of EUR/USD, 1-Month at-the-money forward and 1-Month Risk Reversal

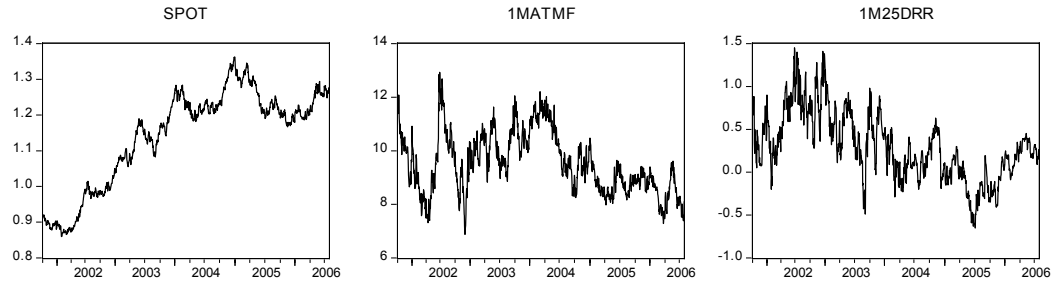

Panel C: Daily Movement of AUD/USD, 1-Month at-the-money forward and 1-Month Risk Reversal

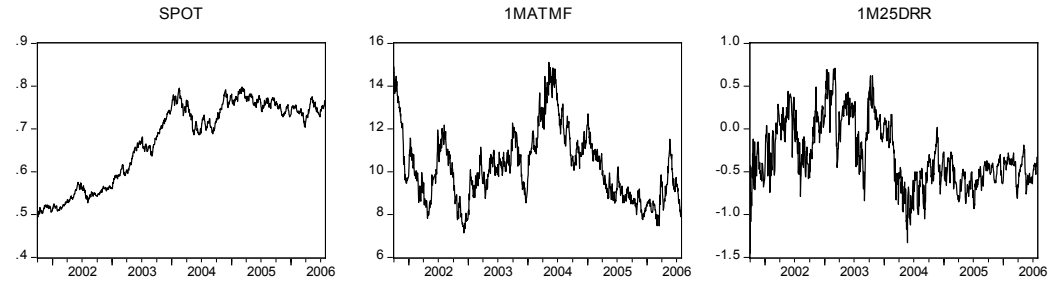

Panel D: Daily Movement of USD/JPY, 1-Month at-the-money forward and 1-Month Risk Reversal

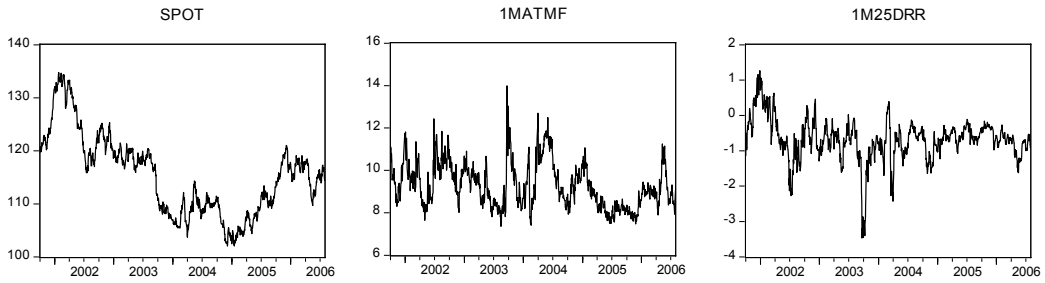

5.5 Methodology

The moving average method is one of the oldest and most widely used strategies in the foreign exchange market. In essence a buy or sell signal is generated when the prevailing market price has risen or declined more than its average value a few periods earlier. Within the context of this study, such a contrarian[98] strategy assumes mean reversion in the volatility process (Engle and Patton, 2001) and is consistent with the findings of Balvers, Wu and Gilliland (2000).

While numerous variations of moving average trading rules exist amongst market practitioners, the moving average of the volatility series in this study is estimated using a 253-day[99] window. This approach is largely motivated by empirical evidence that supports profitability of the contrarian strategies over long time horizons. For instance, Lakonishok, Shleifer, Vishny (1994) and Conrad and Kaul (1998) suggest that contrarian strategies are capable of generating profitable trades over one to five year investment horizons. In this chapter, due to sample size limitations, the window interval for the trading rules is limited to 253 days.

[98] This strategy profits from price reversal in contrast with the "momentum" approach which expects price continuation in one direction (Angel, Christophe and Ferri, 2003).
[99] It is assumed that there are approximately 253 trading days in a year.

Figure 5-2: The Simple Moving Average Trading Rule

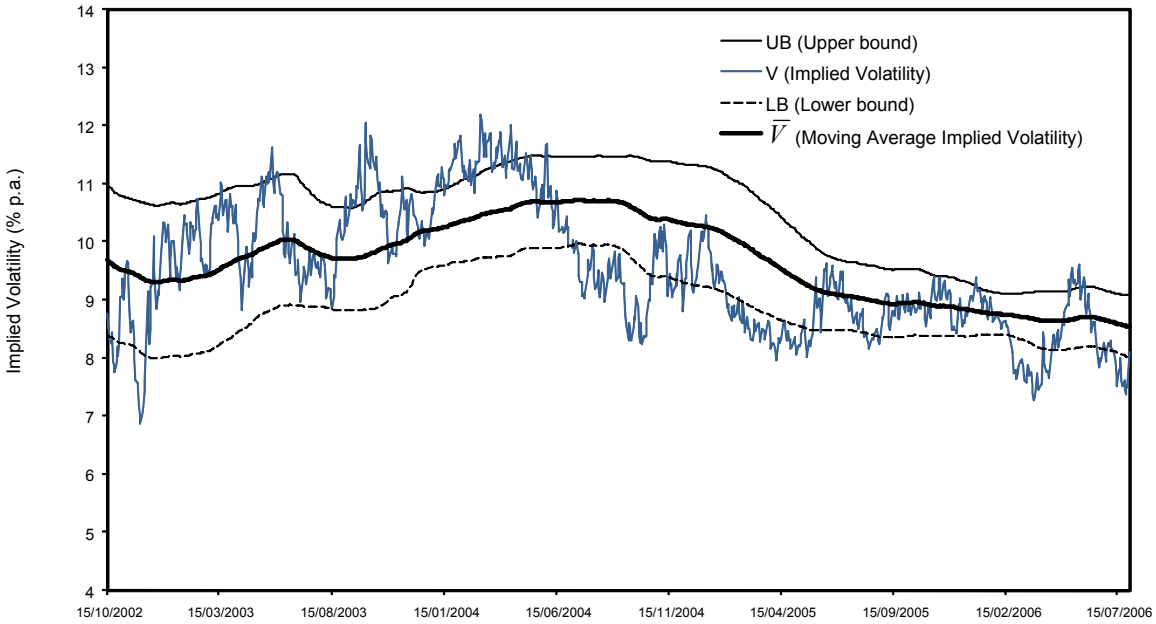

The application of the simple moving average trading rule is illustrated in Figure 5-2. Under this rule, an upper (UB) and a lower bound (LB) are estimated from a 253-day moving average of the implied volatility series ($\overline{V}$). When the prevailing implied volatility series (V) shown in Figure 5-2 breaches the upper bound, a sell signal is registered. Based on the same rationale, a buy signal is generated when the lower bound is breached. Estimations of the upper and lower bounds are described in Equations 5-1 and 5-2 below:

$$UB_{i,t,n} = \overline{V}_{i,t,n} + TV\sigma(n)_{i,t} \quad (5\text{-}1)$$

$$LB_{i,t,n} = \overline{V}_{i,t,n} - TV\sigma(n)_{i,t} \quad (5\text{-}2)$$

where

$UB_{i,t,n}$ = upper bound for series i at period t, calculated over the sample period n,

$LB_{i,t,n}$ = lower bound for series i at period t, calculated over the sample period n,

$\overline{V}_{i,t,n}$ = moving average of series *i* at period *t*, calculated over the sample period *n*, estimated as $\frac{1}{n}\sum_{j=t}^{t+n-1} V_j$, where V_j denotes the at at-the-money or risk reversal series,

$\sigma(n)_{i,t}$ = standard deviation for series *i* at period *t*, calculated over the sample period *n*, estimated as $\sqrt{\frac{1}{n-1}\sum_{j=t}^{t+n-1}(V_j - \overline{V})^2}$,

TV = trigger value for the upper and lower bounds.

To identify the buy or sell signals, two dummy variables are set up as follow:

$$D(V)_{i,t,n} = \begin{cases} +1 & if\ V_{i,t,n} > UB_{i,t,n} \\ -1 & if\ V_{i,t,n} < LB_{i,t,n} \end{cases} \qquad (5\text{-}3)$$

The term $D(V)_{i,t,n}$ is the dummy variable for series *i*, at period *t*. When the prevailing series (V_t) is above the upper bound, the dummy variable registers a value of positive one and a sell position is undertaken. In other words, a sell straddle trade is performed when the prevailing series V_t exceeds the upper bound ($UB_{i,t,n}$) for any give day *t* within the sample period. Conversely, when the prevailing series is below the lower bound, a value of negative one is registered and a buy position is engaged.

The upper and lower bounds are constructed using selected trigger values, which effectively define the distance between the bounds. They are expressed in terms of a given number of standard deviations above or below the moving average of the prevailing series. For instance, when the trigger value is set to one, the upper bound is one standard deviation above the moving average of the prevailing series. Buying and selling of straddles and risk reversals at high trigger values is consistent with the belief that a trend reversal is expected when the prevailing volatility prices are at their

extremes. In other words, the use of large trigger values will not result in a trade if only a small movement in the prevailing prices occurs, but a buy or sell signal is initiated when a large movement is detected.

Figures 5-3 and 5-4 illustrate the effect of using different trigger values to generate buy and sell signals. In Figure 5-3, the bounds are constructed using a trigger value of one; when the prevailing one-month EUR/USD at-the-money forward implied volatility (denoted as V) is inside the lower and upper bounds, no trade signal is registered. However, between 15 January, 2004 and 15 June, 2004, the volatility moved above the upper bound resulting in sell signals over this period. When a larger trigger value of two is used (Figure 5-3), the gap between the upper and lower bound widens. With the wider non-trading range, less trade signals are recorded over the same time period.

This chapter reports the results obtained using trigger values of 0.01, 0.5, 1.0 and 1.5. For most of the currency pairs, less than 30 buy and sell signals are observed when a trigger value greater than 1.50 is used. Consequently these test results are not reported due to limited sample size.

New trades are initiated over the sample period whenever a buy or a sell signal is identified. For both the straddle and risk reversal trades, when a trade signal becomes available, a long or short trade is performed and the contract is held until maturity. This approach is adopted to simplify daily monitoring of the trade positions.

Figure 5-3: EUR/USD Buy and Sell Signals (Trigger Value =1)

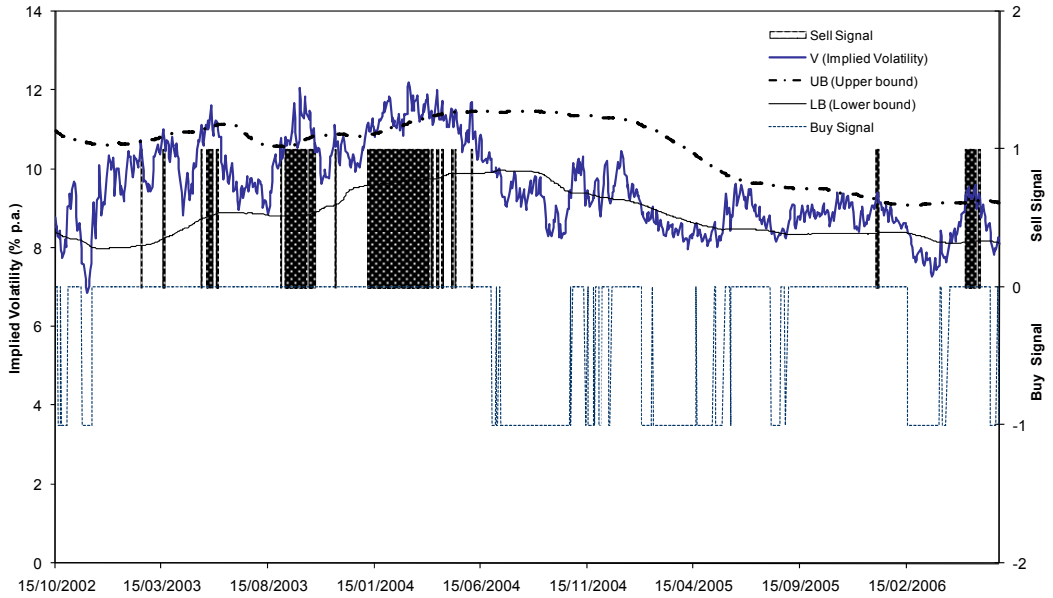

Figure 5-4: EUR/USD Buy and Sell Signals (Trigger Value =2)

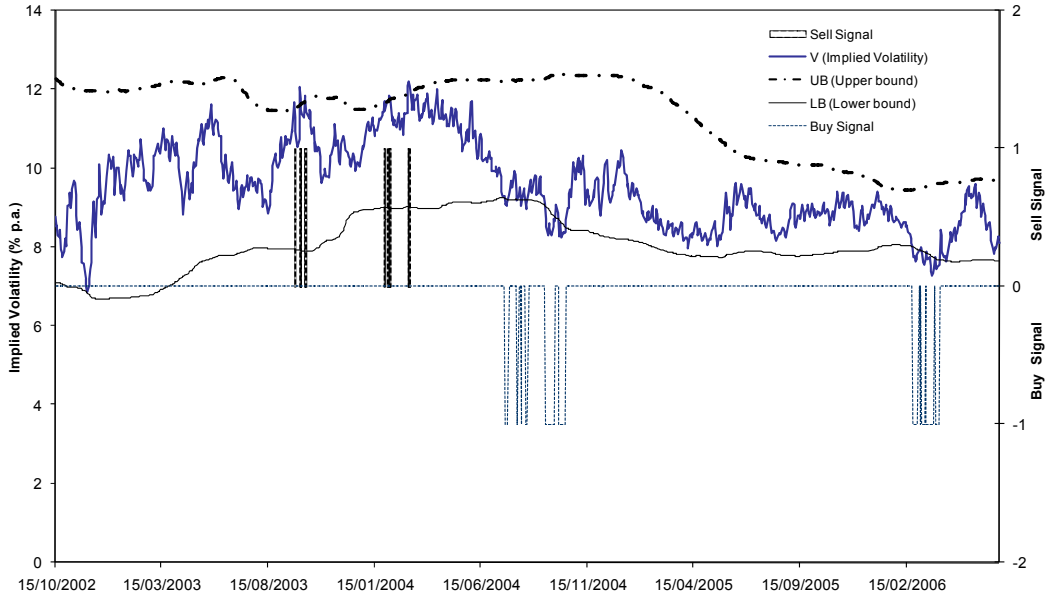

5.5.1 Options Premia Estimations

This study uses the Garman-Kohlhagen model (1983) to price currency options. The option premium is adjusted for trading days and bid and offer spread to reflect the volatility a trader has to pay for trade execution. For example, given a bid and offer spread of 0.5% and a three-month volatility of 20% per annum, the volatility bid is estimated as 19.5% per annum (that is 20% x (1-0.05/2). If a buy signal emerges when the one-year volatility is 8% per annum, the one- year volatility offer will be 8.2% per annum[100] . The bid and offer spreads for the one-month and one-year contracts are assumed to be 0.25% and 0.15% per annum respectively, which are conservative estimates for G-7 currencies according to market conventions. For contracts maturing between one month and one year, linear interpolation technique is employed to estimate the spreads for these contracts. This is given by the following formula:

$$BA_i = (BA_2 - BA_1)\frac{D_i - D_1}{D_2 - D_1} + BA_1 \qquad (5\text{-}4)$$

where

BA_i = estimated i-period bid/offer spread,

D_i = number of trading days that corresponds with $BA_{,i}$,

D_1 = number of trading days for one-month contract,

D_2 = number of trading days for one-year contract,

BA_1 = one-month bid/offer spread,

BA_2 = one-year bid/offer spread.

As an example, the volatility spread for the three-month contract can be estimated using Equation 5-4. Assuming that number of trading days for the one-month, three-month

[100] That is, 8% x (1+0.05/2).

and the one-year contracts is 22, 65 and 260 respectively, the bid and offer spread for the three-month contract is estimated as:

$$BA_{3m} = (0.0015 - 0.0025)\left[\frac{65-22}{260-22}\right] + 0.0025$$

$$BA_{3m} = 0.232\% \text{ per annum}$$

The implied volatility parameter of the Garman-Kohlhagen (1983) model is adjusted for bid and offer spread according to the following specification:

$$\sigma_{i,BA} = V_{i,t} + \left[-\left(\frac{BA_i}{2}\right)(D(V_{i,t})\right] \quad (5\text{-}5)$$

where

$\sigma_{i,BA}$ = Garman-Kohlhagen (1983) implied volatility for maturity *i*, adjusted for bid/offer spread,

$V_{i,t}$ = quoted implied volatility for maturity *i* available at period *t*,

BA_i = estimated bid/offer spread for an option contract with maturity *i*,

$D(V_{i,t})$ = dummy variable for a buy or a sell signal for maturity *i* available at period *t* (see Equation 5-3, + 1 = sell, -1 = buy).

On 5 September, 2003, the AUD/USD call option is quoted at 10.34% per annum and a buy signal is reported using the simple moving average trading rule. Using Equation 5-5, the bid volatility for the call is estimated as:

$$\sigma_{1m,BA} = 0.1034 + [-(0.0025/2)(-1)]$$

$$= 10.47\% \text{ per annum.}$$

If a sell signal is generated instead, the dummy is replaced with a value of plus one, resulting in an offer volatility of 10.22% per annum. The estimated bid/offer volatility is

used to price the call and put options. Under the Garman and Kohlhagen (1983) model, the value of a European currency call option is defined as:

$$C(S_t, T, X, \sigma, r_f, r_d) = S_t e^{-r_f T} N(d_1) - X e^{-r_d T} N(d_2) \quad (5\text{-}6)$$

where

$$d_1 = \frac{\ln(S_t / X) + [r_d - r_f + (0.5\sigma^2)]T}{\sigma\sqrt{T}} \quad (5\text{-}7)$$

and $d_2 = d_1 - \sigma\sqrt{T}$

σ = $\sigma_{i,BA}$ defined above,

S_t = spot exchange rate at maturity,

X = strike price of the underlying currency,

r_f, r_d = foreign and domestic interest rates respectively,

T = option term to maturity.

N(x) is the cumulative normal distribution function for a random variable with upper integral limit of x. The Garman-Kohlhagen (1983) is also used to estimate put option premium. The premium calculation is adjusted for bid and offer spread via the volatility parameter using Equation 5.5.

As the data collected are available in deltas, d_1 and d_2 can be inferred from the deltas. The delta of a call, denoted as δ_c is the first derivative of an option with respect to the spot exchange rate therefore differentiating the call price function using Equation 5.6 with respect to S_t gives:

$$\frac{\partial_c}{\partial_{St}} = e^{-r_f T} N(d_1) \tag{5-8}$$

Given the value of δ_c from market data, the inverse of d_1 can be calculated using the inverse of the cumulative normal distribution function.

$$d_1 = N^{-1}(e^{r_f T} \delta_c) \tag{5-9}$$

In the same manner the value of d_1 for the put option can be estimated,

$$d_1 = -N^{-1}(-e^{r_f T} \delta_p) \tag{5-10}$$

The values for d_1 in Equations 5-9 and 5-10 can be plugged into Equation 5-7 to find the strike prices of the calls and puts in the risk reversal trades. Since the risk reversal data described in Table 5-2 is the net of the combination (not separate implied volatility prices of each leg), implied volatility data for the 25-delta call and 25-delta put are subsequently obtained from UBS Investment Bank to estimate the strike prices[101]. For the at-the-money forward straddle, the strike price of a given currency *f* with maturity *m* is defined as[102]:

$$X_m^f = S_t \frac{\left[1+(d_T/360).i_n\right]}{\left[1+(d_T/360).i_d\right]} \tag{5-11}$$

where

d_T = maturity of the option in days,

S_t = spot exchange rate of the underlying currency,

i_n = BBA-LIBOR rate of the foreign currency,

i_d = BBA-LIBOR rate of the domestic currency.

[101] Further details are provided in the data section of Chapter 6.
[102] For the GBP/USD currency pair, 365 days is used to calculate the strike price.

5.5.2 Estimation of Holding-period Return

At the expiration of the contract, a comparison of the strike price with the closing spot exchange rate is made. The difference is netted off against the total option premium incurred or received to determine the holding-period return for the sample period.

For the straddle trades, the holding-period return is estimated as:

$$R_{i,t,n}^{hpa} = \left[\frac{(P_{i,t,n} - S_d S_T) - \left|(S_T - X_m^f)\right| D(V_{i,t})}{\left|P_{i,t,n}\right|} \right] \text{-1} \times \sqrt{\frac{260}{d_T}} \qquad \text{(5-12)}$$

where

$R_{i,t,n}^{hpa}$	=	t-period holding-period return per annum for series i over sample period n,
$P_{i,t,n}$	=	total option premium for each combination trade,
S_d	=	bid and ask spread of the underlying spot exchange rate,
S_T	=	spot price of the underlying exchange rate at maturity,
X_m^f	=	strike price[103] of the option contracts given the currency f with maturity m,
$D(V_{i,t})$	=	buy or sell dummy variable (+1 = sell, -1 = buy)
d_T	=	option maturity in days,

The term S_d approximates the bid and ask spread of 0.05%, charged on the spot exchange rate at the exit of each trade. Thus $R_{i,t,n}^{hpa} > 0$ reflects a profit and $R_{i,t,n}^{hpa} < 0$ indicates a loss on the trade. The options premia are calculated in U.S. dollar terms for all currency pairs to ensure return comparability across currency. It is assumed that the number of trading days is as follows: i.) 22 trading days for the one month contracts, ii.) 65 days for the three month contracts, iii.) 130 days for the six month contracts, and iv.)

[103] For the straddle, the call and put options are bought and sold at the same strike price.

260 days for the one year contracts. The trading days counts are used to calculate the holding-period returns defined according to Equation 5-12.

As option price increases less than proportionately over time (Hull, 2006), the annualised holding-period returns are measured as a function of the square root of time. The total option premium ($P_{i,t,n}$) used in Equation 5-12 is defined according to the type of option combination. Table 5-3 summaries the calculation of option premium used in this study. The total premium reflects the net option premium incurred or received from the option position. Thus a positive value represents premium received from the option combination and a negative value indicates cost incurred for the option trades.

Table 5-3: Calculation of Total Option Premium

Combination	Position	Total Premium
Buy a straddle	buy a call + buy a put	$P_{i,t,n} \equiv (P^{P}_{i,t,n} + P^{C}_{i,t,n}) \times (-1)$
Sell a straddle	sell a call + sell a put	$P_{i,t,n} \equiv (P^{P}_{i,t,n} + P^{C}_{i,t,n})$
Risk reversal A	buy a call + sell a put	$P_{i,t,n} \equiv (P^{P}_{i,t,n} - P^{C}_{i,t,n})$
Risk reversal B	sell a call + buy a put	$P_{i,t,n} \equiv (P^{C}_{i,t,n} - P^{P}_{i,t,n})$

The holding-period return for risk reversal trades is calculated as:

$$R_{i,t,n}^{hpa} = \left[\frac{(P_{i,t,n} - S_d S_T) + \left[- D(V_{i,t,n}) \max(S_T - X_C, 0) + D(V_{i,t,n}) \max(X_P - S_T, 0) \right]}{\left| P_{i,t,n} \right|} \right] \text{-1} \times \sqrt{\frac{260}{d_T}}$$

(5-13)

$P_{i,t,n} \equiv (P_{i,t,n}^{P} - P_{i,t,n}^{C})$ for buy a call + sell a put,
$P_{i,t,n} \equiv (P_{i,t,n}^{C} - P_{i,t,n}^{P})$ for sell a call + buy a put,

where

$R_{i,t,n}^{hpa}$	=	*t*-period holding-period return per annum for series *i* over sample period *n*,
$D(V_{i,t})$	=	buy or sell dummy variable (+1= sell a call and buy a put,-1 = buy a call and sell a put),
X_C	=	strike price for a 25-delta call option,
X_P	=	strike price for a 25-delta put option,
$P_{i,t,n}$	=	total option premium for each combination trade,
S_d	=	bid and ask spread of the underlying spot exchange rate,
S_T	=	spot price of the underlying exchange rate at maturity,
d_T	=	option maturity in days,

The exercise prices for call and put options are calculated individually using Equation 5-9 and Equation 5-10. The option premia for the call and the put are estimated using the Garman-Kohlhagen (1983) model to give a total option premium for the risk reversal position. If the exchange rate falls between X_P and X_C on the expiration of the contracts, then the total premium is zero. If a sell signal ($D(V_{i,t}) = +1$) is recorded on a particular day of the sample period, a sell-call and buy-put[104] is initiated and the

[104] This is referred to as "risk reversal B" in Table 5-3.

contracts are held until maturity. Similarly, when a buy signal is registered ($D(V_{i,t}) = -1$), a buy-call and sell put position is undertaken.

5.5.3 Examples of Holding-period Return Calculations

The following sections give a detailed holding-period return calculations for the straddle and risk reversal trades based on Equation 5-12 and Equation 5-13. The option parameters are based on the dataset collected on 5 September, 2003.

5.5.3.1 Straddle Holding-period Return

The value of the Australian dollar is AUD/USD 0.6463 on 5 September, 2003. On this day, the one-month BBA-LIBOR interest rate is 4.8025% in Australia and 1.12% in the United States. The one-month at-the-money European call and put have a common strike price of AUD/USD 0.6486 and the implied volatility is quoted at 10.34% per annum. Using the simple moving average trading rule, a buy signal is generated. The estimated bid volatility, $\sigma_{i,BA}$=10.47% per annum (assume a spread of 0.25%). The Garman-Kolhhagen (1983) currency option pricing model thus calculates a total premium of USD 0.0153 for the straddle. A buy straddle trade is performed and the options are held until contract expiration. On maturity, the exchange rate increased to AUD/USD 0.6819. The holding-period return of the buy straddle trade can be calculated using Equation 5-12. In this case, $P_{i,t,n}$ = USD 0.0153, S_d = 0.0005, S_T = 0.6819, X = 0.6486 and the dummy variable, $D(V)$ = -1. Hence:

$$R_{i,t,n}^{hpa} = \left(\left[\frac{\left[(0.0153(-1) - (0.0005)(0.6819) \right] - \left[\left| (0.6819 - 0.6486) \right| (-1) \right]}{\left| 0.0153 \right|} \right] - 1 \right) \times \left(\sqrt{\frac{260}{22}} \right)$$

= 53.01% per annum.

However, if the spot exchange rate decreased from the initial value of AUD/USD 0.6463 to AUD/USD 0.6212, the calculated holding-period return then becomes -78.88% per annum. Alternatively, since the put option expires in-the-money, the net payoff (X-S-P) becomes (USD 0.6486-USD 0.6212-USD 0.0153) which gives a profit of USD 0.0121. The one-month dollar return is therefore USD 0.01179, net of bid/ask spread (that is USD 0.6212 x 0.0005). The annualised holding-period return is therefore [(USD 0.01179/USD 0.0153)-1] x √(260/22) which is approximately -78.88% p.a.

5.5.3.2 Risk Reversal Holding-period Return

On 5 September 2003, the quoted one-month implied volatility for a 25-delta call option is 10.39% and put option of the same maturity and delta value has a quoted volatility of 10.78% per annum. The bid volatility for the call option using Equation 5-5 is calculated as $\sigma_{C,BA}$ = 0.1039+[-(0.0025/2)(-1)] = 10.52%, while the ask volatility for the put, $\sigma_{P,BA}$ = 0.1078+[-(0.0025/2)(+1)] = 10.66%. Using the Garman-Kohlhagen (1983) model, the call option has a value of USD 0.0011 and the put option is worth USD 0.0073, and hence the total premium, $P_{i,t,n}$ = (USD 0.0074 - USD 0.0011) for the buy a call and sell a put risk reversal.

The holding-period return of risk reversal trade can be calculated using Equation 5-13. In this case, $P_{i,t,n}$ = USD 0.0063, S_d = 0.0005, S_T = 0.6819, X_C = 0.6722, X_P = 0.6472 and the dummy variable, $D(V)$ = -1. Accordingly, the holding-period return for the buy-call and sell-put, $R_{i,t,n}^{hpa}$ is calculated as:

$$\left[\frac{[0.0063-0.0005(0.6819)]+[-(-1)\max(0.6819-0.6722,0)+(-1)\max(0.6472-0.6819,0)]}{|0.0063|}\right]\text{-}1\times\sqrt{\frac{260}{22}}$$

= 510.71% per annum.

In this case, the put option expires out-of-money but the call moves in-the-money generating a profit of USD 0.6819-USD 0.6722 = USD 0.0097. The total premium net of the spread of 0.0005 x 0.6819 (S_dS_T) is added and this gives a total profit of USD 0.015659. The annualised holding period return of [(0.015659/0.0063)-1] x 3.4378 = 510.71% per annum is generated over the trading period. If the spot exchange rate decreased to AUD/USD 0.6212 on expiration of the contracts, then the holding-period return becomes -1435.72% per annum.

5.5.4 The Naïve Strategy and the Simple Moving Average Strategy

In Brock, Lakonishok and LeBaron (1992), the performance of technical trading rules are evaluated against the daily unconditional mean returns for the Dow Jones Index[105]. A similar approach is adopted in this study. Trading positions based on naïve trading models are created for each of the option maturities. The average holding-period returns of these positions are recorded for each option maturity over the test period. Statistical tests are then performed to determine if the mean holding-period returns from the simple moving average strategy are statistically different from the naïve strategy.

[105] See Tables I and II of Brock, Lakonishok and LeBaron (1992).

For each maturity, an upper and lower bound for the naïve positions are constructed with trigger values of -10 and +10 respectively, based on Equations (5-1) and (5-2). The rationale for this approach is to conduct buy and sell trades irrespective of any trade signals that may exist over the test period. Using these trigger values, nearly all data points fall outside of the bounds, generating a sufficiently large number of trades for the estimation of mean daily holding-period returns over the sample period. For instance, in Table 5-4, the estimated mean average holding-period return for the GBP/USD one-month at-the-money forward buy straddle is 0.009% per year – this is used as a naive holding-period return for comparison with holding-period return achieved under various trigger values. Since one buy and sell trade is generally initiated each day of the sample period, trading decisions made using this approach do not specifically make use of the information contained in the time pattern of the volatility price series. Thus, if the mean holding-period return of the combination trades is positive and statistically different from the mean holding-period return for the naïve trades, one can conclude that the moving average rules contain useful information.

Table 5-4: Naïve Models for At-the-money Forward Straddles

	Buy Straddle				Sell Straddle			
	N	**% win**	**R^{hpa} (%)**	**R^{hpa}/SD**	**N**	**% win**	**R^{hpa} (%)**	**R^{hpa}/SD**
GBP/USD								
1M	926	48.488	0.009	0.352	926	45.464	-0.023	-0.841
3M	885	41.582	0.000	0.007	885	56.723	-0.010	-0.202
6M	825	50.182	0.006	0.096	825	45.333	-0.015	-0.221
1Y	698	52.436	0.022	0.226	698	44.986	-0.027	-0.289
Mean		**48.172**	**0.009**	**0.170**		**48.127**	**-0.019**	**-0.388**
EUR/USD								
1M	932	42.918	-0.001	-0.032	932	52.468	-0.008	-0.423
3M	891	47.026	0.002	0.065	891	50.730	-0.009	-0.249
6M	831	49.699	0.006	0.118	831	46.811	-0.011	-0.238
1Y	704	46.875	0.000	-0.006	704	49.290	-0.004	-0.057
Mean		**46.630**	**0.002**	**0.036**		**49.825**	**-0.008**	**-0.242**
AUD/USD								
1M	929	42.734	0.001	0.044	929	51.884	-0.006	-0.467
3M	889	42.070	0.003	0.125	889	55.906	-0.008	-0.288
6M	828	48.792	0.012	0.275	828	49.275	-0.015	-0.358
1Y	700	53.857	0.016	0.237	700	44.143	-0.018	-0.276
Mean		**46.863**	**0.008**	**0.170**		**50.302**	**-0.012**	**-0.347**
USD/JPY								
1M	930	41.183	-0.491	-0.285	930	54.301	-0.351	-0.204
3M	890	34.831	-1.215	-0.431	890	61.685	0.574	0.204
6M	829	45.959	-0.223	-0.057	829	50.543	-0.298	-0.076
1Y	702	45.726	-0.292	-0.054	702	51.994	-0.081	-0.015
Mean		**41.925**	**-0.555**	**-0.207**		**54.631**	**-0.039**	**-0.023**

Note: The above results are for trading days from 1 October, 2001 to 31 July, 2006. The upper and lower bounds are estimated using trigger values of -10 and +10 for the at-the-money straddle trades.

The naïve strategies are constructed for at-the-money forward implied volatility and risk reversal trades respectively. The average trade signals reported in Tables 5-4 and 5-5 result in approximately 800 trades over the sample period. The fraction of profitable trades (holding-period returns > 0) is approximately 0.48 for the straddles while it is approximately 0.30 for the risk reversal naïve trades.

Table 5-5: Naïve Models for Risk Reversals

	Buy Call Sell Put				Sell Call Buy Put			
	N	**% win**	**R^{hpa} (%)**	**R^{hpa}/SD**	**N**	**% win**	**R^{hpa} (%)**	**R^{hpa}/SD**
GBP/USD								
1M	926	34.665	0.012	0.451	926	21.922	-0.024	-0.926
3M	885	33.559	0.027	0.608	885	12.655	-0.036	-0.800
1Y	698	50.716	0.053	0.693	698	22.636	-0.059	-0.761
Mean		**39.647**	**0.031**	**0.584**		**19.071**	**-0.039**	**-0.829**
EUR/USD								
1M	932	29.721	0.006	0.364	932	19.850	-0.015	-0.821
3M	891	34.119	0.014	0.440	891	17.621	-0.021	-0.626
1Y	704	38.636	0.015	0.281	704	50.568	-0.019	-0.348
Mean		**34.159**	**0.012**	**0.362**		**29.346**	**-0.018**	**-0.598**
AUD/USD								
1M	929	36.060	0.011	0.972	929	15.070	-0.016	-1.402
3M	889	39.708	0.021	0.942	889	8.436	-0.024	-1.104
1Y	700	59.143	0.037	0.685	700	0.143	-0.040	-0.726
Mean		**44.970**	**0.023**	**0.866**		**7.883**	**-0.027**	**-1.077**
USD/JPY								
1M	930	29.032	-0.076	-0.049	930	20.645	-0.682	-0.443
3M	890	34.719	-0.129	-0.054	890	18.764	-0.417	-0.177
1Y	702	61.254	1.453	0.299	702	23.077	-1.780	-0.366
Mean		**41.668**	**0.416**	**0.065**		**20.829**	**-0.960**	**-0.329**

Note: The above results are for trading days from 1 October, 2001 to 31 July, 2006. The upper and lower bounds are estimated using trigger values of -10 and +10 for the risk reversal trades.

\

5.6 Empirical Results

Tables 5-6 and 5-7 present the results for trading day ranging from 1 October 2001 to 31 July 2006. The first column reports the trading rules used. These are identified according to contract type by maturity with the relevant trigger value. For instance (1M, 0.5) means the trades are performed using a 253-day moving average with a trigger value of 0.5 on the one-month contract. The number of closed trades ("*N*") is reported in the second column and the seventh column. The term "% win" records the percentage of trades with holding-period returns greater than zero at the expiration of the contract. "R^{hpa}" is the mean annualised holding-period return generated over the sample period, while "R^{hpa}/SD" is the ratio of mean holding-period return divided by the standard deviation of the holding-period returns over the corresponding trading period.

The *t*-ratios for the trades are presented in columns five and ten. They are used to test for differences of the mean holding-period returns for the buy and sell trades from the corresponding naïve trades presented in Tables 5-4 and 5-5. The term"Diff" is the mean holding-period return for the buy trade less the mean holding-period return for the sell trade. The corresponding *t*-ratios in the last column test the difference between the mean buy and the mean sell trades with the null hypothesis of zero. All *t*-ratios are 2-tailed tests at various levels of significance.

Across each of the tables, the number of trades decline with the trigger value as expected. As the lower and upper bound move further away from the prevailing rates, less trade signals are generated. For instance, in the one-month AUD/USD buy straddle

trade (see Panel C of Table 5-6), 513 buy signals are generated at the trigger value of 0.01 but only 112 signals are available at the trigger value of 1.5.

Table 5-6: Results for At-the-money Forward Straddle Trades

	Buy Straddle					Sell Straddle					Buy - Sell	
	N	% win	R^{hpa}(%)	*t*-ratio	R^{hpa}/SD	N	% win	R^{hpa}(%)	*t*-ratio	R^{hpa}/SD	Diff	*t*-ratio
Panel A: GBP/USD												
(1M, 0.01)	435	53.793	0.022 **	2.328	0.765	489	49.284	-0.011 **	2.295	-0.461	0.010 **	5.546
(3M, 0.01)	418	45.215	0.004	0.671	0.094	464	59.267	-0.007	0.574	-0.123	0.006	1.614
(6M, 0.01)	400	46.500	-0.004 *	-1.887	-0.073	422	43.128	-0.023	-1.489	-0.299	0.014 **	3.081
(1Y, 0.01)	307	33.876	-0.015 ***	-5.730	-0.173	384	31.771	-0.056 **	-4.757	-0.601	0.041 ***	6.050
(1M, 0.5)	311	55.949	0.031 **	3.432	1.023	326	49.387	-0.010 **	2.176	-0.386	0.012 **	5.363
(3M, 0.5)	291	56.357	0.024 **	3.599	0.570	292	53.767	-0.017	-0.860	-0.287	0.021 **	4.864
(6M, 0.5)	281	40.569	-0.020 **	-4.583	-0.545	264	45.833	-0.017	-0.411	-0.213	-0.002	-0.403
(1Y, 0.5)	221	24.434	-0.030 ***	-7.397	-0.414	239	37.657	-0.038	-1.510	-0.463	0.008	1.076
(1M, 1)	156	65.385	0.048 **	4.781	1.583	195	50.256	-0.005 **	2.410	-0.203	0.016 **	5.199
(3M, 1)	148	67.568	0.043 **	4.745	1.020	166	56.627	-0.008	0.269	-0.131	0.025 **	4.253
(6M, 1)	184	46.196	-0.012 **	-2.596	-0.367	184	51.087	-0.005	1.258	-0.061	-0.005	-0.834
(1Y, 1)	162	12.963	-0.050 ***	-9.303	-1.178	192	40.104	-0.027	0.109	-0.382	-0.023 **	-3.673
(1M, 1.5)	46	73.913	0.069 **	4.231	2.027	125	52.800	0.008 **	3.514	0.327	0.018 **	3.772
(3M, 1.5)	29	96.552	0.102 **	5.272	3.278	115	62.609	0.012 **	2.125	0.202	0.045 **	4.070
(6M, 1.5)	61	26.230	-0.024 **	-2.527	-0.732	140	66.429	0.022 **	4.220	0.314	-0.032 **	-3.491
(1Y, 1.5)	87	22.989	-0.038 ***	-5.734	-0.820	150	38.000	-0.026	0.139	-0.430	-0.012	-1.529
Mean		**48.030**	**0.009**		**0.379**		**49.250**	**-0.013**		**-0.200**	**0.009**	
Panel B: EUR/USD												
(1M, 0.01)	540	48.889	0.007 **	2.186	0.378	387	59.173	0.003 **	2.765	0.152	0.001	0.982
(3M, 0.01)	537	48.603	0.006	0.805	0.151	346	54.046	-0.004	1.110	-0.113	0.005 *	1.910
(6M, 0.01)	497	58.753	0.023 **	4.338	0.465	327	60.245	0.015 ***	6.126	0.356	0.005 *	1.675
(1Y, 0.01)	424	47.170	-0.003	-0.674	-0.046	276	48.913	-0.007	-0.783	-0.122	0.004	0.811
(1M, 0.5)	363	46.832	0.004	1.159	0.224	265	61.132	0.008 **	3.392	0.397	-0.001	-0.648
(3M, 0.5)	402	55.224	0.015 **	2.721	0.384	240	50.000	-0.009	-0.001	-0.254	0.012 **	3.901
(6M, 0.5)	386	62.953	0.026 **	4.941	0.575	208	72.115	0.034 ***	8.925	0.903	-0.005	-1.475
(1Y, 0.5)	344	40.116	-0.013 **	-2.990	-0.208	177	56.497	0.011 **	2.776	0.258	-0.024 **	-4.518
(1M, 1)	243	48.971	0.009 **	2.058	0.482	126	65.079	0.023 **	4.993	1.380	-0.004 **	-1.968
(3M, 1)	270	68.889	0.038 ***	6.846	1.025	126	57.143	0.001	1.485	0.033	0.019 **	4.541
(6M, 1)	255	70.980	0.034 ***	6.082	0.865	104	79.808	0.047 ***	8.475	1.460	-0.009 **	-2.013
(1Y, 1)	245	40.408	-0.015 **	-3.056	-0.246	94	43.617	0.000	0.488	-0.015	-0.015 **	-2.239
(1M, 1.5)	110	49.091	0.013 *	1.941	0.625	42	76.190	0.043 **	4.858	3.355	-0.009 **	-2.613
(3M, 1.5)	145	78.621	0.052 ***	7.388	1.603	36	41.667	-0.027	-1.359	-0.676	0.039 ***	6.234
(6M, 1.5)	147	72.789	0.025 **	3.420	0.971	42	78.571	0.043 **	5.151	1.460	-0.013 **	-2.658
(1Y, 1.5)	142	39.437	-0.018 **	-3.023	-0.383	46	47.826	0.002	0.573	0.080	-0.020 **	-2.755
Mean		**54.858**	**0.013**		**0.429**		**59.501**	**0.011**		**0.541**	**-0.001**	

Note: The above results are for trading days ranging from 1 October 2001 to 31 July, 2006. The t-ratios for the buy and sell straddle in columns 5 and 10 test the difference of the average holding-period returns for the buy and sell trades from the naïve trades. Trading rules are identified as (contract type by maturity, trigger value) in the first column. "N (Buy)" and "N (Sell)" are the number of buy and sell signals generated during the sample period.

**** Significant at the 1% level*

*** Significant at the 5% level*

** Significant at the 10% level*

5.6.1 Buy and Sell At-the-money Forward Straddle

Results for the straddle trades based on the moving average rules are presented in Table 5-6. For the four currency pairs examined, three currency pairs produced positive average holding-period returns for the buy straddle trades.

Table 5-6: Results for At-the-money forward Straddle Trades (continued)

	Buy Straddle					Sell Straddle					Buy - Sell	
	N	% win	R^{hpa}(%)	*t*-ratio	R^{hpa}/SD	N	% win	R^{hpa}(%)	*t*-ratio	R^{hpa}/SD	Diff	*t*-ratio
Panel C: AUD/USD												
(1M, 0.01)	513	40.546	0.000	-0.317	-0.016	412	50.728	-0.007	-0.316	-0.486	0.002 **	2.283
(3M, 0.01)	497	29.376	-0.014 ***	-6.457	-0.748	388	39.691	-0.029 ***	-6.534	-0.972	0.008 **	4.673
(6M, 0.01)	475	37.895	0.001 **	-2.996	0.030	350	34.286	-0.029 **	-3.760	-0.732	0.022 ***	7.373
(1Y, 0.01)	364	46.978	0.027 **	2.440	0.328	331	35.952	-0.006 **	3.156	-0.156	0.033 ***	6.660
(1M, 0.5)	429	36.131	-0.004 *	-1.691	-0.324	298	48.322	-0.009	-0.813	-0.580	0.001	1.465
(3M, 0.5)	414	26.087	-0.017 ***	-7.133	-0.964	263	39.544	-0.032 ***	-6.409	-1.016	0.008 **	4.038
(6M, 0.5)	352	28.693	-0.010 ***	-5.687	-0.242	255	33.725	-0.025 **	-2.288	-0.705	0.010 **	3.352
(1Y, 0.5)	233	35.622	0.020	0.781	0.227	251	35.857	-0.003 **	3.653	-0.104	0.022 **	3.906
(1M, 1)	293	32.082	-0.009 **	-3.367	-0.934	195	45.128	-0.012 *	-1.730	-0.789	0.001	0.871
(3M, 1)	320	23.125	-0.019 ***	-7.218	-1.165	175	45.714	-0.022 **	-3.146	-0.692	0.001	0.517
(6M, 1)	292	19.863	-0.017 ***	-7.219	-0.448	188	35.106	-0.019	-0.926	-0.643	0.002	0.500
(1Y, 1)	176	30.114	0.011	-0.811	0.128	203	36.453	-0.003 **	3.226	-0.129	0.014 **	2.239
(1M, 1.5)	112	28.571	-0.012 **	-2.817	-1.315	128	48.438	-0.005	0.194	-0.366	-0.002	-1.197
(3M, 1.5)	129	22.481	-0.022 **	-5.205	-1.214	122	52.459	-0.012	-0.811	-0.398	-0.005	-1.623
(6M, 1.5)	118	10.169	-0.029 ***	-7.097	-1.043	135	40.741	-0.014	0.177	-0.483	-0.010 **	-2.852
(1Y, 1.5)	80	2.500	-0.044 ***	-7.951	-1.563	149	34.899	-0.003 **	2.764	-0.128	-0.040 ***	-11.523
Mean		**28.140**	**-0.009**		**-0.579**		**41.065**	**-0.014**		**-0.524**	**0.004**	
Panel D: USD/JPY												
(1M, 0.01)	562	44.128	0.206 **	2.212	0.121	363	59.229	0.640 **	2.708	0.374	-0.126	-1.099
(3M, 0.01)	558	46.774	0.169 **	4.362	0.054	327	80.428	2.883 ***	6.957	1.701	-1.357 ***	-7.273
(6M, 0.01)	580	53.448	0.675 **	2.945	0.165	244	66.393	1.786 **	5.444	0.601	-0.785 **	-2.713
(1Y, 0.01)	487	55.852	0.727 **	3.465	0.168	213	77.465	2.287 **	5.280	0.340	-1.560 **	-3.673
(1M, 0.5)	423	48.936	0.657 **	3.320	0.387	237	54.008	-0.001	0.812	-0.001	0.191	1.385
(3M, 0.5)	414	55.314	1.440 ***	7.650	0.462	222	76.577	2.738 **	5.451	1.525	-0.649 **	-2.860
(6M, 0.5)	421	65.321	2.299 ***	7.615	0.587	143	59.441	1.258 **	3.227	0.451	0.736 **	2.073
(1Y, 0.5)	330	54.545	0.750 **	3.104	0.182	124	83.065	3.248 ***	6.088	0.484	-2.499 **	-4.781
(1M, 1)	222	52.252	0.727 **	2.754	0.422	168	53.571	-0.413	-0.125	-0.238	0.332 *	1.876
(3M, 1)	262	60.687	1.910 ***	7.757	0.634	142	82.394	3.292 **	5.579	1.901	-0.691 **	-2.516
(6M, 1)	262	78.626	4.091 ***	11.073	1.073	78	65.385	1.541 **	2.879	0.601	1.803 **	3.920
(1Y, 1)	220	49.091	0.127	1.092	0.040	70	82.857	3.555 **	5.180	0.485	-3.428 **	-5.501
(1M, 1.5)	74	48.649	0.508	1.405	0.321	88	48.864	-0.875	-0.797	-0.532	0.402	1.578
(3M, 1.5)	123	60.976	2.337 ***	6.450	0.741	70	88.571	3.853 **	4.803	2.357	-0.758 *	-1.872
(6M, 1.5)	138	90.580	5.873 ***	12.295	1.855	43	72.093	2.183 **	2.913	0.888	2.609 **	4.955
(1Y, 1.5)	134	58.209	0.512 *	1.692	0.217	28	100.000	7.282 ***	7.203	6.040	-6.770 ***	-14.732
Mean		**57.712**	**1.438**		**0.464**		**71.896**	**2.204**		**1.061**	**-0.784**	

Note: The above results are for trading days ranging from 1 October 2001 to 31 July, 2006. Trading rules are identified as (contract type by maturity, trigger value) in the first column. "N (Buy)" and "N (Sell)" are the number of buy and sell signals generated during the sample period. The t-ratios for the buy and sell straddle in columns 5 and 10 test the difference of the average holding-period returns for the buy and sell trades from the naïve trades.
**** Significant at the 1% level*
*** Significant at the 5% level*
**Significant at the 10% level*

The null hypothesis that the holding-period returns equal the holding-period returns generated by the respective naïve trades is generally rejected. The buy straddle mean holding-period returns range from a mean of –0.009% for the AUD/USD to 1.438% for the USD/JPY currency pair. This compares with the mean holding-period return of –0.555% for the USD/JPY and the highest mean holding-period return of 0.009% reported for the GBP/SUD naive trades. On a risk-adjusted basis, the mean buy straddle holding-period returns are also higher than the corresponding naïve trades. For instance, the "R^{hpa}/SD" ratio for the EUR/USD and the USD/JPY pairs are 0.43 and 0.46 respectively compared with a ratio of 0.036 and –0.207 for the naïve trades. Nearly all of the currency pairs rejected the null hypothesis that the holding-period returns equal the returns generated by the naïve trades at the 5 percent level of significance using a two-tailed test.

Similar results are reported for the sell trades. However, the overall mean holding-period return is less favourable for sell trades with only two out of four currency pairs reporting positive mean holding-period returns. The USD/JPY pair has the highest holding-period return of 2.20% per year. It is interesting to note that the USD/JPY series also has the highest mean holding-period return in the buy straddle trades of 1.44% per year across all trades. For this currency pair, nearly all the returns for the respective maturities and trigger values have positive returns over the sample period.

The third and the eighth columns in Table 5-6 report the fraction of buy and sell trades with holding-period returns greater than zero. For the buy trades, the mean fraction ranges from 0.28 to 0.57 while the sell trades have a range of 0.41 to 0.72 for

the AUD/USD and the USD/JPY straddle trades respectively. These fractions exhibit greater variation compared with the naïve trades with mean fractions of 0.42 to 0.55. If the trading rules did not produce useful trade signals, the mean fraction for moving average and naïve trades would be very close.

The second last column lists the differences between the mean buy and sell holding-period returns for the various maturities and trigger values. Most of the buy-sell differences are above zero with the exception of the EUR/USD and the USD/JPY currency pairs. Such differences appear to become increasingly negative as the triggers increase. This suggests that at higher trigger values, the sell trades perform slightly better than the buy trades. Overall, the *t*-tests for these differences are significant suggesting the null hypothesis of zero difference in trading profits for the buy and sell straddles trades can be rejected. The overall result is consistent with the general market trend observed in Figure 5-1 and the discussion provided in Section 5-2.

Regardless of the market trend, we observe that the buy straddle strategies profit when movement in the spot market is large enough to offset the cost incurred in the option trades. In an upward-trending market, the long straddles produce winning outcomes and positive holding-period returns as the call options move in-the-money at the expiration of the contracts. Likewise, in a declining market put options move in-the-money, generating positive holding-period returns sufficient to offset the option premia incurred. This explains the positive average holding-period returns reported for the GBP/USD, EUR/USD and USD/JPY currency pairs. Further a steady upward movement in the EUR/USD from 0.90 to around 1.30 over the sample period results in average winning trades of 55% and average holding-period return of 0.013% across all

maturities and trigger values. On the other hand, the spot exchange rate for USD/JPY declined from 132.165 on 4 March, 2002 to 114.371 on 31 July, 2006. The profit generated from the put option position produces average winning trade of 57.71% with average holding-period return of 1.438% per year across all trades, after taking into account of transaction costs.

For the sell straddle trades, profitable opportunities exist when the strategies offer large option premia from the sell call and put combination in a relatively less volatile spot market as such a market condition reduces the probability of the call and put moving in-the-money. For the EUR/USD and USD/JPY currency pairs, their respective implied volatility decline from 12.50% to 8.51% and 10.75% to 8.50% over the sample period (see Figure 5-1). Consistent with these patterns, positive mean holding-period returns are reported for these currency pairs over the same period. This is in contrast with the GBP/USD currency pair where the one-year at-the-money forward implied volatility moved from 7.10% on 1 April, 2002 to around 8.00% per year at the end of the sample period. As expected, the increase in volatility results in an average loss of -0.013% per year.

5.6.2 Risk Reversal Trades

The results for the risk reversals trades are presented in Table 5-7. For the buy-call-sell-put strategy, and consistent positive holding-period returns are reported for the AUD/USD, GBP/USD and EUR/USD currency pairs across all maturities.

Table 5-7: Results for Risk Reversal Trades

	Buy Call & Sell Put					Sell Call & Buy Put					Buy - Sell	
	N	% win	R^{hpa}(%)	*t*-ratio	R^{hpa}/SD	N	% win	R^{hpa}(%)	*t*-ratio	R^{hpa}/SD	Diff	*t*-ratio
Panel A: GBP/USD												
(1M, 0.01)	514	32.296	0.005	-1.453	0.203	408	19.608	-0.033	-1.630	-1.153	0.011 ***	6.391
(3M, 0.01)	509	32.809	0.024	-0.512	0.536	366	14.208	-0.039	-0.602	-0.906	0.032 ***	10.387
(1Y, 0.01)	320	32.813	0.030 **	-4.708	0.470	373	31.903	-0.079 **	-4.017	-0.971	0.109 ***	19.382
(1M, 0.5)	403	34.243	0.008	-0.606	0.350	279	18.996	-0.041 **	-2.651	-1.301	0.014 ***	6.735
(3M, 0.5)	363	37.466	0.033	1.129	0.789	218	13.761	-0.046	-1.502	-1.029	0.039 ***	10.726
(1Y, 0.5)	240	36.250	0.035 **	-3.251	0.526	276	26.812	-0.082 **	-4.354	-1.129	0.117 ***	18.971
(1M, 1)	222	31.982	0.012	0.091	0.485	129	19.380	-0.050 **	-3.056	-1.490	0.018 ***	5.745
(3M, 1)	209	45.933	0.054 **	4.095	1.308	125	12.800	-0.046	-1.198	-1.045	0.050 ***	10.439
(1Y, 1)	184	35.326	0.029 **	-4.003	0.478	174	17.241	-0.088 **	-4.716	-1.572	0.117 ***	18.959
(1M, 1.5)	96	25.000	0.008	-0.404	0.245	47	27.660	-0.051 **	-2.011	-1.531	0.017 **	2.998
(3M, 1.5)	109	43.119	0.055 **	3.114	1.263	16	0.000	-0.027	0.368	-1.498	0.041 **	3.730
(1Y, 1.5)	96	50.000	0.043	-1.206	0.642	89	13.483	-0.089 **	-3.604	-1.814	0.132 ***	15.143
Mean		**36.436**	**0.028**		**0.608**		**17.988**	**-0.056**		**-1.287**	**0.058**	
Panel B: EUR/USD												
(1M, 0.01)	574	20.557	-0.001	-2.153	-0.033	355	14.648	-0.027	-3.390	-1.712	0.008	6.522
(3M, 0.01)	585	30.940	0.014	-0.111	0.424	304	13.158	-0.022	-0.271	-0.675	0.018	7.715
(1Y, 0.01)	451	28.825	0.006	-3.366	0.164	250	43.600	-0.037	-3.885	-0.481	0.042	10.068
(1M, 0.5)	415	23.373	0.003	-0.822	0.177	235	13.617	-0.028	-2.958	-1.764	0.009	6.102
(3M, 0.5)	443	27.540	0.013	-0.328	0.423	188	5.851	-0.024	-0.652	-0.857	0.019 ***	7.047
(1Y, 0.5)	342	27.778	0.006 **	-3.135	0.218	155	36.129	-0.057 ***	-7.227	-0.745	0.063 ***	13.557
(1M, 1)	237	24.895	0.007	0.209	0.353	148	11.486	-0.035 **	-3.789	-2.384	0.012 ***	6.207
(3M, 1)	243	28.395	0.017	0.634	0.689	94	2.128	-0.032 *	-1.711	-1.543	0.025 ***	8.511
(1Y, 1)	192	29.688	0.006 **	-2.313	0.362	59	15.254	-0.101 ***	-10.955	-1.699	0.108 ***	22.282
(1M, 1.5)	125	29.600	0.016	1.540	0.658	59	13.559	-0.031 *	-1.953	-2.089	0.014 **	3.969
(3M, 1.5)	119	27.731	0.022	1.168	0.845	37	2.703	-0.027	-0.601	-1.647	0.024 **	5.434
(1Y, 1.5)	134	37.313	0.009	-1.355	0.490	19	5.263	-0.121 ***	-7.992	-2.830	0.130 ***	23.427
Mean		**28.053**	**0.010**		**0.398**		**14.783**	**-0.045**		**-1.535**	**0.039**	

Note: The above results are for trading days ranging from 1 October, 2001 to 31 July, 2006. The t-ratios in columns 5 and 10 test the difference of the average holding-period return for the "buy call & sell put" and "sell call & buy put" trades from the naïve trades. Trading rules are identified as (contract type by maturity, trigger value) in the first column. "N (Buy)" and "N (Sell)" are the number of buy and sell signals generated during the sample period.

**** Significant at the 1% level*

*** Significant at the 5% level*

** Significant at the 10% level*

Table 5-7: Results for Risk Reversal Trades (continued)

	Buy Call & Sell Put					Sell Call & Buy Put					Buy - Sell	
	N	% win	R^{hpa}(%)	*t*-ratio	R^{hpa}/SD	N	% win	R^{hpa}(%)	*t*-ratio	R^{hpa}/SD	Diff	*t*-ratio
Panel C: AUD/USD												
(1M, 0.01)	468	39.530	0.015 *	1.772	1.224	454	19.163	-0.011 **	2.130	-1.121	0.008 ***	10.335
(3M, 0.01)	485	36.701	0.019	-0.649	0.844	401	3.990	-0.026	-0.839	-1.260	0.023 ***	15.420
(1Y, 0.01)	456	41.886	0.011 ***	-10.149	0.636	240	0.000	-0.091 ***	-11.954	-1.410	0.101 ***	31.686
(1M, 0.5)	295	36.610	0.014	0.935	1.060	302	20.199	-0.007 **	3.787	-0.873	0.006 ***	6.853
(3M, 0.5)	315	37.143	0.021	0.058	0.889	278	1.079	-0.031 **	-2.231	-1.635	0.026 ***	14.662
(1Y, 0.5)	333	46.246	0.012 ***	-8.361	0.699	181	0.000	-0.100 ***	-12.677	-1.536	0.111 ***	29.589
(1M, 1)	155	36.129	0.011	-0.027	0.748	143	18.182	-0.005 **	3.397	-0.656	0.005 **	3.350
(3M, 1)	159	32.704	0.018	-0.769	0.702	151	0.662	-0.035 **	-2.958	-2.059	0.027 ***	10.784
(1Y, 1)	216	55.093	0.015 ***	-5.987	0.843	120	0.000	-0.122 ***	-15.022	-2.020	0.136 ***	31.041
(1M, 1.5)	95	34.737	0.009	-0.393	0.609	55	29.091	0.001 **	3.239	0.191	0.002	1.065
(3M, 1.5)	105	25.714	0.008 **	-2.762	0.342	73	0.000	-0.039 **	-2.793	-2.609	0.023 ***	7.538
(1Y, 1.5)	138	65.217	0.018 **	-4.047	1.004	71	0.000	-0.150 ***	-16.786	-4.521	0.168 ***	47.360
Mean		**40.643**	**0.014**		**0.800**		**7.697**	**-0.051**		**-1.626**	**0.053**	
Panel D: USD/JPY												
(1M, 0.01)	390	32.051	-0.160	-0.257	-0.096	523	23.901	-0.764	-0.291	-0.533	0.176 *	1.708
(3M, 0.01)	392	42.602	-0.017	0.419	-0.010	490	26.327	-0.333	0.299	-0.121	0.158	0.985
(1Y, 0.01)	431	58.701	1.247	-0.666	0.235	260	12.308	-2.143	-1.082	-0.554	3.390 ***	8.948
(1M, 0.5)	244	35.656	-0.528	-1.136	-0.283	296	28.378	-0.250	1.226	-0.165	-0.081	-0.555
(3M, 0.5)	218	60.550	-0.333	-0.603	-0.201	295	27.458	-0.727	-0.928	-0.256	0.197	0.915
(1Y, 0.5)	246	73.984	2.029	1.604	0.421	124	4.032	-1.485	0.665	-0.701	3.514 ***	7.740
(1M, 1)	144	38.194	-0.743	-1.332	-0.351	98	34.694	-0.099	1.023	-0.057	-0.187	-0.724
(3M, 1)	117	64.957	-1.383 **	-2.755	-0.727	154	33.117	0.596 **	2.567	0.380	-0.990 **	-4.686
(1Y, 1)	128	89.063	0.426 **	-2.368	0.270	89	0.000	-1.130	1.254	-0.816	1.556 ***	7.508
(1M, 1.5)	81	56.790	0.803	1.402	0.411	15	53.333	5.914 **	4.766	2.920	-1.487 **	-2.691
(3M, 1.5)	57	54.386	-2.560 **	-3.782	-1.170	15	0.000	-0.532	-0.094	-1.792	-1.014 *	-1.781
(1Y, 1.5)	91	96.703	0.201 **	-2.457	2.172	27	0.000	-0.222 *	1.664	-68.596	0.423 ***	23.680
Mean		**58.636**	**-0.085**		**0.056**		**20.296**	**-0.098**		**-5.858**	**0.471**	

Note: The above results are for trading days ranging from 1 October, 2001 to 31 July, 2006. The t-ratios in columns 5 and 10 test the difference of the average holding-period return for the "buy call & sell put" and "sell call & buy put" trades from the naïve trades. Trading rules are identified as (contract type by maturity, trigger value) in the first column. "N (Buy)" and "N (Sell)" are the number of buy and sell signals generated during the sample period.
**** Significant at the 1% level*
*** Significant at the 5% level*
** Significant at the 10% level*

However, only the USD/JPY currency pair produced winning trades above 50 per cent. For the yen, the annual holding-period return is as high as two per cent for the one-year contract, after accounting for volatility and spot exchange rate spread. However, the overall result has a mean holding-period return of -0.085% per year. This is less compelling when compared to the results reported for straddle trades.

Overall, the mean holding-period returns are also less favourable than the corresponding holding-period returns reported in the naïve trades. With the exception of the USD/JPY series, all three currency pairs have a smaller fraction of winning trades compared with the naïve trades. Only 14.80% of closed trades record holding-period returns greater than zero for the EUR/USD sell-call and buy-put combinations while the naïve trade records 29.35% across all maturities for the same combination (refer to Table 5-5).

The averages calculated from all trades executed indicate that sell-call-buy-put risk reversal trades produce negative mean holding-period returns for all four currency pairs. For instance, a loss of -0.098% per annum is reported for the USD/JPY currency pair and this result is consistent with the steady appreciation of the underlying currencies against the U.S. dollar. This has resulted in negative holding-period returns as the call options moved in-the-money. Furthermore, the mean holding-period returns for the sell-call-buy-put risk reversals are consistently below the mean holding-period returns for the buy-call-sell-put positions. This result holds across all currency pairs and this confirms that the sell-call-buy-put combination resulted in greater losses due to the depreciation of the U.S dollar against all four currencies over the sample period.

In terms of winning trades, the sell-call-buy-put trades also performed less favourably. Whenever a positive profit is generated with the buy-call-sell-put strategy, it is unlikely to achieve the same trading outcome for the sell-call-buy-put strategy. This contention is supported by the *t*-ratios reported on the last column of Table 5-7 where the difference in the trading outcomes are statistically significant across all maturities and trigger values. When compared to the straddles trades, the rejections for equal means are stronger in this class of trading strategy.

5.6.3 Straddle Aggregate Result by Trigger Values

Tables 5-8 and 5-9 provide the aggregate mean percentage win ("% win") and the aggregate mean holding-period returns ($\overline{R}^{hpa}$) for the at-the-money forward straddle and risk reversals according to maturity and trigger values. The buy straddle trades consistently report higher holding-period returns and percentage winning trades compared with the naïve trades reported in Panel A. A similar pattern is also noted for the sell straddle trades.

The six-month buy straddle reported in Table 5-8 has the highest holding-period returns across most trigger values. Specifically, the mean holding-period return increases from 0.174% to 1.461% per year while the percentage wining trades increased marginally from 49.149% to 49.942%. This suggests that more profitable trades can be achieved at higher trigger values. This provides support for the notion that when the prevailing volatility series is high, the moving average rules provide useful signals for volatility trades. Similar patterns can be noted for three-month options. Furthermore, it is interesting to note that the one-year straddle has the lowest percentage of winning trades and holding-period returns at trigger values of 1.0 and 1.5.

Table 5-8: Aggregate Result for At-the-money Forward Straddles

	Buy Straddle		Sell Straddle	
	Mean % win	$\overline{R}^{hpa}$ **(%)**	Mean % win	$\overline{R}^{hpa}$ **(%)**
Panel A: Naive Trades:				
(1M, ±10)	43.831	-0.120	51.029	-0.097
(3M, ±10)	41.377	-0.302	56.261	0.137
(6M, ±10)	48.658	-0.050	47.991	-0.085
(1Y, ±10)	49.724	-0.064	47.603	-0.033
Panel B: Aggregate Trades				
(1M, 0.01)	46.839	0.059	54.604	0.156
(3M, 0.01)	42.492	0.041	58.358	0.711
(6M, 0.01)	49.149	0.174	51.013	0.437
(1Y, 0.01)	45.969	0.184	48.525	0.554
(1M, 0.5)	46.962	0.172	53.212	-0.003
(3M, 0.5)	48.246	0.366	54.972	0.670
(6M, 0.5)	49.384	0.574	52.779	0.313
(1Y, 0.5)	38.682	0.182	53.269	0.805
(1M, 1.0)	49.672	0.194	53.509	-0.102
(3M, 1.0)	55.067	0.493	60.472	0.816
(6M, 1.0)	53.916	1.024	57.846	0.391
(1Y, 1.0)	33.144	0.018	50.758	0.881
(1M, 1.5)	50.056	0.145	56.573	-0.207
(3M, 1.5)	64.657	0.617	61.326	0.957
(6M, 1.5)	49.942	1.461	64.458	0.558
(1Y, 1.5)	30.784	0.103	55.181	1.814

Note: $\overline{R}^{hpa}$ is the mean annualised percentage holding-period over the sample period for the GBP/USD, EUR/USD, AUD/USD and USD/JPY currency pairs."Mean % win" is the mean of the corresponding trades with holding-period returns>0 at maturity.

A similar result can be observed for the sell straddle trades. In contrast however, the buy straddle trades reported in columns two and three provide evidence that the one-year straddles has the highest holding-period return for trigger values of 0.5, 1.0 and 1.5. Losses are incurred for the one-month sell straddle at trigger values of 0.5, 1.0 and 1.5, with the largest loss of -0.207% per year when the trigger is set at 1.50. This suggests that the test results are sensitive to the size of the trigger. Further the performance of the straddle trades is also associated with the movement of underlying exchange rates over the sample period.

5.6.4 Risk Reversal Aggregate Result by Trigger Values

Overall, the distinction between risk reversal and corresponding naïve trades are less pronounced in Table 5-9 even at high trigger values. The buy-call-sell-put risk reversal performed marginally better than the naïve trades reported in Panel A. The one-month and one-year risk reversals generate better holding-period returns and winning trades at higher trigger values. This is consistent with the results for the three and six-month straddle reported in Table 5-8.

Table 5-9: Aggregate Result for Risk Reversals

	Buy-Call & Sell-Put		Sell-Call & Buy-Put	
	Mean % win	$\overline{R}_{hpa}$ (%)	Mean % win	$\overline{R}^{hpa}$ (%)
Panel A: Naive Trades:				
(1M, ±10)	32.370	-0.012	19.372	-0.184
(3M, ±10)	35.526	-0.017	14.369	-0.124
(1Y, ±10)	52.437	0.390	24.106	-0.474
Panel B: Aggregate Trades				
(1M, 0.01)	31.108	-0.035	26.459	-0.208
(3M, 0.01)	35.763	0.010	26.667	-0.104
(1Y, 0.01)	40.555	0.323	44.022	-0.587
(1M, 0.5)	32.470	-0.125	26.219	-0.081
(3M, 0.5)	40.674	-0.066	29.326	-0.206
(1Y, 0.5)	46.064	0.520	45.792	-0.430
(1M, 1.0)	32.799	-0.178	26.297	-0.047
(3M, 1.0)	42.997	-0.323	28.147	0.120
(1Y, 1.0)	52.292	0.118	44.162	-0.360
(1M, 1.5)	36.531	0.209	33.186	1.458
(3M, 1.5)	37.737	-0.610	20.700	-0.156
(1Y, 1.5)	62.308	0.067	45.166	-0.145

Note: $\overline{R}^{hpa}$ is the mean annualised percentage holding-period over the sample period for the GBP/USD, EUR/USD, AUD/USD and USD/JPY currency pairs."Mean % win" is the mean of the corresponding trades with holding-period returns >0 at maturity.

The sell-call-buy-put risk reversals have fewer winning trades compared with the buy-call-sell-put risk reversals. The holding-period returns are also lower than those observed for the buy-call-sell-put positions in most instances. The largest trading loss is reported for the one-year position at the trigger value of 0.01. The losses are less severe when a larger trigger value is used. This can be seen at the trigger values of 0.5, 1.0 and 1.5 where the losses improved from -0.430% to -0.145% per year.

5.7 Conclusion

By allowing for volatility and exchange rate spreads, the trading rules examined in this study earn positive returns for the majority of the currency pairs over the test period. The empirical evidence for the straddles indicates that buy signals generate a greater number of profitable trades than the sell signals. The differences in profit size for the buy and sell strategies are also statistically significant. Further, risk reversal trades produce less compelling outcomes with lower winning trades and profits. This could be attributed to the size of the gap between the strike prices as the net cost of the call and put produces a zero position over this range. As a result, the movement in the underlying market has to be sufficiently large to shift the price outside the region for the strategies to generate positive holding-period returns.

Overall, the empirical results in this study are consistent with the market trend over the sample period. They indicate that the use of simple average trading rules provides useful buy and sell signals for volatility trading. This finding contradicts the random walk theory and thus lends support to the results reported in Chapter 4.

Furthermore, consistent with recent literature, the results confirm the usefulness of the moving average trading rules even after adjusting for transaction costs.

As discussed in Chang and Olser (1999), central bank intervention in foreign exchange markets may lead to the violations of random walk behaviour. Since the implied volatility prices reflect spot market sentiment, such a violation may introduce identical price behaviour in the currency option market. In additional, Bonser-Neal and Tanner (1996) find no support for the hypothesis that exchange rate intervention by the Bank of Japan reduced USD/JPY implied volatility. Instead, the intervention seems to have resulted in a significant increase in the USD/JPY implied volatility. Beine, Benassy-Quere and Lecourt (2002) report similar findings in their study of central bank interventions in the foreign exchange market. These studies offer support for the results reported in Tables 5-6 (Panel D) and 5-7 (Panel D) for the USD/JPY currency pair. Since market inefficiency can be demonstrated if exploitable opportunities are revealed by technical trading strategies, the test results reported in this chapter suggest that the over-the-counter currency option market may not be fully efficient. It may further imply that pricing models employed by market traders do not fully capture actual market characteristics.

CHAPTER 6 – THE DYNAMICS OF VOLATILITY SMILE AND FOREIGN EXCHANGE RISK

6.1 Introduction

In Chapters 4 and 5, empirical examinations of the over-the-counter currency option market are performed using implied volatility data from at-the-money option and from various option combinations. It is shown in Chapter 4 that short-dated implied volatility tend to violate the random walk hypothesis over the sample period. The results from the volatility trading analysis in Chapter 5 indicate that moving average trading strategies generate positive returns.

This chapter offers further empirical analysis of the behaviour of the over-the-counter currency option market using a richer dataset that comprises of implied volatility quotes which correspond to various levels of moneyness. The structure of the implied volatility data facilitates close examination of the volatility smile anomaly in the over-the-counter currency option market.

The Garman-Kohlhagen (1983) option-pricing model assumes that the volatility of the underlying exchange rate is constant across all strike values. Empirical evidence, however, suggests that the implied volatility parameter derived from a currency option-pricing model is not a constant function of moneyness. This systematic departure from the theoretical assumption underlying the Garman-Kohlhagen option-pricing model is known as the "volatility smile" where a u-shaped pattern between implied volatility and moneyness is often observed. Specifically in-the-money and out-

of-the-money options have relatively higher implied volatility than at-the-money options.

This chapter is structured as follows. Section 6.2 presents literature on the volatility smile anomaly and describes the nature of the data used in this study. Section 6.3 introduces the process used to estimate the daily volatility smile and the results of quadratic approximation are presented in Section 6.4. Section 6.5 analyses the dynamics of the estimated curvature and slope proxies while Section 6.6 describes the estimation of conditional volatility. Section 6.7 explains the Granger-causality tests and the results from these tests are reported in Section 6.8. A robustness test, using probit analysis, is presented in Section 6.9. Section 6.10 concludes this chapter.

6.2 Volatility Smile Anomaly

The literature supporting the existence of the volatility smile suggests two underlying reasons for this phenomenon. First, some studies report that the smile is a result of the erroneous assumption regarding the probability distribution of the future exchange rate. Specifically, these studies suggest that the probability of asset price distribution is skewed and leptokurtic instead of lognormal. For example, Malz (1997) and Campa, Chang and Reider (1998) show that foreign exchange distributions derived from an asymmetric volatility smile deviate significantly from the lognormal assumption.

In line with the violation of lognormal assumption, a number of researchers have tested smile-consistent classes of model, including Bates (1996a), Gessner and

Poncet (1997), Das and Sundaram (1999) Sarwar and Krehbiel (2000). These authors generally conclude that incorporating jump processes and stochastic volatility components into the Garman-Kohlhagen (1983) option-pricing model does not fully explain or reproduce the pronounced volatility smile observed in empirical studies. Chesney and Scott (1989) suggest that the use of the Garman-Kohlhagen (1983) model with daily revised implied volatility, provides a better estimate of observed currency option prices than more complex models such as the stochastic volatility models. Thus it appears that skewness and leptokurtic effects alone may not fully explain the empirical smile puzzle.

Another explanation for the smile effect that has emerged in recent literature is related to trading activity in response to hedging pressures. Specifically, as currency option traders anticipate significant volatility in the market, out-of-money options are purchased as a form of insurance. Ederington and Guan (2002) argue, for example, that in the stock index options market implied volatility differs because of hedging pressure. When a market crash is anticipated, market players hedge their portfolio from downside risk by purchasing out-of-money puts. As downside movement of the underlying asset eventuates, the option will move in-the-money and thus generates positive payoffs. Such hedging activities would create upward pressure on the option premia as the volume of trade increases. Put-call parity would then result in changes in implied volatility of the put and call with the same moneyness to remove arbitrage opportunities.

Bollen and Rasiel (2003) also support the hedging argument and conclude that the existence of a symmetric u-shaped pattern of quoted implied volatility in the

currency option market reflects demand by hedgers in anticipation of erratic movements in the foreign exchange market. Thus, a trading-based argument may provide further insight into the dynamics of the empirical smile. Finally, the "net buying pressure" argument by Bollen and Whaley (2004) postulates that the supply and demand imbalance due to trading activities by market players push up the implied volatility for out-of-money options in the index option market.

Also consistent with the hedging hypothesis, the 'skewness premium'[106] reported in Bates (1996) fluctuated drastically over the ERM[107] crisis period and became increasingly negative preceding the withdrawal of the British pound from the ERM, after the Bank of England failed to support the pound sterling above its lower limit of DM2.778[108]. In addition, Doran, Peterson and Tarrant (2007) provide empirical evidence that the skewness in option prices resulting from higher implied volatility for out-of-the money relative to at-the-money and in-the-money options provides some information about the future movement of the underlying market.

In the spirit of Doran *et al* (2007), this chapter contributes to the literature by exploring the relation between volatility smile dynamics and future volatility for the following currency pairs - the GBP/USD, EUR/USD, AUD/USD and USD/JPY. Different measures of smile dynamics are used to capture the daily behaviour of the volatility smile, namely, the slope of the put and call volatility curves, the skewness of the foreign exchange rate distribution and curvature of the volatility smile. In addition, the slope coefficient at each level of moneyness is also estimated. In particular, this

[106] This is defined as $(C/P - 1)$, where c and p are call and put option premia. These options are equally out-of-money.
[107] This stands for Exchange Rate Mechanism which was operational from 12 March, 1979 to the 2 August, 1993.
[108] See Figure 1 and Figure 4 of Bates (1996b). Malz (1996) also provides extensive discussion and analysis on the ERM crisis using over-the-counter currency option prices.

study aims to determine whether the daily movement of the smile curve is related to the anticipated volatility in the underlying currency.

A volatility smile is constructed for each trading day using one-month implied volatility quotes for call and put options. A smooth volatility smile is estimated by fitting a quadratic function to the observed volatility smile data. Further, the first derivative of the quadratic approximation is derived to estimate the slope at various points along the smile. For the estimation of future volatility, this study uses a recursive GARCH (1,1) model proposed by Kroner, Kneafsey, Claessens (1995) to obtain comparable one-month ahead GARCH estimate of conditional exchange rate volatility. Granger causality and vector-autoregressive tests are then applied to examine the relations that exist between measures of smile dynamics and anticipated volatility for each currency pair. The robustness of the analysis is confirmed using multivariate probit.

6.2.1 Currency Option Trading and Volatility Smiles

The dynamics of the volatility smile in the over-the-counter currency option market may be induced from the interaction between the supply and the demand of puts and calls resulting from active trading of out-of-money options. As the quoted implied volatility of spot exchange rates reflects traders' assessment of the future currency movement, any anticipated volatility change is likely to be reflected in the currency option market associated with a change in option trading activities. In particular, informed traders who perceive out-of-money options as a cheap form of insurance can enter into a trade with a put option writer to reduce their risk of a large decline in the

spot exchange rate market. If this hypothesis holds for this group of trades in the market then quoted implied volatility for the out-of-money option premia should increase to reflect increased demand.

Out-of-money puts and calls are also attractive to market participants who seek to engage in speculative and highly leveraged option trades. With a relatively low premium, the speculator may purchase out-of-money calls or puts when the foreign exchange market is calm, in the hope that a large upward or downward shock develop within the option expiration period leaving one or more of the options in-the-money at expiration.

The exposure of the option writers to unlimited downside risk can be hedged by taking an offsetting position in the option market. For instance, a put option writer can hedge against market exposure by purchasing a put option on the same currency under the same terms. Their position needs to be rebalanced frequently, thus creating a demand for near or out-of-money options.

6.2.2 Data

Traditionally, the estimation of implied volatility is achieved given the observed option price using the Black-Scholes (1973) formula. The application of this procedure can result in considerable measurement errors due to various market frictions (Hentschel, 2003). A distinct feature of the dataset obtained from the over-the-counter option market is the use of quoted implied volatility to estimate the daily volatility smile. This alleviates estimation errors induced by non-synchronous trades and other

market frictions resulting from separate trading of spot exchange rate from the option market.

The quoted implied volatility used in this study is generously provided by UBS Investment Bank[109] in Switzerland. UBS is a major market-marker of over-the-counter currency option in the European market. The sample consists of daily closing average of bid and ask implied volatility prices of European options with their corresponding delta values for the GBP/USD, EUR/USD, AUD/USD and USD/JPY over different time periods from 27 October, 1999 to 5 May, 2006. The use of average bid-ask implied volatility avoids the bid-ask bounce problem commonly found in empirical research.

Over-the-counter implied volatility are quoted with constant maturity as distinct from the exchange-traded equivalent available at PHLX. Daily closing dealer quotes for the one-month European calls and puts are collected at 6:00 pm, Monday to Friday at New York trading time. The volatility quotes for the each currency pair are available in different delta values of 5 to 45 with increments of 5[110]. Daily quotes for delta-neutral options are also available over the corresponding period. In essence, the delta of an option measures the rate of change of the option price relative to the underlying asset price. Mathematically, this is defined as the first-order partial derivative of the option price with respect to the price of its underlying asset. The delta neutral option is struck when the delta value for the call and put are equal but opposite; the delta value of this option is approximately 50[111]. Market convention also refers to

[109] UBS AG was formed through the merger of Swiss Bank Corporation and the Union Bank of Switzerland in 1998.
[110] This is equivalent to 0.05 in decimal places which is used in the Garman-Kohlhagen (1983) model to calculate the dollar premium for the option contract.
[111] This is equivalent to 0.5 in decimal places.

the delta neutral option as the at-the-money option where the strike price of the option equals or is close to, the underlying spot exchange rate.

This study draws on Covrig and Low (2003) who suggests that the one-month at-the-money implied volatility of currency option is an unbiased estimator of future volatility. According to Covrig and Low (2003), the delta-neutral position should correlate reasonably well with the estimated volatility over time.

The daily spot exchange rate data for each currency pair is obtained from Reuters at 5:00 pm New York trading time. Thus, measurement errors induced by time mismatch for the spot and the currency option are assumed negligible. To obtain daily forecasts of one-month ahead volatility for each of the three currency pairs, a recursive GARCH (1,1) is used to estimate conditional variance following Kroner, Kneafsey and Claessens (1995).

The daily one-month interest rates for the British pound (GBP), euro (EUR), Japanese yen (JPY) and American dollar (USD) are obtained from Reuters-British Bankers' Association database where daily fixing of the one-month interest rates is performed at 11:00 am GMT. A mismatch error might arise between interest rates, option and spot reporting times, but the impact on analysis is assumed to be small as intra-day money market interest rates are usually stable. Matched interest rates, spot rate and option volatility give rise to an aggregate sample of 3,744 daily observations which translates to 71,136[112] useable sets of data. The availability of both time series and

[112] For each day, there are 19 cross-sectional data points that corresponds to different levels of delta. Thus total number of usable observations equals 19 x 3,744 for the entire sample period.

cross-sectional components allow the construction of a reasonably complete volatility smile for each day over the entire sample period.

6.2.3 Implied Volatility vs Deltas

Figure 6-1 presents implied volatility quotes against different levels of delta for the GBP/USD, EUR/USD, AUD/USD and USD/JPY currency pairs on 21 August, 2003. The graphs reveal a very prominent smile pattern in the over-the-counter currency option market data. The complete volatility smile is constructed using both put and call quoted implied volatility of the same moneyness measured in deltas; the put and call volatility curves are connected at the delta-neutral[113] position which has a value of approximately 50. Thus put volatility curve appears to the left of the delta-neutral and call volatility curve is located to the right of the delta-neutral position.

By definition, the absolute values of European put and call deltas should sum to the value of one (Hull, 2006). It should be noted that, the quoted implied volatility for a put with delta value of x must equal the quoted implied volatility for a call with delta value of $(1-x)$. For instance, the implied volatility for a 25-delta put should be identical to that of a 75-delta call option.

[113] This is approximately equivalent to at-the-money position. The terms "delta-neutral" and "at-the-money" are used interchangeably.

Figure 6-1: One-month Quoted Implied Volatility versus Delta on 21/08/2003

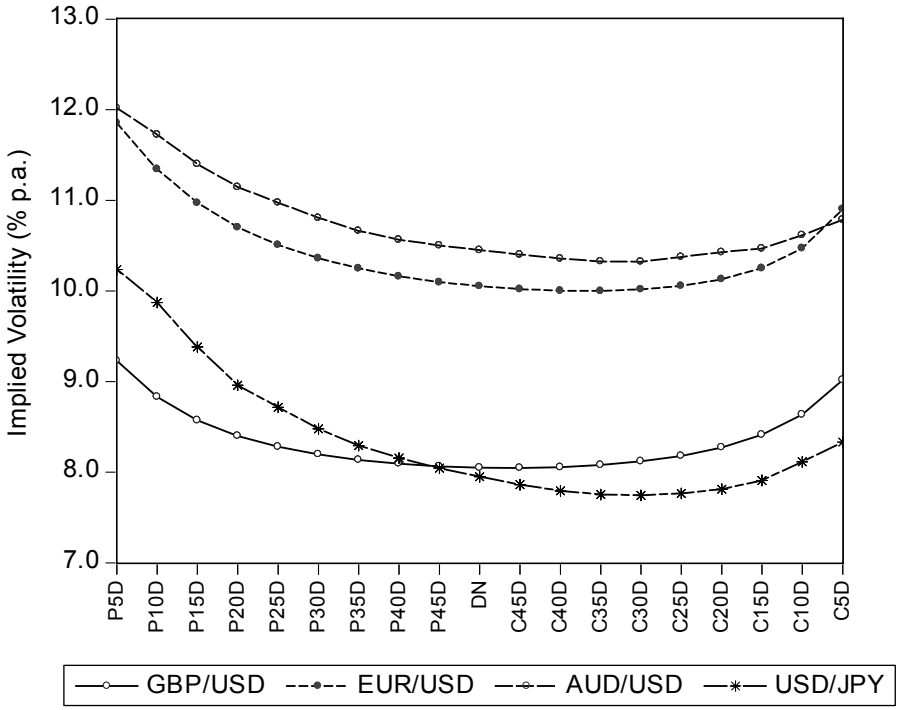

Note: The quoted volatility for each level of moneyness measured in delta are used to construct the smiles. The letters "P" and "C" on the horizontal axis denote put and call option respectively; the value following these letters represents the degree of moneyness. For instance, "C5D" refers to a call option with delta value of five. "DN" represents the delta-neutral position.

Figure 6-1 illustrates that the volatility smiles are less than symmetrical with higher quoted volatility to the left of the volatility smiles. For instance, the 10-delta put and call for the EUR/USD have implied volatility of 11.34% and 10.47% respectively; this could suggest unequal preference for put and call at this level of delta. This is sometimes called a 'smirk' pattern. The existence of a 'smirk' pattern is also reported by Campa *et al* (1998) and is consistent with the post-1987 phenomena discussed in Bates (1991). Asymmetrical smiles may reflect market assessment of anticipated change in volatility for the unit currency – in this case depreciation of the GBP, EUR and AUD exchange rates against the US dollar.

6.2.4 Descriptive Statistics

Table 6-1 displays the summary statistics for the GBP/USD, EUR/USD, AUD/USD and USD/JPY currency pairs. The daily implied volatility series are available on different dates in some cases but most observations cover a common period from 2 October, 2001 to 2 June, 2006. The calls and puts are identified by delta values with their corresponding implied volatility. The series "C" and "P" denote call and put options respectively and the number that follows indicates the degree of moneyness. For instance,"C5D" means call option with a delta value of five while "DN" is the delta-neutral position.

First, the results report that the implied volatility for the out-of-the money calls and puts are consistently higher as the level of delta decreases; this pattern is observed across the four currency pairs. These results are not surprising since a u-shaped pattern is expected from the datasets where the smile applies. For the GBP/USD and EUR/USD currency pairs, calls have higher mean implied volatility compared with the puts of same moneyness. In contrast, if one expects the unit currency to have an equal chance of appreciation or depreciation against the US dollar, the call volatility should mirror the patterns observed in puts; clearly this is not the case. For instance, the 5-delta call for the GBP/USD has a mean of 9.375% but the corresponding mean for put is 9.111%. The gap between the calls and puts of the same moneyness becomes wider as the level of delta ranges from 45 to 5. For example, the GBP/USD gap changes from 0.022% (8.254% - 8.232%) to 0.264% (9.375% - 9.111%); the EUR/USD has slightly larger gaps of 0.078% and 0.947% respectively. Perhaps traders expect the GBP/USD and EUR/USD currency pairs to appreciate over the sample period and trade accordingly.

Table 6-1: Summary Statistics for the Implied Volatility Datasets

	Mean	Maximum	Minimum	Std. Dev.	Skewness	Ex. Kurtosis
Panel A : GBP/USD						
Spot GBP/USD	1.6814	1.9451	1.4082	0.1574	-0.1802	-1.2884
1-Mth GBP	4.2290	4.8831	3.3363	0.4439	0.1809	-1.3608
1-Mth USD	1.9288	4.1213	1.0200	0.8252	1.0465	0.1191
P5D	9.1110	13.2734	6.2070	1.1164	0.7996	1.7683
P10D	8.7592	12.8260	5.8002	1.1095	0.7227	1.7307
P15D	8.5561	12.5291	5.5165	1.1049	0.6689	1.7130
P20D	8.4292	12.3206	5.3405	1.1006	0.6375	1.6898
P25D	8.3463	12.1668	5.2300	1.0969	0.6190	1.6581
P30D	8.2915	12.0495	5.1602	1.0940	0.6079	1.6196
P35D	8.2570	11.9584	5.1180	1.0917	0.6014	1.5750
P40D	8.2380	11.8869	5.0961	1.0900	0.5977	1.5247
P45D	8.2320	11.8311	5.0908	1.0889	0.5965	1.4683
DN	8.2377	11.7898	5.1000	1.0885	0.5972	1.4070
C45D	8.2544	11.7597	5.1233	1.0886	0.5996	1.3375
C40D	8.2842	11.7398	5.1636	1.0893	0.6041	1.2544
C35D	8.3285	11.7318	5.2236	1.0909	0.6107	1.1567
C30D	8.3911	11.7373	5.3091	1.0935	0.6195	1.0397
C25D	8.4776	11.7793	5.4300	1.0975	0.6309	0.8974
C20D	8.5976	11.9060	5.6017	1.1037	0.6441	0.7236
C15D	8.7673	12.0858	5.8462	1.1138	0.6550	0.5170
C10D	9.0137	12.3555	6.1736	1.1319	0.6483	0.3000
C5D	9.3753	12.7922	6.5076	1.1653	0.6008	0.1753
Panel B: EUR/USD						
Spot EUR/USD	1.0876	1.3488	0.8600	0.1375	-0.1404	-1.2864
1-Mth EUR	2.6592	3.8300	2.0145	0.5917	0.2889	-1.6502
1-Mth USD	1.5431	2.6375	1.0200	0.3950	0.4945	-0.7408
P5D	10.7569	14.4068	7.6360	1.1728	-0.1387	-0.2867
P10D	10.3549	13.9295	7.2319	1.1553	-0.1499	-0.2823
P15D	10.1465	13.6291	7.0244	1.1421	-0.1602	-0.2825
P20D	10.0278	13.4247	6.9099	1.1331	-0.1651	-0.2821
P25D	9.9585	13.2777	6.8450	1.1269	-0.1659	-0.2808
P30D	9.9206	13.1684	6.8106	1.1226	-0.1637	-0.2784
P35D	9.9052	13.0861	6.7974	1.1195	-0.1590	-0.2746
P40D	9.9076	13.0241	6.8009	1.1174	-0.1521	-0.2693
P45D	9.9255	12.9786	6.8190	1.1161	-0.1428	-0.2623
DN	9.9574	12.9476	6.8500	1.1155	-0.1315	-0.2536
C45D	10.0041	12.9293	6.8950	1.1155	-0.1172	-0.2424
C40D	10.0692	12.9769	6.9578	1.1162	-0.0986	-0.2272
C35D	10.1550	13.1547	7.0409	1.1176	-0.0748	-0.2074
C30D	10.2671	13.3671	7.1502	1.1199	-0.0442	-0.1811
C25D	10.4141	13.6251	7.2950	1.1235	-0.0045	-0.1457
C20D	10.6097	13.9429	7.4894	1.1290	0.0462	-0.0988
C15D	10.8742	14.3373	7.7525	1.1377	0.1071	-0.0395
C10D	11.2348	14.8169	8.0980	1.1517	0.1629	0.0204
C5D	11.7041	15.3376	8.4807	1.1750	0.1549	0.0259

Note: The series "C" and "P" denote call and put option respectively; the number following these letters represents the degree of moneyness, for instance,"C5D" denotes call option with a delta value of five."DN" is the delta-neutral position;"1-Mth GBP" and "1-Mth USD" are the one-month BBA-Reuters LIBOR for the British pound and US dollar respectively. The sample period for the GBP/USD spans from 1 October, 2001 to 14 November, 2005, with a total of 962 observations. For the EUR/USD series, a total of 772 observations were collected over the period 1 October, 2001 to 23 December, 2004.

Table 6-1: Summary Statistics for the Implied Volatility Datasets (continued)

	Mean	Maximum	Minimum	Std. Dev.	Skewness	Ex. Kurtosis
Panel C: AUD/USD						
Spot AUD/USD	0.6901	0.7978	0.5275	0.0810	-0.6641	-1.0274
1-Mth AUD LIBOR	5.1834	5.7500	4.3713	0.3491	-0.3631	-1.4834
1-Mth USD LIBOR	2.2173	5.0756	1.0200	1.2006	0.9162	-0.5336
P5D	11.3809	17.5913	8.2627	1.8717	0.8720	0.5133
P10D	11.1188	17.1950	8.0562	1.8318	0.8644	0.5050
P15D	10.8399	16.7387	7.7900	1.7862	0.8437	0.4707
P20D	10.6429	16.3440	7.6057	1.7467	0.8080	0.3930
P25D	10.4925	16.0173	7.4679	1.7101	0.7782	0.3307
P30D	10.3503	15.7143	7.3450	1.6780	0.7489	0.2638
P35D	10.2456	15.4722	7.2602	1.6528	0.7193	0.1969
P40D	10.1862	15.2934	7.2179	1.6350	0.6898	0.1298
P45D	10.1489	15.1392	7.1995	1.6193	0.6593	0.0597
DN	10.1227	15.0000	7.1931	1.6049	0.6291	-0.0100
C45D	10.0984	14.8624	7.1899	1.5911	0.5979	-0.0809
C40D	10.0811	14.7290	7.1948	1.5791	0.5637	-0.1575
C35D	10.0828	14.6213	7.2165	1.5724	0.5261	-0.2381
C30D	10.1164	14.5437	7.2693	1.5716	0.4817	-0.3278
C25D	10.1874	14.4800	7.3622	1.5708	0.4287	-0.4315
C20D	10.2602	14.4700	7.3572	1.5738	0.3688	-0.5353
C15D	10.3651	14.4720	7.3795	1.5800	0.2962	-0.6520
C10D	10.5616	14.6410	7.4070	1.6136	0.2077	-0.7571
C5D	10.7604	14.8485	7.4352	1.6563	0.1321	-0.8251
Panel D: USD/JPY						
Spot USD/JPY	115.4272	134.7700	102.0300	7.5644	0.4464	-0.3333
1-Mth JPY LIBOR	0.0566	0.3622	0.0363	0.0406	5.4620	33.7159
1-Mth USD LIBOR	2.3370	5.4000	1.0200	1.2810	0.9800	-0.3212
P5D	11.2904	19.2557	7.8938	1.5133	1.0828	1.8487
P10D	10.8764	18.6149	7.8411	1.4894	1.0512	1.6462
P15D	10.4535	17.6429	7.7140	1.3922	1.0129	1.3782
P20D	10.0910	16.6869	7.6536	1.2887	0.9443	1.1069
P25D	9.8588	16.1191	7.6251	1.2296	0.8867	0.8883
P30D	9.6451	15.5899	7.6314	1.1739	0.8366	0.7012
P35D	9.5020	15.0761	7.5570	1.1326	0.7682	0.4312
P40D	9.3953	14.6463	7.4973	1.1010	0.7078	0.2082
P45D	9.3070	14.2963	7.4394	1.0757	0.6581	0.0396
DN	9.2396	14.0000	7.4000	1.0562	0.6182	-0.0940
C45D	9.1869	13.7055	7.3610	1.0399	0.5845	-0.2099
C40D	9.1510	13.4213	7.3392	1.0284	0.5601	-0.2957
C35D	9.1307	13.1360	7.3040	1.0217	0.5460	-0.3445
C30D	9.1333	12.8710	7.2775	1.0228	0.5484	-0.3380
C25D	9.1849	12.8500	7.3500	1.0383	0.5730	-0.2703
C20D	9.2636	13.2000	7.4373	1.0641	0.6054	-0.1755
C15D	9.4198	13.7875	7.5233	1.1274	0.6881	0.0514
C10D	9.6468	14.4824	7.6799	1.1989	0.7346	0.2234
C5D	9.8411	14.9903	7.7313	1.2710	0.7192	0.2207

Note: The series "C" and "P" denote call and put option respectively; the number following these letters represents the degree of moneyness, for instance, "C5D" denotes call option with a delta value of five. "DN" is the delta-neutral position; "1-Mth AUD" and "1-Mth USD" are the one-month BBA-Reuters LIBOR for the Australian dollar and US dollar respectively. The sample period for the AUD/USD spans from 19 April, 2002 to 5 May, 2006, with a total of 960 observations. For the USD/JPY series, a total of 1150 observations were obtained from 1 October, 2001 to 31 July, 2006.

In contrast, the implied volatility for the AUD/USD reported in Panel C are higher for puts than for calls of the same moneyness; the out-of-money 5-delta put has an implied volatility of 11.381% while the implied volatility for the 5-delta call is 10.760%. This is indicative of more demand for puts over calls. The difference between calls and puts of the same moneyness displayed greater variation the further the strike price from the spot price. Call options generally exhibit lower volatility and out-of-money calls do not show the same level of volatility as the puts. For example, for the 5-delta call, the standard deviation of volatility series is 1.656, which is lower than the corresponding standard deviation for put option of 1.872 while the corresponding skewness coefficients are 0.132 and 0.916 respectively.

Panel D of Table 6-1 reports the highest degree of skewness in the volatility smile for the Japanese yen compared with the other three currency pairs. The gaps between the puts and calls of the same delta values are much wider than the rest of the currency pairs. For example, the 5-delta put has a mean implied volatility of 11.290% while the mean for corresponding call is 9.841%, resulting in a gap of 1.449%. In fact the implied volatility for puts are consistently higher than the corresponding calls across all levels of moneyness. Thus it appears that on average, the market has a bearish view of the US dollar against the Japanese yen over the sample period. Indeed, the average exchange rate for the USD/JPY currency pair dropped from 132.705 in January 2002 to 115.681 in July 2006. Similar with the pattern observed in the AUD/USD currency pair, larger variations in the implied volatility series are also reported for the put options.

6.3 The Volatility Smile

As strike prices of over-the-counter currency options are usually set to equal the forward exchange rate of the same maturity, option moneyness is redefined as M which is a ratio of the strike price X relative to the forward exchange rate. For each delta level i on day t, the relative moneyness of an option with delta level i is measured as $(X_{i,t})$ / (F_t) where $X_{i,t}$ is the strike price relating to delta level i. The variable F_t is the corresponding forward price calculated on day t. Since the daily implied volatility quotes are expressed relative to the option delta, the option pricing parameter d_1 along with other observed option variables has to be inferred from the deltas to estimate the strike price. Given the option's delta is the first derivative of an option value with respect to the spot exchange rate, differentiating the call price function with respect to the spot price results in $e^{rfT}N(d_1)$. The value of d_1 can be then calculated by inverting the cumulative normal distribution function. Finally using the option's expiration, T and quoted implied volatility, σ, the strike price denoted as X can be estimated using Equation (6-2). This transformation is necessary so that the behaviour of the volatility smile can be examined across various strike prices. Figure 6-2 presents the reconstructed smiles using implied volatility and moneyness. The characteristics of the smiles remain consistent with those previously reported in Figure 6-1.

The daily forward rates are calculated using the observed interest rates for the respective exchange rates together with the daily closing spot exchange rates:

$$F = Se^{(r_d - r_f)T} \tag{6-1}$$

$$X = Fe^{1/2\sigma^2 T - d_1\sigma\sqrt{T}} \quad (6\text{-}2)$$

where

r_d	=	1-month LIBOR for the currency *d*, where *d* represents the British pound, euro, Australian dollar and Japanese yen,
r_f	=	1-month LIBOR for the US dollar,
T	=	time to expiration for the option contract,
S	=	Daily closing average bid and ask exchange rate for GBP/USD, EUR/USD, AUD/USD and USD/JPY

Figure 6-2: Implied Volatility versus Moneyness (X/F) for AUD/USD

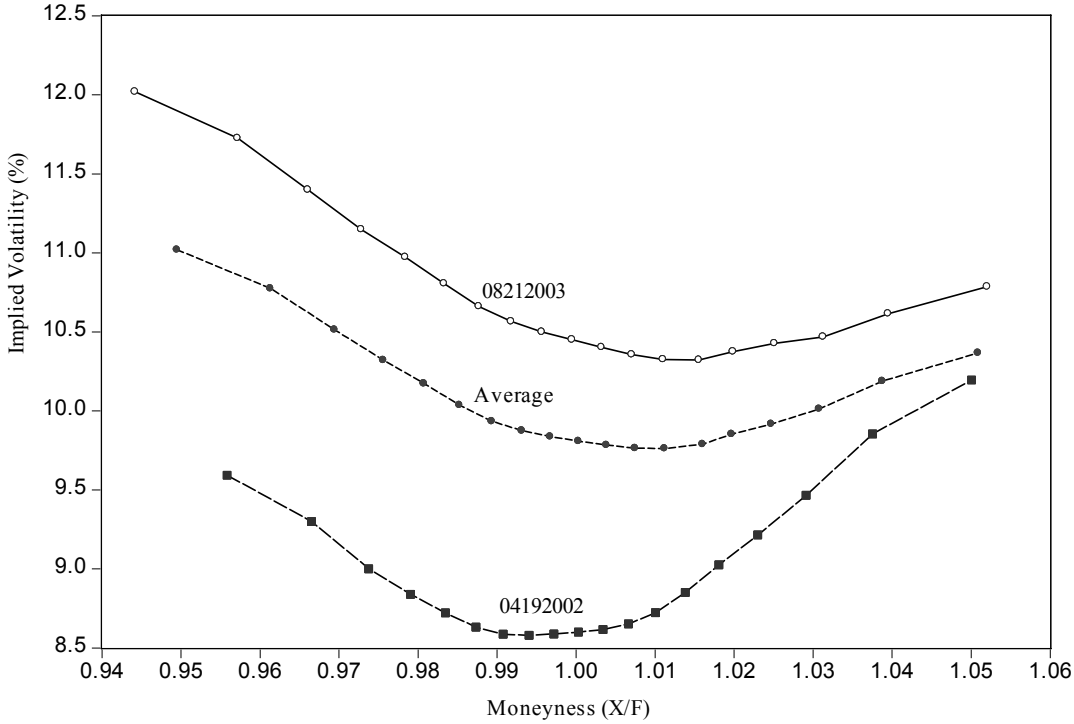

Note: This table plots two AUD/USD volatility smiles together with the average pattern over the sample period. The estimated smile on 19 April, 2002 and 21 August, 2003 vary considerably from the average smile over the sample period.

6.3.1 Smile Asymmetry

In Figure 6-2, the AUD/USD implied volatility of the puts and calls against the estimated moneyness defined as $(X_{i,t})/(F_t)$ is presented for selected trading days. Again significant skewness consistent with the findings of Bollen and Rasiel (2003) can be noted. Notably, a more symmetrical smile pattern is observed on 19 April, 2002 but the smile becomes a smirk on 21 August, 2003. The dynamic nature of the smile pattern may reflects the market sentiment over the trading days. The average closing exchange rate for the Australian dollar over the sample period is USD 0.6564. It appreciates from 0.5402 on 19 April, 2002 to 0.5555 on 20 May, 2002. Conversely it depreciates from 0.6582 on 21 August, 2003 to approximately 0.6450 in early September 2003.

6.3.2 Slope Coefficients for Call and Put Volatility Curves

The summary statistics for the daily volatility smile suggests that the shape of the smile changes considerably over time due mainly to the movement of the out-of-money calls and puts (see Table 6-1). It is possible that when a downward movement in the spot exchange rate is anticipated, market makers sell calls (puts) for lower (higher) implied volatility. To capture these responses from puts and calls separately, the smile slope for the call and put volatility curves are measured separately using a piecewise approximation method:

$$PF_t = \frac{IV_{5DP,t} - IV_{DN,t}}{M_{5DP,t} - M_{DN,t}} \tag{6-3}$$

$$CF_t = \frac{IV_{5DC,t} - IV_{DN,t}}{M_{5DC,t} - M_{DN,t}} \tag{6-4}$$

where

PF_t	=	slope of the estimated put volatility curve at period *t,*
CF_t	=	slope of the estimated call volatility curve at period *t,*
$IV_{5DP,t}$	=	quoted volatility for 5-delta put at period *t,*
$IV_{5DC,t}$	=	quoted volatility for 5-delta call at period *t,*
$IV_{DN,t}$	=	quoted volatility for delta-neutral at period *t,*
$M_{5DP,t}$	=	estimated moneyness $(X_{i,t})/(F_t)$ for 5-delta put for period *t,*
$M_{5DC,t}$	=	estimated moneyness $(X_{i,t})/(F_t)$ for 5-delta call for period *t*.

Using this method the slopes for the call and put volatility curves are calculated using two data points measured from the delta neutral position (which is approximately the lowest point of the call or put volatility curve) to the 5-delta position located which is generally at the highest point of the call and put volatility curves. This effectively measures the steepness of the volatility smile along the put and call volatility curves. The estimated slopes for the put volatility curve located to the left of the minimum point of the smile would generally have a negative value while positive slopes are expected for the call volatility curve.

6.3.3 Measure of Skewness for Volatility Smile

To measure the degree of skewness of the volatility smile, the difference between the absolute values of the slopes for the call and put volatility curves, defined in Equations (6-3) and (6-4) is estimated. Thus, smile skewness, *SKW* is defined as:

$$\left|CF_t\right| - \left|PF_t\right| \tag{6-5}$$

If the slope of the call volatility curve (to the right of the volatility smile) is steeper than the put volatility curve, then the smile skewness measure will report a positive value reflecting the non-symmetrical nature of the smile with a larger skewness to the right of the smile. It follows that for a symmetrical smile, *SKW* should have a value close to zero.

6.4 Quadratic Approximation of Volatility Smile

To capture the time-varying characteristic of the smile, a model for the volatility smile is required. Following Shimko (1993) and Dumas, Fleming and Whaley (1998)[114], estimation of a smooth volatility smile is performed by fitting a quadratic function to the daily observed implied volatility smile. The quadratic function takes the following form:

$$IV_i = a_{0,i} + a_{1,i}M_i + a_{2,i}M_i^2 + u_i \quad (6\text{-}6)$$

where

M_i = estimated moneyness calculated as $(X_{i,t}) / (F_t)$

IV_i = quoted implied volatility for a given level of moneyness i

The regression model specified in Equation (6-6) is estimated using a nonlinear approximation method for each day of the sample period. The sample is constructed using all available put and call data points. In other words, a cross-section of 19 data points by moneyness is used to estimate the volatility smile for each day. For each currency pair, regressions are estimated over the entire sample period, resulting in approximately 900 sets of estimates for the coefficients a_1 and a_2.

[114] See Model 7, pp.2068 of the original article.

Table 6-2: Estimated Smile Coefficients Using Quadratic Approximation

	$IV_i = a_{0,i} + a_{1,i}M_i + a_{2,i}M_i^2 + u_i$				$M = X/F$
Currency	$\hat{a}_0$	$\hat{a}_1$	$\hat{a}_2$	R^2	Mmin = $-\hat{a}_1/2\hat{a}_2$
GBP/USD	5.475	-10.808	5.415	0.987	0.998
EUR/USD	4.466	-8.811	4.445	0.984	0.991
AUD/USD	3.858	-7.445	3.689	0.972	1.009
USD/JPY	5.619	-10.897	5.371	0.992	1.014

Table 6-2 reports the coefficients estimated using the quadratic specification given by Equation (6-6).[115] The quadratic model provides a good fit for the observed smiles across all four currency pairs evidenced by the high average R^2 value. The coefficient $\hat{a}_1$ is directly related to $\hat{a}_2$ where $\hat{a}_1$ is approximately $-2\hat{a}_2$. The minimum point of the smile curve can be calculated as the derivative of Equation (6-6) relative to the degree of moneyness *X/F*, which can be set to zero to find the minimum volatility moneyness value, *X/F*. The results are reported in the last column of Table 6-2. Overall, the minimum point of the volatility smile, "Mmin", is very close to 1.00 as expected. This result is consistent with the volatility smile presented in Figure 6-2 suggesting, on average, the at-the-money option has the lowest implied volatility on any given day of the sample period. This result holds across all currency pairs. In short, the quadratic model appears to provide a good estimate of the daily smile curve.

6.4.1 Measure of Curvature for Volatility Smile

In order to examine the sensitivity of the smile curve to future foreign exchange risk at each level of moneyness, Equation (6-6) is differentiated with respect to moneyness (*M*) to give:

[115] These represent averages of the coefficients estimated from the quadratic model.

$$\frac{\delta IV_t}{\delta M_t} = a_{1,t} + 2a_{2,t}M_{i,t} \quad (6\text{-}7)$$

The coefficients a_1 and a_2 from Equation (6-6) are substituted into Equation (6-7) to calculate the slope of the smile at different values of *M* along the volatility smile. The calls and puts correspond to the delta values from 5 to 45 (increasing by 5). In contrast to the method defined in Equations (6-3) and (6-4), this procedure provides an estimation of a slope coefficient for any given level of moneyness. Taking the second derivative of Equation (6-6) with respect to *M* provides a measure of curvature, *CE,* for the volatility smile, which is calculated as:

$$CE_t = 2a_{2_t} \quad (6\text{-}8)$$

The coefficient for a_2 is obtained from estimation of Equation (6-6). The curvature coefficient is estimated daily resulting in approximately 900 observations for each currency pair. If the observed smile on a given day *t* has become less prominent than the previous day *t-1*, the coefficient for the smile curvature on day *t* is expected to be lower than the day before. The dynamics of the volatility smile proxied by *CF*, *PF*, *SKW* and *CE* are used in the time series and probit models reported in sections 6-8 to 6-9.

6.5 Dynamics of Curvature and Slopes Coefficients over Time

Figure 6-3 displays the estimated daily smile curvature and slope for the call and put volatility curves over the sample period for the GBP/USD, EUR/USD, AUD/USD and the USD/JPY currency pairs. The estimated daily slope coefficients for the call "*CF*" (middle line) and put volatility curves "*PF*" (bottom line) are shown. Equations (6-3) and (6-4) are used for the estimation of these coefficients. On the right axis of the graph, the smile curvature coefficient denoted as "*CE*" is also presented.

This is estimated using the second derivative of the quadratic equation specified in Equation (6-8).

The slope coefficients ("*PF*") estimated from the put volatility curves are mostly below zero and vary considerably over the sample period. However, for the euro, the slope coefficients exceed zero from 26 June, 2002 to 17 January, 2003. When a smile is constructed using average implied volatility over the entire sample period, a virtually linear upward-sloping line is obtained. The shape of smile is nearly flat for the 5-delta to 45-delta puts and starts to slowly increase from delta-neutral onwards with the highest volatility recorded for the 5-delta call. Conversely for the AUD/USD, the average smile curves for the periods from 20 April, 2004 to 27 July, 2004, 13 May, 2005 to 30 December, 2005 and 17 May, 2006 to 4 October, 2006 are generally downward sloping.

Figure 6-3: Time Series Plots of Curvature and Slope Coefficients

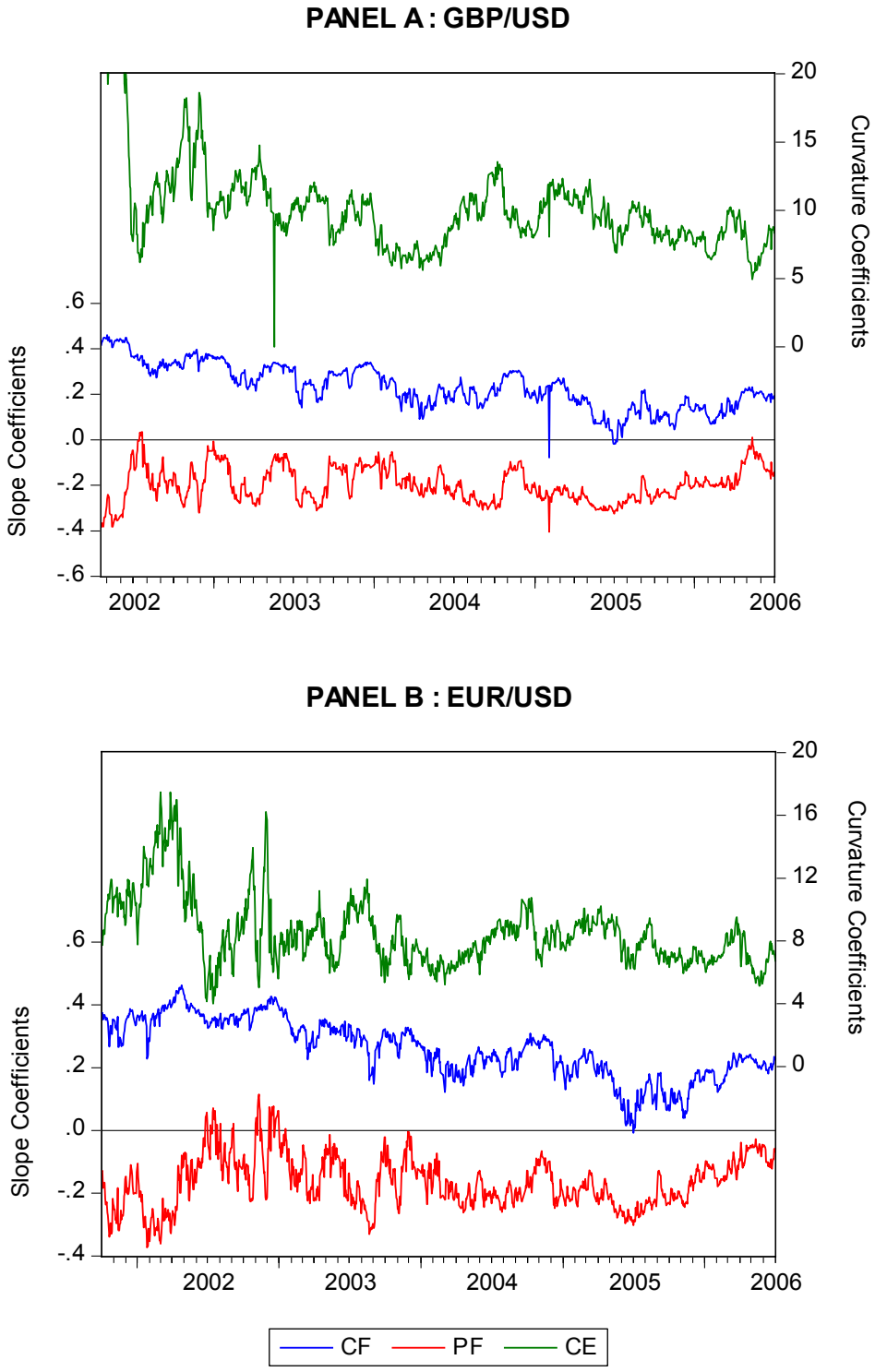

Note: "CE" (top line) is the daily curvature coefficient of the entire volatility smile, estimated using the second derivative of the quadratic equation; "CF" (middle line) and "PF" (bottom line) represent the daily slope coefficients for the call and put volatility curves estimated separately using Equations (6-3) and (6-4).

Figure 6-3: Time Series Plots of Curvature and Slope Coefficients (continued)

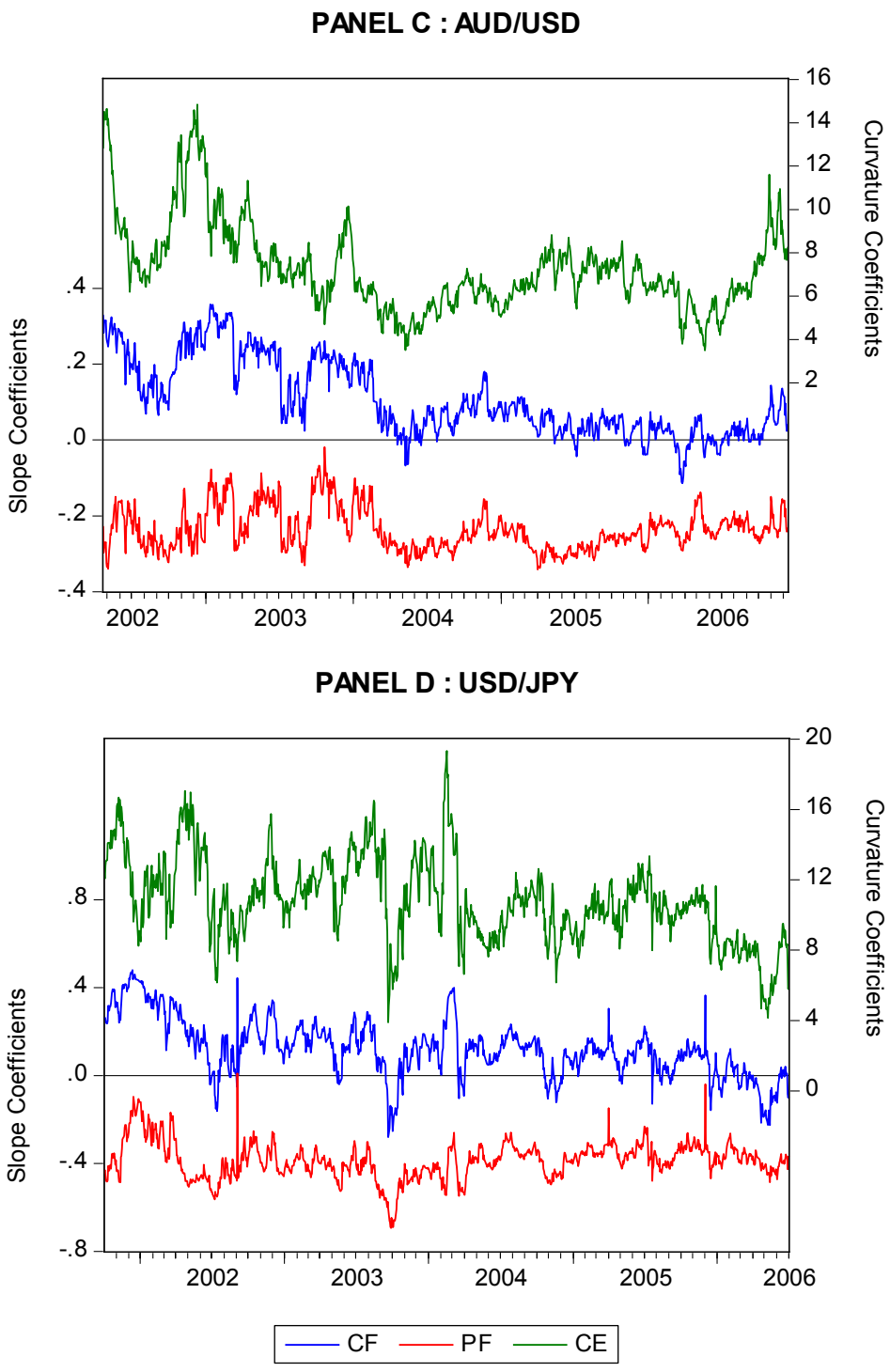

Note: "CE" (top line) is the daily curvature coefficient of the entire volatility smile, estimated using the second derivative of the quadratic equation; "CF" (middle line) and "PF" (bottom line) represent the daily slope coefficients for the call and put volatility curves estimated separately using Equations (6-3) and (6-4).

6.5.1 Summary Statistics for Smile Dynamics

Table 6-3 presents summary statistics for the estimated smile dynamics proxied by the call volatility curve (*CF*), put volatility curve (*PF*), curvature of the volatility smile (*CE*) and skewness of the volatility smile (*SKW*) along with the one-month conditional volatility.

Table 6-3: Statistics for the Shape Proxies and Conditional Volatility

Series	Mean	Min	Max	St.Dev	Skew	Ex.Kurt	PP Test
GBP/USD (obs=962)							
CF	0.222	-0.078	0.397	0.090	-0.171	-0.679	-3.443*
PF	-0.192	-0.405	0.035	0.073	0.426	-0.496	-4.884**
CE	9.635	4.939	18.616	2.174	0.813	1.451	-4.142**
SKW	-0.030	-0.360	0.327	0.145	-0.073	-0.744	-4.084**
σ	0.088	0.074	0.120	0.010	1.537	2.497	
EUR/USD (obs=772)							
CF	0.306	0.122	0.463	0.069	-0.242	-0.634	-2.957*
PF	-0.160	-0.372	0.115	0.089	0.343	-0.040	-5.014**
CE	8.891	4.005	17.479	2.450	1.057	1.160	-4.087**
SKW	0.142	-0.170	0.422	0.124	-0.043	-0.763	-4.498**
σ	0.105	0.084	0.133	0.013	0.099	-0.800	
AUD/USD (obs =960)							
CF	0.088	-0.114	0.357	0.094	0.940	0.127	-3.450**
PF	-0.234	-0.341	-0.019	0.056	0.764	0.080	-5.675**
CE	6.860	3.498	12.138	1.487	0.487	0.163	-3.322*
SKW	-0.114	-0.332	0.277	0.143	0.662	-0.705	-4.818**
σ	0.107	0.071	0.169	0.022	1.109	1.036	
USD/JPY (obs =1150)							
CF	0.118	-0.280	0.480	0.133	0.118	0.154	-4.759**
PF	-0.387	-0.694	0.010	0.084	0.035	1.870	-6.423**
CE	10.742	3.897	19.326	2.450	0.195	0.103	-5.067**
SKW	-0.243	-0.553	0.434	0.161	1.076	1.563	-6.342**
σ	0.099	0.078	0.132	0.011	0.630	0.250	

Note: "σ" is the annualized 1-month conditional volatility."CF" and "PF" are the estimated slope coefficients for the call and put volatility curves."CE" is the curve coefficients of the volatility smile."SKW" is the skewness of the volatility smile, "PP" is the Phillips-Perron (1988) unit root test statistics.
*** Significant at the 1% level*
** Significant at the 5% level*

The mean coefficient for *CF* is positive and for *PF* it is negative. The null hypothesis of a unit root process is rejected across all currency pairs suggesting differencing is not necessary to achieved stationarity. For the estimated conditional volatility, restrictions are imposed on the GARCH (1,1) parameters to ensure stationarity in the volatility process (see discussion in the following section).

6.6 Estimation of one-Month Conditional Volatility

For estimation of future volatility of the underlying exchange rate, this chapter adopts the GARCH (1,1) specification. This method is also used in Jorion (1995) and Covrig and Low (2003) in the study of foreign exchange volatility forecasting, amongst others. The conditional variance using the GARCH (1,1) model is specified as:

$$h_t = \omega + \alpha(r_{t\text{-}1} - \mu)^2 + \beta h_{t\text{-}1} \tag{6-9}$$

$$r_t = \mu + \sqrt{h_t} z_t, \; Z_t \sim N(0,1)$$

The variable r_t is the log return of the daily spot exchange rate, Z_t is the standardised residual and μ is the average daily return of the log series. The parameter ω is the average variance rate, α represents the coefficient of the squared error term and β is the correlation coefficient of the lagged conditional variance. The parameter restrictions, $(\alpha + \beta) < 1.0$ and $\omega > 0$ are imposed in estimating the GARCH process to ensure stationarity in the volatility process. Equation (6-9) provides an estimate of one-day ahead forecasts of the exchange rate volatility. The model uses daily closing average of the bid and ask spot exchange rate from 1 January, 1998 to 13 July, 2007 which results in approximately 2,500 usable observations for each currency pair. The

use of maximum likelihood procedure results in the following GARCH estimates presented in Table 6-4 below:

Table 6-4: Estimated GARCH (1,1) Parameters

Currency	μ	ω	α	β	*L*
GBP/USD	0.000120268	0.000000331	0.028889901	0.957545250	9695.356219000
EUR/USD	0.000158124	0.000000024	0.020080494	0.978919506	8249.540681000
AUD/USD	0.000010000	0.000000030	0.027785550	0.971214450	8946.724741000
USD/JPY	0.000050280	0.000000500	0.043223241	0.945398362	9067.856401000

Note: ***L*** denotes the maximized log-likelihood function.

6.6.1 Recursive GARCH(1,1) of Kroner *et al* (1995)

Since the daily implied volatility used to construct the smile curve have constant maturity of one-month, the conventional GARCH (1,1) model has to be adjusted to generate comparable estimates of one-month volatility for the exchange rates. Following Covrig and Low (2003), a recursive method is used to generate the comparable estimates of one-month ahead volatility. This specification was originally suggested by Kroner *et al* (1995):

$$h_{t,t+N} = \sum_{i=1}^{N} h_{t+i} \qquad (6\text{-}10)$$

N denotes the number of days ahead starting from time t. For simplicity, it is assumed that there are 23 business days within a one-month period. Therefore N as defined in Equation (6-10) takes the value of 23. The square-root of $h_{t,\ t+N}$ is calculated each day and multiplied by a factor of $\sqrt{12}$ to arrive at the estimated yearly volatility parameter.

Evidence provided by Covrig and Low (2003) suggests that quoted implied prices for at-the-money currency options is an unbiased estimator of actual volatility over the option expiration period. Drawing from this result, the soundness of daily volatility estimates using the recursive GARCH (1,1) method can be evaluated against the at-the-money volatility. To do this, the delta neutral volatility series is used as a proxy for at-the-money volatility.

Time series plots[116]of the one-month delta-neutral volatility and the estimated conditional volatility suggests that the recursive method of Kroner *et al* (1995) is a reliable approach and is consistent with Covrig and Low (2003). The GARCH (1,1) predicted one-month exchange rate volatility fluctuates significantly over the sample period consistent with the delta-neutral volatility series. For instance, the estimated conditional volatility for GBP/USD varied from 7.4% to 12.0% per annum (see Table 6-3). These results are similar to the range reported in Table 6-1where the implied volatility of the delta-neutral position moved from 5.1% to 11.8% per annum over the same time period. Both series are strongly correlated producing results consistent with the literature.

6.7 Volatility Smiles Dynamics and Future Exchange Rate Volatility

To investigate whether a relationship exists between future exchange rate volatility and the shape of the volatility smile, a variant of the Granger causality test based on Koch (1993) is used. Kyriacou and Sarno (1999) and Sarwar (2003) have previously employed this method to investigate the existence of Granger causality in the

[116] See Figure A1 provided in Appendix A.

futures and options markets respectively. Peiers (1997) uses a similar approach to examine the foreign exchange trading patterns in the interbank market. Specifically, this chapter provides a test for correlation between future exchange rate volatility and the slope of the volatility smile:

$$\sigma_t = \alpha_0 + \sum_{i=1}^{p} \gamma_{1i} \sigma_{t-i} + \sum_{j=L}^{q} \alpha_{1j} S_{t-j} + \varepsilon_t \qquad (6\text{-}11)$$

$$S_t = \gamma_0 + \sum_{i=L}^{p} \gamma_{2i} \sigma_{t-i} + \sum_{j=1}^{q} \alpha_{2j} S_{t-j} + \upsilon_t \qquad (6\text{-}12)$$

where $t = 0,1,\ldots\ldots, n$

L = value of the lag structure and takes a value of 1.0 for the conventional Granger-causality test and a value of 0.0 when the Granger test is performed following Koch (1993),

σ_t = daily forecast of one-month exchange rate using the recursive GARCH (1,1) model specified in Equation (6-10),

S_t = measure of smile dynamics defined in Equations (6-3) – (6-5) and (6-8) namely, the slope of the call volatility curve (CF_t); slope of the put volatility curve (PF_t) and degree of skewness in the smile curve (SKW_t) ; curvature of the smile (CE_t) and slope of the smile estimated at different levels of moneyness (M_t).

The variable α_0 and γ_0 in Equations (6-11) and (6-12) are intercepts; p and q are the number of lag period used in the regression model, and ε_t, υ_t represent the respective error terms resulting from these equations. Equation (6-11) tests the null hypothesis that the coefficients of the daily smile dynamics jointly do not have any predictive ability over future volatility of the exchange rate. The test of significance is performed for up to total number of q lags. This is a joint test for q zero coefficients on the independent variable S_t using a standard F-test. The test postulates that the anticipated volatility

measured at period t is related to past values of itself, as well as the volatility smile dynamics denoted as S_t.

In Equation (6-12), the null hypothesis suggests that past values of the estimated exchange rate volatility do not have any predictive ability over the smile dynamics. If this is true, then the coefficients, $\gamma_{21} \ldots \gamma_{2q}$, should equal zero up to p lags. Significant lagged coefficients indicate that the association between the GARCH (1,1) estimated exchange rate volatility and the dynamics of the smile curve is not spontaneous. This suggests that it takes some time for option traders to react to the anticipated volatility in the underlying currency.

A possible concern with running the regressions from lag 1 is the exclusion of possible contemporaneous interaction between the variables since informed traders in the currency option market may act quickly to cause a change in the smile dynamics within a one day interval. Following Koch (1993), the same test is repeated from lag zero to examine any simultaneous relationship between the variables. Both regression models are performed from lag zero and 1 respectively resulting in a total of 88 regression outputs per currency pair[117]. Rejection of the joint hypothesis is consistent with the information content of the volatility estimator and the volatility smile characteristics.

The choice of lagged terms for Equations (6-11) and (6-12) is determined using the Akaike information criterion (AIC) commonly used in distributed lagged model. The AIC indicates 4 lags to be used in the regression models for the GBP/USD series

[117] There are 4 different measures of smile dynamics used in Equations (6-11) and (6-12). The slope of the smile measured at 5-delta to 45-delta (in increments of 5) for calls and puts provides another 18 slope measures for the daily smile curvature. The total regression output is therefore (4x2x2+18x2x2) per currency pair.

while 5, 8 and 3 lags are selected for the EUR/USD, AUD/USD and USD/JPY series respectively. The standard errors of the regression models are corrected for autocorrelation using the heteroscedasticity-and-autocorrelation-consistent method of Newey-West (1987). The test of stationarity on the smile dynamics is performed using the Phillips-Perron (1988) unit root test. All the test results are significant and therefore the null hypothesis of nonstationary can be rejected for the smile dynamics defined in Equation (6-3) – (6-5) and (6-8) (see column 7 of Table 6-3).

6.8 Empirical Results

Tables 6-5 and 6-6 report the *F*-test statistics for the bilateral Granger causality tests along with the corresponding *p*-values for the individual currency. The results of Equation (6-12) are reported in the first and third columns while the second and fourth columns provide the results for Equation (6-11). The mean values for the *F*-statistics and *p*-values are calculated from the individual results for each currency pair. Results reported in Panel A are for tests with lag starting at one using Equations (6-11) and (6-12). Panel B, reports the results for the same test but with lags beginning at zero.

Table 6-5: Granger Causality Tests on Dynamics of Volatility Smile (CF & PF)

			Measures of Dynamics			
			Call Function (CF)		Put Function (PF)	
			Dependent var (*Eq.6-12*)	Dependent var (*Eq.6-11*)	Dependent var (*Eq.6-12*)	Dependent var (*Eq.6-11*)
Currency pair	**Lags**	**Obs**	**Slope (CF)**	**GARCH (σ)**	**Slope (PF)**	**GARCH (σ)**
Panel A: ***lag 1 to p,q***						
GBP/USD						
F-stats	4	962	0.057	2.199	2.649	0.923
p -value			0.084	0.066	0.031	0.449
Adj-R^2			0.942		0.899	
EUR/USD						
F-stats	5	772	2.014	1.778	2.712	0.444
p -value			0.073	0.114	0.060	0.818
R^2			0.940		0.860	
AUD/USD						
F-stats	8	960	2.528	0.482	2.710	0.972
p -value			0.009	0.870	0.005	0.456
Adj-R^2			0.949		0.858	
JPY/USD						
F-stats	3	1105	2.652	0.973	1.634	2.507
p -value			0.047	0.404	0.179	0.057
Adj-R^2			0.902		0.837	
Mean F-stats			1.813	1.358	2.426	1.212
Mean *p* -value			0.053	0.364	0.069	0.445
Panel B: ***lag 0 to p,q***						
GBP/USD						
F-stats	4	962	0.742	1.909	2.643	0.916
p -value			0.563	0.106	0.032	0.453
Adj-R^2			0.942		0.899	
EUR/USD						
F-stats	5	772	1.946	1.611	1.986	0.570
p -value			0.083	0.153	0.077	0.723
Adj-R^2			0.940		0.860	
AUD/USD						
F-stats	8	960	2..521	0.428	4.913	1.199
p -value			0.010	0.905	0.000	0.295
Adj-R^2			0.949		0.859	
JPY/USD						
F-stats	3	1150	11.054	1.208	1.158	2.445
p -value			0.000	0.305	0.320	0.062
Adj-R^2			0.901		0.838	
Mean F-stats			4.581	1.289	2.675	1.283
Mean *p* -value			0.164	0.367	0.107	0.383

Note: Panel A reports the results for the bilateral Granger causality tests performed from lag 1 to the optimal lag term p and q. Panel B provides the results for the same test performed from lag 0 to p and q; R^2 is the adjusted goodness of fit. The following regression models are performed using autocorrelation and heteroscedasticity consistent covariance matrix of Newey-West (1987):

$$\sigma_t = \alpha_0 + \sum_{i=1}^{p} \gamma_{1i}\sigma_{t-i} + \sum_{j=L}^{q} \alpha_{1j} S_{t-j} + \varepsilon_t \; ; \; S_t = \gamma_0 + \sum_{i=L}^{p} \gamma_{2i}\sigma_{t-i} + \sum_{j=1}^{q} \alpha_{2j} S_{t-j} + \upsilon_t$$

The estimated slope coefficients are measured from the delta-neutral implied volatility to the 5-delta call ("CF") and put ("PF") implied volatility respectively using the piecewise method; the annualized 1-month conditional variance ("σ") of the underlying currencies is estimated using the recursive GARCH model.

6.8.1 Bilateral Granger-causality Test along Volatility Smile

An autocorrelation and heteroscedasticity consistent covariance matrix (Newey-West, 1987) is used to calculate the standard errors of the regression models. The estimated smile dynamics are defined previously in Equations (6-3) – (6-5) and (6-8). The annualized one-month conditional variance (σ) of the underlying currencies is estimated using the recursive GARCH model specified in Equation (6-10).

The results presented in Panel A of Table 6-5 that report a significant unidirectional relationships exist between the anticipated currency volatility and the smile dynamics. Specifically, the joint test for *q* zero coefficients on the smile dynamics *S* cannot be rejected, with the exception of the GBP/USD currency pair. These results are reported in columns two and four. In contrast, the results for Equation (6-12) reported in columns one and three demonstrate rejections of the null hypothesis of zero lagged coefficients on the anticipated volatility σ. The rejections of the null are slightly stronger when the put volatility curve (*PF*) is used as the dependent variable in the regression tests. For instance, the *p*-values for *PF* are consistently lower than *CF* for the GBP/USD, EUR/USD and AUD/USD currency pairs. For the USD/JPY series, however, rejection of the null hypothesis is only reported for the call volatility curve in column one of Panel A. This suggests that the estimated volatility has the ability to predict the smile dynamics proxied by put and call volatility curves.

In Panel B contemporaneous interactions among the variables are allowed in the Granger causality test. With the exception of the USD/JPY series, the results remain unchanged for Equation (6-11) although the *F*-statistics are slightly lower and have higher *p*-values for *CF*. Notably, the overall results for Equation (6-12) are considerably

different for the call volatility curve. When contemporaneous interactions amongst the variables are allowed, rejections of the null become less apparent for the GBP/USD, EUR/USD and the AUD/USD currency pairs. However, the results for the Japanese yen become more significant at the 1% level. This confirms the importance of modelling the variables contemporaneously as suggested by Koch (1993). For the put volatility curve, the overall results remained unchanged.

Table 6-6 gives the Granger test results using skewness (*SKW*) and curvature (*CE*) measures. As in Table 6-5, the test statistics for Equation (6-12) are provided in columns one and three and the results for Equation (6-11) are available in columns two and four. For Equation (6-11), the null hypothesis of zero coefficients values for the independent variable *SKW* cannot be rejected except for the AUD/USD currency pair. Thus, overall, it seems that the measure of skewness in the smile curve does not have any predictive ability for the future volatility of the exchange rate. When the causality test is repeated from lag zero, the overall results remain unchanged.

Across all currency pairs, the results for Equation (6-12) reported in Panel A are consistently rejected at the 1% level. When the regression is performed from lag zero, rejection of the null remains. Therefore similar to the results reported for *PF*, skewness of the smile curve is linked to the estimated currency volatility contemporaneously and over time. The unidirectional causality from the recursive GARCH volatility to the smile dynamics is stronger for *PF*. Similarly, the null of zero lagged coefficients for the estimated volatility specified in Equation (6-12) is rejected.

Table 6-6: Granger Causality Tests on Dynamics of Volatility Smile (SKW and CE)

			Measures of Dynamics			
			Skewness (SKW)		Curvature (CE)	
			Dependent var (*Eq.6-12*)	Dependent var (*Eq.6-11*)	Dependent var (*Eq.6-12*)	Dependent var (*Eq.6-11*)
Currency pair	**Lags**	**Obs**	**Skewness (SKW)**	**GARCH (σ)**	**Slope (CE)**	**GARCH (σ)**
Panel A: ***lag 1 to p,q***						
GBP/USD						
F-stats	4	962	3.622	1.929	7.263	2.866
p -value			0.006	0.103	0.000	0.022
Adj-R^2			0.928		0.927	
EUR/USD						
F-stats	5	772	13.511	1.827	4.164	0.547
p -value			0.000	0.121	0.000	0.741
Adj-R^2			0.873		0.907	
AUD/USD						
F-stats	8	960	3.963	2.095	4.207	3.222
p -value			0.003	0.079	0.000	0.001
Adj-R^2			0.911		0.958	
JPY/USD						
F-stats	3	1105	0.700	3.256	16.595	17.222
p -value			0.552	0.206	0.000	0.000
Adj-R^2			0.841		0.896	
Mean F-stats			5.449	2.277	8.057	5.964
Mean *p* -value			0.140	0.127	0.000	0.191
Panel B: ***lag 0 to p,q***						
GBP/USD						
F-stats	4	962	3.020	1.250	11.316	2.012
p -value			0.017	0.287	0.000	0.090
Adj-R^2			0.928		0.928	
EUR/USD						
F-stats	5	772	2.249	1.472	3.523	0.418
p -value			0.061	0.208	0.003	0.837
Adj-R^2			0.873		0.910	
AUD/USD						
F-stats	8	960	7.531	1.574	3.774	3.244
p -value			0.000	0.178	0.000	0.001
Adj-R^2			0.911		0.958	
JPY/USD						
F-stats	3	1150	0.970	2.952	13.032	16.072
p -value			0.405	0.031	0.000	0.000
Adj-R^2			0.841		0.896	
Mean F-stats			3.442	1.812	7.911	5.437
Mean *p* -value			0.121	0.176	0.001	0.232

Note: Panel A reports the results for the bilateral Granger causality tests performed from lag 1 to the optimal lag term p and q. Panel B provides the results for the same test performed from lag 0 to p and q; R^2 is the adjusted goodness of fit. The following regression models are performed using autocorrelation and heteroscedasticity consistent covariance matrix of Newey-West (1987):

$$\sigma_t = \alpha_0 + \sum_{i=1}^{p} \gamma_{1i}\sigma_{t-i} + \sum_{j=L}^{q} \alpha_{1j} S_{t-j} + \varepsilon_t \; ; \; S_t = \gamma_0 + \sum_{i=L}^{p} \gamma_{2i}\sigma_{t-i} + \sum_{j=1}^{q} \alpha_{2j} S_{t-j} + \upsilon_t$$

Skewness ("SKW") of the volatility smile is measured as |CF|-|PF|. The curvature ("CE") coefficients of the volatility smile are estimated using the second derivative of the daily fitted quadratic function. The annualized 1-month conditional variance ("σ") of the underlying currencies is estimated using the recursive GARCH model.

For estimated smile curvature, *CE*, the results suggest the existence of feedback between anticipated currency volatility and the curvature of the smile. This is reported for the GBP/USD, AUD/USD and the USD/JPY currency pairs. This relationship remains in the contemporaneous model.

The mean *p*-value is high due to non-rejection of the null for the EUR/USD series. In three out of four currency pairs, a bilateral relationship between smile curvature and anticipated currency volatility is reported in this study. Again the results for Equation (6-12) are much stronger with an overall *F*-statistic of 7.911, significant at the 1% level. This suggests that, the direction of causality from future volatility (σ) to measure of smile dynamics (*S*) is stronger.

In short, the results of this analysis suggest a unidirectional causality from the anticipated volatility of the underlying currency to the daily smile dynamics. The results based on analysis of the curvature of the smile indicate the existence of significant feedback between the smile curvature and the estimated volatility. Further, the conventional and contemporaneous Granger causality tests suggest that a unidirectional relationship between anticipated volatility and smile dynamics, measured with *PF*, *SKW* and *CE*, is robust to varying time intervals.

6.8.2 Granger-causality Test at Individual Delta Levels

To extend the findings tabulated in Tables 6-5 and 6-6, the Granger causality tests defined in Equations (6-11) and (6-12) are repeated using moneyness M_D in place of *S*. This allows a closer examination of the smile dynamics at individual point of the

smile curve. Thus the dynamics of the smile can be specifically assessed at the 5-delta level or 15-delta and so forth.

The moneyness variable M_D measures the slope of the volatility smile using the first derivative of the fitted smile defined in Equation (6-7). The value of moneyness that corresponds to the delta value of 5 to 45 is used in Equation (6-7) to estimate the slope coefficient that corresponds with each individual point on the volatility smile curve. For instance, the slope coefficient for the call on day t is calculated as $M_D = a_{1,t} + 2a_{2,t}M_{i,t}$, where the coefficients a_1 and a_2 are estimated daily using ordinary least squares regression. The level of moneyness for a given delta value is estimated as $M_{i,t} = X_i/F_t$, and i denotes delta values of 5 to 45 (in increments of 5).

As in the former approach, the standard errors from the regression models are corrected for autocorrelation and heteroscedasticity using the Newey-West (1987) procedure. Recursive GARCH models specified in Equation (6-10), provide the one-month ahead volatility estimates for each currency pair. Both the conventional and contemporaneous Granger causality tests are performed. The results for the put and call options are provided in Tables 6-7 and 6-8 respectively. For brevity, only the p-values of the regression tests are presented.

Table 6-7: Granger Causality Test on Individual Slope for Put Options

	Put Options							
	GBP/USD		EUR/USD		AUD/USD		USD/JPY	
	Eq.6-12 Dep var Slope (M_D)	Eq.6-11 Dep var GARCH (σ)	Eq.6-12 Dep var Slope (M_D)	Eq.6-11 Dep var GARCH (σ)	Eq.6-12 Dep var Slope (M_D)	Eq.6-11 Dep var GARCH (σ)	Eq.6-12 Dep var Slope (M_D)	Eq.6-11 Dep var GARCH (σ)
Panel A: ***Lag 1 to p,q***								
P5D	0.014	0.571	0.020	0.640	0.004	0.641	0.887	0.074
P10D	0.025	0.573	0.012	0.596	0.005	0.699	0.741	0.132
P15D	0.039	0.541	0.007	0.552	0.007	0.734	0.546	0.204
P20D	0.057	0.500	0.005	0.509	0.010	0.756	0.417	0.288
P25D	0.075	0.457	0.003	0.469	0.015	0.772	0.322	0.372
P30D	0.095	0.413	0.002	0.430	0.021	0.785	0.258	0.461
P35D	0.114	0.368	0.001	0.392	0.030	0.796	0.214	0.551
P40D	0.132	0.329	0.001	0.356	0.040	0.805	0.181	0.640
P45D	0.148	0.290	0.001	0.321	0.051	0.813	0.156	0.722
Panel B: ***lag 0 to p,q***								
P5D	0.011	0.568	0.062	0.667	0.001	0.317	0.907	0.093
P10D	0.024	0.571	0.109	0.666	0.002	0.408	0.885	0.162
P15D	0.039	0.547	0.157	0.658	0.005	0.488	0.676	0.226
P20D	0.055	0.515	0.209	0.649	0.010	0.555	0.466	0.296
P25D	0.073	0.481	0.267	0.638	0.017	0.615	0.297	0.368
P30D	0.091	0.443	0.333	0.627	0.026	0.668	0.185	0.452
P35D	0.110	0.403	0.406	0.613	0.035	0.714	0.117	0.543
P40D	0.131	0.365	0.485	0.595	0.046	0.755	0.075	0.631
P45D	0.155	0.326	0.568	0.572	0.056	0.792	0.049	0.702

Note: Panel A reports the p-values for the bilateral Granger causality tests performed from lag 1 to the optimal lag term p and q. Panel B provides the p-values for the same test performed from lag 0 to p and q; The following regression models are performed using autocorrelation and heteroscedasticity consistent covariance matrix of Newey-West (1987):

$$\sigma_t = \alpha_0 + \sum_{i=1}^{p} \gamma_{1i}\sigma_{t-i} + \sum_{j=L}^{q} \alpha_{1j} M_{D_{t-j}} + \varepsilon_t \; ; \; M_{D_t} = \gamma_0 + \sum_{i=L}^{p} \gamma_{2i}\sigma_{t-i} + \sum_{j=1}^{q} \alpha_{2j} M_{D_{t-j}} + \upsilon_t$$

M_D is the slope of the smile curve measured at moneyness level M using Equation (6-7). The moneyness measure M defined in Equation (6-6) corresponds to the delta value of 5 to 45 (in increments of 5).

The regression tests reported in Tables 6-7 and 6-8 reveal several notable findings. First, the Granger test for the puts in Table 6-7 confirms the existence of unidirectional causality from the estimated volatility to the slope M_D. The mean *p*-values are significant in most instances for all but the USD/JPY pair. The evidence is particularly strong for the out-of-money puts with delta values of 5 to 35 in most instances. In the contemporaneous Granger test reported in Panel B, the results remain significant for delta values of 5 to 25 with the exception of the USD/JPY series.

Table 6-8: Granger Causality Test on Individual Slope for Call Options

	Call Options							
	GBP/USD		EUR/USD		AUD/USD		USD/JPY	
	Eq.6-12 Dep var Slope (M_D)	Eq.6-11 Dep var GARCH (σ)	Eq.6-12 Dep var Slope (M_D)	Eq.6-11 Dep var GARCH (σ)	Eq.6-12 Dep var Slope (M_D)	Eq.6-11 Dep var GARCH (σ)	Eq.6-12 Dep var Slope (M_D)	Eq.6-11 Dep var GARCH (σ)
Panel A: ***Lag 1 to p,q***								
C5D	0.030	0.096	0.000	0.143	0.108	0.620	0.079	0.435
C10D	0.055	0.086	0.001	0.081	0.116	0.787	0.088	0.584
C15D	0.083	0.095	0.006	0.101	0.160	0.930	0.089	0.706
C20D	0.111	0.110	0.033	0.135	0.054	0.905	0.084	0.812
C25D	0.135	0.127	0.054	0.166	0.072	0.828	0.088	0.865
C30D	0.167	0.149	0.035	0.193	0.057	0.763	0.089	0.904
C35D	0.165	0.168	0.013	0.211	0.044	0.920	0.101	0.889
C40D	0.170	0.192	0.005	0.234	0.270	0.919	0.110	0.872
C45D	0.168	0.223	0.002	0.260	0.749	0.454	0.123	0.835
Panel B: ***lag 0 to p,q***								
C5D	0.245	0.141	0.000	0.168	0.077	0.855	0.001	0.243
C10D	0.441	0.142	0.000	0.123	0.102	0.924	0.001	0.327
C15D	0.527	0.148	0.002	0.107	0.158	0.967	0.002	0.417
C20D	0.512	0.158	0.075	0.101	0.076	0.970	0.004	0.514
C25D	0.448	0.170	0.362	0.148	0.233	0.974	0.005	0.593
C30D	0.370	0.184	0.641	0.294	0.203	0.891	0.007	0.674
C35D	0.311	0.205	0.756	0.352	0.149	0.963	0.011	0.711
C40D	0.259	0.229	0.764	0.438	0.337	0.934	0.016	0.745
C45D	0.216	0.260	0.719	0.499	0.758	0.796	0.023	0.756

Note: Panel A reports the p-values for the bilateral Granger causality tests performed from lag 1 to the optimal lag term p and q. Panel B provides the p-values for the same test performed from lag 0 to p and q; The following regression models are performed using autocorrelation and heteroscedasticity consistent covariance matrix of Newey-West (1987):

$$\sigma_t = \alpha_0 + \sum_{i=1}^{p} \gamma_{1i}\sigma_{t-i} + \sum_{j=L}^{q} \alpha_{1j} M_{Dt-j} + \varepsilon_t \; ; \; M_{Dt} = \gamma_0 + \sum_{i=L}^{p} \gamma_{2i}\sigma_{t-i} + \sum_{j=1}^{q} \alpha_{2j} M_{Dt-j} + \upsilon_t$$

M_D is the slope of the smile curve measured at moneyness level M using Equation (6-7). The moneyness measure M defined in Equation (6-6) corresponds to the delta value of 5 to 45 (in increments of 5).

Second, the *p*-values of the regression models in Table 6-7 seem to relate directly to the level of moneyness. That is, lower delta options also have lower *p*-values. Therefore the out-of-money puts show stronger support for a unidirectional relationship than near-money options. The results for the GBP/USD and AUD/USD currency pairs still hold when the Granger causality is performed from lag zero. For the EUR/USD currency pair, contemporaneous modelling of the variable produces significant test results compared to the conventional Ganger method except for the far out-of-money option of 5-delta which remains significant in Panel B. There is little evidence of links for the USD/JPY currency pair. On the whole, the evidence suggests that far out-of-money puts relate strongly with the volatility of the underlying currency.

Third, the *p*-values for Equation (6-12) (Table 6-8) are generally higher both in Panels A and B than the corresponding values reported previously for the put options in Table 6-7. The unidirectional relations between conditional volatility and the slope M_D do not hold under the contemporaneous Granger test. Again, this is consistent with previous results reported for *CF* in Table 6-5. As in Table 6-7, the *p*-values of the regression tests are still stronger for more out-of-the money options.

6.8.3 Trivariate vector autoregressive model

To this point, the analysis of the relationship between currency volatility and the behaviour of the smile has been restricted to a two-variable model. The preceding analyses reported in Tables 6-5, 6-6, 6-7 and 6-8 provide evidence of causality between currency volatility and the put volatility curve, as well as currency volatility and the call volatility curve. It is plausible that the causality that exists may not be solely due to the anticipated volatility in the foreign exchange market as call and put volatility curves will be tend to move together due to the put-call parity relationship. In this section, further analysis is performed using the vector autoregressive (VAR) technique to examine the linkages between three anticipated volatility (σ), the put volatility curve (*PF*) and call volatility curve (*CF*).

As all the three endogenous variables are stationary according the Phillips-Person unit root test results (see Table 6-3), vector autoregressive modelling can be applied to ascertain the causal dynamics among the three endogenous variables. The unrestricted trivariate VAR is specified as:

$$\sigma_{FX,t} = \alpha_{\sigma FX} + \sum_{i=1}^{k} \gamma^{\sigma FX}_{\sigma FX,i\sigma FX,t-i} + \sum_{i=1}^{k} \beta^{CFFX}_{\sigma FX,iCFFX,t-i} + \sum_{i=1}^{k} \theta^{PFFX}_{\sigma FX,iPFFX,t-i} + \varepsilon_{\sigma} \quad (6\text{-}13)$$

$$CF_{FX,t} = \alpha_{CFFX} + \sum_{i=1}^{k} \gamma^{\sigma FX}_{CFFX,i\sigma FX,t-i} + \sum_{i=1}^{k} \beta^{CFFX}_{CFFX,iCFFX,t-i} + \sum_{i=1}^{k} \theta^{PFFX}_{CFFX,iPFFX,t-i} + \varepsilon_{CF} \quad (6\text{-}14)$$

$$PF_{FX,t} = \alpha_{PFFX} + \sum_{i=1}^{k} \gamma^{\sigma FX}_{PFFX,i\sigma FX,t-i} + \sum_{i=1}^{k} \beta^{CFFX}_{PFFX,iCFFX,t-i} + \sum_{i=1}^{k} \theta^{PFFX}_{PFFX,iPFFX,t-i} + \varepsilon_{PF} \quad (6\text{-}15)$$

where $\boldsymbol{\sigma}_{FX,t}$ is the estimated conditional volatility for currency *FX*; $CF_{FX,t}$ and $PF_{FX,t}$ are the slopes of the call and put volatility curves defined in Equations (6-3) and (6-4) at time *t* ; *k* is the lag choice determined using the AIC specification. The trivariate specification allows for a reliable analysis of the shock transmission mechanism among the variables in the system. Further, impulse response and variance decompositions analyses are undertaken to trance the impact of shocks in conditional volatility on smile slope (call volatility curve and put volatility curve).

A generalized impulse response function is employed to avoid issues associated with the ordering of the endogenous variables. Variance decomposition determines the fraction of variation in the endogenous variables resulting from the innovations in other variables within the trivariate system – that is, the relative magnitude of the effect of one variable on other variables within the model.

6.8.4 Residuals Autocorrelation and Results for VAR(3) model

In Table 6-9, the Breusch-Godfrey LM test is performed to test autocorrelation in the residuals. The initial VAR (3) specification shows evidence of autocorrelation up to 10 lags. To alleviate this problem, a time trend in the VAR (3) model is specified. The summary statistics in Table 6-9 indicate that the adjusted specification is adequate

for the purposes of this study. Specifically, for the LM test, the null of zero autocorrelation in the residuals cannot be rejected in all cases. This is further confirmed using the *Q*-test statistic for the null of zero joint residual autocorrelation.

Table 6-9: Residuals Autocorrelation Tests for VAR (3) Model

		LM(10) Test on Residuals						Q(10) Joint Test	
Currency	**Obs**	**σ**	***p*-value**	**CF**	***p*-value**	**PF**	***p*-value**	**Chi-Sqr(63)**	***p*-value**
GBP/USD	962	11.102	0.350	8.739	0.557	13.220	0.212	51.999	0.837
EUR/USD	772	15.345	0.120	9.615	0.475	14.279	0.161	52.347	0.829
AUD/USD	960	8.595	0.571	14.527	0.150	12.361	0.262	64.569	0.422
USD/JPY	1050	12.725	0.239	4.564	0.918	7.763	0.652	64.045	0.440

Note: LM(10) denotes the LM test with 10 lags. The tests are performed on the individual unrestricted trivariate VAR model specified with a trend component. Columns 2, 4 and 6 present the test statistics for the regression models specified with the dependent variables "σ", "CF" and "PF". The corresponding p-values are reported in columns 3, 5 and 7. The Portmanteau Test ("Q(10)") for joint residual autocorrelation is estimated over 10 lags.

The test results using the VAR (3) specification are provided in Table 6-10. The *F*-statistics for the system indicates that the VAR (3) model is highly significant with high R^2 values. This is consistent with the results reported in Table 6-5. The *F*-statistic has the highest value when the VAR (3) model is performed using the estimated conditional volatility as the dependent variable.

Table 6-10: Test Results for the Trivariate VAR Model

	GBP/USD, $k=4$			EUR/USD, $k=5$			AUD/USD, $k=5$			USD/JPY, $k=3$		
Dep Var	***F*-stats**	***p*-value**	**Adj. R^2**	***F*-stats**	***p*-value**	**Adj. R^2**	***F*-stats**	***p*-value**	**Adj. R^2**	***F*-stats**	***p*-value**	**Adj. R^2**
σ	1263.40	0.000	0.999	2219.11	0.000	0.999	1683.42	0.000	0.999	1806.85	0.000	0.999
CF	12.96	0.000	0.942	3.09	0.000	0.857	2.36	0.000	0.856	10.71	0.000	0.903
PF	7.11	0.000	0.899	8.18	0.000	0.941	7.38	0.000	0.948	4.22	0.000	0.838

Note: The table above reports the system F-test statistics with the corresponding p-values. The optimal lag k (using AIC specification) adjacent to the currency pair is used to perform the regression tests.

6.8.5 Impulse Response Analysis

To examine the impact of a shock in anticipated volatility on the future values of the endogenous variables within the VAR (3) system, an impulse response function is estimated for each of the currency pairs using generalized one standard deviation shocks on the endogenous variables. The impulse response functions due to a shock in the anticipated volatility for the calls and puts are presented separately in Figure 6-4. They are reproduced in Figures 6-5, 6-6, 6-7 and 6-8 together with impulse response functions for all other endogenous variables using different scales.

The impulse response functions for the slope coefficients of puts and calls volatility curves can be characterized as a sine wave pattern which reflects a dynamic system (Greene, 2003). This pattern is consistent with the findings of Sarwar (2003) which suggests that an over or under-reaction in the currency option market occurs as informed trader adjust their trading positions over time due to the impending risk in the spot foreign exchange market.

In response to one standard deviation volatility shock, the slope of the put volatility curve results in an immediate flattening of the smile associated with both the put and the call volatility curves. The slope of the put volatility curve becomes less negative (positive reaction) and slope for the call volatility curve becomes less positive (negative reaction). There is a tendency toward “overshooting” over a period of 25 days for the currency pairs with respect to the slope coefficient for the put volatility curve but this is not evident with the slope of the call volatility curve where the initial reaction to the volatility shock produced negative reaction and remains so over the next 50 to130 days.

Figure 6-4: Impulse Reponses for Smile Slopes due to Volatility Shock

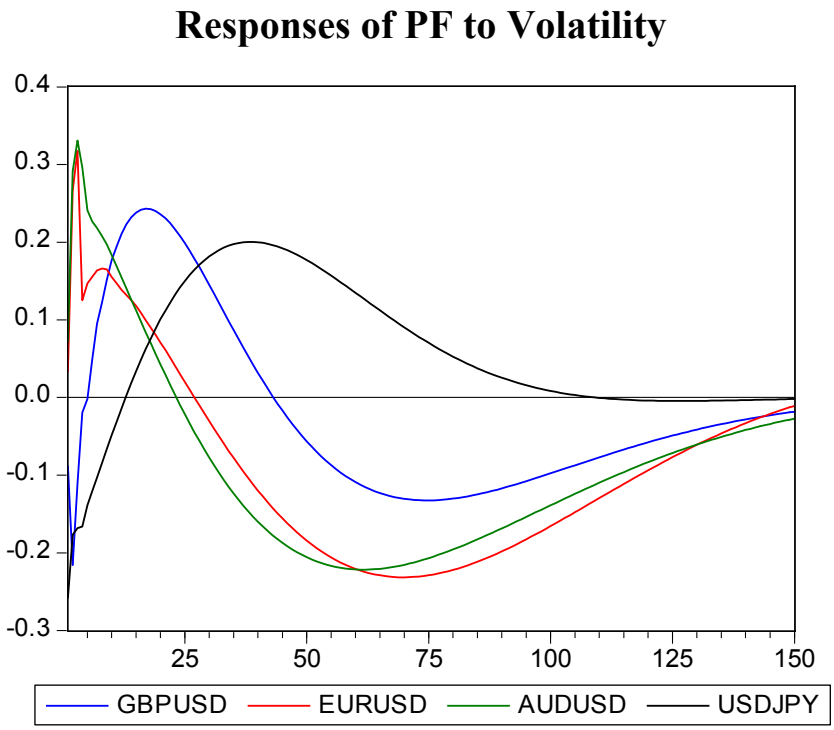

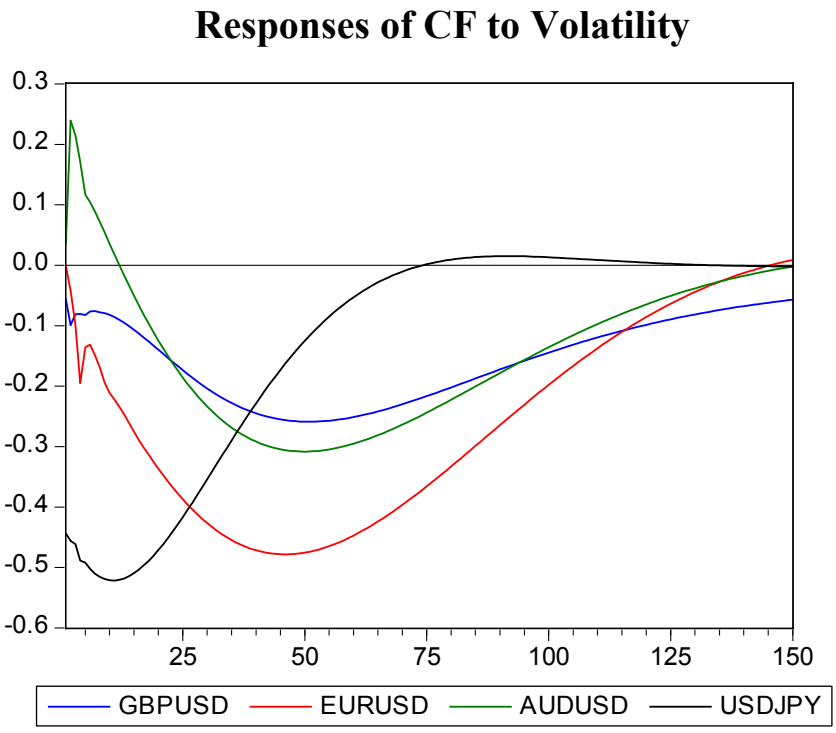

Figures 6-5, 6-6, 6-7 and 6-8 show the impulse response functions for the endogenous variables according to the trivariate VAR model for each of the three currency pairs respectively. The patterns for the impulse response functions and variance decompositions are largely identical across all four currency pairs. The notation GVOL stands for GARCH estimated conditional volatility, *CF* and *PF* are the slope coefficients defined in Equation (6-3) and (6-4). For ease of comparison, a common scale for all responses of a single variable is used, for instance the shock of GVOL on GVOL, *CF* and *PF* have a common scale. The 95% confidence bands using Monte Carlo simulation is drawn around the impulse response functions (dotted lines). The corresponding variance decompositions analysis is presented on the bottom panels.

The impulse response function for the GBP/USD put volatility curve to a shock in volatility is presented on the bottom left panel of the impulse response chart in Figure 6-5. GVOL shocks have a positive effect on future GVOL values. However, a shock to the *CF* or the *PF* coefficients does not produce any significant response in GVOL. This further supports the existence of the unidirectional relationship identified in Table 6-5. Further, a shock in *CF* generates a significant response from *PF* but a shock in *PF* only produces a modest response in *CF*. There is some asymmetry in the relationship between *CF* and *PF* with a relatively large reaction reported for *PF* due to a shock to *CF*.

The variance decomposition analysis shows that the anticipated volatility in the underlying currency is not explained by changes in the *CF* or *PF*. However, the anticipated volatility of the underlying currency appears to have significant impact on the call and put volatility curves. Approximately 5% to 20% of 150 days ahead variance

Figure 6-5: GBP/USD Impulse Reponses for Trivariate VAR

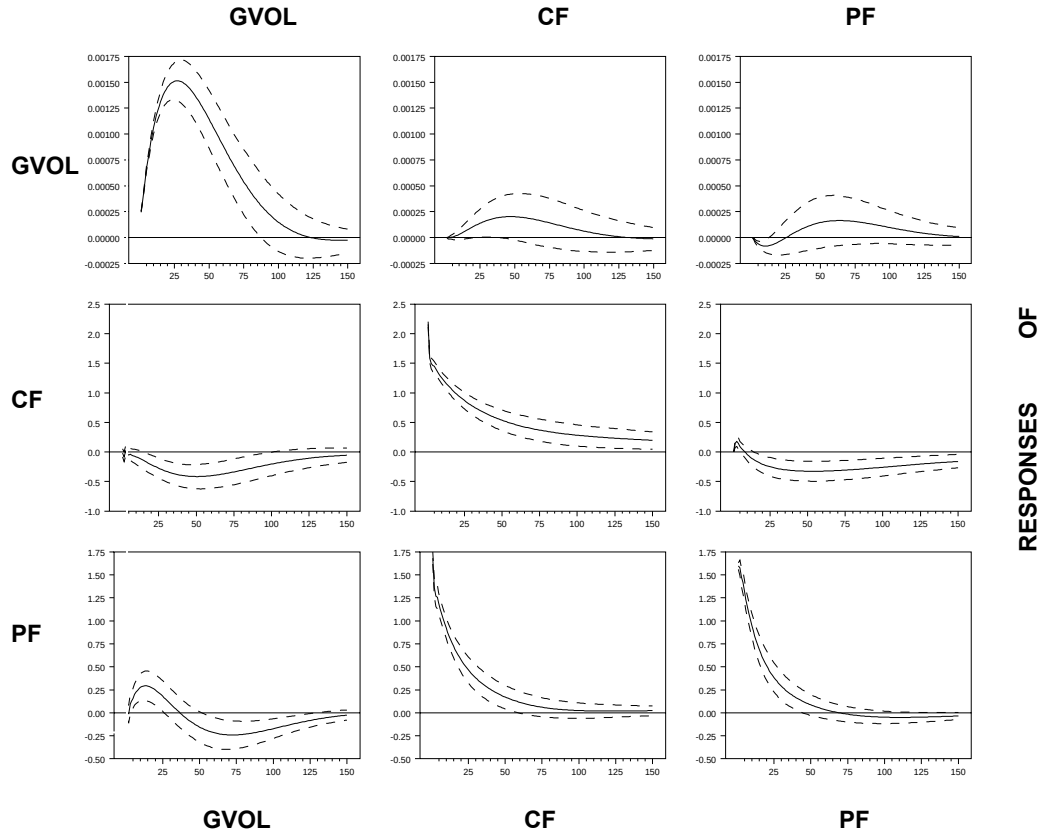

Variance Decomposition

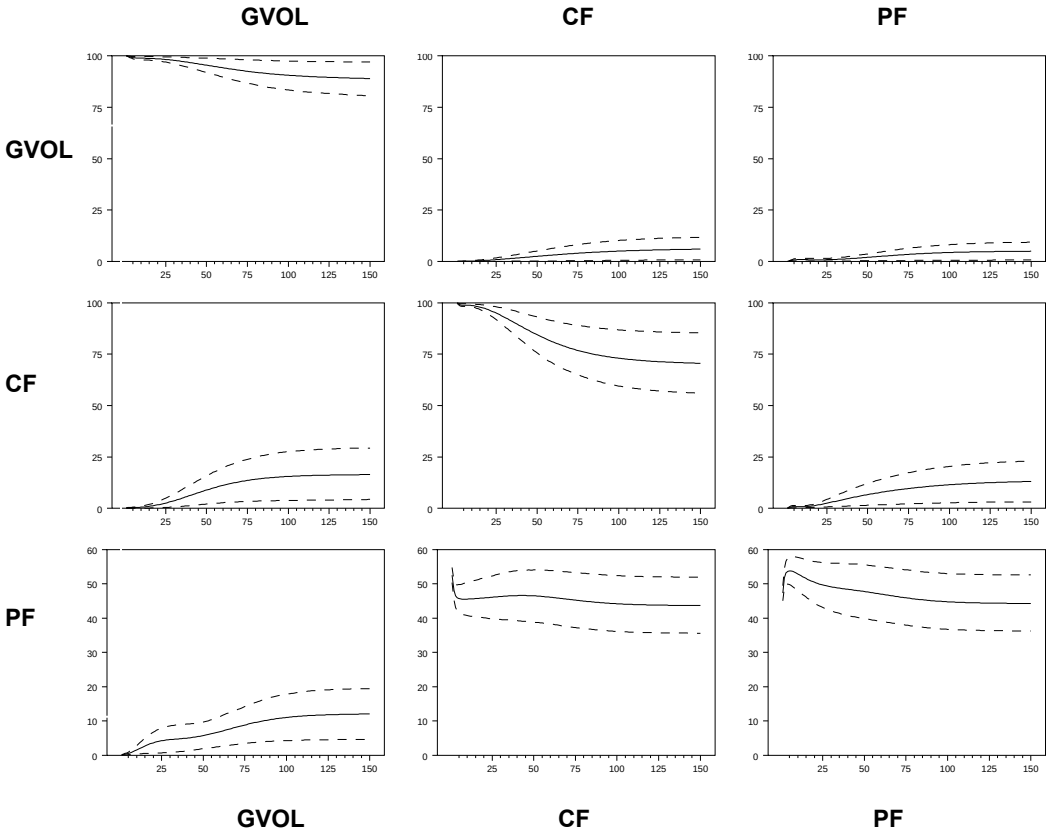

Figure 6-6: EUR/USD Impulse Reponses for Trivariate VAR

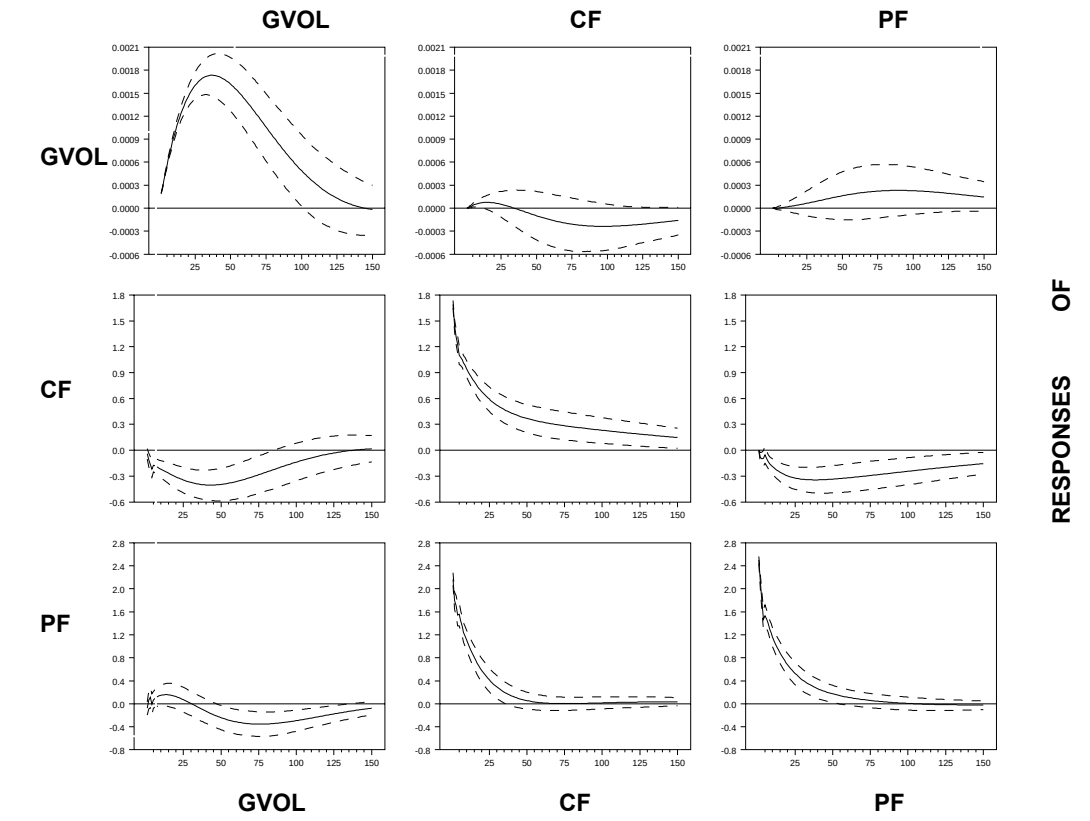

Variance Decomposition

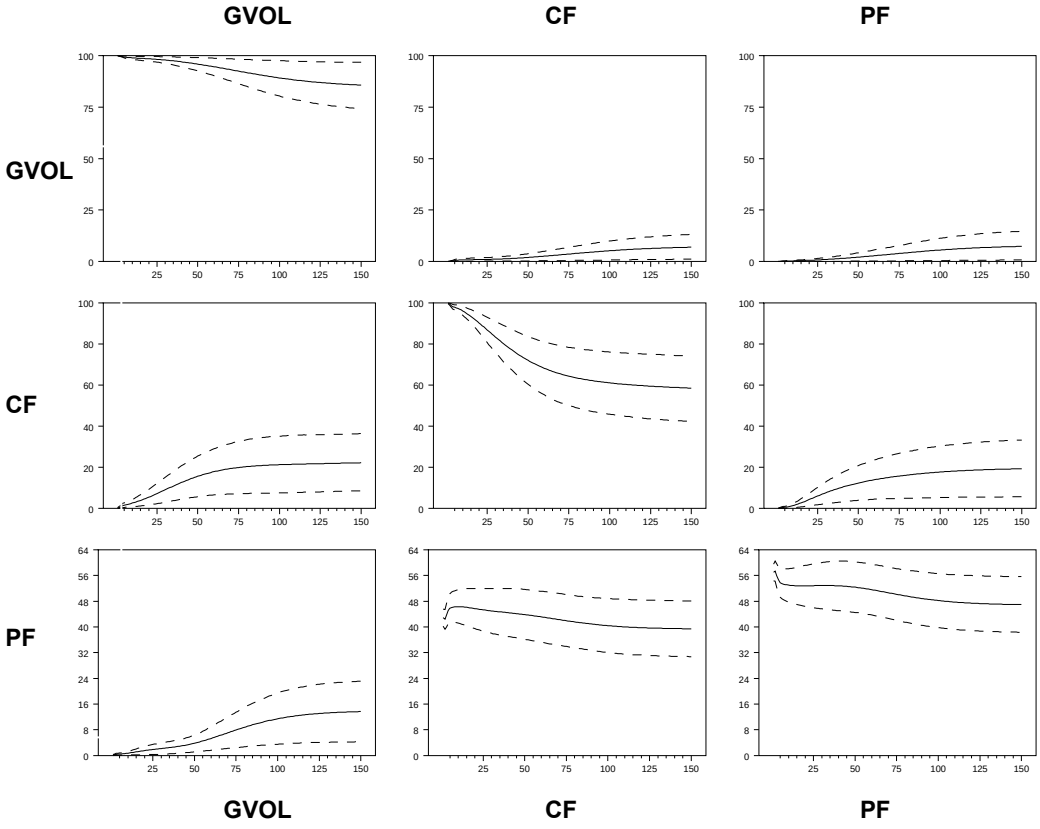

Figure 6-7: AUD/USD Impulse Reponses for Trivariate VAR

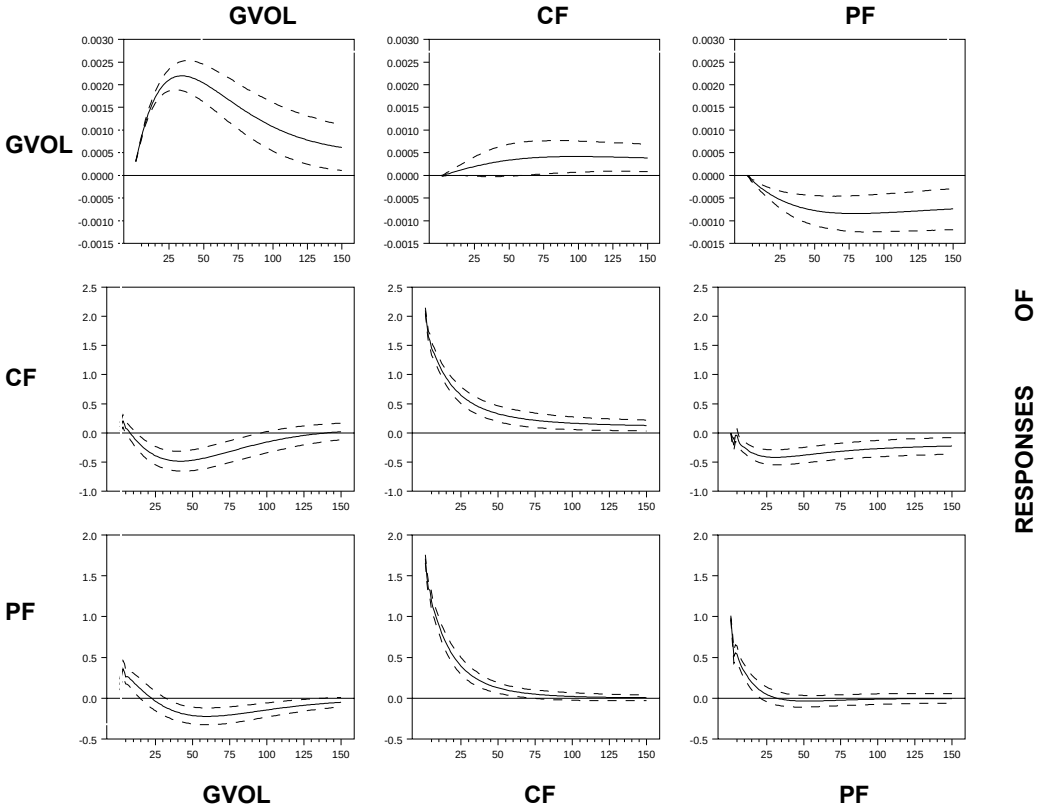

Figure 6-8: USD/JPY Impulse Reponses for Trivariate VAR

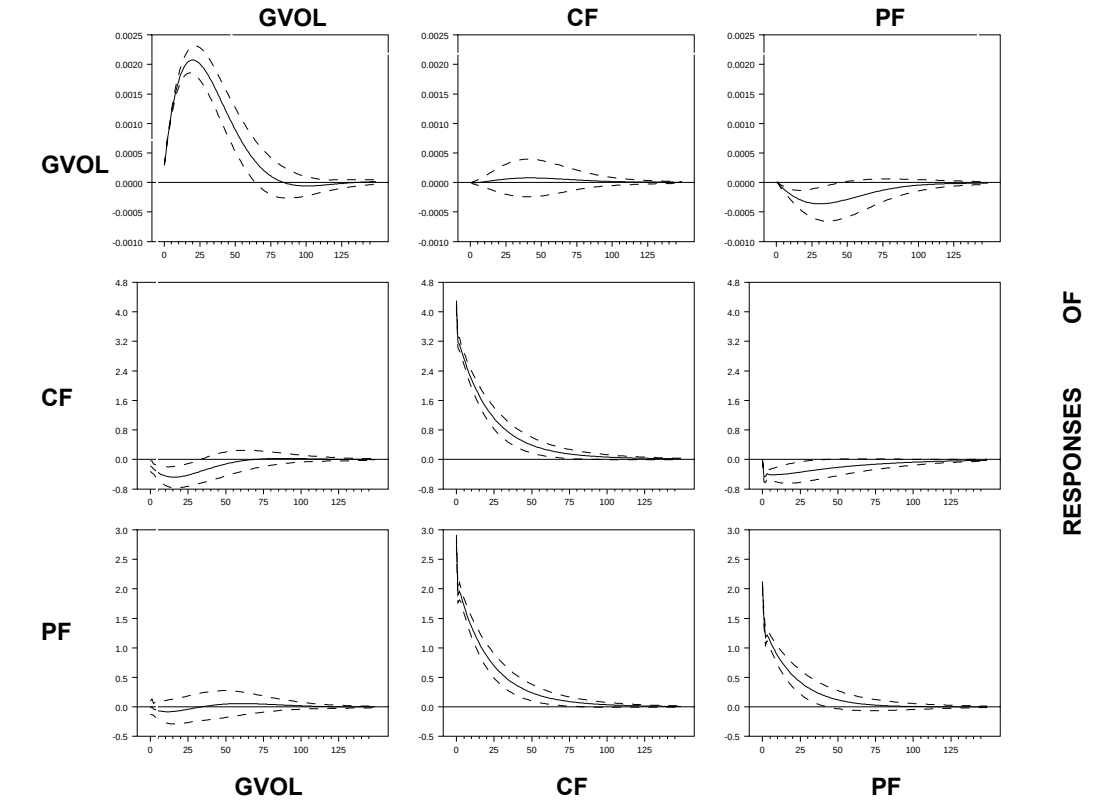

Variance Decomposition

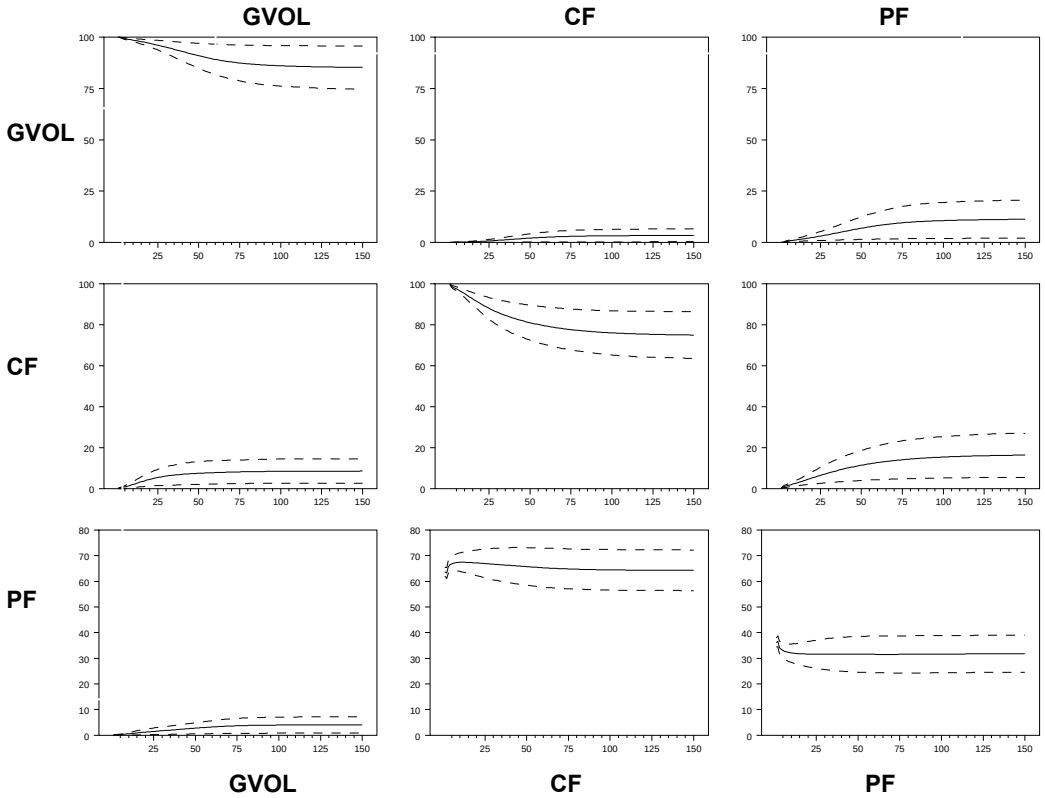

forecast of the put volatility curve is attributed to the innovations in the anticipated currency volatility. The call volatility curves have similar results with higher weights of 10% to 22% over the same interval. Therefore consistent with the findings in the previous section, the slope of the call and put volatility curves are related to the anticipated currency volatility. Further, evidence of feedback between the call and put volatility curves is also identified using the impulse response analysis.

6.9 Jumps and the Smile Dynamics

The findings from the preceding sections suggest that a significant relationship exists between the different measures of smile dynamics and the anticipated volatility of the underlying exchange rates. As a robustness check and further extension of this analysis, it is of interest to examine whether the information embedded in the smile dynamics is capable of providing insights into the behaviour of prices in the spot exchange rate market. Specifically, this section investigates whether the absolute change in the smile dynamics explains the likelihood of significant movements in the underlying currency. Following Doran *et al* (2007), jumps over the maturity of the option contracts are estimated and this is followed by a multivariate probit analysis using different measures of volatility smile dynamics as explanatory variables. These measures of smile dynamics are formally defined in Equations (6-3)-(6-4) and (6-7)-(6-8).

For the detection of jumps in the daily spot exchange rates, this study adopts the nonparametric method of Lee and Mykland (2007) which is defined as:

$$L(i) \equiv \frac{\log S(t_i)/S(t_{i-1})}{\hat{\sigma}(t_i)} \tag{6-16}$$

where

$$\hat{\sigma}(t_i)^2 \equiv \frac{1}{K-2}\sum_{j=i-K+2}^{i-1}\left|\log S(t_j)/S(t_{j-1})\right|\left|\log S(t_{j-1})/S(t_{i-2})\right| \tag{6-17}$$

K = window size measured in days

$S(t_i)$ = daily closing spot exchange rate at period t_i

J = $t + T$

A threshold of ± 4.6001[118] is adopted from Lee and Mykland (2007) to detect the presence of a jump on any given day t_i to the expiration of the option contract $t+T$; when the threshold is breached on day t_i, a jump is recorded and a value of one is assigned for that day. If the estimated $L(i)$ statistic specified in Equation (6-16) stays within the thresholds, day t_i receives a value of zero. The null hypothesis of no jump at t_i can be rejected at the 1% level of significance when the thresholds are violated.

The choice of K in Equation (6-17) can be determined by sampling frequency as noted in theorem 2 of Lee and Mykland (2007). However, the determination of the optimal size for K is by no means straightforward. According to Lee and Mykland (2007), if daily data is used, the optimal size for K should range from 15.87 to 252.

Table 6-11 summarises estimated jump frequency using three different window sizes. Negative jumps are denoted as "JN" while "JP" represents positive jumps that occurred over the option expiration period. A total of 245 and 58 jumps are reported

[118] See pp.9 of their paper for further details.

when a window size of 5 and 16 days are used respectively. On the other hand, a window size of 30 days reduces the sample size of the dependent variable significantly, resulting in a limited observation of 22 jumps from the currency pairs. For simplicity, since the data are sampled on daily intervals, *K* is set to a value of 16 trading days following Lee and Mykland (2007). This appears to generate a reasonable aggregate sample size of 58 jumps over the option expiration period[119].

Table 6-11: Jump Frequencies and Window Sizes

Currency	Window Size (*K*)								
	5			16			30		
	JP	JN	Total	JP	JN	Total	JP	JN	Total
GBP/USD	32	35	67	4	8	12	2	3	5
EUR/USD	36	27	63	0	10	10	0	0	0
AUD/USD	23	27	50	3	9	12	3	4	7
USD/JPY	31	34	65	10	14	24	4	6	10
Observations	122	123	245	17	41	58	9	13	22

Note: This table indicates the frequencies of positive and negative jumps using various window sizes. The jumps are estimated using the nonparametric procedure of Lee and Mykland (2007). The terms "JP" and "JN" denote positive and negative jumps respectively.

In terms of currency type, when a window size of 16 days is used, a total of 12 jumps are recorded for the AUD/USD and the GBP/USD, while the EUR/USD and the USD/JPY report 10 and 24 jumps respectively. The USD/JPY has the greatest number of negative jumps of 14, followed by the EUR/USD with 10 negative jumps, while AUD/USD and GBP/USD each with 9 and 8 negative jumps. Positive jumps comprise approximately 29% of the aggregate sample and are mostly recorded by the USD/JPY currency pair.

[119] Further analysis is also performed using a window size of 5 days. See Tables B1 and B2 reported in Appendix B of this dissertation.

Figures 6-9 and 6-10 present the estimated jumps for the AUD/USD and the USD/JPY currency pairs over the sample period. The at-the-money implied volatility series (*IV*) is shown on the left axis while the spot exchange rate is displayed on the right axis. The estimated jumps reflect much of the upward and downward movement in the series over the sample period.

Figure 6-9: Estimated Jumps for AUD/USD

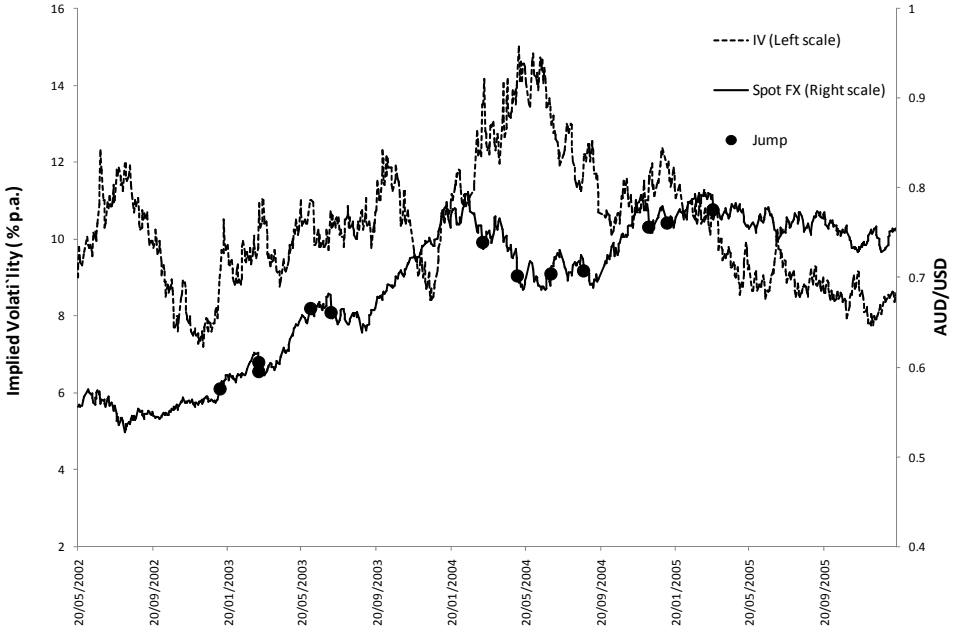

Figure 6-10: Estimated Jumps for USD/JPY

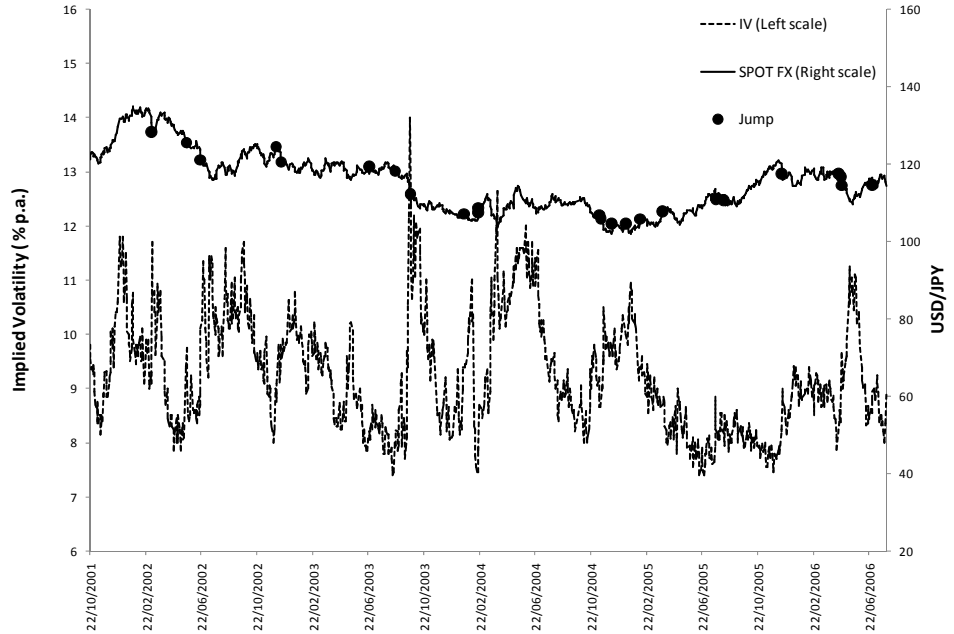

6.9.1 Probit Model Analysis

To maintain a reasonably parsimonious model, it is assumed that the daily dynamics of the volatility smile can be reasonably estimated using the slope of the volatility smile measured at 5-delta, 10-delta and 15-delta. In addition, the curvature and slope coefficients for put and call volatility curves are also included in probit model analysis. The following probit model tests the relationship between jumps and volatility smile dynamics using call options:

$$Pb(Jump_{t+T}=1) = F(\beta_0 + \beta_1 \Delta CF_t + \beta_2 \Delta CE_t + \beta_3 \Delta C5D_t + \beta_4 \Delta C10D_t + \beta_5 \Delta C15D_t) + \varepsilon_t \quad (6\text{-}18)$$

where

$Pb(Jump_{t+T}=1)$	=	probability that jumps occur within periods t to $t+T$, T denotes the maturity of the option contract,
F	=	the standardized cumulative distribution function,
ΔCF	=	natural logarithm of the absolute change in CF measured as $\log(\lvert CF_t / CF_{t-1} \rvert)$,
ΔCE	=	natural logarithm of the absolute change in the curvature coefficients measured as $\log(\lvert CE_t / CE_{t-1} \rvert)$,
$\Delta C5D$	=	natural logarithm of the absolute change in the slope coefficient for 5-delta call measured as $\log(\lvert C5D_t / C5D_{t-1} \rvert)$. For the 10-delta and 15-delta calls, the same method is used.

The null hypothesis of simultaneous zero coefficients in the regressors ($\beta_0=\beta_1=\beta_2\ldots=\beta_5=0$) is tested using the likelihood ratio test ("LR"). The reported z-statistics for the individual regressors are based on standard errors and covariance from the Huber/White quasi-maximum likelihood method. This ensures consistent estimates

of the regression coefficients which are robust to distributional bias in the standard error. The estimation of the jumps is performed over the option expiration period of one month. For simplicity, this study assumes the one month option contracts has 30 trading days to expiration.

The probit regression model is repeated using put option contracts. Thus, the test using the put option contracts is specified as:

$$Pb(Jump_i=1) = F(\beta_0 + \beta_1 \Delta PF_t + \beta_2 \Delta CE_t + \beta_3 \Delta P5D_t + \beta_4 \Delta P10D_t + \beta_5 \Delta P15D_t) + \varepsilon_t \quad (6\text{-}19)$$

6.9.2 Results for Probit Model Analysis

Table 6-12 presents the aggregate test results of the multivariable probit estimation for the put and call options. The joint test of zero coefficients in the dependent variables using the likelihood ratio "LR" is strongly rejected for both calls and puts at the 1% level.[120] This suggests the change in the curvature, the slope of the call and put volatility curves together with the out-of-money options are capable of generating insights into the likelihood of jumps in the underlying currencies. Compared with call options, the result is marginally stronger for the put options, with a higher likelihood ratio of 51.68. This is broadly consistent with the findings reported in the previous sections using Granger causality and VAR methodologies.

[120] A similar result is reported when the window size of 5 days is used to estimate the jumps. See Appendix B for further details.

The probit model demonstrates positive and significant coefficients for ΔPF,ΔP5D, indicating the larger the change in the slope of the put volatility curve, and more out-of-money the put, the greater the likelihood of a jump in the underlying currency. For the slope of the call volatility curve, a negative significant coefficient for ΔCF is reported instead. This suggests a lower slope coefficient for call volatility curve is associated with higher probability of a jump in the underlying currency. Overall, the results for put and call volatility curves appear to indicate that when the volatility smile becomes steeper to the left of at-the-money implied volatility (put volatility curve), and relatively flat to the right of at-the-money implied volatility (call volatility curve), the more likely is a jump. This is consistent with the view that a "smirk" pattern exists when a large movement of the underlying exchange rate is anticipated.

Table 6-12: Probit Regressions for the Aggregate Sample

$$Pb(Jump_{t+T}=1) = F(\beta_0 + \beta_1 \Delta CF_t + \beta_2 \Delta CE_t + \beta_3 \Delta C5D_t + \beta_4 \Delta C10D_t + \beta_5 \Delta C15D_t) + \varepsilon_t$$
$$Pb(Jump_{t+T}=1) = F(\beta_0 + \beta_1 \Delta PF_t + \beta_2 \Delta CE_t + \beta_3 \Delta P5D_t + \beta_4 \Delta P10D_t + \beta_5 \Delta P15D_t) + \varepsilon_t$$

	Put Options		Call Options	
	Coefficient	*z* -statistics	Coefficient	*z* -statistics
ΔPF (ΔCF)	0.541 **	(2.191)	-0.291 ***	(-3.475)
ΔCE	-0.991 ***	(-6.742)	-0.689 ***	(-3.527)
ΔP5D (ΔC5D)	0.334 ***	(2.878)	-0.154	(-0.739)
ΔP10D (ΔC10D)	-0.057	(-0.668)	0.161	(0.885)
ΔP15D (ΔC15D)	-0.296 ***	(-3.844)	0.018	(0.245)
LR	51.684 ***		50.203 ***	

Note: The Jump parameter is estimated using the Lee and Mykland (2007) method to detect for the presence of a on day t to (t+T).When the threshold is breached, a value of one is assigned or zero otherwise. A total of 58 jumps are used in the probit models. To save space, the constant term is omitted from the table.
**** Significant at the 1% level*
*** Significant at the 5% level*
** Significant at the 10% level*

The curvature coefficient for the smile is negative and significantly related to the probability of jumps, suggesting that a significant skewness exists in the put volatility curve while the call volatility curve is relatively flat when a jump is expected. This is due to a significant adjustment in the shape of the volatility smile, that is, as a spike is anticipated (upward or downward), puts are bid up relative to calls causing a considerable increase in the slope coefficient for the put volatility curve while the call volatility curve moved in the opposite direction. The combined effect of this adjustment is a decrease in the curvature coefficient for the volatility smile. Again, these findings are consistent with the "smirk" pattern reported in Campa and Chang (1995).

To further examine the robustness of the test results presented in Table 6-12, positive and negative jumps are identified separately and the probit regression is repeated in the total sample. If puts are preferred over calls when a negative jump occurs, the regression coefficients for the puts should register positive values while negative values are expected for the corresponding calls. To test this conjecture, positive ($L(i) >$ threshold) and negative jumps ($L(i) <$ threshold) are identified separately in the total sample and the probit regression is repeated. This is undertaken for both calls and puts, and results in four estimated models presented in Table 6-13.

For the prediction of negative jumps, the LR statistics are consistently higher than the corresponding statistics reported for positive jumps although the joint hypothesis of zero coefficients in the dependant variables remains significant at the 1% level in both instances. However, the relatively low LR statistics for positive jumps may be due to less frequent positive jumps reported over the sample period and thus the results should be interpreted with caution considering the limited sample size.

Table 6-13: Aggregate Results for Probit Regressions

	Put options				Call options			
	Positive Jumps		Negative Jumps		Positive Jumps		Negative Jumps	
	Coefficient	*z* -statistics	Coefficient	*z* -statistics	Coefficient	*z* -statistics	Coefficient	*z* -statistics
ΔPF (ΔCF)	-0.835 ***	(-4.464)	0.860 ***	(4.873)	0.194 ***	(2.411)	-0.331 ***	(-3.905)
ΔCE	-0.469	(-1.616)	-0.555 ***	(-3.446)	-0.887 ***	(-3.332)	-0.700 ***	(-3.924)
ΔP5D (ΔC5D)	-0.500 ***	(-4.537)	0.132	(0.881)	0.795 ***	(4.047)	0.236	(1.081)
ΔP10D (ΔC10D)	0.365 ***	(3.364)	-0.062	(-0.501)	-0.604 ***	(-3.047)	-0.151	(-0.666)
ΔP15D (ΔC15D)	0.238 ***	(2.971)	-0.134 *	(-1.824)	-0.178 ***	(-3.362)	-0.153 **	(-2.447)
LR	20.424 ***		66.500 ***		24.904 ***		69.188 ***	

Note: The dependent variable is the Jump parameter estimated using the Lee and Mykland (2007) method. A threshold of +4.6001(-4.6001) is used to detect for the presence of positive (negative) jumps on day t to (t+T). The term "LR" is the likelihood ratio statistics for the joint test of $\beta_0=\beta_1=\beta_2\ldots=\beta_5=0$. The reported z-statistics are based on standard errors and covariance from the Huber/White method. For brevity, the constant term is omitted from the table.
**** Significant at the 1% level*
*** Significant at the 5% level*
** Significant at the 10% level*

The regression coefficients for the put volatility curve are positive and statistically significant when negative jumps are detected. It demonstrates that there is a higher probability of a downward spike in the underlying exchange rate when the slope of the put volatility curve increases. On the contrary, a negative significant coefficient is reported for the call volatility curve suggesting that the probability of a market crash is associated with a flattening of the call volatility curve. Similar to the result previously reported in Table 6-12, the coefficient for out-of-money put of 15-delta remains negative and significant. Except for positive jumps reported for the put options, the curvature coefficients remain negative and significant in Table 6-13.

In summary, the results presented are consistent with the notion that information contained in the smile dynamics is useful for the prediction of jumps in daily exchange rates. This is consistent with Doran *et al* (2007) in their analysis of the equity market. The curvature of the smile and the slopes of the put and call volatility

curves are important explanatory variables for predicting jumps in the underlying currency.

6.10 Conclusion

In this chapter, the dynamics of volatility smiles are investigated using a trader-quoted currency option dataset, collected from the over-the-counter market. The relationship between the behaviour of the volatility smile and the anticipated volatility for the underlying currency is investigated. The results and analysis lead to three important conclusions about the behaviour of volatility smile. First, the dynamics of the volatility smile is related to the anticipated volatility of the currency market. Second, a large downward movement in the underlying currency appears to be related to an increase in slope coefficient for the put volatility curve and a decrease in slope coefficient for the call volatility curve. Third, the curvature of the volatility smile contains an important signal about market expectations and the findings of this chapter show that smile curvature has significant predictive ability.

CHAPTER 7 – FOREIGN EXCHANGE VOLATILITY PREDICTION: INTEGRATING VOLATILITY SMILE WITH IMPLIED VOLATILITY

7.1 Introduction

The information content of option-implied volatility has been actively studied in both the academic and practitioner literature. However, the forecasting power of traded implied volatility and its relationship with the smile anomaly has not been fully investigated. In the previous chapter, it is shown that the dynamics of the volatility smile is related to the anticipated volatility in the underlying currency. The current chapter extends these findings by investigating the usefulness of information embedded in the shape of the volatility smile for the prediction of future realised volatility. In particular, it adds to the literature on volatility prediction that uses at-the-money implied volatility forecasts by studying how the shape of the volatility smile affects the forecasting ability of implied volatility.

The analysis first examines the relationship between the level of implied volatility and the shape of the volatility smile. Second, the relative information content of the forecasting model is analysed using encompassing regression tests. The overall results suggest that the shape of the volatility smile, proxied by slope and curvature provides useful predictions of realised volatility over the remaining life of the option contract. Information embedded in volatility smile is forward-looking and is important in prediction of foreign exchange volatility. In addition, the results reported in this

chapter suggest that the forecasting ability of at-the-money implied volatility is affected by the shape of the volatility smile.

The following section briefly reviews the volatility smile literature. Section 7.3 surveys previous literature on volatility forecasting. The data and methodology used in this chapter are discussed in Sections 7.4 and 7.5 respectively. Data analysis and test results are presented in Sections 7.6 to 7.10. The conclusion of this chapter is offered in Section 7.11.

7.2 Shapes of Volatility Smiles and Volatility of the Underlying Assets

It is widely acknowledged that the volatility smile effect became more pronounced in the equity option markets after the October 1987 stock market crash. In a recent paper, Liu, Pan and Wang (2005) argue that option prices are very sensitive to market crashes and they suggest that the smile effect is attributable to extreme events in the financial markets. In the currency option market, Campa and Chang (1995) and Bollen and Rasiel (2003) note that the volatility smile effect occurs as a result of expectations of increasing risk in the underlying currency. Further, probit model analysis by Doran, Peterson and Tarrant (2007) provides evidence that information about volatility skew can be used to predict positive and negative jumps in the equity market.

The economic determinants of the volatility smile effect are examined by Pena, Rubio and Serna (1999) using implied volatility from the Spanish equity IBEX-35 index. They find that the curvature of the volatility smile is both significant and

negatively related to actual volatility in the underlying index. Slope and curvature estimates for the volatility smile are positively related to the option bid-ask spread. They note that as market makers anticipate higher volatility in the underlying market, out-of-money calls and puts are more highly valued than what the Black-Scholes (1973) model would suggest. A recent investigation by Deuskar, Gupta, and Subrahmanyam (2008) suggests that the volatility smile effect in the interest rate option market is affected by the degree of uncertainty in the underlying market. The volatility smile becomes steeper and more skewed over high-interest periods, but when the yield curve is sloping downwards, the smile effect becomes less pronounced. These results are generally consistent with the forward-looking nature of option-implied volatility.

7.3 Previous Studies on Volatility Forecasting

Implied volatility can be viewed as the *ex-ante* estimate of market volatility over the option expiration period. Therefore it is no surprise that a number of authors have examined the information content of implied volatility for option markets (for example, Jorion (1995), Fleming Ostdiek and Whaley (1995), Christensen and Prabhala (1998), Covrig and Low (2003), and Corrado and Miller (2005). These studies generally agree that option-implied volatility is capable of generating reliable forecasts of future volatility for the underlying asset.

Yet, earlier work by Day and Lewis (1992) and Canina and Figlewski (1993) find little evidence of implied volatility as a superior source of volatility forecast. Christensen and Prabhala (1998) argue that the Canina and Figlewski study suffers from mis-specified tests arising from highly autocorrelated errors due to the use of an overlapping sampling procedure.

When at-the-money implied volatility is used as a forecast for future volatility, it is commonly assumed that the shape of the smile has no impact on this forecast. Based principally on the studies by Christensen and Prabhala (1998), and Pena, Rubio and Serna (1999), it is therefore hypothesised in this chapter that while at-the-money implied volatility provides a valid forecast of future volatility, the shape of the implied volatility smile may also change significantly with changes in the level of future volatility as market sentiment evolves over time. A significant relationship may exist between the shape of the volatility smile and the level of at-the-money implied volatility and thus information about the smile may be included in the volatility forecasting model to increase explanatory power. In this study both the level of at-the-money implied volatility and the shape proxies of the smile are used for the prediction of realised volatility following the work documented in previous chapters.

7.4 Data

The over-the-counter currency option sample used in this chapter consists of daily closing quoted implied volatility corresponding to various levels of delta. To avoid the issue of bid-ask bounce, the mid-point of the bid-ask implied volatility for calls and puts is used in the analysis, with the spread obtained from UBS Investment Bank of Switzerland. The various implied volatility series are available on different periods but most observations cover the common period from 2 of October, 2001 to 2 June, 2006. These option series have constant time-to-maturity of one-month at any point in time of the sample period.

Quoted implied volatility for four major currency pairs are considered in this chapter, namely, the GBP/USD, the EUR/USD, the AUD/USD and the USD/JPY currency pairs. The traded implied volatility corresponds to call and put options with delta values ranging from 5 to 45, increasing by increments of 5. The at-the-money implied volatility is proxied using option contracts with a delta value of 0.50 where the exercise price is either close or equal to the underlying exchange rate. The structure of the data allows a fairly complete volatility smile to be observed on any given day over the entire sample period. This alleviates implied volatility estimation errors due to non-synchronous trades in the spot and option markets.

The daily average closing bid-ask quotes for the spot exchange rates are obtained from Reuters over the period 1 January, 1998 to 28 June, 2006. The spot exchange rate series extends over a longer time period relative to the option series in order to ensure sufficient observations are available for the estimation of conditional volatility using a 1000-day rolling GARCH (1,1) model. The corresponding one-month interest rates for each of the currency pairs are obtained from the British-Bankers' Association database.

7.5 Methodology

In Chapter 4, it is revealed that the levels of at-the-money implied volatility exhibit a significant non-normal distribution over the sample period. Accordingly in the following analysis, log transformation is applied to the volatility data to reduce skewness and kurtosis of the data so that the volatility series are approximately normally distributed. This transformation is also consistent with other studies that

employ volatility data, including Christensen and Hansen (2002) and Corrado and Miller (2005).

7.5.1 The Relationship between Implied Volatility and the Shape of Volatility Smile

The first analysis involves investigating the relationship between the levels of at-the-money implied volatility and the shape of the volatility smile. The at-the-money implied volatility is often used as a forecast for future volatility because as shown in Feinstein (1989), it represents an unbiased estimate of average variance over the life of the option. Furthermore, the use of at-the-money options result in less estimation error (Day and Lewis, 1992). Since at-the-money implied volatility is frequently used as an *ex-ante* forecast for realised volatility, any significant relationship that exists between the levels of at-the-money implied volatility and the shape of the volatility smile imply that the latter may contain useful information for volatility forecasting.

The shape of the volatility smile is proxied using slope and curvature coefficients estimated from each day's volatility smile. The methodology for estimating the shape of the volatility smile is previously discussed in Chapter 6[121]. The average slope of the smile (*AS*) is also included as an additional proxy in the regression tests. This is estimated as the first derivative of the quadratic form defined in Chapter 6.[122] For simplicity, the daily moneyness coefficient (X_t/F_t) is calculated by taking the average of moneyness that corresponds to 50-delta, 40 delta, 30-delta, 20 delta and 10-

[121] See Equations 6-3, 6-4, 6-7 and 6-8.

[122] See Equation 6-7.

delta for call and put options. Furthermore, this chapter uses absolute values of these of these proxies since it is hypothesised that the levels of at-the-money implied volatility are related to the shape of the volatility smile. In other words, this study focuses on the steepness of the slope rather than its direction.

In order to account for the possibility of non-linear dependence and to minimise the impact of extreme values of the implied-volatility series, nonparametric Spearman rank order correlation coefficients are estimated over the sample period. A *t*-statistics test is conducted for the null hypothesis that the correlation between at-the-money implied volatility and the shape of the volatility smile is zero. Correlation analysis also allows examination of the relationship that may exist between different proxies for the shape of the volatility smile.

7.5.2 Estimation of Realised Volatility

To assess the forecasting ability of the various proxies used in this study, the *ex-post* realised volatility of the underlying currency is estimated using the average of daily closing bid-ask prices. Since the option implied volatility has a constant maturity of one month, the realised volatility has to be estimated over the corresponding option time-to-maturity to ensure comparability. E*x-post* realised volatility for the underlying currency over the option expiration period *t* to *T* is estimated as:

$$RV_{t,T} = \sqrt{\sum_{t=1}^{T} [\ln(S_t / S_{t-1})]^2 (259 / T)} \qquad (7\text{-}1)$$

where $RV_{t,T}$ is the estimated *ex-post* realised volatility of the exchange rate over the option expiration period t to T and S_t is average bid-ask price for 1 unit of spot exchange rate available at period t. The square of the daily log returns are annualised by assuming 259 trading days per year. Consistent with the approach used in previous studies, (for instance Christoffersen and Mazzotta (2005), and Covrig and Low (2003)), this study assumes 20 trading days in a one month period.

7.5.3 Estimation of Conditional Volatility

A GARCH forecast series is constructed using a rolling window of 1000 observations[123]. That is, on any given day of the sample period, spot exchange rate returns over the last 1000 days are used to estimate the GARCH (1,1) parameters. The procedure involves the use of a constant sample size for each forecast, adding the return on day (t-1) and omitting the return on day t-(1000+1) from the sample to arrive at the variance forecast for day t. This assumes that market participants use of market information available to them at the time when the forecast is made. The GARCH parameters are estimated using the Broyden, Fletcher, Goldfarb and Shanno algorithm[124].

[123] Various rolling windows are also used in the estimation process. However the choice of 1000-day window is adopted as the estimated GARCH parameters are closer to previous studies such as Jorion (1995).
[124] See Press, Flannery, Teukolsky and Vettering (1988).

7.5.4 The Relationship between Realised Volatility and the Shape of Volatility Smile

Following Christensen and Prabhala (1998), the forecasting ability of the independent variable is evaluated by regressing the *ex-post* realised volatility on the proxies for the shape of the smile. Thus the univariate regression model takes the following form:

$$\ln RV_{t,T} = \gamma_0 + \beta_1 \ln SM_{t,T} + \varepsilon_t \qquad (7\text{-}2)$$

where $SM_{t,T}$ includes a range of estimation capturing the shape of the volatility smile according to the methodology provided in chapter 6[125], and $RV_{t,T}$ is the realised volatility estimated from Equation (7-1). The standard errors of the OLS regression tests are corrected for autocorrelation and heteroscedasticity using the Newey-West (1987) procedure.

Using the same univariate specification defined in Equation (7-2), the regression test is repeated using at-the-money implied volatility $IV_{t,T}$ as the independent variable. If the at-the-money implied volatility forecast is the true expected value of the realised volatility, $RV_{t,T}$, regressing $RV_{t,T}$ on $IV_{t,T}$ should produce regression coefficients of 0.00 for the intercept γ_0, and 1.00 for coefficient β_1. However, if the estimated coefficients are statistically different from 0.00 and 1.00, it is concluded that the forecasting model is inefficient and produces a biased estimate of realised volatility over the forecasting horizon.

[125] See section 6.3.2 to 6.4.1.

7.5.5 Forecasting Realised Volatility using Smile-adjusted Implied Volatility

To examine forecasting power using information in the volatility smile, the predictive ability of the implied volatility forecasts is examined using bivariate and multivariate models. First, Equation (7-2) is redefined as:

$$\ln RV_{t,T} = \gamma_0 + \beta_1 \ln IV_{t,T} + \beta_2 \ln IV_{t,T} \ln SM_t + \varepsilon_t \qquad (7\text{-}3)$$

where $IV_{t,T}SM_t$ is an interaction term. This regression model allows for interactions between IV_t and SM_t to be included in the forecasting procedure. It suggests that the evolution of at-the-money implied volatility is related to the shape of volatility smile over time.

Unbiasedness[126] and efficiency[127] tests that account for the interaction term $IV_{t,T}SM_t$ described in Equation (7-3) can be evaluated using the Wald coefficient restriction test. If the forecast is an unbiased and efficient predictor of future realised volatility, regressing $RV_{t,T}$ on $IV_{t,T}$ and the interaction term $IV_{t,T}SM_t$ should result in failure to reject the joint coefficient restriction test, with the null hypothesis specified as γ_0 =0 and (β_1+β_2)=1. The alternative null hypothesis can be tested by restricting the regression coefficients jointly as γ_0 =*0* and β_1=1, β_2 =0 to evaluate the performance of the $IV_{t,T}$ forecasts when the interaction term is included in the forecasting model. Failure to reject the null suggests that $IV_{t,T}$ is an unbiased and efficient estimate of realised volatility.

[126] That is, the slope coefficient is not statistically different from 1.00.
[127] This means the coefficient for the intercept term is not significantly different from zero.

7.5.6 Forecasting Realised Volatility Using, Smile Characteristics, Implied Volatility and Rolling-GARCH (1,1) Model

To further examine the relative performance of the at-the-money implied volatility and the GARCH (1,1) conditional volatility, the following regression is constructed with the interaction term described in Equation (7-3):

$$\ln RV_{t,T} = \gamma_0 + \beta_1 \ln IV_{t,T} + \beta_2 \ln IV_{t,T} \ln SM_{t,T} + \beta_3 \ln GV_{t,T} + \varepsilon_t \qquad (7\text{-}4)$$

where the variable GV_t is the estimated future volatility of the underling currency using the rolling-GARCH (1,1) framework. This model extends the earlier work of Jorion (1995), Day and Lewis (1992) and Covrig and Low (2003) by incorporating a third explanatory variable into the forecasting model – that is, the interaction term $IV_{t,T}SM_{t,T}$. This is used in addition to the option-implied volatility and GARCH (1,1) predictions of volatility.

Several hypotheses can be tested within the encompassing regression test according to Equation (7-4). The first test involves imposing restrictions on the estimated OLS coefficients with γ_0 =0, (β_1+ β_2) =1 and β_3 =0. This allows the *IV* series to be tested when interactions between *IV* and the shape of the volatility are considered. The rationale rests on the premise that the predictive ability of at-the-money implied volatility is related to the shape of the volatility smile.

The second test adopts the conventional specification used in previous studies to test the predictive power of the at-the-money implied volatility series. The coefficient restrictions for the null hypothesis are γ_0 =0, β_1 =1 and β_3 =0. Finally, the third

coefficient restrictions test is performed with the null hypothesis of γ_0 =0, β_1 =0 and β_3 =1. This tests the information content of the estimated GARCH (1,1) forecast.

7.6 Descriptive Statistics

Table 7-1 reports the descriptive statistics for the slope, curvature and volatility series for the currency pairs. The quoted at-the-money implied volatility (*IV*) series are based on the average of the bid and ask volatility prices for the one-month options. The realised volatility (*RV*) and the conditional volatility (*GV*) are estimated over the corresponding periods. The series *CF* denotes the slope of the call volatility curve and the series *PF* is the slope of the put volatility curve. The slope and curvature of the smile are represented by the series *AS* and *CE*. The realised volatility estimated over the maturity of the option period is denoted by the series *RV*. The GBP/USD series comprises of 1109 observations while 847 observations are used for the EUR/USD currency pair while the AUD/USD and the USD/JPY currency pairs have daily observations of 1104 and 1126 respectively.

There are no systematic differences in the mean realised volatility, mean quoted implied volatility, and mean conditional volatility for the currency pairs GBP/USD and USD/JPY. However, the mean conditional volatility series for the EUR/USD and the AUD/USD exchange rates are consistently greater than the mean realised volatility series.

Table 7-1: Descriptive Statistics for Implied Volatility and Estimated Series

	CF	*PF*	*AS*	*CE*	*RV*	*IV*	*GV*
Panel A : GBP/USD (2/10/2001 - 3/7/2006)							
Mean	0.236	0.202	0.160	10.434	8.487	8.197	8.401
Median	0.244	0.219	0.163	10.029	8.352	8.050	8.277
Maximum	0.460	0.405	0.284	28.430	14.549	11.790	11.802
Minimum	0.001	0.003	0.097	4.939	3.748	5.100	5.915
Std. Dev.	0.093	0.072	0.032	3.297	2.012	1.043	0.639
Skewness	-0.094	-0.443	0.766	2.208	0.434	0.651	1.342
Kurtosis	2.515	2.715	4.638	10.536	3.375	4.699	6.698
Panel B : EUR/USD (4/12/2002 - 28/6/2006)							
Mean	0.224	0.167	0.153	7.842	7.794	9.555	10.235
Median	0.225	0.176	0.153	7.737	7.554	9.400	10.108
Maximum	0.427	0.330	0.281	11.933	15.123	12.948	13.761
Minimum	0.008	0.002	0.107	5.139	2.919	7.325	6.003
Std. Dev.	0.082	0.068	0.029	1.271	1.983	1.083	0.684
Skewness	-0.187	-0.254	0.943	0.354	0.771	0.372	0.956
Kurtosis	2.909	2.330	5.161	2.603	3.983	2.397	7.904
Panel C : AUD/USD (22/4/2002 - 8/12/2006)							
Mean	0.112	0.236	0.139	7.295	9.959	9.868	11.096
Median	0.076	0.246	0.135	6.856	9.574	9.700	10.958
Maximum	0.357	0.341	0.233	14.846	18.100	15.000	16.206
Minimum	0.000	0.019	0.073	3.498	4.593	5.900	8.439
Std. Dev.	0.095	0.056	0.030	2.024	2.855	1.700	1.230
Skewness	0.766	-0.760	0.527	1.239	0.579	0.488	1.212
Kurtosis	2.338	3.104	3.084	4.895	2.789	3.010	5.747
Panel D : USD/JPY (2/10/2001 - 28/6/2006)							
Mean	0.146	0.387	0.238	10.836	9.135	9.244	9.071
Median	0.127	0.387	0.231	10.734	9.165	9.100	9.118
Maximum	0.480	0.694	0.565	19.326	14.304	14.000	10.620
Minimum	0.000	0.010	0.154	3.897	4.470	7.400	4.517
Std. Dev.	0.104	0.083	0.050	2.387	1.950	1.054	0.366
Skewness	0.928	-0.081	2.130	0.247	0.093	0.581	-3.285
Kurtosis	3.402	4.773	11.845	3.173	2.522	2.837	31.929

Note: This table displays the summary statistics for levels of the series used in this study. The statistics are calculated on levels of the individual series. The absolute values for the slopes are used in this study. The GBP/USD series comprises of 1109 observations, 847 observations are used for the EUR/USD while the AUD/USD and the USD/JPY consist of 1104 and 1126 observations respectively.

The realised volatility, quoted at-the-money implied volatility and the conditional volatility estimates fluctuate considerably over the sample period. For example, in Panel B, the EUR/USD *IV* series vary from 7.33% p.a. to 12.95% p.a. in line with the *RV* series. These series also have similar values for mean, median, maximum, minimum, skewness and kurtosis. However, it is clear that the implied volatility series exhibit consistently greater volatility for daily levels than the

corresponding GARCH-estimated conditional volatility series. Except for the AUD/USD currency pair, the conditional volatility standard deviations for the currencies are less than 1.00. In contrast, the implied volatility series have values in excess of 1.00 across all currency pairs from time to time.

The estimated slope coefficients for the calls (*CF*), puts (*PF*) and average slope of the volatility smile (*AS*) have relatively small variance compared with the curvature coefficients (*CE*). Nonetheless noticeable movements in the coefficient for *CF* and *PF* can be seen over the sample periods. For instance, the GBP/USD slope coefficient for the call volatility curve has a minimum and maximum value of 0.001 and 0.460 respectively. A similar pattern is noted for the put volatility curves. This empirical observation is consistent with the "smirk" or "sneer" patterns due to marked-perceived volatility in the currency market. In other words, the daily volatility smiles are 'skewed' in one direction. An examination of the third and fourth moments indicates the existence of both excess skewness and kurtosis. This suggests a violation of normal distribution in the data series.

7.7 Stationarity Tests

To test for the possibility of spurious regression, stationarity tests are applied to the individual data series. Table 7-2 provides the Phillips-Perron (1988) nonparametric unit root tests for (i) stationarity of the estimated slopes for the call and put volatility curves, (ii) the slope and curvature of the volatility smile, (iii) the realised volatility of the underlying currency, (iv) the at-the-money implied volatility, and (v)

the estimated GARCH (1,1) volatility series. The hypothesis that the estimated slopes and curvatures are nonstationary is rejected at the 5% level of significance. Similarly for the estimated realised and GARCH (1,1) volatility series, the nonstationary hypothesis for each series is rejected at the 1% level. For the quoted-at-the money implied volatility series, the nonstationary hypothesis is rejected at the 5% level for all currencies except the AUD/USD, which is stationary at the 10% level of significance. Overall, the rejections of the null of nonstationary suggest that differencing is not required to achieve stationary data series.

Table 7-2: Phillips-Perron(1988) Unit Root Tests

	GBP/USD		EUR/USD		AUD/USD		USD/JPY	
Series	*p* -values	BW	*p* -values	BW	*p* -values	BW	*p* -values	BW
CF	0.001	4	0.008	6	0.002	3	0.000	5
PF	0.000	4	0.000	3	0.000	2	0.000	0
AS	0.001	6	0.000	4	0.034	2	0.000	4
CE	0.001	6	0.000	9	0.001	2	0.000	7
RV	0.003	3	0.000	9	0.006	1	0.000	6
IV	0.039	2	0.000	3	0.079	2	0.000	12
GV	0.000	13	0.000	23	0.000	4	0.000	25

Note: This table provides the nonparametric Phillips-Perron (1988) unit root tests for the null of a unit root in the individuate series. The tests are performed on levels of the individual series. The Newey-West (1994) bandwidth ("BW") is selected using the Barlet kernel function. The GBP/USD series comprises of 1109 observations, 847 observations are used for EUR/USD while AUD/USD and USD/JPY consist of 1104 and 1126 observations respectively.

7.8 At-the-money Implied Volatility and the Shape of Volatility Smile

This section provides a preliminary analysis of whether there is a significant correlation between at-the-money implied volatility and the shape of volatility smiles proxied by the slope of the call (*CF*) and put (*PF*) volatility curves, the average slope of the volatility smile (*AS*) and the curvature of the volatility smile (*CE*).

The results for the Spearman correlation tests are displayed in Table 7-3. Across all currency pairs, the shape of the smile proxied by the size of the smile curvature (*CE*) exhibits the highest correlation with the at-the-money implied volatility. In addition, the relationship between these two series is consistently negative across all currency pairs. The *p*-values for the Spearman correlation are less than 0.000 suggesting strong rejections of the null hypothesis of zero correlation at the 1% level of significance. Thus, when at-the-money implied-volatility is low, the smile curvature coefficient has a considerable degree of curvature.

Drawing from the findings of Pena *et al* (1999), it appears that at higher levels of volatility, the curvature of the volatility smile becomes flatter reflecting lower bid-ask spreads. On the other hand, when a less volatile market is anticipated, the size of the curvature coefficient becomes larger with a higher bid-ask spread. In the foreign exchange market when higher levels of volatility are anticipated, out-of-money calls and puts are demanded by market players. Trading activity under such market conditions creates strong liquidity and, as a result, the bid-ask spread becomes narrower. In turn, this causes the curvature of the volatility smile to flatten. This interpretation is consistent with the "hedging pressure" argument proposed by Ederington and Guan (2002) who conjecture that the smile anomaly may be partially attributed to active trading of out-of-money calls and puts when less favourable market conditions are anticipated.

Table 7-3: Correlations Between Parameter Estimates and Implied Volatility

Series	*CF*	*PF*	*AS*	*CE*	*IV*
Panel A: GBP/USD					
CF	1.000				
PF	-0.411	1.000			
	-14.995				
	(0.000)				
AS	0.796	0.130	1.000		
	43.713	4.366			
	(0.000)	(0.000)			
CE	0.519	0.420	0.840	1.000	
	20.203	15.402	51.466		
	(0.000)	(0.000)	(0.000)		
IV	-0.160	-0.358	-0.398	-0.702	1.000
	-5.396	-12.749	-14.460	-32.856	
	(0.000)	(0.000)	(0.000)	(0.000)	
Panel B: EUR/USD					
CF	1.000				
PF	-0.600	1.000			
	-21.788				
	(0.000)				
AS	0.778	-0.032	1.000		
	36.021	-0.918			
	(0.000)	(0.359)			
CE	0.225	0.372	0.529	1.000	
	6.728	11.654	18.144		
	(0.000)	(0.000)	(0.000)		
IV	0.358	-0.067	0.402	-0.370	1.000
	11.159	-1.956	12.758	-11.599	
	(0.000)	(0.051)	(0.000)	(0.000)	

Note: This table shows the Spearman rank-order correlations corrected for degrees-of-freedom. The t-test statistic for the null of zero correlation coefficient is reported immediately below the Spearman correlation coefficient. The p-values for the test statistics are available in the parentheses.

For the average slope of the volatility smile (*AS)*, the correlation coefficients are again highly significant across all currency pairs. Positive relationships between the slope of volatility smile and at-the-money implied volatility are reported for the currency pairs EUR/USD, AUD/USD and USD/JPY, while the GBP/USD has a negative correlation coefficient of -0.398 as indicated in Panel A.

Table 7 3: Correlations Between Parameter Estimates and Implied Volatility (continued)

Series	*CF*	*PF*	*AS*	*CE*	*IV*
Panel C: AUD/USD					
CF	1.000				
PF	-0.527	1.000			
	-20.588				
	(0.000)				
AS	0.826	-0.097	1.000		
	48.613	-3.221			
	(0.000)	(0.001)			
CE	0.568	-0.116	-0.346	1.000	
	22.938	-3.888	-12.265		
	(0.000)	(0.000)	(0.000)		
IV	0.088	0.091	0.127	-0.566	1.000
	2.922	3.049	4.240	-22.814	
	(0.004)	(0.002)	(0.000)	(0.000)	
Panel D: USD/JPY					
CF	1.000				
PF	-0.506	1.000			
	-19.634				
	(0.000)				
AS	0.163	0.653	1.000		
	5.551	28.866			
	(0.000)	(0.000)			
CE	0.508	-0.073	-0.008	1.000	
	20.203	20.203	20.203		
	(0.000)	(0.000)	(0.000)		
IV	0.058	0.156	0.432	-0.537	1.000
	1.939	5.307	16.066	-21.332	
	(0.000)	(0.000)	(0.000)	(0.000)	

Note: This table shows the Spearman rank-order correlations corrected for degrees-of-freedom. The t-test statistic for the null of zero correlation coefficient is reported immediately below the Spearman correlation coefficient. The p-values for the test statistics are available in the parentheses

The sign and size of the slope coefficient varies significantly over the sample period suggesting that the shape of the volatility curve is responsive to expected volatility in the underlying currency. Since the slope of the smile is constructed using both call and put volatility curves, this result suggests that average skewness in the volatility smile and at-the-money implied volatility are strongly correlated over time.

The correlation coefficients for call and put volatility curves range from 0.058 to 0.358 while slopes and curvatures have larger coefficients of 0.127 to -0.702. The fact that call and put volatility curves are less correlated with the at-the-money implied volatility indicates that daily movement in the at-the-money implied volatility is mainly related to the slope and curvature coefficients of the volatility smile. Nonetheless, except for the EUR/USD currency pair reported in Panel B, the slope coefficients for calls and puts remain significant at the 1% level.

Of note is the negative correlation between calls and puts across all currency pairs. This is consistent with the notion that the demand for calls and puts reflects different market sentiment over the sample period. For instance, some market players would prefer to use puts rather than calls when the underlying currency is expected to depreciate in the coming month.

In summary, the overall findings from this preliminary analysis suggest that daily movements in the at-the-money implied volatility series is associated with the shape of the volatility smiles. Further, the degree of uncertainty in the underlying foreign exchange market appears to be associated with the shape of the smile.

To further illustrate the relationship between the at-the-money implied volatility series and the size of the volatility smile coefficients, the time series plots for the GBP/USD at-the-money implied volatility series are graphed together with the curvature coefficients of the same currency. The GBP/USD is chosen because of the four currency pairs, it has the strongest correlation with the at-the-money volatility series.

Figure 7-1: Movement of Implied Volatility and Smile Curvature over Time

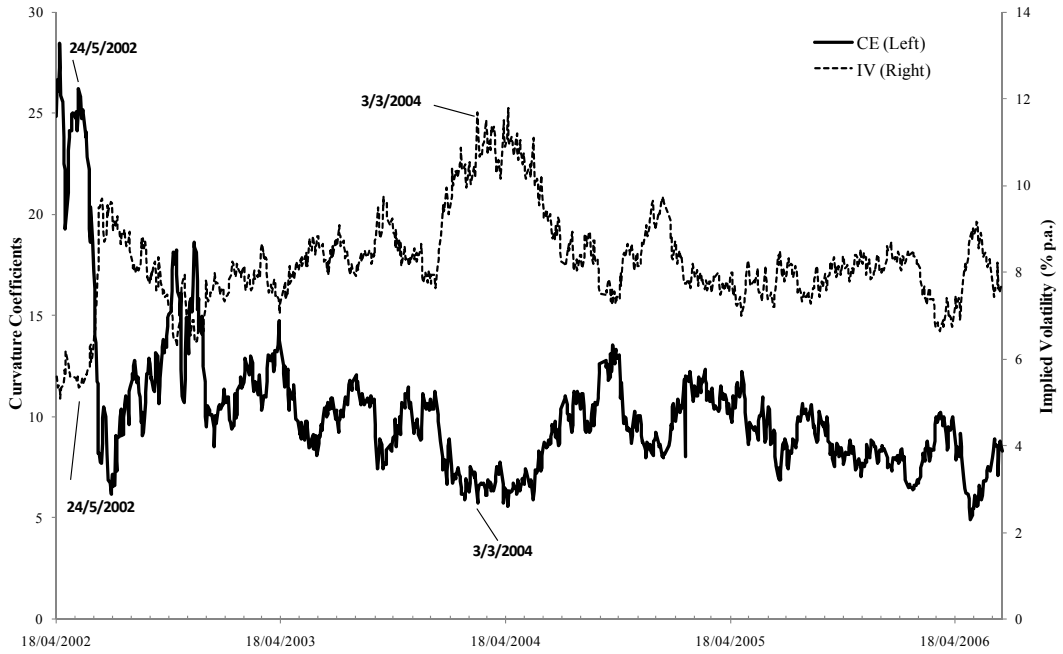

Note: This figure shows the time series plots of at-the-money implied volatility series ("IV", right-scale) and the volatility smile curvature coefficients ("CE", left-scale) from 18 April, 2002 to 3 July, 2006.

The time series plots in Figure 7-1 illustrate the movement of at-the-money implied volatility series and the estimated curvature coefficients for the GBP/USD. The two series are observed to move in the opposite direction over the period 18 April, 2002 to 3 July, 2006 and the resultant correlation coefficient is -0.72 (*t*-statistic of -32.856 with *p*-value of 0.000). Of note are the level of at-the-money implied volatility and the size of the curvature coefficients on two particular days within this sample period. These are 24 May, 2002 and 3 March, 2004. Specifically on 24 May, 2002 the at-the-money implied volatility is 5.35% p.a., while the smile curvature coefficient is approximately 26.2. In contrast, the at-the-money implied volatility increased to approximately 11.7% p.a. and at the same time the size of the smile curvature

decreased to approximately 5.7 on 3 March, 2004. The volatility smiles on these two days are displayed in Figure 7-2.

Figure 7-2: Volatility Smiles for GBP/USD

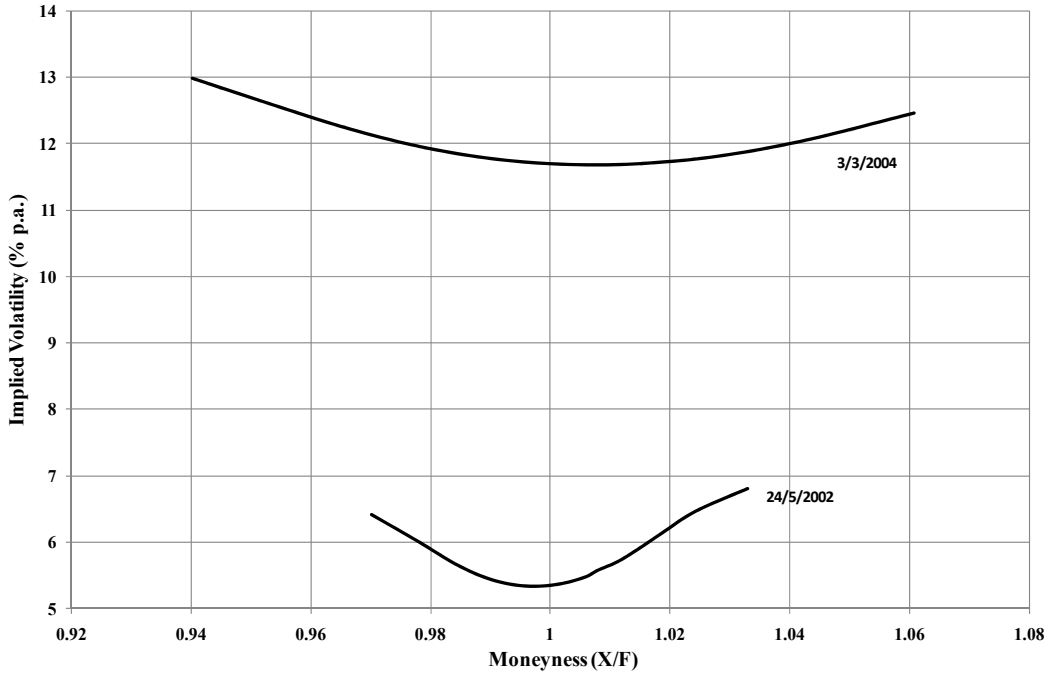

Note: This figure shows the volatility smiles on 24 May, 2002 and 3 March, 2004. The smiles are constructed using trader-quoted implied volatility.

Two interesting observations can be made from Figure 7-2. First, the volatility smile on 3 March, 2004 is relatively flat compared with that on 24 May, 2002. In the former, the smile extends over a wider range of moneyness from 0.94 to around 1.06. In contrast, on 24 May, 2002, the smile spans over a relatively smaller range of moneyness from 0.97 to around 1.03.

Second, on 24 May, 2002 the level of at-the-money implied volatility is about half the implied volatility reported on 3 March, 2004 but the size of the smile curvature

is about 5 times greater. Thus, the size of the smile curvature appears to be inversely related to the level of implied volatility. These findings are consistent with the previous analysis using Spearman rank-order correlation presented in Table 7-3 where a significant negative relationship is reported.

Table 7-4 displays the GBP/USD implied volatility levels for the at-the-money option ("*IV*") together with the shape proxies and the moneyness ratio for each level of deltas. The ratio is estimated relative to the at-the-money implied volatility denoted as "*DN*". For example, the quoted implied volatility for 5-delta put ("*P5D*") on 24 April, 2002 is 6.21% while at-the-money option has volatility of 5.10%, giving an estimate of 1.217 in column six.

Table 7-4: Estimated Shape Proxies and Volatility Smile

Date	*IV*	*CF*	*PF*	*AS*	*CE*	*P5D*	*P20D*	*P35D*	*DN*	*C35D*	*C20D*	*C5D*
24/04/2002	5.100	0.448	0.382	0.284	28.430	1.217	1.047	1.004	1.000	1.024	1.098	1.276
16/09/2003	8.425	0.223	0.256	0.170	10.840	1.134	1.038	1.008	1.000	1.005	1.030	1.122
21/04/2004	11.789	0.091	0.244	0.122	5.615	1.126	1.045	1.014	1.000	0.995	1.001	0.047

Note: This table displays the at-the-money implied volatility levels, proxies for the slope and curvature of the smile along with the corresponding moneyness ratios. The values are shown in columns six to twelve.

Table 7-4 shows that the curvature coefficients ("*CE*") on 24 April, 2002 and 21 April, 2004 are distinctly different from the mean curvature coefficient of 10.83 (estimated for the entire sample period). However, on 16 September, 2003, the estimated curvature coefficient is 10.84, which is nearly identical to the mean value. At the same time, the size of the slope coefficients for the put and call volatility curves (denoted as "*PF*" and "*CF*") are nearly equal (0.256 and 0.223 respectively). This suggests that on average, the smile is fairly symmetrical over the sample period.

On 24 April 2002, the smile curvature coefficient has the highest value and decreases to 10.840 and 5.615 on 16 September, 2003 and 21 April, 2004 respectively. Over the same period, the slope proxies also decrease steadily in tandem with the size of the curvature coefficient. The shape of the smile presented in Figure 7-3 provides a graphical representation of the smile dynamics over the same time period and indicates that the smile effect becomes less pronounced over the two year period. This is consistent with the size of the slope coefficients reported in columns two to five of Table 7-4. The average slope of the smile proxied by *AS*, is approximately equal to the mean of slope for the put (*PF*) and call volatility curve (*CF*) when the difference between *PF* and *CF* are small. As expected, when the smile is more symmetrical, the coefficient for *AS* is approximately the average of the *PF* and *CF* slope coefficients. This is particularly the case on 16 September, 2003. Notably the level of at-the-money implied volatility increased from 5.10% to 11.80% over the same period. This is also consistent with the pattern reported in Figure 7-2.

Figure 7-3: Volatility Smile Dynamics for GBP/USD

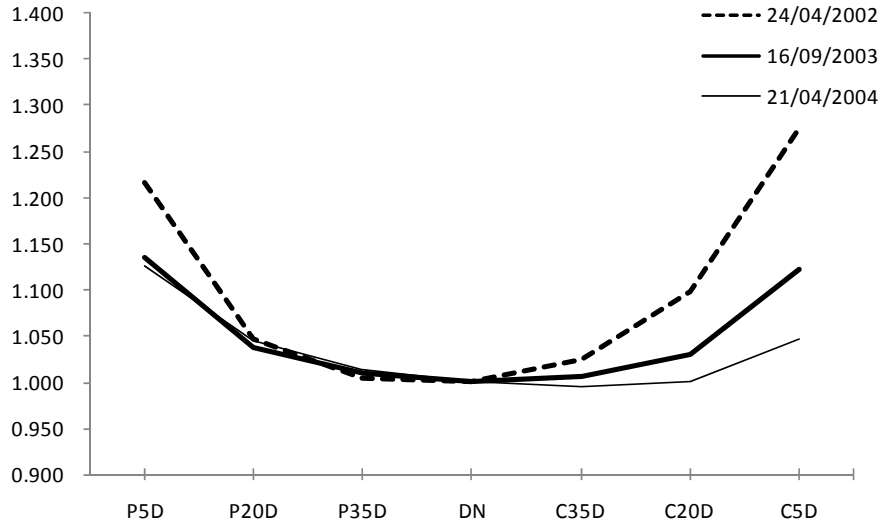

Note: The volatility smiles are constructed using the estimated moneyness values presented in columns six to twelve of Table 7-4.

7.9 Univariate Regression Test Results

Two different regression test results are presented in this section. First, the predictive power of the proxies for the shapes of the volatility smile is evaluated. Second, the univariate model is repeated using at-the-money implied volatility as the independent variable to examine the information content of the implied volatility series.

7.9.1 Regressing RV on SM

Table 7-5 reports the OLS estimates using Equation (7-2). The regressions are performed independently by regressing the realised volatility (*RV*) on the shape of the smile (*SM*), which is proxied by (i) the slope coefficient of the call volatility curve (*CF*) and put (*PF*), (ii) the average slope of the volatility smile (*AS*) and (iii) the curvature of the volatility smile (*CE*).To reduce the impact of incorrect inference from tests using overlapping data, the regressions are performed with Newey-West (1987) adjusted standard errors. This adjustment is also applied to all other regression tests undertaken in this chapter.

The results indicate that the shape of the volatility smile contains information about future realised volatility. The β_1 coefficients for the slopes and curvature measures produce significant results in all cases with the exception of the *CF* series for the EUR/USD and the USD/JPY currency pairs. It is clear that in most instances, the *t*-test statistic for the null hypothesis of zero β_1 coefficients is rejected at the 1% level of significance. It is also important to note that amongst all other proxies, *CF* has the

Table 7-5: Univariate Regression Tests Using Shape Proxies of Volatility Smile

γ_0		β_1			
ct.	***CF***	***PF***	***AS***	***CE***	R^2
Panel A: GBP/USD					
2.256 ***	-0.618 ***				0.054
(0.042)	0.168				
2.297 ***		-0.926 ***			0.074
(0.043)		0.200			
2.601 ***			-3.068 ***		0.159
(0.077)			0.463		
2.489 ***				-0.036 ***	0.241
(0.055)				0.005	
Panel B: EUR/USD					
1.984 ***	0.167				0.002
(0.061)	0.245				
1.864 ***		0.943 ***			0.063
(0.053)		0.258			
1.727 ***			1.930 **		0.047
(0.138)			0.885		
2.226 ***				-0.100 *	0.003
(0.110)				0.052	
Panel C: AUD/USD					
2.319 ***	0.022 ***				0.009
(0.020)	0.006				
2.533 ***		0.190 **			0.032
(0.114)		0.080			
1.911 ***			2.777 **		0.031
(0.153)			1.215		
2.984 ***				-0.112 ***	0.252
(0.102)				0.015	
Panel D: USD/JPY					
2.218 ***	-0.203				0.008
(0.024)	0.133				
2.093 ***		0.245 ***			0.008
(0.027)		0.070			
2.051 ***			0.575 **		0.017
(0.056)			0.227		
2.429 ***				-0.022 ***	0.057
(0.068)				0.007	

Note: This table displays the univariate regression tests performed using autocorrelation and heteroscedasticity consistent covariance matrix of Newey-West (1987). The corrected standard errors are reported in the parentheses. The regression model is specified as:

$$\ln RV_{t,T} = \gamma_0 + \beta_1 \ln SM_{t,T} + \varepsilon_t$$

where SM denotes the shapes of volatility smile proxied using "CF", "PF","AS", "CE" which represents the slope for the call volatility curve, slope for the put volatility curve, average slope of the volatility smile and curvature of the smile respectively.

**** Significant at the 1% level*

*** Significant at the 5% level*

** Significant at the 10% level*

lowest R^2. In contrast, the put volatility curve (*PF*) rejects the null hypothesis in all currency pairs and also has a higher R^2.

The average slope of the volatility smile (*AS*) has the greatest β_1 coefficients. The OLS estimates are -3.068 for the GBP/USD, 1.930 for the EUR/USD, 2.777 for the AUD/USD, and 0.575 for the USD/JPY currency pair respectively. Thus, the shape of the smile proxied by *AS* appears to exhibit significant upward and downward bias, reflecting average skewness of the volatility smile over the sample period. The results for the put volatility curve (*PF*) are also highly significant with lower β_1 coefficients. For example, the OLS estimated β_1 coefficient for EUR/USD is 0.943 (R^2 = 0.063). Overall, the results in this table are fairly consistent with the Spearman rank-order statistics presented in Table 7-3.

The smile curvature has the best goodness-of-fit with the exception of the EUR/USD currency pair. The Australian dollar has the highest R^2 of 0.252. Again, consistent with the previous analysis using the Spearman rank order correlation, the OLS estimates for the smile curvatures have negative coefficients across all currency pairs.

7.9.2 Regressing RV on IV

Consistent with previous studies using over-the-counter currency option contracts[128], the OLS estimated β_1 coefficients reported in column two of Table 7-6 strongly reject the null hypothesis of zero coefficients at the 1% level of significance. The unbiasedness and efficiency test is performed by imposing joint coefficient

[128] For instance, earlier work by Covrig and Low (2003) also find similar results using one-month at-the-money implied volatility from the OTC currency option market.

restrictions ($\alpha_0 = 0$ *and* $\beta_1 = 1$). The Wald test statistic indicates that the null hypothesis cannot be rejected for the GBP/USD and the AUD/USD currency pairs. Thus, there is evidence to support the hypothesis that implied volatility of foreign exchange option contracts are unbiased and efficient predictors of future realised volatility since the intercepts, α_0, are insignificantly different from zero and the β_1 coefficients are close to and insignificantly different from 1.0.

Table 7-6: Univariate Regression Tests Using At-the-money Implied Volatility

Currency		γ_0	β_1	R^2	*WT*
GBP/USD					
	ct.	-0.043	1.027 ***	0.282	0.506
	s.e.	(0.215)	(0.101)		
EUR/USD					
	ct.	-1.057 ***	1.368 ***	0.371	101.856 ***
	s.e.	(0.286)	(0.127)		
AUD/USD					
	ct.	-0.179	1.068 ***	0.315	1.909
	s.e.	(0.178)	(0.080)		
USD/JPY					
	ct.	1.070 ***	0.504 ***	0.064	11.701 ***
	s.e.	(0.289)	(0.128)		

Note: This table provides the univariate regression tests performed using autocorrelation and heteroscedasticity consistent covariance matrix of Newey-West (1987). The corrected standard errors are reported in the parentheses. The regression model is specified as: $\ln RV_{t,T} = \gamma_0 + \beta_1 \ln IV_{t,T} + \varepsilon_t$

The Wald test statistics reported in column four test the biasness of the forecasting model with the null of $\alpha_0 = 0$ *and* $\beta_1 = 1$.

*** *Significant at the 1% level*

** *Significant at the 5% level*

* *Significant at the 10% level*

7.10 Multiple Regression Test Results

The analysis in the previous sections suggests that the shape of the smile is a significant explanatory variable for future realised volatility. It is also shown that significant correlation exists between the level of at-the-money implied volatility and the shape of the smile. In this section, the at-the-money implied volatility are used

jointly with the proxies for the smile shape to forecast future realised volatility. This approach enables one to examine the forecasting ability of the implied volatility series when interactions between the shapes of smile and the implied volatility series are permitted.

7.10.1 Regressing RV on IV and SM

The test results for the multiple regressions performed by regressing the realised volatility (*RV*) on the at-the-money implied volatility (*IV*) series and the shapes of the volatility smile (*SM*) are reported in Tables 7-7 to 7-10. In each of the tables, the implied volatility and proxies for the shape of the smile are used jointly as explanatory variables.

Table 7-7 reports that the *IV* series remains significant at the 1% level and the size of the β_1 coefficients are approximately the same as reported in Table 7-6. However the slope coefficients (β_2) for the at-the-money implied volatility and *CF* interaction term are only marginally significant for the EUR/USD and the USD/JPY at the 5% and 10% level respectively.

Not surprisingly the size of the β_2 coefficients is relatively small compared with the slope coefficient β_1 for the *IV* series. Further, the interaction term is only marginally significant for two of the four currencies examined. The Wald test with the null hypotheses of $\gamma_0 = 0$ and $(\beta_1 + \beta_2) = 1$, and $\gamma_0 = 0$ and $\beta_1 = 1$, $\beta_2 = 0$ cannot be rejected for the GBP/USD and the AUD/USD currency pairs.

Table 7-7: Regression Tests Using At-the-money Implied Volatility and CF

Currency	γ_0	β_1	β_2	***Adj-R^2***	***WT-1***	***WT-2***
GBP/USD						
ct.	-0.058	1.006 ***	-0.117	0.289	0.935	1.310
s.e.	(0.236)	(0.106)	(0.079)			
EUR/USD						
ct.	-1.239	1.489 ***	-0.178 **	0.385	18.739 ***	75.988 ***
s.e.	(0.266)	(0.118)	(0.086)			
AUD/USD						
ct.	-0.077	1.016 ***	0.089	0.377	0.519	1.301
s.e.	(0.072)	(0.074)	(0.198)			
USD/JPY						
ct.	1.038 ***	0.535 ***	-0.114 *	0.078	10.113 ***	9.166 ***
s.e.	(0.285)	(0.127)	(0.059)			

Note: This table provides the regression tests performed using autocorrelation and heteroscedasticity consistent covariance matrix of Newey-West (1987). The corrected standard errors are reported in the parentheses. The regression model is specified as: $\ln RV_{t,T} = \gamma_0 + \beta_1 \ln IV_{t,T} + \beta_2 \ln IV_{t,T} \ln CF_t + \varepsilon_t$

The Wald test statistics reported in columns five and six test the biasness of the forecasting model with the null of 1.): $\gamma_0 = 0$ *and* $(\beta_1 + \beta_2) = 1$*; 2.):* $\gamma_0 = 0$ *and* $\beta_1 = 1$, $\beta_2 = 0$ *respectively.*

*** *Significant at the 1% level*

** *Significant at the 5% level*

* *Significant at the 10% level*

The result for regressing *RV* on *IV* and *PF* is displayed in Table 7-8. The overall pattern remains similar to that reported in Table 7-7, although the coefficient for the GBP/USD interaction term is marginally significant at the 10% level. The size of the β_2 coefficient increases from -0.117 to -0.145, suggesting the interaction between at-the-money implied volatility and the put volatility curve has slightly greater explanatory power than the call volatility curve reported in the previous table.

Table 7-8: Regression Tests Using At-the-money Implied Volatility and PF

Currency	γ_0	β_1	β_2	*Adj-R^2*	*WT-1*	*WT-2*
GBP/USD						
ct.	0.086	0.994 ***	-0.145 *	0.288	1.259	1.227
s.e.	(0.236)	(0.106)	(0.079)			
EUR/USD						
ct.	-1.143 ***	1.328 ***	0.467 ***	0.451	18.004 ***	83.027 ***
s.e.	(0.266)	(0.118)	(0.086)			
AUD/USD						
ct.	-0.071	1.035 ***	-0.049	0.373	0.102	0.493
s.e.	(0.072)	(0.074)	(0.198)			
USD/JPY						
ct.	1.108 ***	0.463 ***	0.060	0.067	7.306 ***	7.879 ***
s.e.	(0.285)	(0.127)	(0.059)			

Note: This table provides the regression tests performed using autocorrelation and heteroscedasticity consistent covariance matrix of Newey-West (1987). The corrected standard errors are reported in the parentheses. The regression model is specified as: $RV_{t,T} = \gamma_0 + \beta_1 IV_{t,T} + \beta_2 IV_{t,T} PF_t + \varepsilon_t$

The Wald test statistics reported in columns five and six test the biasness of the forecasting model with the null of 1.): $\gamma_0 = 0$ *and* $(\beta_1 + \beta_2) = 1$*; 2.):* $\gamma_0 = 0$ *and* $\beta_1 = 1$, $\beta_2 = 0$ *respectively.*

*** *Significant at the 1% level*

** *Significant at the 5% level*

* *Significant at the 10% level*

For the USD/JPY currency pair, the β_2 coefficient is not significant and the Wald statistics for the coefficient restriction tests decreased more sharply. The Wald test statistic for the joint coefficient restriction test with the null of $\gamma_0 = 0$ and $(\beta_1 + \beta_2) = 1$ remains significant at the 1%. The same pattern can be noted when the null hypothesis for the at-the-money implied volatility is specified as $\gamma_0 = 0$ and $\beta_1 = 1$, $\beta_2 = 0$. Similar with the results reported in Table 7-7, the null hypotheses for the AUD/USD currency pairs still hold.

Table 7-9: Regression Tests Using At-the-money Implied Volatility and AS

Currency	γ_0	β_1	β_2	*Adj-R^2*	*WT-1*	*WT-2*
GBP/USD						
ct.	0.334	0.957 ***	-0.703 **	0.305	3.098 **	2.627 **
	(0.236)	(0.106)	(0.079)			
EUR/USD						
ct.	-0.948 ***	1.397 ***	0.041 **	0.374	6.595 ***	70.190 ***
	(0.266)	(0.118)	(0.086)			
AUD/USD						
ct.	-0.067	0.996 ***	0.187	0.374	0.319	0.776
	(0.072)	(0.074)	(0.198)			
USD/JPY						
ct.	1.115 ***	0.473 ***	0.044	0.064	8.224 ***	7.981 ***
	(0.358)	(0.185)	(0.218)			

Note: This table provides the regression tests performed using autocorrelation and heteroscedasticity consistent covariance matrix of Newey-West (1987). The corrected standard errors are reported in the parentheses. The regression model is specified as: $\ln RV_{t,T} = \gamma_0 + \beta_1 \ln IV_{t,T} + \beta_2 \ln IV_{t,T} \ln AS_t + \varepsilon_t$

The Wald test statistics reported in columns five and six test the biasness of the forecasting model with the null of 1.): $\gamma_0 = 0$ *and* $(\beta_1 + \beta_2) = 1$*; 2.):* $\gamma_0 = 0$ *and* $\beta_1 = 1$, $\beta_2 = 0$ *respectively.*

**** Significant at the 1% level*

*** Significant at the 5% level*

** Significant at the 10% level*

In Table 7-9, the OLS estimated GBP/USD coefficient for the interaction between at-the-money implied volatility and the average slope of the smile (*IVAS*) is significant at 5% level. These are in contrast to the results reported in Tables 7-8 and 7-7 where the same coefficient is either not significantly differently from zero or is only marginally significant at the 10% level. It is also interesting to note that both the unbiasedness and efficiency hypotheses, not previously rejected, have Wald statistics of 3.098 and 2.627 (both rejected at the 5% level of significance). This suggests that the rejection of the unbiasedness and efficiency hypotheses seems to be related to the significance of the interaction term. That is, the slope of the smile has a significant impact on the forecasting ability of the at-the-money implied volatility series – the more significant is the size of the slope coefficient, the less accurate is the at-the-money implied volatility forecast. Conversely, when the interaction term is not significant, the Wald tests cannot be rejected. Further evidence is provided in the AUD/USD test results

where the Wald statistic is not rejected when the interaction term is insignificant. This result is also evident for the AUD/USD currency pair presented in Tables 7-7, 7-8 and 7-10.

Table 7-10: Regression Tests Using At-the-money Implied Volatility and CE

Currency	γ_0	β_1	β_2	*Adj-R^2*	*WT-1*	*WT-2*
GBP/USD						
ct.	0.853 **	0.710 ***	-0.010 **	0.306	3.384 **	2.757 **
	(0.236)	(0.106)	(0.079)			
EUR/USD						
ct.	-1.509 ***	1.419 ***	0.019 ***	0.410	18.731 ***	79.096 ***
	(0.266)	(0.118)	(0.086)			
AUD/USD						
ct.	-235	1.062 ***	-0.030	0.492	0.965	0.997
	(0.072)	(0.074)	(0.198)			
USD/JPY						
ct.	1.443 ***	0.405 ***	-0.007 *	0.080	10.214 ***	8.654 ***
	(0.326)	(0.132)	(0.218)			

Note: This table provides the regression tests performed using autocorrelation and heteroscedasticity consistent covariance matrix of Newey-West (1987). The corrected standard errors are reported in the parentheses. The regression model is specified as: $\ln RV_{t,T} = \gamma_0 + \beta_1 \ln IV_{t,T} + \beta_2 \ln IV_{t,T} \ln CE_t + \varepsilon_t$

The Wald test statistics reported in columns five and six test the biasness of the forecasting model with the null of 1.): $\gamma_0 = 0$ *and* $(\beta_1 + \beta_2) = 1$*; 2.):* $\gamma_0 = 0$ *and* $\beta_1 = 1$, $\beta_2 = 0$ *respectively.*

*** Significant at the 1% level

** Significant at the 5% level

* Significant at the 10% level

On the whole, using smile curvature as a proxy for the shape of volatility smile shows the highest adjusted-R^2 (see column four of Table 7-10). This is consistent with the univariate test results reported in Table 7-5 where the *RV* series is regressed on the *CE* series. The interaction between at-the-money implied volatility and the smile curvature (*IVCE*) is significantly different from zero for the GBP/USD, the EUR/USD and the USD/JPY currency pairs. Furthermore, the Wald test statistics for the null hypotheses of $\gamma_0 = 0$ and $(\beta_1 + \beta_2) = 1$, and $\gamma_0 = 0$ and $\beta_1 = 1$, $\beta_2 = 0$ are rejected at the 1% and 5% level of significance for these three currency pairs.

Thus compared with other proxies, the curvature of the volatility smile appears to be a more robust explanatory variable in predicting the variation of realised volatility across the currency pairs. Furthermore the effect of including smile curvature into the regression tests has a greater impact on the forecasting ability of the *IV* series.

In summary, it is noted that the rejection of the null hypotheses of unbiasedness and efficiency occurs whenever the interaction term is reported to be significant. Thus when the shape of volatility smile is found to be significant in the regression model, the forecasting ability of the *IV* series worsens and the unbiasedness and efficiency hypotheses is more likely to be rejected. Stronger empirical evidence is provided when the smile curvature (*CE*) is used in the forecasting procedure.

7.10.2 Regressing RV on IV, SM and GV

The final regression tests involve forecasting future realised volatility using currency option-implied volatility together with the GARCH-estimated conditional volatility. This provides a further extension to the testing methodology by focusing on the relative performance of the option-implied volatility and the GARCH (1,1) estimated volatility when the shape of the volatility smile is accounted for in the forecasting procedure.

The first encompassing regression test results are presented in Table 7-11 using a bivariate model. They indicate that unbiasedness and efficiency (null hypothesis of γ_0 =0 and β_1=0, β_2=1) is strongly rejected for the GARCH (1,1) forecasts across all currency pairs while evidence for implied volatility forecasts (null hypothesis of γ_0 =0

and β_1=1, β_2=0) is not rejected for AUD/USD. The coefficient for the *IV* series denoted as β_1 is significant at the 1% level for the currency pairs GBP/USD, EUR/USD and AUD/USD while the estimates for β_2 are only significant for the GBP/USD and the EUR/USD currency pairs (marginally significant at the 10% level). Notably the size of the β_1 coefficients is consistently larger than that of β_2, suggesting that the option-implied volatility explain a much greater share of the variation in future realised volatility than the GARCH (1,1) estimated volatility. In a broad sense, while support for the unbiasedness and efficiency hypotheses is weaker in the bivariate analysis, the *IV* series still captures much of the variation in realised volatility.

Table 7-11: Regression Tests with At-the-money Implied Volatility and GARCH (1,1) Estimates

Currency	γ_0	β_1	β_2	***Adj-R^2***	***WT-1***	***WT-2***
GBP/USD						
ct.	-0.849 ***	0.897 ***	0.506 ***	0.301	4.021 ***	24.128 ***
	(0.409)	(0.108)	(0.194)			
EUR/USD						
ct.	-1.725 ***	1.239 ***	0.412 *	0.380	71.238 ***	159.848 ***
	(0.412)	(0.157)	(0.222)			
AUD/USD						
ct.	-0.418	0.9377 ***	0.227	0.377	0.619	79.623 ***
	(0.128)	(0.251)	(0.262)			
USD/JPY						
ct.	1.306 *	0.503	-0.106	0.066	7.447 ***	14.902 ***
	(0.748)	(0.136)	(0.267)			

Note: This table provides the encompassing regression tests performed using autocorrelation and heteroscedasticity consistent covariance matrix of Newey-West (1987). The corrected standard errors are reported in the parentheses.The regression model is specified as:

$$\ln RV_{t,T} = \gamma_0 + \beta_1 \ln IV_{t,T} + \beta_2 \ln GV_{t,T} + \varepsilon_t$$

The Wald test statistics reported in columns five and six test the biasness of the forecasting model with the null of 1.): γ_0 =0 and β_1=1, β_2=0; 2.): γ_0 =0 and β_1=0, β_2=1 respectively.
**** Significant at the 1% level*
*** Significant at the 5% level*
** Significant at the 10% level*

The magnitude for the estimated adjusted *R*-square is quite high in most instances. Using implied volatility of currency option from the Chicago Mercantile Exchange (CME), Jorion (1995) reports R^2 results between 0.100 and 0.152 whereas the R^2 reported in Table 7-11 range from 0.066 to 0.380. Specifically, GBP/USD, EUR/USD and AUD/USD all have adjusted R^2 greater than 0.300.

In Tables 7-12 to 7-15, the encompassing regressions are performed by including different proxies for the shape of the smile as a third explanatory variable. Together with the existing unbiasedness and efficiency hypotheses, a third unbiasedness and efficiency hypotheses is employed for the GARCH-estimated volatility series. The Wald test statistic for the multivariate regression with the null hypothesis of $\gamma_0=0$, $\beta_1=0$ and $\beta_3=1$ is available in column eight of each table.

In sharp contrast with the *GV* forecasts, the *IV* series are highly significant and the null hypothesis of zero coefficients is rejected in all cases. The size of the β_1 coefficients is always larger than the β_3 coefficients. This result holds across all currencies. For instance, in Table 7-14, the GBP/USD coefficients for β_1 and β_3 are 0.901 and 0.293 respectively. Further, for AUD/USD, the unbiasedness and efficiency hypotheses cannot be rejected when the forecasting test is performed using different proxies represented by *CF*, *AS* and *CE* (see Tables 7-12, 7-14 and 7-15). Consistent with the previous analysis, the empirical evidence suggests that at-the-money implied volatility has stronger predictive power than the GARCH-estimated conditional volatility. In fact, the unbiasedness and efficiency hypotheses are rejected for the *GV* forecast at the 1% level of significance in all of the forecasting tests.

Table 7-12: Regression Tests Using At-the-money Implied Volatility with CF and GARCH (1,1) Estimates

Currency		γ_0	β_1	β_2	β_3	*Adj-R^2*	*WT-1*	*WT-2*	*WT-3*
GBP/USD									
	ct.	-0.752	0.905 ***	-0.031	0.462 **	0.298	2.083	3.176 **	24.991 ***
	s.e.	(0.507)	(0.105)	(0.096)	(0.221)				
EUR/USD									
	ct.	-1.826 ***	1.368 ***	-0.168 **	0.368	0.391	13.911 ***	10.788 ***	43.854 ***
	s.e.	(0.175)	(0.218)	(0.233)	(0.201)				
AUD/USD									
	ct.	-0.946 **	0.942 ***	-0.089 ***	0.443 **	0.517	2.071	1.827	69.280 ***
	s.e.	(0.407)	(0.089)	(0.167)	(0.207)				
USD/JPY									
	ct.	1.557 **	0.523 ***	-0.117 **	-0.222	0.079	6.501 ***	4.270 ***	16.091 ***
	s.e.	(0.788)	(0.134)	(0.059)	(0.288)				

Note: This table provides the encompassing regression tests performed using autocorrelation and heteroscedasticity consistent covariance matrix of Newey-West (1987). The corrected standard errors are reported in the parentheses. The regression model is specified as: $\ln RV_{t,T} = \gamma_0 + \beta_1 \ln IV_{t,T} + \beta_2 \ln IV_{t,T} \ln CF_t + \beta_3 \ln GV_{t,T} + \varepsilon_t$

$RV_{t,T}$ is the estimated realised volatility over the period t to T. The independent variable $IV_{t,T}$ is the quoted at-the-money implied volatility series and GV_t denotes the estimated future volatility of the underlying exchange rate using a rolling GARCH (1,1) model. "CF_t" represents the slope of the call volatility curve estimated using piecewise method. The Wald test statistics (WT-1, WT-2, WT-3) reported in columns six to eight test the biasness of the forecasting model with the null of 1.) $\gamma_0 = 0$, $(\beta_1 + \beta_2) = 1$ and $\beta_3 = 0$; 2.) $\gamma_0 = 0$, $\beta_1 = 1$ and $\beta_3 = 0$; 3.) $\gamma_0 = 0$, $\beta_1 = 0$ and $\beta_3 = 1$ respectively. Column five reports the adjusted R-squares for the regression models.

**** Significant at the 1% level*

*** Significant at the 5% level*

** Significant at the 10% level*

Table 7-13: Regression Tests Using At-the-money Implied Volatility with PF and GARCH (1,1) Estimates

Currency		γ_0	β_1	β_2	β_3	*Adj-R^2*	*WT-1*	*WT-2*	*WT-3*
GBP/USD									
	ct.	-0.809	0.831 ***	-0.202 **	0.594 ***	0.312	3.291 **	4.238 ***	21.679 ***
	s.e.	(0.396)	(0.116)	(0.089)	(0.201)				
EUR/USD									
	ct.	-1.289 ***	1.300 ***	0.459 ***	0.091	0.452	12.387 ***	42.988 ***	82.296 ***
	s.e.	(0.400)	(0.154)	(0.089)	(0.198)				
AUD/USD									
	ct.	-0.824 **	0.884 ***	0.171	0.401 *	0.520	2.126 *	2.244 *	60.848 ***
	s.e.	(0.442)	(0.120)	(0.197)	(0.219)				
USD/JPY									
	ct.	1.191	0.466 ***	0.067	-0.0425	0.067	4.549 ***	4.337 ***	15.658 ***
	s.e.	(0.749)	(0.149)	(0.074)	(0.278)				

Note: This table provides the encompassing regression tests performed using autocorrelation and heteroscedasticity consistent covariance matrix of Newey-West (1987). The corrected standard errors are reported in the parentheses. The regression model is specified as: $\ln RV_{t,T} = \gamma_0 + \beta_1 \ln IV_{t,T} + \beta_2 \ln IV_{t,T} \ln PF_t + \beta_3 \ln GV_{t,T} + \varepsilon_t$

$RV_{t,T}$ is the estimated realised volatility over the period t to T. The independent variable $IV_{t,T}$ is the quoted at-the-money implied volatility series and GV_t denotes the estimated future volatility of the underlying exchange rate using a rolling GARCH (1,1) model. "PF_t" represents the slope of the put volatility curve estimated using piecewise method. The Wald test statistics (WT-1, WT-2, WT-3) reported in columns six to eight test the biasness of the forecasting model with the null of 1.) $\gamma_0 = 0$, $(\beta_1 + \beta_2) = 1$ and $\beta_3 = 0$; 2.) $\gamma_0 = 0$, $\beta_1 = 1$ and $\beta_3 = 0$; 3.) $\gamma_0 = 0$, $\beta_1 = 0$ and $\beta_3 = 1$ respectively. Column five reports the adjusted R-squares for the regression models.

*** Significant at the 1% level*

** Significant at the 5% level*

* Significant at the 10% level*

Table 7-14: Regression Tests Using At-the-money Implied Volatility with AS and GARCH (1,1) Estimates

Currency		γ_0	β_1	β_2	β_3	*Adj-R^2*	*WT-1*	*WT-2*	*WT-3*
GBP/USD									
	ct.	-0.227	0.901 ***	-0.521 *	0.293	0.309	2.725 *	3.315 **	25.168 ***
	s.e.	(0.518)	(0.110)	(0.308)	(0.204)				
EUR/USD									
	ct.	-1.659 ***	1.196 ***	0.145	0.404 *	0.379	7.361 ***	10.036 ***	36.764 ***
	s.e.	(0.385)	(0.165)	(0.274)	(0.218)				
AUD/USD									
	ct.	-1.059 **	0.941 ***	-0.202	0.508 **	0.571	2.014	02.028	46.884 ***
	s.e.	(0.435)	(0.121)	(0.454)	(0.236)				
USD/JPY									
	ct.	1.213 *	0.468 ***	0.062	-0.043	0.066	5.003 ***	3.642 **	15.915 ***
	s.e.	(0.721)	(0.181)	(0.135)	(0.284)				

Note: This table provides the encompassing regression tests performed using autocorrelation and heteroscedasticity consistent covariance matrix of Newey-West (1987). The corrected standard errors are reported in the parentheses. The regression model is specified as: $\ln RV_{t,T} = \gamma_0 + \beta_1 \ln IV_{t,T} + \beta_2 \ln IV_{t,T} \ln AS_t + \beta_3 \ln GV_{t,T} + \varepsilon_t$

$RV_{t,T}$ is the estimated realised volatility over the period t to T. The independent variable $IV_{t,T}$ is the quoted at-the-money implied volatility series and GV_t denotes the estimated future volatility of the underlying exchange rate using a rolling GARCH (1,1) model. "AS_t" represents the average slope of the volatility smile estimated using quadratic approximation. The Wald test statistics (WT-1, WT-2, WT-3) reported in columns six to eight test the biasness of the forecasting model with the null of 1.) $\gamma_0 = 0$, $(\beta_1 + \beta_2) = 1$ and $\beta_3 = 0$; 2.) $\gamma_0 = 0$, $\beta_1 = 1$ and $\beta_3 = 0$; 3.) $\gamma_0 = 0$, $\beta_1 = 0$ and $\beta_3 = 1$ respectively. Column five reports the adjusted R-squares for the regression models.

**** Significant at the 1% level*

*** Significant at the 5% level*

** Significant at the 10% level*

Table 7-15: Regression Tests Using At-the-money Implied Volatility with CE and GARCH (1,1) Estimates

Currency		γ_0	β_1	β_2	β_3	*Adj-R^2*	*WT-1*	*WT-2*	*WT-3*
GBP/USD									
	ct.	0.111	0.683 ***	-0.010 **	0.351 *	0.313	3.735 **	3.673 **	20.533 ***
	s.e.	(0.563)	(0.168)	(0.004)	(0.181)				
EUR/USD									
	ct.	-1.845	1.347 ***	0.018 ***	0.222	0.411	13.193 ***	12.396 ***	27.387 ***
	s.e.	(0.378)	(0.164)	(0.005)	(0.193)				
AUD/USD									
	ct.	-1.010	0.893 ***	-0.011	0.518	0.516	1.978	1.991	27.939 ***
	s.e.	(0.459)	(0.128)	(0.063)	(0.231)				
USD/JPY									
	ct.	2.327 **	0.455 **	-0.085 *	-0.320	0.089	7.111 ***	3.728 **	13.632 ***
	s.e.	(1.083)	(0.197)	(0.047)	(0.317)				

Note: This table provides the encompassing regression tests performed using autocorrelation and heteroscedasticity consistent covariance matrix of Newey-West (1987). The corrected standard errors are reported in the parentheses. The regression model is specified as: $\ln RV_{t,T} = \gamma_0 + \beta_1 \ln IV_{t,T} + \beta_2 \ln IV_{t,T} \ln CE_t + \beta_3 \ln GV_{t,T} + \varepsilon_t$

$RV_{t,T}$ is the estimated realised volatility over the period t to T. The independent variable $IV_{t,T}$ is the quoted at-the-money implied volatility series and GV_t denotes the estimated future volatility of the underlying exchange rate using a rolling GARCH (1,1) model. "CE_t" represents the slope of the curvature of the volatility smile estimated using quadratic approximation. The Wald test statistics (WT-1, WT-2, WT3) reported in columns six to eight test the biasness of the forecasting model with the null of 1.) $\gamma_0 = 0$, $(\beta_1 + \beta_2) = 1$ and $\beta_3 = 0$; 2.) $\gamma_0 = 0$, $\beta_1 = 1$ and $\beta_3 = 0$; 3.) $\gamma_0 = 0$, $\beta_1 = 0$ and $\beta_3 = 1$ respectively. Column five reports the adjusted R-squares for the regression models.

**** Significant at the 1% level*

*** Significant at the 5% level*

** Significant at the 10% level*

Similar to the results reported previously in Tables 7-7 to 7-10, there is still evidence to suggest that rejection of the unbiasedness and efficiency hypotheses is related to the interaction term defined in Equation (7-4). This empirical evidence is particularly strong in Table 7-15 where the forecast regression is performed by incorporating smile curvature as the chosen measure of volatility smile shape. It appears that smile curvature is the most robust and statistically important in virtually all the regression tests reported in this chapter.

7.11 Conclusion

In this chapter, an empirical analysis is undertaken to examine the usefulness of information embedded in the shape of the volatility smile for the purpose of foreign exchange volatility prediction. In addition, the study examines how the shape of the volatility smile affects the forecasting ability of implied volatility forecasts. The regression tests are performed using traded implied volatility data which is directly observable in the over-the-counter market place. There are three main findings reported in this chapter.

First, the shape of the volatility smile, proxied by the slope and curvature coefficient, is significantly correlated with the level of at-the-money implied volatility. In particular, the coefficient for the smile curvature appears to be both significant and negatively related to the level of implied volatility. This confirms the findings of Pena *et al* (1999). In univariate analysis, it is also shown that these proxies are significant explanatory variables for future realised volatility.

Second, the validity of the unbiasedness and efficiency hypotheses for implied volatility forecasts is attributable to the shape of the smile. The more pronounced is the smile, the more likely is the rejection for the null hypothesis. In other words, when the smile effect is more pronounced, the forecast performance of at-the-money volatility is expected to deteriorate. These empirical findings are reported consistently across both the bivariate and multiple regression analyses when the curvature of the smile is incorporated into the forecasting model.

Third, the overall results are consistent with recent empirical findings that suggest implied volatility data from the over-the-counter currency option provide good forecasts for realised volatility. The results also confirm the empirical findings of Christensen and Prabhala (1998), Christensen and Hansen (2002), Covrig and Low (2003) but contradicts earlier findings of Day and Lewis (1992) and Canina and Figlewski (1993). In short, implied volatility does predict realised volatility both in the univariate specification as well as in more complex models that include conditional volatility estimates.

CHAPTER 8 – CONCLUSIONS AND FUTURE RESEARCH

8.1 Introduction

As stated in Chapter 1 and in Chapter 3, a better understanding of implied volatility behaviour has important implications to the pricing of option contracts, hedging and risk estimation. Option implied volatility cannot be directly observed and often obtaining an accurate estimate has proven to be a difficult task. This dissertation provides four analyses of the empirical characteristics of currency option implied volatility. To this end, the behaviour of implied volatility is examined using data for four major currency pairs. The analyses presented in this dissertation are performed using trader-quoted implied volatility prices obtained from the over-the-counter market.

Chapter 2 provides an overview of the over-the-counter currency option market. It gives an introduction to the size of the currency option market, the trading conventions used in the industry, volatility trading strategies, details of two sources of implied volatility data available from this market, and finally, a comparison of contract features for exchange-traded and over-the-counter currency option contracts is also considered. Chapter 3 offers a broad survey of the key literature concerning two aspects of implied volatility - first, estimating and modelling the behaviour of implied volatility, and second, the volatility smile effect and explanations for this anomaly. In this chapter, issues concerning the estimation of implied volatility are also discussed, highlighting the potential problems associated with the calculation of implied volatility estimates and

arguing that the use of quoted implied volatility data can potentially alleviate measurement errors arising from the use of these procedures. Option pricing models that assume random volatility parameters appear to provide better pricing performance than the traditional Garman-Kohlhagen (1983) model but fail to provide a good fit to market data. Thus modelling implied volatility as a random walk process may not be entirely consistent with empirical data.

8.2 Contributions of the Dissertation

Empirical analyses are presented in Chapter 4 through Chapter 7. Chapter 4 investigates the behaviour of quoted implied volatility of various maturities. This chapter extends the literature on implied volatility in several ways. First, by testing the random walk hypothesis across implied volatility of different maturities, the implied volatility characteristics across the term structure can be better understood. The results using in-sample tests provide evidence of random walk violations in the volatility series. This evidence is reported across all currency pairs, notably with strong rejections of random walk hypothesis for the short-dated volatility of one week and one month. Contrary to the Garman-Kohlhagen (1983) and Hull-White (1987) models, the results reported in this chapter suggest that option-implied volatility is not constant over time and is not well described as a random walk process. Second, the study also suggests that option pricing and volatility models that assume a random walk component across the volatility term structure are not consistent with empirical findings. Third, the in-sample test result is further supported in the out-of-sample tests involving forecasting implied volatility changes from a random walk model, artificial neural networks and ARIMA frameworks. These findings suggest that short-dated implied volatility is better

characterised as a mean-reverting process while the random walk process captures variation in long-dated implied volatility. The results are broadly consistent with the recent literature in option pricing methodology.

Chapter 5 extends the key findings of Chapter 4 by testing the profitability of volatility trading using simple technical trading strategies. It is shown in Chapter 4 that the random walk hypothesis is violated and therefore trading rules could be profitable. The trading rules used in this chapter assume that when prevailing quoted volatility departs considerably from its moving average, a buy or sell trade will emerge. Two main contributions stem from Chapter 5. First, the focus on option combination trades, including straddles and risk reversals, provides an important extension to standard trading rule analysis. Second, consistent with previous studies, the results presented in this chapter indicate that volatility trading using moving average trading rules is capable of generating profitable trades even after adjusting for transaction costs. In particular, the buy straddle trades generate positive holding-period returns for three of the four currency pairs tested. However, risk reversal trades produced less compelling outcomes across all currency pairs.

In Chapter 6, the moneyness of implied volatility is examined using quoted implied volatility data. This chapter draws attention to the dynamic behaviour of volatility as little empirical research exists with respect to how the volatility smile evolves over time. It examines the relationship between different proxies for the shape of volatility smile and the anticipated volatility for the GBP/USD, the EUR/USD, the AUD/USD and the USD/JPY exchange rates. This chapter provides two important findings with regard to the dynamics of volatility smile. First, variation in the volatility

smile is related to increasing risk of the underlying currency. This result is particularly strong when the curvature of the smile and the slope of the put volatility curve are included in both the Granger-causality analysis and trivariate vector autoregression based analysis. Second, the results reveal significant feedback between the curvature of the volatility smile and the anticipated volatility of the underlying currencies. Robustness test using probit model provides similar findings with respect to jumps in the underlying foreign exchange rate series.

Chapter 7 explores the implication of these findings by incorporating the proxies for the shape of the volatility smile in predicting future realised volatility. This extends the current literature on volatility forecasting by introducing an interaction term between the shape of the volatility smile and the at-the-money implied volatility. Three key contributions are made to the existing literature. First, it is shown that proxies for the shape of the volatility smile are significantly correlated with at-the-money implied volatility. Curvature coefficients are found to be both significant and negatively related to the level of at-the-money implied volatility. Second, acceptance of the unbiasedness and efficiency hypothesis for at-the-money implied volatility is a function of the shape of the smile. The more pronounced is the smile, the more likely is the rejection of the null hypothesis. Third, in terms of volatility forecasting, preference for the use of quoted implied volatility data is supported.

8.3 Further Extensions to the Dissertation

The extensions of this dissertation can be categorised, but not limited to, three main areas: the predictability of implied volatility, forecasting ability of out-of-money

options and finally, the dynamics of volatility smile across maturities. The findings reported in Chapters 4 and 5 provide evidence of the predictability of at-the-money implied volatility. Stemming from this result, the predictability of out-of-money call and put options may also be explored using similar in and out-of-the sample methods. The analysis can be further improved using larger sample sizes and more currency pairs. Predictability of implied volatility across different level of moneyness will provide important insight into the evolution and predictability of the volatility smile.

Based on the results presented in Chapter 6, a second extension involves the use of out-of-the money implied volatility data for the prediction of realised volatility. This approach is in contrast with the use of at-the-money implied volatility which is often considered in empirical studies. However, it is pointed out in Chapter 2 that currency options are heavily traded in the over-the-counter market, even for out-of-the-money options. The rationale for this extension is consistent with the findings of Chapter 6 that suggest out-of-the money options can be used to predict future market sentiment, especially when large adverse movement in the underlying exchange rate is imminent.

The analyses presented in Chapter 6 and in Chapter 7 are based on implied volatility data of one-month maturity. A natural extension to these analyses is to employ data of various maturities to see if the test results are robust across the term structure. Differences in test results may be attributed to differences in liquidity since market liquidity generally decreases as maturity increases since long term contracts are usually less actively traded in the derivative markets. Future research could also employ different indicators of uncertainty such as inflation rates, unemployment and credit

spreads as a means of understanding how the dynamics of the smile are related to alternative measures of uncertainty. Any seasonal behaviour of volatility smile could also be examined by introducing a dummy variable that captures seasonal effects, such as day-of-the week. Finally the same analysis may also be extended to other over-the-counter derivative instruments which have yet to be explored, for example, options on interest rate swaps.

8.4 Conclusion

This dissertation provides four empirical analyses relating to the behaviour of implied volatility. The time series behaviour of implied volatility appears to be inconsistent with the random walk hypothesis both in the analysis of in-sample and out-of-sample data. This is particularly the case for short-dated volatility. A volatility trading strategy based on simple average trading rules suggests evidence of profitable trades even after adjusting for transaction costs. This is contrary to the notion that volatility of the underlying asset can be characterised as a random walk process.

This study confirms the notion that the volatility smile anomaly is not solely attributable to the erroneous assumptions underlying in the Garman-Kohlhagen (1983) option pricing model. The analysis suggests that the shape of the volatility smile can affect the forecasting ability of at-the-money implied volatility. Furthermore, the shape of the volatility smile also appears to have predictive power over future volatility in excess of that provided by implied volatility.

APPENDIX A – CONDITIONAL AND IMPLIED VOLATILITY

Figure A1: Implied Volatility and Conditional Volatility

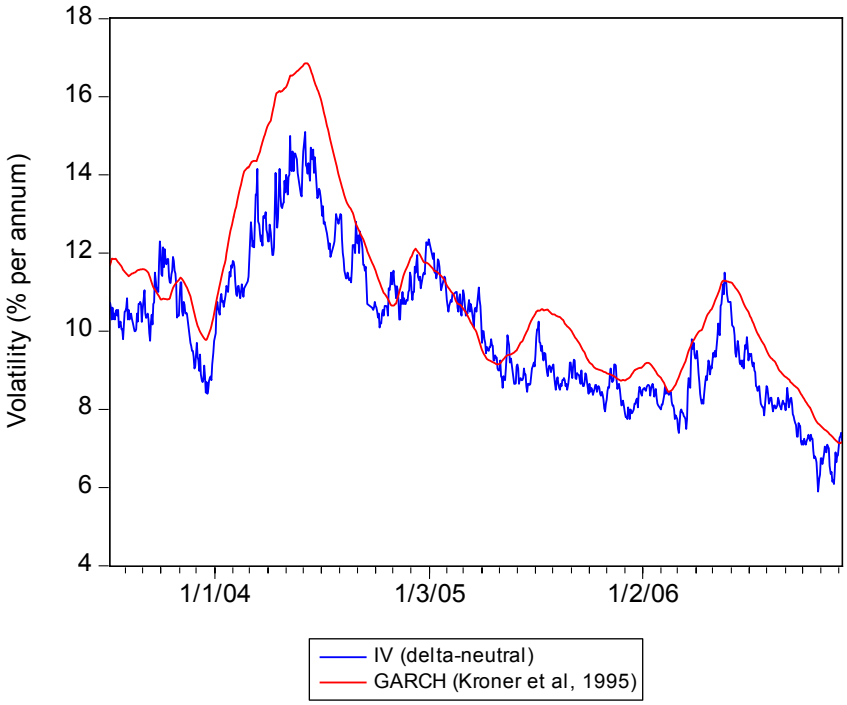

APPENDIX B – ADDITIONAL PROBIT MODEL ANALYSIS

Table B1: Probit Regressions for Put Options

(The Lee and Mykland (2007) Jump Estimated with $K=5$)

$$Pb(Jump_{t+T}=1) = F(\beta_0 + \beta_1 \Delta PF_t + \beta_2 \Delta CE_t + \beta_3 \Delta P5D_t + \beta_4 \Delta P10D_t + \beta_5 \Delta P15D_t) + \varepsilon_t$$

	Put Options							
	GBP/USD		EUR/USD		AUD/USD		USD/JPY	
	Coefficient	z-statistics	Coefficient	z-statistics	Coefficient	z-statistics	Coefficient	z-statistics
ΔPF	2.099 **	(1.766)	-0.449	(-1.474)	-16.981 **	(-2.008)	-37.241 *	(-1.841)
ΔCE	-4.738 ***	(-2.927)	-2.617 **	(-2.169)	-9.184 ***	(-2.631)	-0.528 **	(-2.022)
ΔP5D	16.013 ***	(1.791)	0.421 **	(2.244)	85.183	(1.623)	1.624 **	(2.119)
ΔP10D	-13.251	(-1.524)	0.152 *	(1.755)	-106.274	(-1.629)	-4.586 **	(-2.457)
ΔP15D	-0.109	(-0.205)	0.194	(0.942)	48.938 **	(2.041)	3.301 ***	(2.652)
LR	21.476 ***		9.856 *		15.08 **		25.602 ***	

Note: "ΔPF" denotes the natural logarithm of the absolute change in the slope coefficients for the put function measured as $\log(|PF_t/PF_{t-1}|)$, "ΔCE" is the natural logarithm of the absolute change in the curvature coefficients of the daily volatility smile estimated as $\log(|CE_t/CE_{t-1}|)$, "ΔP5D" is the natural logarithm of the absolute change in the slope coefficients for the 5-delta put estimated as $\log(|P5D_t/P5D_{t-1}|)$; the same method is used for the 10-delta and 15-delta puts. The dependent variable is the Jump parameter estimated using the Lee and Mykland (2007) method; this study employs a threshold of ±4.6001 to detect for the presence of jumps on any given day t to t+T; when the threshold is breached, a value of one is assigned or zero otherwise. Positive and negative jumps were not identified separately due to sample size limitation. "LR" is likelihood ratio statistics for the joint test of $\beta_0=\beta_1=\beta_2\ldots=\beta_5=0$. The reported z-statistics are based on standard errors and covariance from the Huber/White method. For brevity, the constant term is omitted from the table.

**** Significant at the 1% level*

*** Significant at the 5% level*

** Significant at the 10% level*

Table B 2: Probit Regressions for Call Options

(The Lee and Mykland (2007) Jump Estimated with $K=5$)

$$Pb(Jump_{t+T}=1) = F(\beta_0 + \beta_1 \Delta CF_t + \beta_2 \Delta CE_t + \beta_3 \Delta C5D_t + \beta_4 \Delta C10D_t + \beta_5 \Delta C15D_t) + \varepsilon_t$$

	Call Options							
	GBP/USD		EUR/USD		AUD/USD		USD/JPY	
	Coefficient	*z* -statistics	Coefficient	*z* -statistics	Coefficient	*z* -statistics	Coefficient	*z* -statistics
ΔCF	0.066	(0.302)	2.162	(1.469)	-0.081	(-0.759)	-45.589 **	(-2.222)
ΔCE	-1.734	(-1.547)	-3.95	(-1.236)	-2.677 *	(-1.809)	-0.628 ***	(-2.724)
ΔC5D	5.075 **	(2.292)	24.05	(0.905)	-0.138	(-0.523)	1.078	(1.426)
ΔC10D	-7.323 **	(-2.153)	-27.473	(-1.082)	0.019	(0.144)	-1.793	(-0.938)
ΔC15D	1.219 *	(1.670)	3.606	(1.213)	0.015	(0.292)	1.044	(0.779)
LR	9.483 *		10.924 *		9.167		30.669 ***	

Note: "ΔCF" denotes the natural logarithm of the absolute change in the slope coefficients for the call function measured as $\log(|CF_t/CF_{t-1}|)$, "ΔCE" is the natural logarithm of the absolute change in the curvature coefficients of the daily volatility smile estimated as $\log(|CE_t/CE_{t-1}|)$, "ΔC5D" is the natural logarithm of the absolute change in the slope coefficients for the 5-delta call estimated as $\log(|C5D_t/C5D_{t-1}|)$; the same method is used for the 10-delta and 15-delta call. The dependent variable is the Jump parameter estimated using the Lee and Mykland (2007) method; this study employs a threshold of ±4.6001 to detect for the presence of jumps on day t to t+T; when the threshold is breached, a value of one is assigned or zero otherwise. Positive and negative jumps were not identified separately due to sample size limitation. "LR" is likelihood ratio statistics for the joint test of $\beta_0=\beta_1=\beta_2\ldots=\beta_5=0$. The reported z-statistics are based on standard errors and covariance from the Huber/White method. For brevity, the constant term is omitted from the table.

**** Significant at the 1% level*

*** Significant at the 5% level*

** Significant at the 10% level*

BIBLIOGRAPHY

Abraham, A., Seyyed, F. J., & Alsakran, S. A. (2002). Testing the Random Walk Behavior and Efficiency of the Gulf Stock Markets. *The Financial Review, 37*(3), 469-480.

Alam, M. I., Hasan, T., & Kadapakkam, P. R. (1999). An Application of Variance Ratio Test to Five Asian Stock Markets. *Review of Pacific Basin Financial Markets and Policies, 2*(3), 301-315.

Altman, E. I., Marco, G., & Varetto, F. (1994). Corporate Distress Diagnosis - Comparisons Using Linear Discriminant-Analysis and Neural Networks (The Italian Experience). *Journal of Banking & Finance, 18*(3), 505-529.

Angel, J. J., Christophe, S. E., & Ferri, M. G. (2003). A Close Look at Short Selling on Nasdaq. *Financial Analysts Journal, 59*(6), 66-74.

Baillie, R. T., & Bollerslev, T. (1989). The Message in Daily Exchange Rates: A Conditional-Variance Tale. *Journal of Business & Economic Statistics, 7*(3), 297-305.

Bali, T. G., & Demirtas, K. O. (2008). Testing Mean Reversion in Financial Market Volatility: Evidence from S&P 500 Index Futures. *Journal of Futures Markets, 28*(1), 1-33.

Balvers, R., Wu, Y., & Gilliland, E. (2000). Mean Reversion Across National Stock Markets and Parametric Contrarian Investment Strategies. *The Journal of Finance, 55*(2), 745-772.

Bank for International Settlements Quarterly Review. (December 2004). Basel, Switzerland: Bank for International Settlements.

Bank for International Settlements Quarterly Review. (September 2007). Basel, Switzerland: Bank for International Settlements.

Bank for International Settlements Quarterly Review. (March 2009). Basel, Switzerland: Bank for International Settlements.

Bank for International Settlements Quarterly Review. (June 2009). Basel, Switzerland: Bank for International Settlements.

Bank for International Settlements Triennial Central Bank Survey. (December 2007). Basel, Switzerland: Bank for International Settlements.

Barberis, N., Shleifer, A., & Vishny, R. (1998). A Model of Investor Sentiment. *Journal of Financial Economics, 49*(3), 307-343.

Bates, D. S. (1991). The Crash of '87: Was It Expected? The Evidence from Options Markets. *The Journal of Finance, 46*(3), 1009-1044.

Bates, D. S. (1996a). Jumps and Stochastic Volatility: Exchange Rate Processes Implicit in Deutsche Mark Options. *Review of Financial Studies, 9*(1), 69-107.

Bates, D. S. (1996b). Dollar Jump Fears, 1984-1992: Distributional Abnormalities Implicit in Currency Futures Options. *Journal of International Money and Finance, 15*(1), 65-93.

Beckers, S. (1981). Standard Deviations Implied in Option Prices As Predictors of Future Stock Price Variability. *Journal of Banking & Finance, 5*(3), 363-381.

Beine, M., Benassy-Quere, A., & Lecourt, C. (2002). Central Bank Intervention and Foreign Exchange Rates: New Evidence from FIGARCH Estimations. *Journal of International Money and Finance, 21*(1), 115-144.

Belaire-Franch, J., & Opong, J. K. (2005). A Variance Ratio Test of Behaviour of Some FTSE Equity Indices Using Ranks and Signs. *Review of Quantitative Finance and Accounting, 24*(1), 93-107.

Black, F. (1976). The Pricing of Commodity Contracts. *Journal of Financial Econometrics, 3*(1-2), 167-179.

Black, F. (1989a). How We Came Up With The Option Formula. *The Journal of Portfolio Management, 15*(2), 4-8.

Black, F. (1989b). How to Use the Holes in Black-Scholes. *Journal of Applied Corporate Finance, 1*(4), 67-73.

Black, F., & Scholes, M. (1972). The Valuation of Option Contracts and a Test of Market Efficiency. *Journal of Finance, 27*(2), 399-417.

Black, F., & Scholes, M. (1973). The Pricing of Options and Corporate Liabilities. *The Journal of Political Economy, 81*(3), 637-654.

Blume, L., Easley, D., & O'Hara, M. (1994). Market Statistics and Technical Analysis - The Role of Volume. *Journal of Finance, 49*(1), 153-181.

Bollen, N. P. B., & Rasiel, E. (2003). The Performance of Alternative Valuation Models in the OTC Currency Options Market. *Journal of International Money and Finance, 22*(1), 33-64.

Bollen, N. P. B., & Whaley, R. E. (2004). Does Net Buying Pressure Affect the Shape of Implied Volatility Functions? *The Journal of Finance, 59*(2), 711-753.

Bollerslev, T. (1986). Generalized Autoregressive Conditional Heteroskedasticity. *Journal of Econometrics, 31*(3), 307-327.

Bollerslev, T. (2001). Financial Econometrics: Past Developments and Future Challenges. *Journal of Econometrics, 100*(1), 41-51.

Bollerslev, T., Engle, R. F., & Nelson, D.B. (1994). ARCH Models. In R. F. Engle & D. McFadden (Eds.), *Handbook of Econometrics* (Vol. 4, pp. 2959-3038). Amsterdam: Elsevier B.V.

Bollerslev, T., & Mikkelsen, H. O. A. (1996). Modelling and Pricing Long-memory in Stock Market Volatility. *Journal of Econometrics, 73*(1), 151-184.

Bond Markets Report. (July 2009). London: International Financial Services.

Bonser-Neal, C., & Tanner, G. (1996). Central Bank Intervention and the Volatility of Foreign Exchange Rates: Evidence from the Options Market. *Journal of International Money and Finance, 15*(6), 853-878.

Bookstaber, R. M. (1981). Observed Option Mispricing and the Nonsimultaneity of Stock and Option Quotations. *The Journal of Business, 54*(1), 141-155.

Box, G. E. P., & Pierce, D. A. (1970). Distribution of Residual Autocorrelations in Autoregressive-Integrated Moving Average Time Series Models. *Journal of the American Statistical Association, 65*(332), 1509-1526.

Brenner, M., Eldor, R., & Hauser, S. (2001). The Price of Options Illiquidity. *The Journal of Finance, 56*(2), 789-805.

Brenner, M., & Subrahmanyam, M. G. (1988). A Simple Formula to Compute the Implied Standard Deviation. *Financial Analysts Journal, 44*(5), 80-83.

Brock, W., Lakonishok, J., & LeBaron, B. (1992). Simple Technical Trading Rules and the Stochastic Properties of Stock Returns. *The Journal of Finance, 47*(5), 1731-1764.

Brooks, C. (2002). *Introductory Econometrics for Finance* (1 ed.). Cambridge: Cambridge University Press.

Byoun, S., Kwok, C. C. Y., & Park, H. Y. (2003). Expectations Hypothesis of the Term Structure of Implied Volatility: Evidence from Foreign Currency and Stock Index Options. *Journal of Financial Econometrics, 1*(1), 126-151.

Campa, J. M., & Chang, P. H. K. (1995). Testing the Expectations Hypothesis on the Term Structure of Volatility in Foreign Exchange Options. *Journal of Finance, 50*(2), 529-547.

Campa, J. M., Chang, P. H. K., & Reider, R. L. (1998). Implied Exchange Rate Distributions: Evidence from OTC Option Markets. *Journal of International Money and Finance, 17*(1), 117-160.

Campbell, J. Y., A. W. Lo, & A. C. MacKinlay. (1997). *The Econometrics of Financial Market*. Princeton, New Jersey: Princeton University Press.

Canina, L., & Figlewski, S. (1993). The Informational Content of Implied Volatility. *The Review of Financial Studies, 6*(3), 659-681.

Carr, P., & Wu, L. (2007). Stochastic Skew in Currency Options. *Journal of Financial Economics, 86*(1), 213-247.

Chan, K., Hameed, A., & Tong, W. (2000). Profitability of Momentum Strategies in the International Equity Markets. *The Journal of Financial and Quantitative Analysis, 35*(2), 153-172.

Chang, P. H. K., & Osler, C. L. (1999). Methodical Madness: Technical Analysis and the Irrationality of Exchange- Rate Forecasts. *The Economic Journal, 109*(458), 636-661.

Chang, Y. (2004). A Re-examination of Variance-Ratio Test of Random Walks in Foreign Exchange Rates. *Applied Financial Economics, 14*(9), 671-679.

Chaput, J. S., & Ederington, L., H. . (2005). Volatility Trade Design. *Journal of Futures Markets, 25*(3), 243-279.

Chesney, M., & Scott, L. (1989). Pricing European Currency Options: A Comparison of the Modified Black-Scholes Model and a Random Variance Model. *Journal of Financial and Quantitative Analysis, 24*(03), 267-284.

Chiras, D. P., & Manaster, S. (1978). The Information Content of Option Prices and a Test of Market Efficiency. *Journal of Financial Economics, 6*(2/3), 213-234.

Chowdhury, I., & Sarno, L. (2004). Time-Varying Volatility in the Foreign Exchange Market: New Evidence on Its Persistence and on Currency Spillovers *Journal of Business Finance and Accounting, 31*(5-6), 759-793.

Christensen, B. J., & Hansen, C. S. (2002). New Evidence on the Implied-Realized Volatility Relation. *The European Journal of Finance, 8*(2), 187 - 205.

Christensen, B. J., & Prabhala, N. R. (1998). The Relation Between Implied and Realized Volatility. *Journal of Financial Economics, 50*(2), 125-150.

Christoffersen, P., & Mazzotta, S. (2005). The Accuracy of Density Forecasts from Foreign Exchange Options. *Journal of Financial Econometrics, 3*(4), 578-605.

Cincibuch, M. (2004). Distributions Implied by American Currency Futures Options: A Ghost's Smile? *Journal of Futures Markets, 24*(2), 147-178.

Clews, R., Panigirtzoglou, N., & Proudman, J. (2000) Recent Developments in Extracting Information from Options Markets. *Bank of England Quarterly Bulletin, 40*(1), 50-60.

Conrad, J., & Kaul, G. (1998). An Anatomy of Trading Strategies. *The Review of Financial Studies, 11*(3), 489-519.

Cooper, N., & Talbot, J. (1999) The Yen/Dollar Exchange Rate in 1998: Views from Options Markets. *Bank of England Quarterly Bulletin, 39*(1), 68-76.

Corrado, C., J., & Miller Jr, T., W. (1996). Efficient Option-implied Volatility Estimators. *Journal of Futures Markets, 16*(3), 247-272.

Corrado, C., J., & Miller, Jr, T., W. (2005). The Forecast Quality of CBOE Implied Volatility Indexes. *Journal of Futures Markets, 25*(4), 339-373.

Covrig, V., & Low, B. S. (2003). The Quality of Volatility Traded on the Over-the-counter Currency Market: A multiple horizons study. *Journal of Futures Markets, 23*(3), 261-285.

Darrat, A., F. , & Zhong, M. (2000). On Testing the Random-Walk Hypothesis: A Model-Comparison Approach. *Financial Review, 35*(3), 105-124.

Das, S. R., & Sundaram, R. K. (1999). Of Smiles and Smirks: A Term Structure Perspective. *Journal of Financial and Quantitative Analysis, 34*(2), 211-239.

Day, T. E., & Lewis, C. M. (1992). Stock Market Volatility and the Information Content of Stock Index Options. *Journal of Econometrics, 52*(1-2), 267-287.

DeBondt, W. F. M. D., & Thaler, R. (1985). Does the Stock Market Overreact? *The Journal of Finance, 40*(3), 793-805.

DeRosa, D. F. (2000). *Options on Foreign Exchange* (second ed.). New York: John Wiley & Sons.

Deuskar, P., Gupta, A., & Subrahmanyam, M. G. (2008). The Economic Determinants of Interest Rate Option Smiles. *Journal of Banking & Finance, 32*(5), 714-728.

Dickey, D. A., & Fuller, W. A. (1979). Distribution of the Estimators for Autoregressive Time Series with a Unit Root. *Journal of the American Statistical Association, 74*(366), 427-431.

Dickey, D. A., & Fuller, W. A. (1981). Likelihood Ratio Statistics for Autoregressive Time Series with a Unit Root. *Econometrica, 49*(4), 1057-1072.

Diebold, F. X., & Mariano, R. S. (1995). Comparing Predictive Accuracy. *Journal of Economics and Business Statistics, 13*(3), 253-263.

Diebold, F. X., & Nerlove, M. (1989). The Dynamics of Exchange Rate Volatility: A Multivariate Latent Factor Arch Model. *Journal of Applied Econometrics, 4*(1), 1-21.

Doran, J., S. , Peterson, D., R. , & Tarrant, B., C (2007). Is There Information in the Volatility Skew? *Journal of Futures Markets, 27*(10), 921-959.

Duffie, D., Pan, J., & Singleton, K. (2000). Transform Analysis and Asset Pricing for Affine Jump-Diffusions. *Econometrica, 68*(6), 1343-1376.

Dumas, B., Fleming, J., & Whaley, R. E. (1998). Implied Volatility Functions: Empirical Tests. *The Journal of Finance, 53*(6), 2059-2106.

Dunis, C., & Keller, A. (1995). Efficiency Tests with Overlapping Data: An Application to the Currency Options Market. *The European Journal of Finance, 1*(4), 345 - 366.

Ederington, L., & Guan, W. (2002). Why Are Those Options Smiling? *Journal of Derivatives, 10*(2), 9-34.

Engle, R. F. (1982). Autoregressive Conditional Heteroscedasticity with Estimates of the Variance of United Kingdom Inflation. *Econometrica, 50*(4), 987-1007.

Engle, R. F., & Bollerslev, T. (1986). Modelling the Persistence of Conditional Variances. *Econometric Reviews, 5*(1), 1 - 50.

Engle, R. F., & Gonzalez-Rivera, G. (1991). Semiparametric Arch Models. *Journal of Business & Economic Statistics, 9*(4), 345-359.

Engle, R. F., & Patton, A. J. (2001).What is a Good Volatility Model? *Quantitative Finance, 1*(2), 237 - 245.

Equity Markets Report. (June 2009). London: International Financial Services.

Feinstein, S., P. (1989). *A Theoretical and Empirical Investigation of the Black-Scholes Implied Volatility, Dissertation.* Yale University, New Haven, CT.

Ferland, R., & Lalancette, S. (2006). Dynamics of Realized Volatility and Correlations: An Empirical Study. *Journal of Banking & Finance, 30*(7), 2109-2130.

Fleming, J., Ostdiek, B., & Whaley, R. E. (1995). Predicting Stock Market Volatility: A New Measure. *Journal of Futures Markets, 15*(3), 265-302.

Fouque, J. P., Pananicolaou, G., & Sircar, K. R. (2000). *Derivatives in Financial Markets with Stochastic Volatility*. Cambridge, United Kingdom: Cambridge University press.

Garman, M. B., & Kohlhagen, S. W. (1983). Foreign Currency Option Values. *Journal of International Money and Finance, 2*(3), 231-237.

Geske, R., & Roll, R. (1984). On Valuing American Call Options with the Black-Scholes European Formula. *The Journal of Finance, 39*(2), 443-455.

Gessner, V., & Poncet, P. (1997). Volatility Patterns: Theory and Some Evidence from the Dollar-Mark Option Market. *Journal of Derivatives, 5*(2), 46-61.

Greene, W. H. (2003). *Econometric Analysis* (fifth ed.). Upper Saddle River, New Jersey: Prentice Hall.

Harvey, A., Ruiz, E., & Shephard, N. (1994). Multivariate Stochastic Variance Models. *The Review of Economic Studies, 61*(2), 247-264.

Hentschel, L. (2003). Errors in Implied Volatility Estimation. *The Journal of Financial and Quantitative Analysis, 38*(4), 779-810.

Heston, S. L. (1993). A Closed-Form Solution for Options with Stochastic Volatility with Applications to Bond and Currency Options. *The Review of Financial Studies, 6*(2), 327-343.

Hicks, A. (2000). *Managing Currency Risk using Foreign Exchange Options*. Cambridge, England: Woodhead Publishing Ltd & the Association of Corporate Treasurers.

Hsu, P.-H., & Kuan, C.-M. (2005). Reexamining the Profitability of Technical Analysis with Data Snooping Checks. *Journal of Financial Econometrics, 3*(4), 606-628.

Hull, J., & White, A. (1987). The Pricing of Options on Assets with Stochastic Volatility. *The Journal of Finance, 42*(2), 281-300.

Hull, J. C. (2006). *Options, Futures, and other Derivatives* (sixth ed.). Upper Saddle River, New Jersey: Prentice Hall.

Jackwerth, J. C., & Rubinstein, M. (1996). Recovering Probability Distributions from Option Prices. *The Journal of Finance, 51*(5), 1611-1631.

James, F. E., Jr. (1968). Monthly Moving Averages-An Effective Investment Tool? *The Journal of Financial and Quantitative Analysis, 3*(3), 315-326.

Jegadeesh, N., & Titman, S. (1993). Returns to Buying Winners and Selling Losers: Implications for Stock Market Efficiency. *Journal of Finance, 48*(1), 65-91.

Jiang, G. J., & Tian, Y. S. (2005). The Model-Free Implied Volatility and Its Information Content. *The Review of Financial Studies, 18*(4), 1305-1342.

Jorion, P. (1995). Predicting Volatility in the Foreign-exchange Market. *Journal of Finance, 50*(2), 507-528.

Jorion, P. (2000). *Value at Risk: The New Benchmark for Managing Financial Risk* (second, International ed.). Singapore: McGraw-Hill.

Kim, M. J., Nelson, C. R., & Startz, R. (1991). Mean Reversion in Stock Prices? A Reappraisal of the Empirical Evidence. *Review of Economic Studies, 58*(3), 515-528.

Koch, P. D. (1993). Reexamining Intraday Simultaneity in Stock Index Futures Markets. *Journal of Banking & Finance, 17*(6), 1191-1205.

Kroner, K. F., Kneafsey, K. P., & Claessens, S. (1995). Forecasting Volatility in Commodity Markets. *Journal of Forecasting, 14*(2), 77-95.

Kyriacou, K., & Sarno, L. (1999).The Temporal Relationship Between Derivatives Trading and Spot Market Volatility in the U.K.: Empirical Analysis and Monte Carlo Evidence. *Journal of Futures Markets, 19*(3), 245-270.

Lai, M. M., Balachander, K., & Mat Nor, F. (2002). An Examination of the Random Walk Model and Technical Trading Rules in the Malaysian Stock Market. *Quarterly Journal of Business Economics, 41*, 81-104.

Lakonishok, J., Shleifer, A., & Vishny, R.W. (1994). Contrarian Investment, Extrapolation, and Risk. *The Journal of Finance, 49*(5), 1541-1578.

Latane, H. A., & Rendleman Jr, R. J. (1976). Standard Deviations of Stock Price Ratios Implied in Option Prices. *Journal of Finance, 31*(2), 369-381.

Lee, S. S., & Mykland, P. A. (2007). Jumps in Financial Markets: A New Nonparametric Test and Jump Dynamics. *Review of Financial Studies, 21*(6), 2535-2563

Lima, E. J. A., & Tabak, B. M. (2004).Test of the Random Walk Hypothesis for Equity Markets: Evidence for China, Hong Kong and Singapore. *Applied Economics Letters, 11*, 255-258.

Liu, C. Y., & He, J. (1991). A Variance-Ratio Test of Random Walks in Foreign Exchange Rates. *The Journal of Finance, 46*(2), 773-785.

Liu, J., Pan, J., & Wang, T. (2005). An Equilibrium Model of Rare-Event Premia and Its Implication for Option Smirks. *Review of Financial Studies, 18*(1), 131-164.

Lo, A. W., & MacKinlay, A. C. (1988). Stock Market Prices Do Not Follow Random Walks: Evidence From a Simple Specification Test. *Review of Financial Studies, 1*(1), 41-66.

Lo, A. W., & MacKinlay, A. C. (1989). The Size and Power of the Variance Ratio Test in Finite Samples - a Monte-Carlo Investigation. *Journal of Econometrics, 40*(2), 203-238.

Malz, A. M. (1996). Using Option Prices to Estimate Realignment Probabilities in the European Monetary System: The Case of Sterling-Mark. *Journal of International Money and Finance, 15*(5), 717-748.

Malz, A. M. (1997). Estimating the Probability Distribution of the Future Exchange Rate from Option Prices. *Journal of Derivatives, 5*(2), 18-36.

Manaster, S., & Koehler, G. (1982). The Calculation of Implied Variances from the Black-Scholes Model: A Note. *The Journal of Finance, 37*(1), 227-230.

Mayhew, S. (1995). Implied Volatility. *Financial Analysts Journal 51*(4), 8-20.

McCauley, R., & Melick, W. (1996). Risk Reversal Risk. *Risk, 9*(10), 54-57.

Melino, A., & Turnbull, S. M. (1995). Misspecification and the Pricing and Hedging of Long-term Foreign Currency Options. *Journal of International Money and Finance, 14*(3), 373-393.

Neely, C., Weller, P., & Dittmar, R. (1997). Is Technical Analysis in the Foreign Exchange Market Profitable? A Genetic Programming Approach. *Journal of Financial & Quantitative Analysis, 32*(4), 405-426.

Nelson, D. B. (1991). Conditional Heteroskedasticity in Asset Returns: A New Approach. *Econometrica, 59*(2), 347-370.

Newey,W. K., & West, K. D. (1987). A Simple, Positive Semi-Definite, Heteroskedasticity and Autocorrelation Consistent Covariance Matrix. *Econometrica, 55*(3), 703-708.

Newey,W. K., & West, K. D. (1994). Automatic Lag Selection in Covariance Matrix Estimation. *Review of Economic Studies, 61*(4), 631-653.

Nison, S. (1991). *Japanese Candlestick Charting Techniques: A Contemporary Guide to the Ancient Investment Techniques of the Far East*. New York: New York Institute of Finance.

Pan, M.S., Chan, K. C., & C.W. Fok, R. (1997). Do Currency Futures Prices Follow Random Walks? *Journal of Empirical Finance, 4*(1), 1-15.

Peiers, B. (1997). Informed Traders, Intervention, and Price Leadership: A Deeper View of the Microstructure of the Foreign Exchange Market. *The Journal of Finance, 52*(4), 1589-1614.

Pena, I., Rubio, G., & Serna, G. (1999). Why Do We Smile? On the Determinants of the Implied Volatility Function. *Journal of Banking & Finance, 23*(8), 1151-1179.

Phillips, P. C. B., & Perron, P. (1988). Testing for a Unit Root in Time Series Regression. *Biometrika, 75*(2), 335-346.

Pilbeam, K. (1995). The Profitability of Trading in the Foreign Exchange Market: Chartists, Fundamentalists, and Simpletons. *Oxford Economic Papers, 47*(3), 437-452.

Poon, S.H., & Granger, C. (2005). Practical Issues in Forecasting Volatility. *Financial Analysts Journal, 61*(1), 45-56.

Poon, S.H., & Granger, C. W. J. (2003). Forecasting Volatility in Financial Markets: A Review. *Journal of Economic Literature, 41*(2), 478-539.

Poterba, J. M., & Summers, L. H. (1988). Mean Reversion in Stock-prices - Evidence and Implications. *Journal of Financial Economics, 22*(1), 27-59.

Press, W. H., Flannery, B. P., Teukolsky, S. A., & Vettering, W. T. (1988). *Numerical Recipes in C*. New York: Cambridge University Press.

Psaradakis, Z. (2000). p-Value Adjustments for Multiple Tests for Nonlinearity *Studies in Nonlinear Dynamics & Econometrics. , 4*(3), 95-100.

Rendleman Jr, R. J., & O'Brien, T. J. (1990). The Effects of Volatility Misestimation on Option-Replication Portfolio Insurance. *Financial Analysts Journal, 46*(3), 61-70.

Rubinstein, M. (1994). Implied Binomial Trees. *The Journal of Finance, 49*(3), 771-818.

Sabanis, S. (2003). Stochastic Volatility and the Mean Reverting Process. *Journal of Futures Markets, 23*(1), 33-47.

Sarwar, G. (2003). The Interrelation of Price Volatility and Trading Volume of Currency Options. *Journal of Futures Markets, 23*(7), 681-700.

Sarwar, G., & Krehbiel, T. (2000). Empirical Performance of Alternative Pricing Models of Currency Options. *Journal of Futures Markets, 20*(3), 265-291.

Schmalensee, R., & Trippi, R. R. (1978). Common Stock Volatility Expectations Implied by Option Premia. *The Journal of Finance, 33*(1), 129-147.

Scholes, M., S. . (1998). Derivatives in a Dynamic Environment. *The American Economic Review, 88*(3), 350-370.

Scott, L. O. (1987). Option Pricing when the Variance Changes Randomly: Theory, Estimation, and an Application. *The Journal of Financial and Quantitative Analysis, 22*(4), 419-438.

Sentana, E. (1995). Quadratic ARCH Models. *The Review of Economic Studies, 62*(4), 639-661.

Shastri, K., & Wethyavivorin, K. (1987). The Valuation of Currency Options for Alternative Stochastic Processes. *Journal of Financial Research, 10*(2), 283-294.

Shimko, D. (1993). Bounds of Probability. *Risk, 6*(4), 33-37.

Smith, G., & Ryoo, H. J. (2003). Variance Ratio Tests of the Random Walk Hypothesis for European Emerging Stock Markets. *The European Journal of Finance, 9*(3), 290-300.

Smithson, C. W. (1998). *Managing Financial Risk: A Guide to Derivative Products* (third ed.). New York ,NY: McGraw-Hill.

Stein, J. (1989). Overreactions in the Options Market. *The Journal of Finance, 44*(4), 1011-1023.

Stoll, H. R., & Whaley, R. E. (1993). *Futures and Options: Theory and Applications*. Cincinnati, Ohio: South-Western Publishing Co.

Sutton, W. (1990). *The Currency Option Handbook* (second ed.). Cambridge, England: Woodhead-Faulkner Limited.

Taylor, M., & Allen, H. (1992). The Use of Technical Analysis in the Foreign Exchange Market. *Journal of International Money and Finance, 11*(3), 304-314.

Taylor, S., J. . (1994). Modelling Stochastic Volatility: A Review and Comparative Study. *Mathematical Finance, 4*(2), 183-204.

Taylor, S. J. (2005). *Asset Price Dynamics, Volatility, and Prediction*. New Jersey: Princeton University Press.

Taylor, S. J., & Xu, X. (1994). The Magnitude of Implied Volatility Smiles. *Review of Futures Markets, 13*, 355-380.

Trippi, R. R., & Desieno, D. (1992). Trading Equity Index Futures with a Neural Network - A Machine Learning-Enhanced Trading Strategy. *Journal of Portfolio Management, 19*(1), 27-33.

Whaley, R. E. (1982). Valuation of American Call Options on Dividend-paying Stocks: Empirical Tests. *Journal of Financial Economics, 10*(1), 29-58.

Whaley, R. E. (2003). Derivatives. In G. M. Constantinides, M. Harris & R. Stulz (Eds.), *Handbook of the Economics and Finance* (pp. 1131-1155): Elsevier B.V.

World Bank Development Indicator Database. (1 July 2009). Washington, USA: World Bank.

Wright, J., H.(1999). Testing for a Unit Root in the Volatility of Asset Returns. *Journal of Applied Econometrics, 14*(3), 309-318.

Wright, J. H. (2000). Alternative Variance-Ratio Tests Using Ranks and Signs. *Journal of Business & Economic Statistics, 18*(1), 1-9.

Xu, X., & Taylor, S. J. (1994). The Term Structure of Volatility Implied by Foreign Exchange Options. *Journal of Financial and Quantitative Analysis, 29*(1), 57-74.

Zakoian, J.-M. (1994). Threshold Heteroskedastic Models. *Journal of Economic Dynamics and Control, 18*(5), 931-955.